ERAGROSTIS NINDENSIS: UNRAVELLING SENESCENCE IN AN AFRICAN DESICCATION TOLERANT GRASS

by

Christine Frances Madden

MDDCHR005

Thesis Presented for the Degree of

DOCTOR OF PHILOSOPHY

In the Department of Molecular and Cell Biology

UNIVERSITY OF CAPE TOWN

Supervisor:

Prof. Jill M. Farrant

Department of Molecular and Cell Biology
University of Cape Town

South Africa

Co-Supervisor:

Prof. Sagadevan G. Mundree

Centre for Tropical Crops and Biocommodities
Queensland University of Technology

Australia

October 2019

Biographical background

Christine Madden, born 23rd March 1986, completed her BSc degree in Botany and Environmental Science at Rhodes University, South Africa in 2007. She then received her honours degree in Botany and Plant Ecology at the University of Cape Town in 2008, where her two projects investigated functional traits in indigenous trees and the impacts of indigenous herbivore grazing on the vegetation types of the Little Karoo. Between 2009 and 2011 she lived in the Republic of Korea, where she taught English as a Foreign Language at a middle school while concurrently publishing a paper from her honours. In 2012 she returned to South Africa to undertake her MSc in Conservation Biology at the Percy FitzPatrick Institute of African Ornithology, University of Cape Town. There, she undertook course work and two research projects: one, on understanding the impacts of corvids on biodiversity, and another, to quantify changes in abundances and range shift of *Corvus albus* (pied crow). After completing her MSc in 2013 she worked for the conservation NGO BirdLife South Africa, where she worked in the Albatross Task Force as a seabird bycatch specialist to mitigate seabird interactions with the demersal trawl fishery industry in South Africa. In 2016, she began her PhD investigating resurrection plants in the Department of Molecular and Cell Biology, University of Cape Town.

Publications:

Cunningham*, S. J., **Madden*, C. F**., Barnard, P., & Amar, A. (2016). Electric crows: Powerlines, climate change and the emergence of a native invader. Diversity and Distributions, 22(1), 17–29. https://doi.org/10.1111/ddi.12381. *the authors contributed equally

Hoffman, M. T., **Madden, C. F.**, Erasmus, K., Saayman, N., & Botha, J. C. (2009). The impact of indigenous ungulate herbivory over five years (2004-2008) on the vegetation of the Little Karoo, South Africa. African Journal of Range and Forage Science, 26(3), 169–179. https://doi.org/10.2989/AJRF.2009.26.3.8.953

Madden, C. F., Arroyo, B., & Amar, A. (2015). A review of the impacts of corvids on bird productivity and abundance. Ibis, 157(1), 1–16. https://doi.org/10.1111/ibi.12223

Declaration

I, **Christine Frances Madden**, hereby declare that the work on which this dissertation/thesis is based is my original work (except where acknowledgements indicate otherwise) and that neither the whole work nor any part of it has been, is being, or is to be submitted for another degree in this or any other university.

I empower the university to reproduce for the purpose of research either the whole or any portion of the contents in any manner whatsoever.

Signature: Signed by candidate

Date: 4 October 2019

Abstract

Food security is one of the most important global challenges facing the world today, especially in the context of climate change. Research has been conducted into a unique group of plants, called "resurrection plants", that can withstand up to 95% tissue water-loss without compromising viability by, *inter alia,* undergoing extensive metabolic reprogramming and suppressing senescence. In this thesis the African desiccation tolerant grass *Eragrostis nindensis* (Fical & Hiern) was used as a model plant to identify which biological processes are unique to senescence and critical for desiccation tolerance. When desiccated, the older leaves of *E. nindensis* senesce, whereas, the younger leaves recover fully upon rehydration, thereby displaying two phenotypes in a single species. Comparing these two tissue types can show how senescence upon abiotic stress is regulated. Differences in transcript abundances between the two tissue types during drying and rehydration was analysed through RNA-seq analysis, coupled with physiological quantitative traits, mass spectrometry analyses and immunoblotting. The transcriptome reflected a transcriptomic reprogramming towards desiccation tolerance by maintaining transcription of genes that control desiccation tolerance traits in both tissue types, however, only the desiccation tolerant (non-senescent) tissue appeared to suppress senescence and maintained translational control. It was hypothesised that the non-senescent tissues regulate and stabilise RNA. The older tissues were unable to suppress senescence, which resulted in cell death. Lipids accumulated in the non-senescent tissue, particularly unsaturated triacylglycerols. It was proposed that lipid droplets that accumulated during drying were stabilised through, in part, the protein expression of oleosin. These lipid droplets appeared to provide a mechanical stabilisation and energy-providing role in the non-senescent tissue. The transcription of genes that control desiccation tolerance traits was generally maintained in both tissue types, however, translation was prevented in the senescent tissue. The non-senescent tissue therefore appeared to engage in a regulation of senescence at the translational level, rather than a fine-tuned transcriptional regulation. The aim of this work was to provide a critical baseline for future studies working on *E. nindensis,* and desiccation tolerance and senescence in resurrection plants in general. Ultimately, understanding water-deficit stress in the context of senescence can help to improve drought resistance in crops to ensure food security, particularly in Africa.

Acknowledgments

This work was supported in part by the National Research Foundation (NRF). Thank you to Prof. Jill Farrant and Prof. Sagadevan Mundree for the financial contribution.

I would like to express my gratitude to my supervisor Prof. Jill Farrant, who fiercely rallied behind me and whose never-ending encouragement and advice supported me through this thesis. I am honoured to have undertaken this PhD under the guidance of such an incredible woman. Jill, your passion for science and compassion for students is outstanding and thank you for having faith in me.

Other than my supervisor I would like to thank the Centre for Tropical Crops and Biocommodities (CTCB) in Australia under the leadership of Prof. Sagadevan Mundree for inviting me to sequence my RNA and start analysis on the transcriptome. I would like to especially thank Dr Brett Williams for his dedication to my research and the constant encouragement along the way. Brett went above and beyond and could have fulfilled a role as a co-supervisor. Thank you to Michal Lorenc, David Wood and Harm Nijveen for the valuable bioinformatics support. Thank you Dr Suhail Rafudeen for all your assistance with the protein work, your warmth and encouragement are greatly appreciated.

Thank you to Dr Henk Hilhorst for gifting the oleosin antibody and for the good chats about resurrection plants, music and life. Thank you to Halford Dace for sharing the metabolome data.

Keren Cooper, thank you for all your guidance. Heartfelt thank you to the Electron Microscope Unit.

I would like to deeply thank Dr Maria Cecilia Costa for her endless support throughout this PhD. Thank you for teaching me to think critically and for your guidance.

This PhD journey would not have had so many laughs and help around the Plant Stress Lab had it not been for my lab mates, especially my dear friend Astrid Radermacher. Thank you to my friends Kate, Kim, Kat, Hayley, Sam, and Daniël for the support.

In Australia I was supported by my family Lisa, Gerard, Caitlin and Dave. Thank you for your hospitality and letting me experience your life. The trip to Australia would not have been the same without you, and I am so grateful for your love and support.

Finally, I would like to honour my family. I am grateful to my loving parents, Antje and Bernard Madden, who are a constant source of encouragement and inspiration. Thank you to my siblings Gisela, Patrick and Renate for believing in me and keeping me entertained on weekends. Lastly, I am incredibly lucky to have had the love and support from my husband, Richard Parry, without which, I would not have made it through the tough times. Thank you for keeping me laughing.

Table of Contents

List of Abbreviations

ATP	adenosine triphosphate
DEG	differentially expressed gene
DG	diacylglycerols
DGAT1	diacylglycerol acyltransferase 1
DGDG	digalactosyldiacylglycerol
DNA	deoxyribonucleic acid
DW	dry weight
ELIPs	early light-induced proteins
ER	endoplasmic reticulum
EtOH	ethanol
FA	fatty acid
FW	fresh weight
GM	genetically-modified
GOI	gene of interest
HSP	heat-shock protein
LC	liquid chromatography
LD	lipid droplet
LEA	late embryogenesis abundant protein
MeOH	methanol
MGDG	monogalactosyldiacylglycerol
mRNA	messenger RNA
MS	mass spectrometry
MS/MS	tandem mass spectrometry
NST	non-senescent tissue
OB	osmophilic body
P-body	processing body
PC	phosphatidylcholine
PCA	principal component analysis
PCR	polymerase chain reaction
PSI	photosystem I
PSII	photosystem II
RFO	raffinose family oligosaccharide
RNA	ribonucleic acid
RNP	ribonucleoprotein
ROS	reactive oxygen species
RT-qPCR	quantitative real-time PCR
RWC	relative water content
SEM	scanning electron microscopy
SG	stress granule
SMP	seed maturation protein
SQDG	sulfoquinovosyl diacylglycerol
ST	senescent tissue
TAG	triacylglycerol
TEM	transmission electron microscopy
TOR	target of rapamycin
TW	turgor weight

UPR	unfolded protein response
VLCFA	very long chain fatty acids

Disclaimer

When I began this research the *E. nindensis* genome was not yet sequenced. I therefore approached my RNA-seq analysis using methods appropriate for a *de novo* assembly. This affected my PhD in the following ways: Firstly, fewer samples were sequenced than desired, as constructing an assembly *de novo* requires paired-end sequencing, which is of higher quality but more expensive. Therefore, only three RWC (100%, 60%, 25%) were utilised for the dehydration series of both non-senescent tissue (NST) and senescent tissue (ST). The ST had an additional 18% RWC timepoint to avoid sequencing completely degraded tissue but to capture transcript abundance changes at lower water contents. I chose these water contents because they reflected dramatic changes according the physiology (**Chapter 2**) and major genetic reprogramming was expected to occur at, or prior, to these reduced water contents relative to full turgor. Despite that, a full time-course of NST was sequenced (100%, 60%, 40%, 25%, <10% and 12h rehydration), as this thesis was also exploring the global transcriptome of *E. nindensis* upon desiccation and recovery thereof. Secondly, several *de novo* assemblies were constructed using Trinity (Grabherr *et al.* 2011) and differential gene expression (DEG) conducted in edgeR. In December 2017, after the *de novo* assembly had been constructed and analysed, it became known that the genome was being sequenced by Dr Robert VanBuren (Michigan State University, MI, USA). To increase the quality of my transcriptome and to develop a robust analysis, the transcriptome was re-constructed based on the first version of the genome (received in April 2018). The *de novo* assembly was therefore not further utilised, however, the constructed assembly was used to train the genome, along with sequenced samples, and formed a key part in developing the *E. nindensis* genome. A subsequent paper was written (citation below). **Appendix 2** briefly describes the bioinformatic pipeline used to construct the *de novo* assembly. The analyses in all other **Chapters** was derived from the genome-based assembly.

Pardo J., Wai C. M., Chay H., **Madden C. F.**, Hilhorst H. W. M., Farrant, J. M., Vanburen, R. (2019). Intertwined signatures of desiccation and drought tolerance in grasses. BioRxiv. https://doi.org/10.1101/662379

https://www.biorxiv.org/content/10.1101/662379v1

Chapter 1

DESICCATION TOLERANCE AND SENESCENCE IN PLANT GENETICS

1.1. THE CHALLENGES OF ESTABLISHING FOOD SECURITY

Food security is one of the most important social and scientific challenges of our century (Godfray *et al.* 2010; Alexandratos *et al.* 2012; Van Loon *et al.* 2016; Mekonnen *et al.* 2016; FAO 2017; Bechtold *et al.* 2018). Globally, 80% (1.2 billion ha) of the world's cultivated area is rainfed, from which 60% of the global crop output is produced (FAO 2011; Cominelli *et al.* 2013; Dempewolf *et al.* 2017). The majority of our food therefore depends on the timing and availability of rainfall, and any perturbations to this (e.g. drought) will result in insufficient soil moisture availability at seed sowing and during the growing season, affecting nutrient uptake, and ultimately, yield (FAO 2011; Varshney *et al.* 2018). Agricultural production can determine the health of a nation, and according to the Millennium Ecosystem Assessment, poverty is consistently an outcome of undernutrition (Corvalan *et al.* 2005; FAO 2011; Kumar 2015; Ismail *et al.* 2017). Food security is under pressure, especially with the world's population predicted to increase to 9.8 billion by 2050, the bulk of this being in Africa. This increase in demand will put additional strain on existing resources, which will exacerbate food shortages, famine, economic instability, and political unrest (Kumar 2015, Heffernan 2013; Massawe *et al.* 2016; Springman *et al.* 2018). In 2017, over 821 million people were undernourished and this, coupled with the population increase predictions, requires a rise in food production of 50 – 70% (FAO, IFAD, UNICEF 2018). Given the timeline and rate of the impending food crisis in sub-Saharan Africa, together with unpredictable and prolonged droughts, drastic improvements to food production are of utmost importance. Furthermore, croplands are further constrained with the increasing demand for fodder, coupled with rapid urbanisation and land degradation, which results in more crops and fodder being grown on unsuitable and insufficiently arable land (Panunzi 2008; Brown *et al.* 2014).

1.2. RESURRECTION PLANTS: EXPLORING GENETIC VARIATION OF DESICCATION TOLERANCE

All living organisms are dependent on water. Plants require water for adequate metabolic functioning, evaporative cooling, transporting solutes, facilitating biochemical reactions, and due to water being non-compressible, also provides structural support (Bohnert *et al.* 1995; Farrant *et al.* 2017). Water loss is deleterious and most angiosperms are desiccation sensitive, which means they cannot survive water loss below a critical value (generally ~55% of their relative water content (RWC), a measure of plant water status relative to the water content at full turgor), after which early senescence and rapid plant death ensues (Veljovic-Jovanovic *et al.* 2006; Farrant *et al.* 2015).

Approximately 135 flowering plants have been identified that possess the unique ability to withstand desiccation to the air-dry state without severely compromising metabolic processes (Gaff *et al.* 2013; Blum *et al.* 2018). These plants are aptly named "resurrection plants" due to their ability to tolerate loss of ≥ 95% tissue water content (relating to ≥ 0.1g H_2O g dry mass^{1}) for prolonged periods (weeks to months, depending on the species) and "resurrect" from the air-dried state upon rehydration (Gaff 1971). There is little to no free water available at these low RWCs, and resurrection plants engage specific mechanisms to protect membranes and macromolecules during severe water-deficit stress (Oliver *et al.* 2000). During drying, all resurrection plants redirect their metabolic processes towards limiting oxidative damage, ensuring protection of membranes and proteins, maintaining of protein synthesis and the supply of ATP (Gaff *et al.* 2009). Although each species of resurrection plant has different mechanisms to achieve these processes, they are all underlying principles of vegetative desiccation tolerance.

Resurrection plants can be divided into two groups: true desiccation tolerance, where plants recover from rapid water loss and where protective mechanisms are constitutive (e.g. bryophytes), and modified desiccation tolerance, where the induction of protective mechanisms are employed to mitigate damage and slow the rate of drying, with increased repair mechanisms upon rehydration (e.g. angiosperms) (Oliver *et al.* 1998). Similar to orthodox seeds, which are also desiccation tolerant and metabolically quiescent yet viable in the air-dried state, there is a redirection of metabolism in desiccation tolerant tissues upon desiccation, and several seed-associated transcripts are expressed within leaf tissues of resurrection plants (Oliver *et al.* 2000; Costa *et al.* 2017a, 2017b; VanBuren *et al.* 2017). Resurrection plants have evolved numerous adaptations to avoid lethal damage arising predominantly from oxidative and mechanical stresses (Mundree *et al.* 2002; Oliver *et al.* 2004; reviewed in Griffiths 2015; Karbaschi *et al.* 2016; Costa *et al.* 2017a; Yobi *et al.* 2017; Farrant *et al.*

2017). It can be contended that understanding how resurrection plants cope with these two major stresses, from physiological responses to genetic traits, will contribute to the scientific understanding of what is required to confer drought resistance in crops.

1.2.1. How resurrection plants respond to mechanical stress

At the cellular level, mechanical stress is the exertion of pressure on cellular components, particularly the cell wall, due to the loss of turgor from water-deficit stress (Ijin 1957; Levitt, 1980). As water is lost from vacuoles and cytoplasm, tension is placed on the plasma membrane as it shrinks from plasmodesmatal attachments to the cell wall (Vicré *et al.* 2004; Morse *et al.* 2011). Further water loss results in increased compaction of organelles and macromolecules and the ultimate rupture of the plasmalemma, allowing entry of extracellular hydrolases, proteases and nucleases (Hoekstra *et al.* 2001; Morse *et al.* 2011; Farrant *et al.* 2015; Bresson *et al.* 2018). This is often coupled with cytorrhysis (collapsed cell wall), which collectively leads to cell death (Walters *et al.* 2002; Vicré *et al.* 2004; Ginbot *et al.* 2011; Tuba *et al.* 2011).

Resurrection plants prevent such mechanical stresses by a combination of increased vacuole formation and reversible cell wall folding, usually with an inverse correlation (reviewed in Farrant *et al.*, 2007; 2017). To maintain cellular volume the central vacuole is subdivided or new vacuoles are synthesised *de novo* (termed vacuolation), which increases the surface-to-volume ratio preventing tonoplast folding, providing a "bubble-wrap" effect (Mundree *et al.* 2002; Griffiths *et al.* 2014; Sharma *et al.* 2016b; Farrant *et al.* 2017). Vacuolar content has not been determined for most species, but it is likely to be a combination of anthocyanins, other polyphenols with antioxidant activities and various compatible solutes, which are possibly species specific, such as 3, 4, 5 tri-*O*-galloylquinic acid in *Myrothamnus flabellifolia* (Moore *et al.* 2005, 2007). The content of isolated vacuoles was biochemically determined by Vander Willigen *et al.* (2004), who showed that desiccated leaves of the resurrection plant *Eragrostis nindensis* contained at least proline, sucrose, glucose, fructose and protein, in similar proportions in the bundle-sheath cells. Other than vacuolation, cytorrhysis can be avoided through strategic cell wall folding (Moore *et al.* 2013; Vicré *et al.* 2004; Farrant *et al.* 2017). This is achieved by increasing cell wall flexibility of cell wall specific proteins, such as expansins or pectins, as seen in *Craterostigma plantagineum* (Jones *et al.* 2004a), arabinogalactans and pectins in *Mohria caffrorum* and *M. flabellifolia* and arabinoxylans in *E. nindensis* and *Xerophyta* species (Moore *et al.* 2013). The inverse relationship between vacuolation and cell wall folding is demonstrated in *E. nindensis*, where the mesophyll cell walls contain arabinoxylans, making them constitutively flexible,

and fold upon desiccation, whereas, the more rigid bundle-sheath cells prevent cytorrhysis through vacuolation (Vander Willigen *et al.* 2004; Moore *et al.* 2013).

An additional strategy employed by resurrection plants to avoid mechanical injury is cellular vitrification. Within the cytoplasm and organelles, the lack of water changes the physical and biochemical nature of macromolecules, altering their reactivity and increasing the chances of deleterious interactions through molecular crowding adding to mechanical stress (Vertucci and Farrant 1995). This mechanical stress has been proposed to be alleviated by the accumulation of stabilising and protective molecules, such as, *inter alia,* heat-shock proteins (HSP), late embryogenesis associated proteins (LEAs), sucrose, raffinose family oligosaccharides (RFOs), etc. (Juszczak *et al.* 2017; Sun *et al.* 2018b). This process is called vitrification, the formation of a "glassy state" as they (e.g. LEAs, sucrose) act as a water substitute, physically preventing protein aggregation and promoting protein stabilisation, thus enabling subcellular stabilisation (Farrant *et al.* 2015; Artur *et al.* 2019). This accumulation of solutes, particularly sugars, has been associated with desiccation tolerance in both resurrection plants and seeds and is well documented (Bartels *et al.* 2001). For example, *Xerophyta schlechteri* has been observed to increase sucrose by 30- to 50-fold, raffinose and stachyose by 25-fold, and verbascose by 10-fold during desiccation (Whittaker *et al.* 2001; Peters *et al.* 2007; Farrant *et al.* 2007). A similar trend is seen in *Sporobolus stapfianus*, where sucrose increased by 10-fold upon desiccation, and raffinose and stachyose increased by 74- and 62-fold compared to the hydrated state (Oliver *et al.* 2011). Vitrification is a common trait amongst desiccation tolerant plants as it not only protects the cell against the physical loss of water and hence avoids mechanical stress, but it also prevents deleterious interactions, such as oxidation, between macromolecules by accumulating antioxidants or stabilising molecules (discussed below) thus reducing oxidative stress. Although the strategies involved to avoid mechanical damage caused by significant loss of water differ across species, all resurrection plants have developed some mechanisms to avoid this stress.

1.2.2. How resurrection plants respond to oxidative stress

Oxidative stress can compromise cell wall integrity and cause irreversible damage to subcellular organisation (Ruan *et al.* 2010; Dinakar *et al.* 2013; Farrant *et al.* 2017). The most common form of oxidative stress comes from the generation of free radicals as a by-product of photosynthesis (Leprince *et al.* 2015; Farrant *et al.* 2015; Consentino *et al.* 2015; Dinakar *et al.* 2018). Free radicals, or reactive oxygen species (ROS), are highly reactive molecules with unpaired electrons that oxidise other molecules by spontaneously reacting to lipids, proteins and nucleic acids (Farrant *et al.* 2007; Mittler *et al.* 2011; Bobik *et al.* 2015; Mittler 2017). ROS are important signalling molecules that enable the

plant to elicit stress responses, but once the equilibrium of ROS production and scavenging through antioxidants is disrupted, excess ROS become harmful (Zhang *et al.* 2016; Mittler 2017). The redox status is therefore tightly regulated in all living cells (Dietz *et al.* 2016; Bresson *et al.* 2018). Major shifts in the transcriptome, proteome and metabolome occur during drying and most processes aim to prevent chlorophyll interactions and quench ROS products via antioxidants (Vicré *et al.* 2004; Farrant *et al.* 2015).

Resurrection plants attempt to limit ROS by reversibly shutting down photosynthesis (Christ *et al.*, 2014; Farrant *et al.*, 2015, Zia *et al.* 2016). Resurrection plants display two major mechanisms whereby this occurs; homoiochlorophylly, in which the majority of chlorophyll is retained with considerable protection of the thylakoid apparatus during drying, and poikilochlorophylly, in which chlorophyll and thylakoid membranes are dismantled during drying and resynthesised upon rehydration (Tuba *et al.* 1993; Oliver *et al.* 1998; Farrant 2000; Farrant *et al.* 2007; Charuvi *et al.* 2015; Challabathula *et al.* 2016; Dinakar *et al.* 2018). Both mechanisms involve complex processes that reduce or inhibit the activation of photosynthesis during water deficit to minimise the excessive production of ROS due to electron transport disruption (Vicré *et al.* 2004).

Homoiochlorophyllous species, mostly dicots (e.g. *Craterostigma spp., M. flabellifolia, Boea hygroscopica, Lindernia brevidens*), use leaf curling and the production of anthocyanins to reduce light intensity and ultimately prevent light reaching the chloroplasts and prevent ROS generation from photosystem II (PSII) (Xiao *et al.* 2015; Farrant *et al.* 2015; Shivaraj *et al.* 2018). It is hypothesised that this is further facilitated at the molecular level by early-light induced proteins (ELIPs) that bind to chlorophyll, protecting the photosynthetic apparatus, and therefore preventing photo-oxidative damage (Alamillo *et al.* 2001; Giarola *et al.* 2017; VanBuren *et al.* 2019a; Artur *et al.* 2019), although the molecular function of ELIPs has not been fully resolved. Partial dismantling of the photosynthetic machinery is evident in homoiochlorophyllous species, as seen in *Craterostigma pumilum* where the cytochrome b-6-f complex is deactivated, thus resulting in the production of ATP through cyclic electron transfer whilst preventing excessive ROS forming from linear electron flow (Zia *et al.* 2016).

Poikilochlorohyllous species are usually monocots, with the most studied species belonging within the Velloziaceae, from the genus *Xerophyta*, which have C3 photosynthetic metabolism (Sherwin *et al.* 1998; Challabathula *et al.* 2016; Dinakar *et al.* 2012). In poikilochlorohyllous species, the photosynthetic machinery is dismantled, virtually all chlorophyll is lost and thylakoids are disassembled upon desiccation, as reported in *Xerophyta humilis* (Beckett *et al.* 2012), *X. schlechteri* (Sherwin *et al.* 1998), and *E. nindensis* (Vander Willigen *et al.* 2001b). This strategy requires the photosynthetic machinery to be reassembled and chlorophyll to be resynthesised during rehydration

(Sherwin *et al.* 1998; Dinakar *et al.* 2013; Challabathula *et al.* 2016). The reassembly of the photosynthetic machinery delays metabolic restoration, and poikilochlorophyllous species therefore take longer to recover (days vs hours) from desiccation compared to homoiochlorophyllous species (Bajic 2006; Challabathula *et al.* 2016). All resurrection plants shutdown photosynthesis upon water-deficit stress, however, poikilochlorohyllous species degrade the machinery responsible for the most ROS production and can therefore remain desiccated for months to years rather than weeks to months as in homoiochlorophyllous species, which suggests that this strategy enhances stability in a desiccated state (Bajic 2006).

Another oxidative stress mitigation mechanism is the accumulation of antioxidants upon water-deficit stress. Molecules scavenging free radicals occur in all plants and include antioxidants, such as glutathione, ascorbate, tocopherol and several enzymes (peroxidases – ascorbate peroxidase, glutathione peroxidase, thioredoxin peroxidase, catalase, glutathione reductase, superoxide dismutase), α-tocopherol, and polyphenols (Illing *et al.* 2005; Georgieva *et al.* 2017a; Dinakar *et al.* 2018; Dussert *et al.* 2018). Alleviating the stresses induced by water deficit, much like the mechanical and oxidative stresses outlined above, is achieved through a co-ordinated sequence of genetic and molecular regulatory mechanisms, which in turn enable the protection of subcellular organisation in a viable but quiescent state such that metabolism can resume immediately upon rehydration. Understanding these mechanisms is important to achieving desiccation tolerant crops.

1.3. CLASSICAL SENESCENCE AND THE UNKNOWN IN RESURRECTION PLANTS

Senescence is the eventual death of a cell, organ or organism associated with aging or stress. This process is slow and can occur long before leaf maturity (Breeze *et al.* 2011; Bresson *et al.* 2018). The senescence process can be perceived as having three distinct stages; initiation, re-organisation and termination (Bresson *et al.* 2018). Initiation often coincides with the onset of flowering or stresses, which lead to dramatic cellular re-organisation including the breakdown of chloroplasts and remobilisation of salvaged nutrients, and finally termination, where raptured vacuoles release proteases and nucleases into the cell, degrading cellular structures and resulting in cell death (Bresson *et al.* 2018).

Leaf senescence is a universal phenomenon, described as the final stage in leaf development, and involves a coordinated degeneration process that ultimately leads to cell death (Guiboileau *et al.* 2010;

Woo *et al.* 2013; Guo 2018). At the early stages of senescence, large-scale cellular reorganisation takes place, such as thylakoid membrane degradation and the emergence of clustered plastoglobuli. At the later stages of senescence collapsing of the vacuoles, membrane disintegration and chromatin condensation occurs (Lim *et al.* 2007). Senescence is a way of optimising resources through "nutrient salvage" by remobilising nutrients accrued during growth from senescing (source) to developing (sink) tissues and organs (Lim *et al.* 2007; Watanabe *et al.* 2013). Catabolic reactions increase during senescence as macromolecules (such as chlorophyll and ribulose-1,5-bisphosphate carboxylase/oxygenase (RUBISCO)) are broken down into transportable products (amino acids, fatty acids, sugars etc.), and transported into sink tissues to be reused to synthesise new proteins (Woo *et al.* 2013; Esteves *et al.* 2013). This breakdown is followed by decreases in nucleic acids, total RNA as well as translational mechanisms for protein synthesis, such as ribosomes (Lim *et al.* 2007; Woo *et al.* 2013).

The classical view of senescence as age-related cell death is different to prematurely induced senescence due to environmental stress, such as low-light, nitrogen starvation, salinity, drought and pathogen attack (Wingler *et al.* 2009; Allu *et al.* 2014; Yolcu *et al.* 2018; Durgud *et al.* 2018). Senescence is therefore both a genetically regulated age-dependant process as well as a process induced by exogenous factors, such as disease or drought (Lim *et al.* 2007; Bresson *et al.* 2018; Yolcu *et al.* 2018; Guo *et al.* 2019). Both responses undergo key processes that breakdown, remove and recycle nutrients. For example, senescence is developmentally triggered on the onset of flowering in annuals, where the death process was programmed and initiated once the plant reached a certain size and maturity (Thomas 2013). In contrast, starving *Arabidopsis thaliana* (Arabidopsis) of light caused dark-induced environmental stress, which induced the senescence programme (Law *et al.* 2018; Yolcu *et al.* 2018). Although the initial signal that determines senescence remains unclear, there are known pathways of genetic reprogramming once senescence is triggered (Yolcu *et al.* 2018). Senescence-associated genes (SAGs) are typically expressed and regulated by senescence-associated transcription factors, such as NAC and WRKY (Guo *et al.* 2004; Woo *et al.* 2013). The activation of transcription factors is coupled with complex hormonal, redox and metabolic signalling to evoke the organised regulation of senescence (Bresson *et al.* 2018).

Senescence involves a complex genetic cascade from chromain-remodelling through transcriptional, post-transcriptional, translational and post-translational regulation, to protein modification and hormone signalling (Woo *et al.* 2013; Yolcu *et al.* 2018). Stress alters cellular homeostasis and activates the accumulation of metabolites, such as lipids, sucrose or ROS, which act as signalling molecules that prompt epigenetic changes that initiate senescence (Mittler 2017; Durgud *et al.* 2018; Zhang *et al.* 2018). For example, hydrogen peroxide (H_2O_2) in Arabidopsis induces a DEHYDRATION-RESPONSIVE

ELEMENT BINDING gene (DREB2A) that is regulated by the drought-stress related NAC transcription factor, and the overexpression of this gene increases tolerance to drought, salinity and heat-shock in transgenic Arabidopsis (Sakuma *et al.* 2006). Moreover, glucose and fructose are associated with senescence, whereas sucrose accumulation is associated with desiccation tolerance, demonstrating the protective role of non-reducing sugars in resurrection plants (Pourtau *et al.* 2006). Hormonal signals, such as abscisic acid (ABA), auxin and cytokinin trigger stress-responsive gene expression and are linked to the regulation of senescence**.**

In addition, age-related senescence is not a discrete event but rather a continuous process, from the initiation signal followed by cellular and metabolic reorganisation, to termination (Bresson *et al.* 2018). Furthermore, not all cells in a leaf undergo simultaneous senescence, but rather patches of cells die, triggering a coordinated senescence process in other cells and organs (Lim *et al.* 2007). Whole leaf death occurs when the ratio of dead cells is too high. Although senescence has been an acknowledged aspect of resurrection plants since the 1980s, where the older leaves do not recover from desiccation, these reports are largely based on observations and correlation of metabolite accumulation during drying-induced senescence (Gaff *et al.* 1986; Veljovic-Jovanovic *et al.* 2006). Nevertheless, several studies acknowledge that most resurrection plants do exhibit some form of senescence upon desiccation, such as the leaf tip of *X. schlechteri* (unpublished data) or the outer leaves of *S. stapfianus* (Martinelli *et al.* 2007), *Tripogon loliiformis* (Karbaschi *et al.* 2016), *C. plantagineum* (Christ *et al.* 2014)**,** amongst others (Gaff *et al.* 2013). However, the mechanisms of senescence and its regulation in those tissues that die upon desiccation have not been experimentally explored. There is a large degree of cross-talk between developmental and stress induced senescence, however, the causes are very different and detailed knowledge is lacking on the regulatory differences that control age-related vs stress-induced senescence. Ghasempour *et al.* (1998) observed that roughly 50% of *E. nindensis* leaves survive desiccation, illustrating the different phenotypes of tolerant and sensitive tissues. However, how resurrection plants differentially regulate senescence between these two tissue types has not been established.

1.4. CASE STUDY: *ERAGROSTIS NINDENSIS* (FICAL & HIERN)

Because cereals (grasses) make up the bulk of our food, understanding their physiological and metabolic adaptations to water stress can inform crop improvement strategies. Several grasses have been characterised to be desiccation tolerant in their vegetative tissues, mainly within the Eragrostoideae (*Eragrostis, Tripogon*), Sporoboleae (*Sporobolus*), and Chrlorideae (*Oropetium, Brachachme, Microchloa*) tribes (Gaff *et al.* 1974). The genus Eragrostis is from the family Poaceae and

occurs in sub-Saharan Africa, from Democratic Republic of Congo and Tanzania southwards to South Africa (van Outshoorn 1992). There are nine desiccation tolerant species in the family Poacae (Gaff *et al.* 2013), however, only one genus within this family contains an important agricultural crop species: Eragrostis.

Eragrostis is characterised by having several florets, which are small, flat and longitudinal with small, often nutritious, seeds (van Outshoorn 1992, Tadele 2009). There are 83 species of Eragrostis within Africa, with only one known species acquiring vegetative desiccation tolerance; *E. nindensis* (Gaff *et al.* 1974). Interestingly, of the 39 grass species that are desiccation tolerant, only two have been recorded being grazed by animals – *T. loliiformis* and *E. nindensis* (Blomstedt *et al.* 2018). In conversations with farmers during fieldwork, they confirmed that *E. nindensis* is highly palatable and sheep graze on the rehydrated leaves within a week after rainfall. Although some Eragrostis species are used for fodder (e.g. *Eragrostis curvula*), only *E. tef* (Teff) is of commercial importance, which is mainly cultivated in the Horn of Africa. Teff is one of the main agricultural and pastoral crops in East Africa and accounts for over 20% of Ethiopia's farmlands and 75% of staple food supplies in the region (Tadele 2009). Its seed, albeit small, is of high nutritional value, providing dietary fibre, iron, protein and calcium (Tadele 2009). Furthermore, Teff is an orphan crop, which are typically under-studied and under-researched (Tadele 2009). These crops are locally important, often well adapted to extreme climatic conditions, nutritious, culturally valued, and form part of local economies and rural employment (Naylor *et al.* 2004, Tadele 2009). Teff is also gluten free, giving it a recent status of a super food, which is spreading into European and North American markets (Knorr *et al.* 2019).

The *E. nindensis*-Teff combination is by far the closest resurrection plant-crop model addressed to date. The genome of *E. nindensis* shows a 2:4 synteny to Teff, showing direct genomic region overlap (Pardo *et al.* 2019). Teff is relatively drought resistant but is not desiccation tolerant like *E. nindensis*. These two phylogenetically similar species represent an advantageous opportunity for the application of desiccation tolerance in biotechnology by using Teff as a valuable model for transformation using the understanding gained from this study on *E. nindensis*. Understanding what genes in the genetic toolbox are required of a C4 monocot (like several cereals) to confer desiccation tolerance could bridge the gap to transforming Teff or other subsistence crops through biotechnology.

E. nindensis exhibits a strong contrast between desiccation tolerant and desiccation sensitive leaves upon desiccation. Furthermore, this species exhibits two distinctly different phenotypes. When dried below 10% RWC older leaves senesce and die, whereas the younger leaves fully recover upon rehydration (Vander Willigen *et al.* 2003). This provides a useful model to study senescence in a single species. The mechanism behind the activation of senescence in senescent tissue (ST) and the

suppression of senescence in non-senescent tissue (NST) in this species is unknown. We know that resurrection plants suppress senescence in desiccation tolerant tissues. We also know that some resurrection plant leaves die during desiccation. However, it is unknown what gene regulation mechanisms are involved in the senescence processes that allow only some tissue to survive. Whether there is a senescence signal in resurrection plants, and if it is the same as classical senescence has not been determined. Comparing the global transcript abundance patterns between NST and ST upon desiccation aims to gain a better understanding of how senescence functions in leaf tissues that do not recover upon rehydration in the context of desiccation tolerance.

1.5. SCOPE OF THE THESIS

Oliver *et al.* (2011) remarked that "without a relevant comparison between the responses of sensitive and tolerant tissues, any insight into the adaptive processes [of desiccation tolerance] remains simply speculative". Currently no studies have investigated the differences in transcript abundance between desiccation tolerant and desiccation sensitive leaves on a single plant.

Transcriptomes contain a wealth of data and the popularity of high-throughput techniques and the availability of such databases can be overwhelming. To narrow the focus of transcript abundance regulation of desiccation tolerance and senescence processes, the comparison of the ST against the NST within a resurrection plant species should be explored. The rationale behind this direct comparison is the notion that transcripts not expressed in the ST are critical for both desiccation tolerance and to prevent desiccation-induced senescence, whereas those not expressed in the NST are likely to be linked to senescence or represent a failure to withstand desiccation, at the resolution of transcript regulation.

To understand desiccation tolerance in the context of crops or pasture grasses, we first need to understand how desiccation tolerance works on a physiological, genetic and metabolic level, and secondly, how resurrection plants regulate (suppress) senescence and cell death. Here, bioinformatic and molecular techniques were employed to investigate senescence in a resurrection plant. Because *E. nindensis* is a modified desiccation tolerant plant, stress-induced expression of transcripts was bioinformatically investigated. A functional genomics approach was used that combined water-deficit stress induced physiological and ultrastructural changes on NST and ST with transcript abundance patterns in the context of major functional group trends (transcriptome), metabolome (lipidomics) and protein expression in *E. nindensis*.

As indicated above, *E. nindensis* is a highly suitable candidate for the development of drought-tolerant crops and was selected as it is desiccation tolerant, is closely related to an existing crop (Teff), and that the molecular aspect of this species was unexplored. The main research aim was to characterise the transcriptome of *E. nindensis* under different water-deficit stress conditions in order to contribute to the scientific understanding of the regulation of desiccation tolerance in this species, and its senescence, and further understanding of these phenomena in resurrection plants in general. This was an explorative thesis. Using *E. nindensis*, the function and regulation of desiccation tolerance and senescence was interrogated in relation to the fully-hydrated, NST state (the control). Each **Chapter** characterised broad trends of *E. nindensis*, focused in-depth on key or interesting findings, which then informed the next **Chapter** to place desiccation tolerance and associated senescence in the context of resurrection plants.

Firstly, the physiological phenotypes of NST and ST in *E. nindensis* was characterised (**Chapter 2**). Drought is the strongest abiotic stress affecting photosynthesis, and thus understanding how water-deficit stress affects photosynthesis, in relation to transcript abundance, was a key objective. Comparisons of gas exchange parameters, photosynthetic rates, chlorophyll fluorescence and cellular ultrastructure through Transmission and Scanning Electron Microscopy (TEM) of ST in relation to NST was described in **Chapter 2**. It was essential to confirm that the water contents selected capture critical physiological (and therefore molecular) changes during drying and ensure that the sampling strategy consistently differentiated between tissue types for downstream molecular work. Next, the transcriptomic signature of desiccation tolerance in *E. nindensis* in the NST was investigated to understand the regulation of molecular changes that result in a quiescent metabolic state (**Chapter 3**). The aim was to provide a comprehensive overview of the metabolic reprogramming required to convey desiccation tolerance in the surviving tissue upon water-deficit stress and rehydration.

Chapter 4 discusses an in-depth investigation into the differences and similarities of the transcriptomes of the NST and ST by focussing on overrepresented gene ontology (GO) categories in each RWC. An untargeted approach, highlighting transcript abundance patterns of common biological pathways, coupled with a targeted approach, investigating known desiccation tolerance traits, was used to unravel how senescence is regulated between tissue types. GO categories exclusively enriched in each tissue type were analysed to determined key components that regulate desiccation tolerance and senescence.

Since this thesis was explorative, findings were pursued that could not have been pre-determined. One such finding was the consistent appearance of the importance of lipids – from their prominent appearance in the ultrastructural studies through to their overrepresentation in the transcriptome. To

date, there has been no previous analysis of the lipid composition or protein expression in *E. nindensis*. The lipid signature showed promising differences between tissue types and was used as a case study to validate findings from previous **Chapters**. Global changes in targeted lipids and lipid species composition upon water-deficit stress between tissue types was explored. The expression of oleosin, a lipid droplet specific protein, was confirmed through western blotting to elucidate the role of lipid droplets in conveying desiccation tolerance in *E. nindensis*.

Finally, **Chapter 6** highlights key findings and outlines future work. Despite *E. nindensis* being phylogenetically similar to *E. tef* this species is greatly understudied, with only one Master's thesis (Ginbot *et al.* 2011) and one PhD thesis exploring the desiccation tolerance of this species being conducted in 2001 (Vander Willigen *et al.* 2001b). Unravelling senescence and desiccation tolerance in *E. nindensis* therefore has a large scope of exploration and has the potential to reveal novel findings that will aid crop engineering to develop drought tolerance in crops to boost food security in Africa.

Chapter 2

COMPARING DESICCATION-INDUCED PHYSIOLOGICAL CHANGES BETWEEN NST AND ST

2.1. INTRODUCTION

Extreme water loss causes death in most plants. Resurrection plants, referring specifically to species that can recover from near-complete protoplasmic water loss (> 90%), are desiccation tolerant and have evolved incredible strategies to prevent *inter alia* mechanical and photo-oxidative stress, and repair desiccation associated damage (Oliver *et al.* 2000; Zia *et al.* 2016; Charuvi *et al.* 2019). Photosynthesis is the greatest determinant of plant productivity but it is also the main site of damage under abiotic stresses, particularly drought (Miller *et al.* 2010; Charuvi *et al.* 2019). Water loss can become deleterious when electron sinks, such as in the Benson-Calvin cycle, become unavailable when stomatal shutdown, due to turgor loss, reduces intercellular CO_2 concentrations (Erb *et al.* 2018). This shutdown of electron-accepting processes results in an excess of highly energised singlet oxygen (e.g. ROS) in the thylakoid lumen (Pintó-Marijuan *et al.* 2014; Dietz *et al.* 2016; Dinakar *et al.* 2018). ROS are highly reactive and cause oxidation of molecules and peroxidation of lipids if not adequately quenched by oxygen-scavenging molecules, such as the antioxidants α-tocopherol and β-carotene (Kranner *et al.* 2002; Zhu *et al.* 2015; Yobi *et al.* 2017; Bresson *et al.* 2018; Sun *et al.* 2018). Hence, water-deficit stress prevents carbon-gain, and thus plant growth, which can cause irreparable damage to the photosynthetic machinery if not mitigated (Blomstedt *et al.* 2010; Farrant *et al.* 2017). Resurrection plants undergo significant changes to cope with the oxidative and mechanical stress of desiccation, which are reflected by the changes in physiology and ultrastructure, coupled with the genetic reprogramming of important biological processes, such as the shutdown of photosynthesis and the inhibition of senescence (Griffiths *et al.* 2014; Giarola *et al.* 2017; Costa *et al.* 2017a; VanBuren *et al.* 2018).

Ultrastructural changes are induced to avoid damage linked to desiccation. Common features that contribute to desiccation tolerance include cell wall folding and/or the fragmentation of the central vacuole into several smaller vacuoles, collectively maintaining cell volume and thus minimising mechanical stress as seen in *Eragrostis nindensis, Xerophyta schlechteri, Craterostigma wilmsii, Craterostigma pumilum, Myrothamnus flabellifolia,* and *Sporobolus stapfianus* (Sherwin *et al.* 1998;

Farrant *et al.* 2015; Georgieva *et al.* 2017a). Formation of lytic compartments for the breakdown of toxic components, which themselves might ultimately become vacuoles, occurs (Williams *et al.* 2015; Charuvi *et al.* 2019). The decompartmentalisation and reorganisation of organelles can reduce surface area tension, as well as prevent photosynthesis and its harmful by-products by, *inter alia,* dismantling and reorganising thylakoids (Farrant 2000; Vander Willigen *et al.* 2004; Farrant *et al.* 2015; Zia *et al.* 2016; Giarola *et al.* 2017). However, anatomical changes are not consistent across species, as in *Boea hygroscopica*, where thylakoid membranes did not disassemble upon desiccation but remained tightly stacked (Navari-Izzo *et al.* 1995), demonstrating that membrane compositional changes are variable and that there is not a universal strategy in resurrection plants. The shutdown of photosynthesis is reflected by the accompanying decrease in starch abundance and size in most species (Whittaker *et al.* 2007; Farrant *et al.* 2007, 2015; Zia *et al.* 2016). One of the major differences between resurrection plants and desiccation sensitive species is that in desiccation sensitive plants, RUBISCO is broken down and is a major sources of nitrogen (up to 75% of cellular nitrogen) that contributes to the energy status of the cell in the absence of carbon-gain (Lim *et al.* 2007; Avila-Ospina *et al.* 2014). In resurrection plants, RUBISCO is retained, even in poikilochlorophyllous species (Christ *et al.* 2014). Due to their maintenance of chlorophyll, homoichlorophyllous species tend to recycle nutrients through autophagic processes (e.g. *Tripogon loliiformis*), whereas the need for autophagy-derived nutrients is less in poikilochlorohyllous species due to the thylakoid dismantling (Williams *et al.* 2015; Asami *et al.* 2018). Drying induces the accumulation of osmolytes, especially stabilising sugars, such as RFOs, sucrose, trehalose, proline and putative protective proteins, such as LEAs, chaperones, HSPs (Artur *et al.* 2018, 2019; Dussert *et al.* 2018). The cells therefore maintain their subcellular organisation and prevent mechanical stress during desiccation.

All resurrection plants alter their chlorophyll contents, to varying degrees, as a strategy to minimise photo-oxidative damage (Christ *et al.* 2014). The breakdown of chlorophyll and the disassembly of key components of chloroplasts, such as the thylakoid membranes, are similar to the senescence processes occurring in all plants (Otegui 2018; Charuvi *et al.* 2019), however, this breakdown is only reversible in resurrection plants. Senescence in resurrection plants is an intriguing phenomenon as it is actively avoided in desiccation tolerant tissues (Beckett *et al.* 2012; Griffiths *et al.* 2014; Williams *et al.* 2015). Yet, most resurrection plants do display some age-related tissue senescence. However, the physiological processes associated with such senescence have not been fully described in resurrection plants, work by Vander Willigen (2001a, 2001b; 2003; 2004) described basic differences between NST and ST in *E. nindensis*, most notably observing the inability for the ST to recover. While this standalone work is seminal in addressing the response to desiccation in non-surviving tissues, a comprehensive understanding of the performance of ST in a resurrection plant is still not understood. Vander Willigen

et al. (2001b) observed a shutdown of photosynthesis in both the NST and ST. Differences between the two tissue types became apparent by 50% RWC, when the increase in electrolyte leakage in ST indicated the failure to maintain membrane stability (Vander Willigen *et al.* 2001b). This irreparable damage of the cell membrane in ST was supported ultrastructurally through transmission electron microscopy (TEM), where cell membrane disruption is evident at 27% RWC in the ST (Vander Willigen *et al.* 2003). The bundle sheath cells of *E. nindensis* became vacuolated upon severe dehydration and largely maintained their shape upon desiccation (Vander Willigen *et al.* 2004). The tonoplast length of *E. nindensis* almost doubled during drying, from 74.43 to 125.32 µm cell^{-1}, despite the vacuolar volume remaining unaltered, illustrating the role of vacuole fragmentation in the bundle sheath cells negating the need to reduce cell volume (Vander Willigen *et al.* 2003). Finally, some inferences were made in the differences in the accumulation of vacuolar osmolytes, as the tonoplast-intrinsic protein (TIP 3;1), speculated to promote sucrose, proline and protein mobilisation within vacuoles, was only observed in NST upon desiccation (Vander Willigen *et al.* 2004). A deeper investigation into the molecular mechanisms and processes that differ between NST and ST has not been conducted until now.

To understand senescence processes in a resurrection plant it is essential to first elucidate physiological differences upon severe water-deficit stress. These changes need to be analysed in connection with the transcript abundance changes that shed light on the regulation of the biological processes governing physiological function and their metabolic by-products (although the metabolism was beyond the scope of this thesis). A strict characterisation of the whole plant growth format is therefore required to clearly distinguish between NST and ST for downstream molecular investigation using RNA-seq (explored in **Chapter 3 - 6**). The present **Chapter** aims to characterise the physiology of the NST and ST from the *E. nindensis* under desiccation and rehydration by comparing changes in photosynthesis determined by gas exchange and chlorophyll fluorescence. Chlorophyll and anthocyanin content were determined spectrophotometrically and the leaf ultrastructure investigated using TEM. Investigating how resurrection plants undergo senescence is a good path to elucidating the features that are essential for desiccation tolerance (those that are present in NST only), or not (those that are common to both NST and ST).

2.2. METHODS

2.2.1. Germination and propagation

Seeds collected from plants grown in the field near Aggeneys, Northern Cape, South Africa, (29°16'41.1"S 19°00'25.4"E) with permission from the land manager Pieter Venter, were germinated on a 0.8% agar growth medium containing 0.22% Murashige and Skoog (MS) without vitamins. Tissue

culture jars containing 40 ml of the agar medium were autoclaved and left for 48 hours to ensure that there was no contamination. Seeds were surface sterilised by swirling in 70% ethanol for 10 seconds, rinsed with sterile water, dried on filter paper and plated in a laminar flow chamber. Jars were kept in a growth chamber with a 16-hour photoperiod (light intensity of 300 µmol m^{-2} s^{-1}) maintained at 24°C during the day and 15°C at night. After approximately one-month, seedlings from the MS jars were hardened for four days by removing the lids and allowed them to transpire for two hours on the first day, four hours on the second day, and so forth. After acclimation over four days, seedlings were transplanted into seedling trays containing vermiculite and 0.4% Phostrogen All Purpose Plant Food (Bayer, South Africa) with additional 2% calcium. Seedlings were watered three times a week, with a light spray of Phostrogen nutrient solution once a week. After another month, seedlings were transplanted into 10.5-cm pots with a sand:vermiculite:perlite mixture (2:1:1) and kept for another six months to reach a biomass sufficient for the dehydration curve. Mature plants were lightly watered (~250 mL) once a week.

Two weeks prior to experimentation, the plants were transferred into a Percival© (Percival Intellus control system, model number: I-41LL) for acclimation. Plants were kept well hydrated and incubated under controlled conditions of a 16 h photoperiod using a light intensity of approximately 300 µmol.m^{-2}.sec^{-1} with 24 °C daytime and 15 °C night-time temperatures. Plants were randomised by shuffling them around throughout the acclimation and experimentation periods.

2.2.2. Defining the senescent leaf phenotype

It is imperative to correctly distinguish and identify leaf tissues that are desiccation tolerant and will resurrect (NST) versus those that do not recover upon rehydration and senesce (ST), to quantify differences in physiological, metabolic and genetic changes between these distinct tissue types. NST leaves were identified as young, fully-mature (unrolled) leaves, the highest on the tiller (the “inner” leaf, Figure 2.1). ST leaves were identified as the oldest leaf on the tiller (the “outer” leaf), which is the lowest on the tiller.

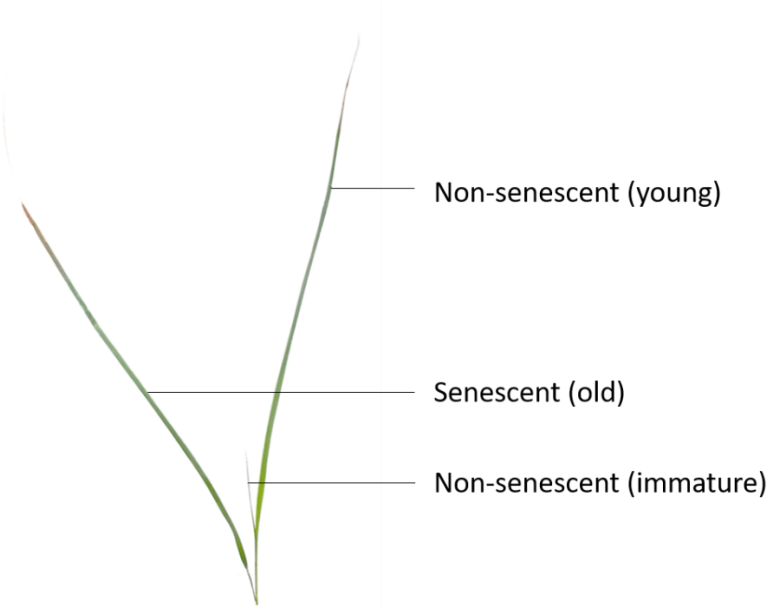

Figure 2.1: Tillers of the resurrection plant *Eragrostis nindensis* identifying younger, desiccation tolerant (non-senescent tissue, NST) and desiccation sensitive (senescent tissues, ST) leaves used for all physiological and molecular assays through this thesis. Note the higher position of the NST compared to the ST, which extends away from the tiller sheath. The ST does not recover during rehydration after a desiccation event.

2.2.3. Desiccation stress treatment and sampling of *E. nindensis*

Five dehydration curves were performed to obtain the different physiological and molecular parameters (Table A5). *E. nindensis* reaches maturity and is completely desiccation tolerant by eight months (Vander Willigen *et al.* 2003). All plants used for the dehydration curve were mature, established eight-month-old or field-collected plants. Individual plants with leaf discolouration, any signs of stress, or significantly different biomass were discarded. All plants were subjected to several cycles of desiccation and rehydration for "genetic priming". Furthermore, since the older leaves of *E. nindensis* die successively during dehydration, the plants were desiccated and then rehydrated six weeks prior to each dehydration experiment to ensure that all dead leaves were pruned prior to stress treatment initiation. This guaranteed that the senescent (oldest) leaves were the same age for each experiment and avoided the compounding effects of age-dependant senescence across dying tissues. The senescent tips were pruned prior to the stress treatment to ensure that all leaf material collected throughout the experiment was alive, so that any senescence was water-deficit induced.

Plants were dehydrated by withholding water until they reached an air-dry state (RWC below 10%). They were left in the air-dry state for two weeks prior to rehydration. All plant samples were randomly selected and harvested in (a minimum) triplicate for each RWC category (100%, 60%, 40%, 25%, <10%). Additional 75% RWC dehydration time points were included in the gas exchange measurements.

Rehydration involved generous watering and misting with a spray bottle until the leaves and soil were saturated. Measurements were taken 12h, 24h, 36h, 72h, 84h, 144h and 204h (hours) post-rehydration.

Throughout this thesis, in the context of the dehydration curve, the period from fully hydrated to air-dry is referred to as “drying”.

2.2.4. Time-lapse photography

A time-lapse sequence visually illustrating the physiological changes of *E. nindensis* during drying and rehydration was performed (https://youtu.be/gV6_CJXM0sw). A mature plant, collected from the wild and kept in the plant growth room for one year, was subjected to desiccation and rehydration by withholding water. A photo was taken every five minutes using a Canon EOS 40D with the following settings: f/10, exposure time 1/20s, ISO 200 and focal length 100 mm.

2.2.5. Relative water content determination

To quantify leaf water status during drying and rehydration, RWC was determined gravimetrically according to Barrs and Weatherley’s (1962) formula:

$$RWC\ (\%) = ((\text{fresh weight} - \text{dry weight}) / (\text{turgid weight} - \text{dry weight})) \times 100$$

A minimum of three individual plants were used as biological replicates per RWC category for all assays. For each plant, approximately three leaves from both NST and ST were harvested and immediately weighed in grams (fresh weight) accurate to 10 ug, then placed in a microtube filled with water and kept at 4°C in the dark overnight. Leaves were blotted on tissue paper to remove external water and weighed (turgid weight). The same sample was placed in a labelled foil packet, dried at 70°C for 48 hours, and weighed (dry weight).

Due to the leaf absorbing water into the intercellular tissues, some measured turgid weights were less accurate and therefore had an under or over-estimated RWC. Several hundred additional RWCs were measured to establish the correlation between absolute water content (AWC = (fresh weight – dry weight)/dry weight) and RWC (Figure 2.2). There is a greater standard deviation at higher water contents. Therefore, AWC was used to group tissues at specific dehydration timepoints, compared to the calculated RWC, and reported on a RWC category basis when there was congruency (Table 2.1). Rehydration was difficult to categorise due to the variable rehydration rates between individual plants

(Appendix, Figure A1). The RWC of individual plants differed in hours after re-watering. Despite this variation, the hours post-rehydration was reported to standardise with previous studies.

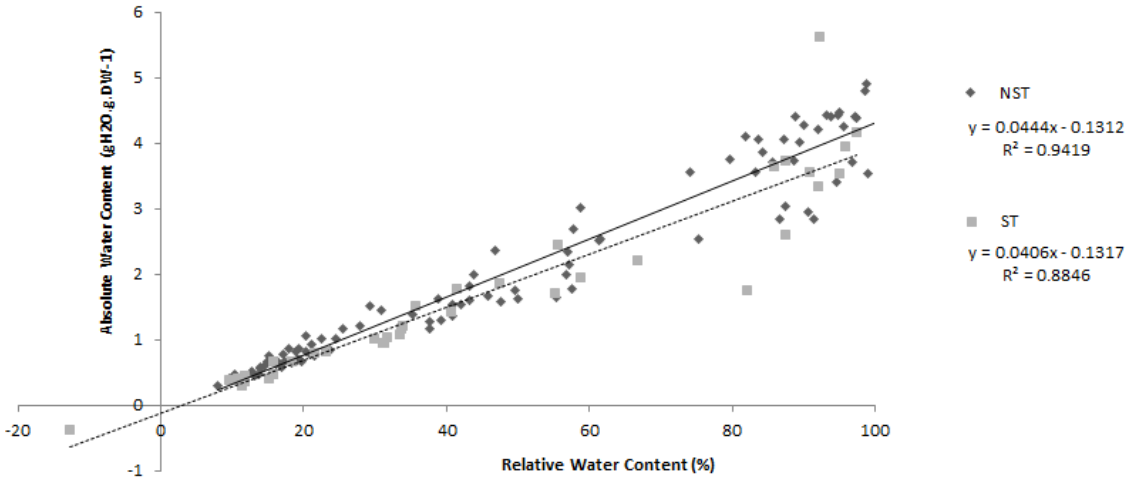

Figure 2.2: The relationship between absolute water content (AWC) and relative water content (RWC) of the resurrection plant *Eragrostis nindensis* for desiccation tolerant, non-senescent tissue (NST) and desiccation sensitive, senescent tissue (ST) upon water-deficit stress.

Table 2.1: The range of absolute water content (AWC) and relative water content (RWC) classification used in the physiological and molecular (RNA-seq) experiments of desiccation tolerant, non-senescent tissue (NST) and desiccation sensitive, senescent tissue (ST) in the resurrection plant *Eragrostis nindensis* grown from seed under laboratory conditions. AWC categories were calculated based on the linear relationship established in Figure 2.2. The range of AWC was ±0.2. For actual RWC values, see Appendix, Table A2.

	AWC	
RWC	NST	ST
100%	3.62	3.21
75%	2.72	2.41
60%	1.99	1.77
40%	1.45	1.28
25%	0.91	0.8
<10%	<0.3	<0.3

For the gas exchange parameters, one control plant continued the once-a-week light watering regime. The fully hydrated plants, defined as those harvested one-day post-watering, were used as the control for the molecular experiments.

2.2.6. Gas exchange and chlorophyll fluorescence

Twenty plants were utilised for these studies (Appendix, Table A1). Gas exchange measurements were performed using a LI-COR 6400XT infrared gas analyser (IRGA) portable photosynthesis system (LI-COR Biosciences Inc., NE, USA) with a fluorescent chamber. Leaves were measured at the same time every day (9–11 am) to avoid the confounding effects of changes in circadian rhythms and photosynthesis. As *E. nindensis* has thin leaves, a minimum of four leaves (unrolled) was required to fill the majority of the chamber area. For the accurate calculation of total leaf area, the leaf was photographed and the leaf area was calculated in ImageJ (Schneider *et al.* 2012). The gas exchange formulas were corrected accordingly. The reference CO_2 concentration was set at 400 $\mu mol.m^{-2}.sec^{-1}$, the light intensity was set at 1000 $\mu mol.m^{-2}.sec^{-1}$ of PAR (photosynthetically active radiation), the flow was set to 100 $\mu mol.m^{-2}.sec^{-1}$. Due to stomata occurring on both the abaxial and adaxial surfaces of the leaf, the stomata ratio was set to 0.5. Samples were inserted into the chamber, the IRGA was matched and the samples were allowed sufficient time to equilibrate (i.e. carbon assimilation or fluorescence stabilised) before measurements were recorded.

Leaves were dark-adapted overnight before measuring chlorophyll fluorescence, as recommended by LI-COR (2012). The LI-COR protocol and settings for determining F_v/F_m was followed with the following parameters: measurement intensity 1, fixed flow 100µmol/s, CO_2 concentration 400 $\mu mol.m^{-2}.sec^{-1}$, flash duration of 0.8 and intensity of 7. Leaves were then light-adapted for a minimum of 20 minutes before photosynthesis (A) and quantum efficiency of photosystem II (ΦPSII) gas exchange measurements were collected. At least five technical replicate measurements (recorded every 15 seconds) were taken to assess stability and data quality. Due to leaf curling at lower water contents, it was difficult to measure gas exchange effectively at RWCs less than 40%. However, gas exchange measurements were still taken despite this change in leaf morphology to investigate the trends in photosynthetic shutdown and resumption. These limitations were acknowledged, and the trends were supported with microscopy and pigment content. Where possible, a two-tailed Student's t-test was used to determine differences between tissue types.

2.2.7. Pigment concentration

Changes in chlorophyll and anthocyanin contents during drying are indicators of a stress-response and therefore pigment concentrations were measured spectrophotometrically using a Beckman DU-64 spectrophotometer (Fullerton, California, USA). For the chlorophyll extraction, 3–10 mg (depending on RWC) of leaf material was harvested from a minimum for three plants per RWC. The weight of each sample was recorded, and the tissue was placed in a 1.5 mL microtube with 800 µl of DMF (N,N-

dimethylformamide, Sigma©) and briefly vortexed and centrifuged. Samples were left to extract on a shaker at 4°C in the dark for 24 hours. Equal amounts (200 µl) were pipetted, in triplicate, into a plate reader and the absorbance was read at 647 nm and 664 nm. DMF was used as a blank. Absorbances (A) were corrected for volume (800 µl) and the blank absorbance was subtracted. The leaf tissue was oven dried for 48h at 75°C to record the dry weight. Chlorophyll concentrations were measured according to Porra *et al.* (1989) using the following equations and expressed on a dry weight basis:

$$\text{Total Chlorophyll} = (17.67 * A_{647}) - (7.17 * A_{664})$$

$$\text{Chlorophyll a} = (12 * A_{664}) - (3.118 * A_{647})$$

$$\text{Chlorophyll b} = (20.78 * A_{647}) - (4.88 * A_{664})$$

Anthocyanin extraction followed the protocol of Neff & Chory (1998). Leaves (3–10 mg, depending on RWC) were weighed, placed in a 1.5 mL tube and snap-frozen in liquid nitrogen. Tissue was ground using a microcentrifuge pestle before adding 300 µl of acidified methanol (MeOH) containing 1% HCl. Samples were briefly vortexed then centrifuged and were left to extract on a shaker at 4°C in the dark for 24 hours. Next, 200 µl of Milli-Q H_2O and 500 µl of chloroform were added to each tube and centrifuged at 13.4 rpm for 5 minutes. The aqueous layer was extracted (~400 µl), placed in a new tube, and brought back to 800 µl volume by adding a 60:40 ratio of acidified MeOH to Milli-Q H_2O. Absorbance was read at 530 nm and 647 nm. Acidified MeOH was used as a blank and absorbances were corrected for volume (800 µl) and the blank absorbance was subtracted. As dry weight of the tissue was not recorded, this was calculated using the fresh and RWC weights. Anthocyanin concentrations were calculated as follows:

$$\text{Anthocyanin} = (A_{530} – (0.25 * A_{657}))$$

According to Rabino & Manchinelli (1986) this formula corrects for the absorption of 530 nm due to chlorophyll and its degradation products.

2.2.8. Cellular ultrastructure

To determine the changes in subcellular organisation upon desiccation and rehydration, TEM was utilised. Sections of approximately 4 mm^2 of leaf tissue, from three different plants at each RWC, were fixed and processed according to Cooper and Farrant (2002) with slight modifications. Briefly, tissues were fixed in 2.5% glutaraldehyde in 0.1 m phosphate buffer (pH 7.4) containing 0.5% caffeine and

then post-fixed in 1% osmium in phosphate buffer. After dehydration in a graded ethanol series, the tissues were immersed in a 50% Spurr's resin solution (1:1 ratio of acetone and room temperature Spurr's resin) and left at 4°C overnight. This step was repeated with a 75% resin solution, and again with an 87.5% resin solution (both kept at 4°C overnight). After incubation, the tissue was carefully placed in a resin block mould filled with 100% Spurr's resin. It was ensured that the samples were placed towards the tapered end of the block for sectioning and that the adaxial surface of the leaf blade faced upwards. Samples were labelled and baked at 60°C overnight. These were cross-sectioned using a microtome (Ultracut-S, Reichert, Germany) and stained with 2% uranyl for 10 minutes. This was repeated with 1% lead citrate (Reynolds 1963). Samples were viewed with a transmission electron microscope (FEI Tecnai T20 TEM).

External features of fully hydrated and desiccated leaves were examined using Scanning Electron Microscopy (*SEM).* Small sections (approximately 2–5 mm^2) of leaf tissue were placed on an SEM stub and visualised using a Phenom™ proX (Eindhoven, Netherlands). An elemental scan determined the dominant elements occurring on the leaf surfaces.

2.3. RESULTS AND INTERPRETATION

2.3.1. Time course of RWC

There was no difference in RWC between the NST and ST when fully hydrated (100% RWC, Figure 2.3). The dehydration curve illustrated in Figure 2.3 was performed on plants collected in the wild grown in their natural soil, which consists of course sand with high drainage properties. Dehydration curves from plants grown from seed under laboratory conditions had higher AWCs when fully hydrated (see Figure 2.2). This is likely due to the field-grown plants being genetically primed to harsher environments that have resulted in anatomical and physiological changes that enable a more efficient use of available water. Regardless of origin, upon drying plants maintained relatively high leaf water contents (~75% RWC) for nine days after water was withheld, and subsequently incurred rapid water loss that resulted in an airdry state by day 14. After a further two weeks in the airdry state, the NST recovered fully during rehydration, whereas the ST did not rehydrate and was dead (see the time-lapse referred to on page 18 for visualisation of the dehydration-rehydration process). Vander Willigen (2001b) observed an increase in electrolyte leakage in the ST by 40% RWC and confirms the inability of the ST to tolerate desiccation. The NST had a higher AWC by 48h post rehydration than hydrated leaves prior to dehydration. Both the NST and ST exhibited a similar rate of water loss (Figure 2.3).

This suggests that senescence is not induced by rapid water loss but is rather a regulated and selected response to drying. It is thus hypothesised that *E. nindensis* adopts a controlled and regulated senescence programme in response to drying.

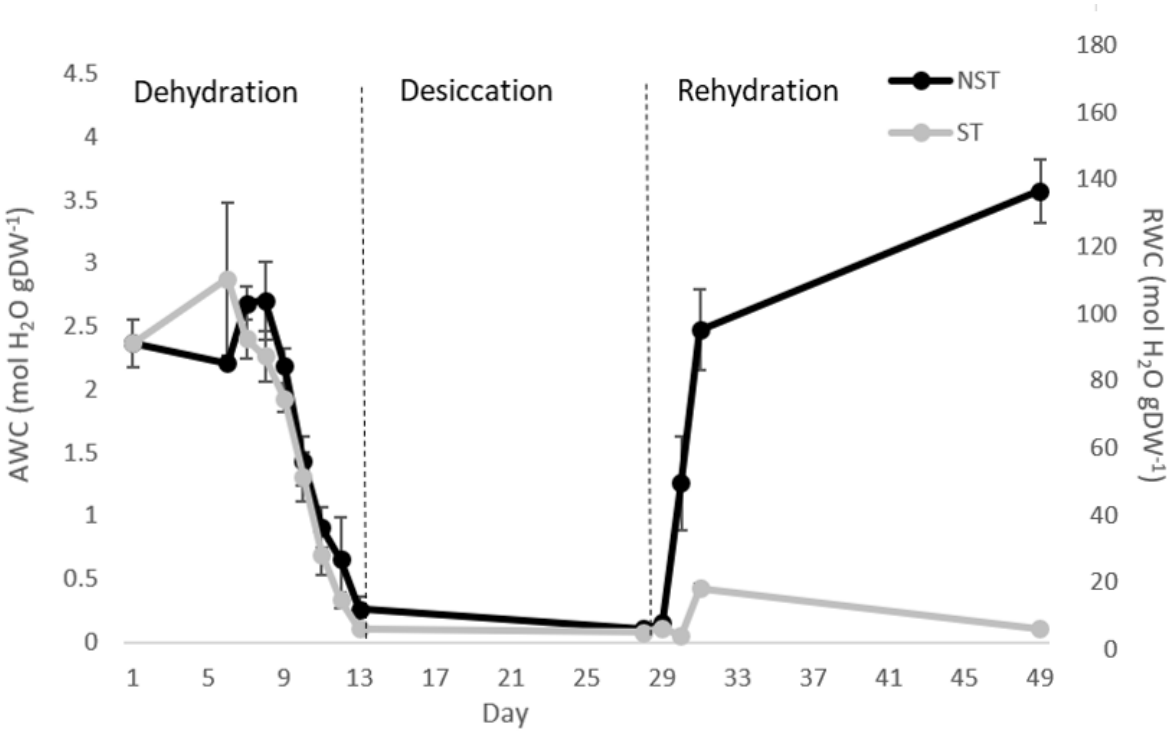

Figure 2.3: Changes in absolute water content (AWC) and relative water content (RWC) over time in the resurrection plant *Eragrostis nindensis* for desiccation tolerant, non-senescent tissue (NST) and desiccation sensitive, senescent tissue (ST) during water-deficit stress. Vertical bars represent standard errors.

2.3.2. Leaf morphology

There was a distinct change in leaf morphology during drying in both leaf types (Figure 2.4). At 100% RWC both the NST and ST appeared green and unfurled. Leaves began to initiate rolling as an early response to drying (around 75% RWC, data not shown), however, with progressive dehydration, the ST showed irregular rolling with sections of the leaf remaining unrolled. Differences in leaf morphology were most striking in the desiccated state. The ST had irregular leaf rolling and displayed a non-uniform morphology. The NST, however, remained tightly rolled and straight, and exhibited a more uniform morphology (see <5%, Figure 2.4). In contrast to *S. stapfianus*, where the NST and ST were distinguishable based on leaf colour (Gaff *et al.* 2009), it is the position on the tiller and the irregular shape that is a better indicator of tissue type in *E. nindensis*.

The biggest differences between the two tissue types were seen during rehydration. There was a stark contrast between the two tissue types, showing their survival and senescence. After 12h post-

watering, the NST swelled yet remained rolled and had a lighter straw-colour (Figure 2.4). Leaves returned to their morphological fully hydrated state within 72h, characterised as unrolled green leaves that had clearly survived desiccation. In contrast, the ST showed no change; leaves were irregularly rolled, the colour remained unchanged, and they did not recover during rehydration.

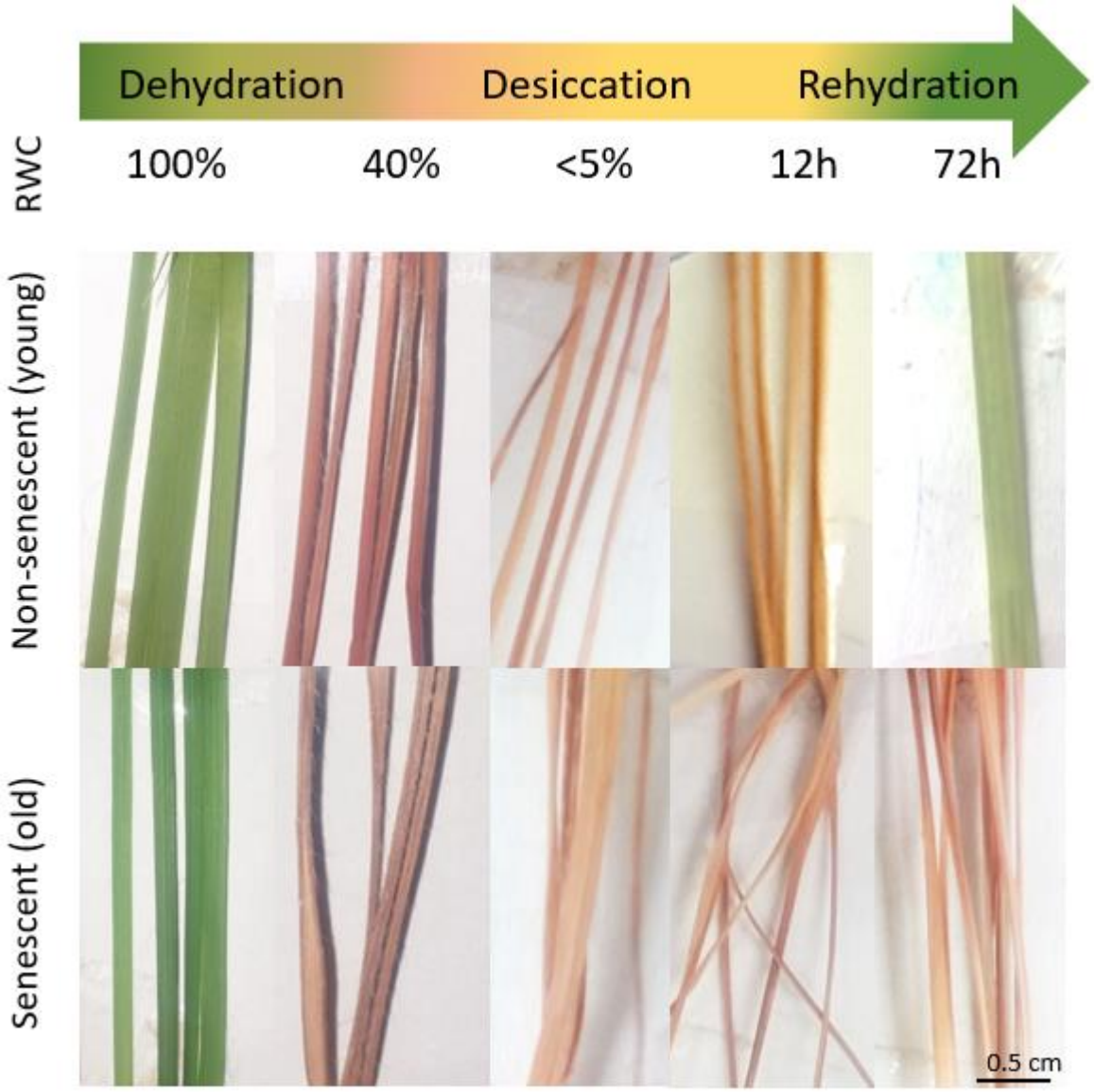

Figure 2.4: Leaf morphological changes between desiccation tolerant, non-senescent tissue (NST) and desiccation sensitive, senescent tissue (ST) upon dehydration (represented as relative water content RWC, %), desiccation (<5% RWC) and rehydration (12 and 72h). The colour in the arrow is a representative illustration of loss and regain of chlorophyll and anthocyanins in the NST. Scale bar is 0.5 cm and applies to all images.

The reduction in leaf area of NST upon desiccation and the corresponding degradation of chlorophyll can be clearly seen in Figure 2.5. SEM observations of leaf topology showed the presence of light-scattering hairs on the adaxial surfaces (Figure 2.5, C) and highly reflective silica bodies (Figure 2.5, D, E) that increased in abundance upon dehydration on the abaxial surface (Figure 2.5). Plants, especially

monocots, accumulate silicon from the soil, which is deposited as silica in the cell walls of leaves, stems and hulls (Yoshida 1965; Guo-chao *et al.* 2018). Silicon accumulation has been associated with increased abiotic and biotic resistance (Liu *et al.* 2014; Ma *et al.* 2006), as the mechanical-barrier minimises transpiration loss and is thought to mediate physiological, metabolic and biochemical pathways that result in increased drought resistance (Biju *et al.* 2017). For example, the silicon knockout mutant of rice had a 50% reduction in husk silicon concentration compared to the wild-type, which increased water loss (Yamaji *et al.* 2009). Silicon has been attributed to increased fungal pathogen resistance (Ma *et al.* 2006), can promote mechanical strength, plays a role in light scattering, and is required for optimal rice production (Guo-chao *et al.* 2018; Ma *et al.* 2006; Yamaji *et al.* 2009). The silicon-related mechanisms that mediate damage incurred under water-deficit stress include the reduction in transpiration rate through the maintenance of water content and controlled osmotic adjustments by regulating osmolytes and antioxidants (Biju *et al.* 2017). Furthermore, Hossain *et al.* (2018) demonstrated that silicon increased activity of antioxidant enzymes (catalases, peroxidases and superoxide dismutase) and reduced electrolyte leakage in wheat seedlings under arsenic stress. Silicon therefore increases membrane stability and antioxidant efficiency, traits that are beneficial during water-deficit stress.

There were no obvious differences in silica deposition between the tissue types in the hydrated or dehydrated state, although distribution analyses were not conducted. Representative SEM images of the NST are therefore displayed in Figure 2.5. The role of silicon as an effective strategy for improving drought resistance has been demonstrated in several crops e.g. maize, rice, wheat, sorghum and soybean (reviewed in Liu *et al.*, 2014). The accumulation and deposition of silica in *E. nindensis* has not been previously observed, and presumably increases the protection from UV-radiation damage by reflecting light, in conjunction with the abovementioned metabolic and physiological effects. This demonstrates the importance of reporting on the physiological changes at the whole-plant level, coupled with adjustments in transcript abundance and metabolism, to gain insights in the ability of *E. nindensis* to survive desiccation.

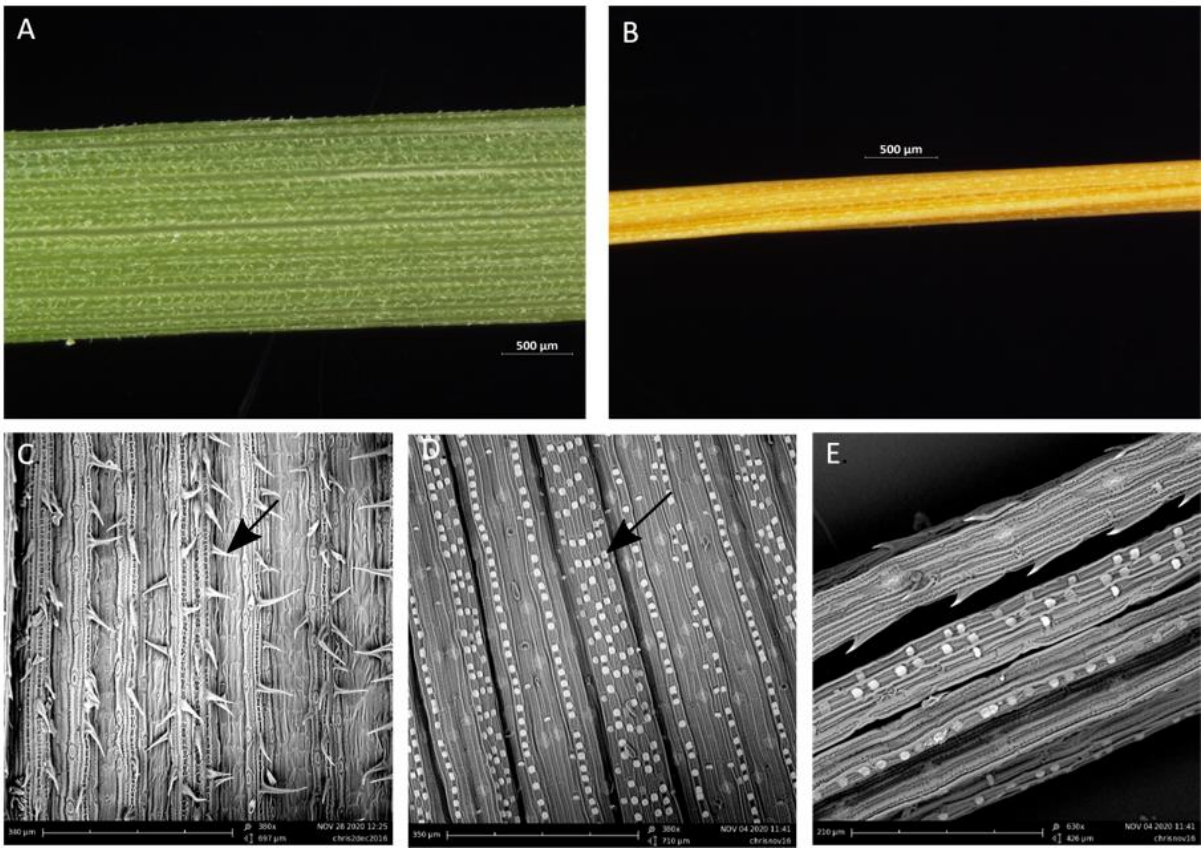

Figure 2.5: Scanning electron microscopy images of desiccation tolerant, non-senescent tissue (NST) of the resurrection plant *Eragrostis nindensis* during drying. (A) Hydrated adaxial leaf, and (B) desiccated chlorotic leaf tightly rolled exposing the abaxial surface. (C) Hydrated adaxial leaf displaying hairs (arrow). (D) Abaxial NST at moderate dehydration (~60% RWC) showing silica bodies (arrow) detected by elemental scan analysis. (E) Desiccated NST exhibiting tight rolling and the presence of reflective silica bodies.

E. nindensis has a leaf turnover typical of grasses. High leaf turn-over is uncommon amongst resurrection plants, where many species, such as *M. flabellifolia* and all *Xerophyta* species studied to date, retain their leaves. In *E. nindensis*, the oldest leaves show whole leaf senescence, whereas the tips of NST also exhibit senescence or 'tip-burning' (Figure 2.6, D, solid arrow), as reported in other resurrection plants, such as *S. stapfianus* (Martinelli 2008). Therefore, the tips of NST and whole ST do not survive rehydration and were not used in any assays. Interestingly, *E. nindensis* exhibits rapid growth post watering as seen by the increase in new biomass (Figure 2.6, D, dashed arrow).

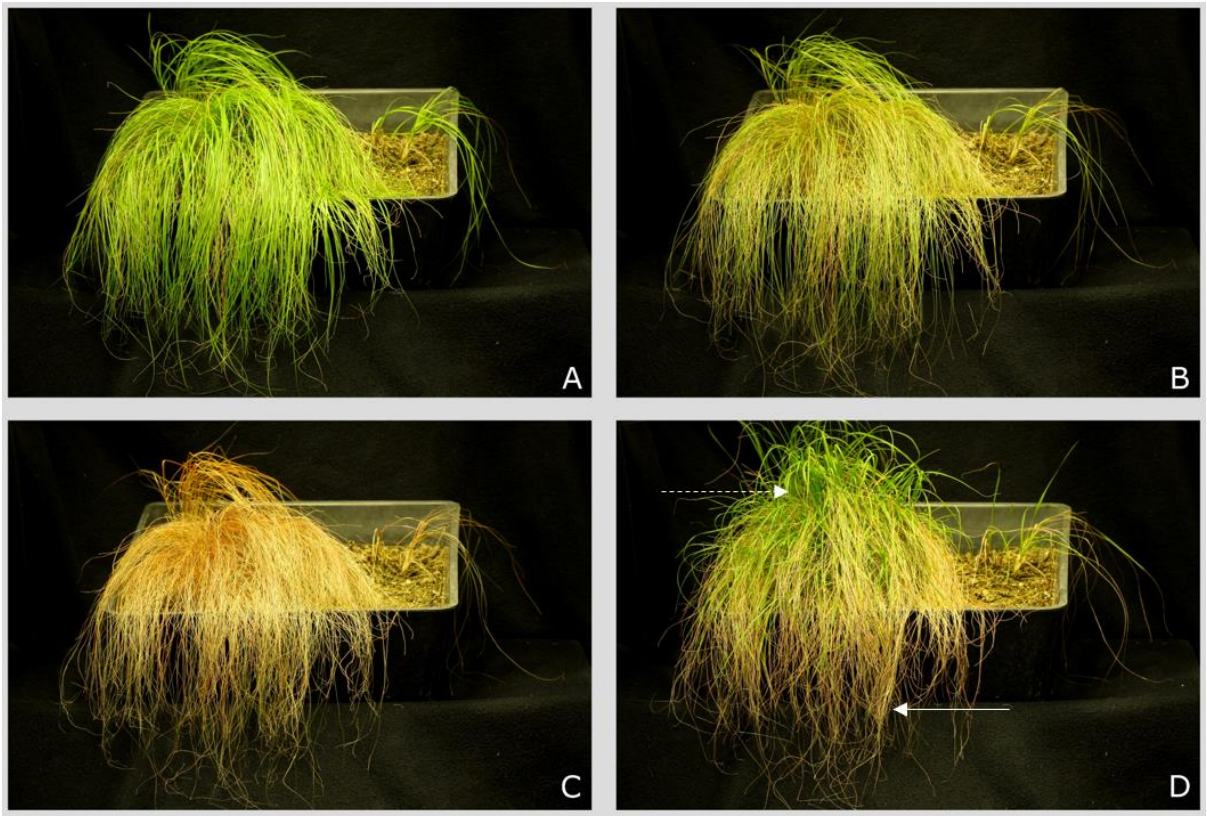

Figure 2.6: Key dehydration timepoints taken from the time-lapse of the resurrection plant *Eragrostis nindensis* during drying and rehydration. (A) Fully hydrated (100% relative water content, RWC, %), (B) ~50% RWC, (C) Airdry (desiccated, <10% RWC), (D) 72 hours post watering (rehydration). Solid arrow indicates tip burning (senescence) of non-senescent tissues. Note the whole-leaf senescing of older leaves. Dashed arrow highlights the rapid post-rehydration growth rate.

2.3.3. Gas exchange and chlorophyll fluorescence

As indicated elsewhere, photosynthesis is affected by water-deficit stress and is actively shutdown in resurrection plants. In *E. nindensis* the range of photosynthesis (CO_2 assimilation) at 100% RWC showed high variation in photosynthetic activity and efficiency between individual plants (Figure 2.7) but was not significantly different between the two leaf tissue types ($p = 0.244$). At 75% RWC, below which water-deficit stress becomes more severe, the mean rate of CO_2 assimilation had declined by 48% and 73% RWC in NST and ST, respectively. Photosynthesis in the ST was therefore more affected by water-loss than the NST. After this initial decrease in response to drying to 75% RWC, *E. nindensis* maintained photosynthesis at relatively stable photosynthetic rates until ~40% RWC, after which photosynthesis was not observed in either tissue type. Photosynthesis was initiated in the NST once the leaves had rehydrated to ~75% RWC (Figure 2.7), corresponding to ~72h post rehydration. This delay in photosynthetic resumption has been reported for several poikilochlorohyllous species and is attributed to the time needed to reconstitute the thylakoid membranes (Ginbot *et al.* 2011; Challabathula *et al.* 2016). The ST did not recover any photosynthetic capacity after rehydration.

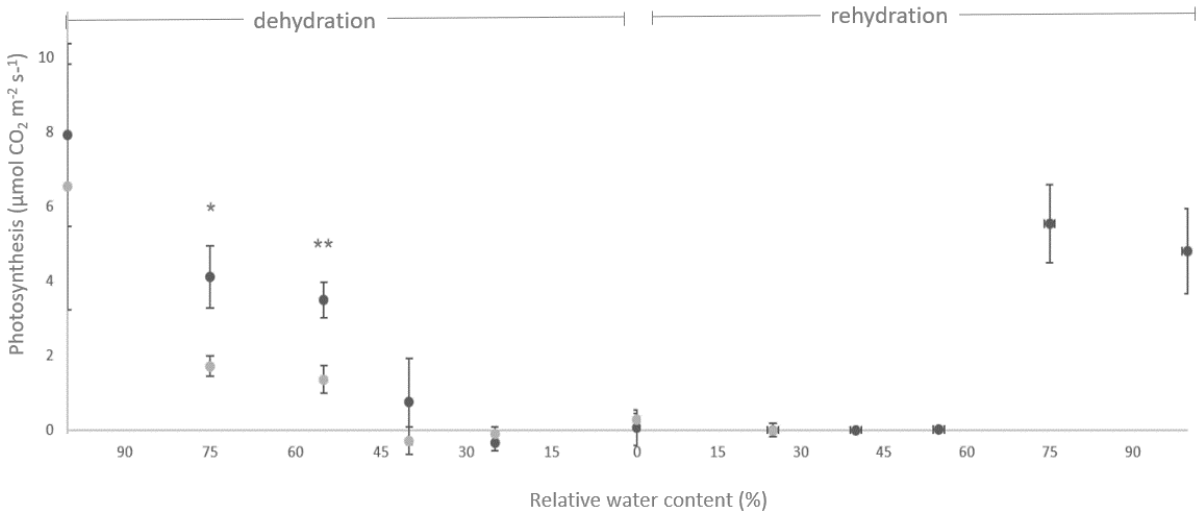

Figure 2.7: Photosynthetic carbon assimilation rates between desiccation tolerant, non-senescent tissue (NST, dark grey) and desiccation sensitive, senescent tissue (ST, light grey) of the resurrection plant *Eragrostis nindensis* upon severe water-deficit stress and recovery thereof (represented as relative water contents, RWC, %). The senescent tissue did not rehydrate beyond 20% RWC. Vertical bars represent standard errors. Student's t-test showed significance * ($p<0.05$, ** $p<0.01$).

ΦPSII indicates the proportion of light (photons) absorbed by PSII, which is used in photochemistry (Gently *et al.* 1989) and is therefore a measure of photosynthetic efficiency. The absorbed electrons require the thylakoid membranes and their photopigments to be intact to drive linear electron flow. NST maintained PSII efficiency until ~60% RWC, indicating that membrane integrity is preserved during the early stages of dehydration (Figure 2.8). In contrast, ΦPSII of ST declined by 75% - 60% RWC (Figure 2.8). Upon further drying to 25% RWC, PSII was deactivated in both tissue types, indicating the attenuation of electron flow across membranes. This is in accordance with the thylakoid membrane dismantling of the poikilochlorohyllous nature of *E. nindensis*. During rehydration, electron flow was resumed in NST around 75% RWC (~3 days), suggesting that thylakoid membranes were sufficiently reorganised to begin functional electron transport. ST did not recover ΦPSII upon rehydration, suggesting that thylakoid reassembly did not occur.

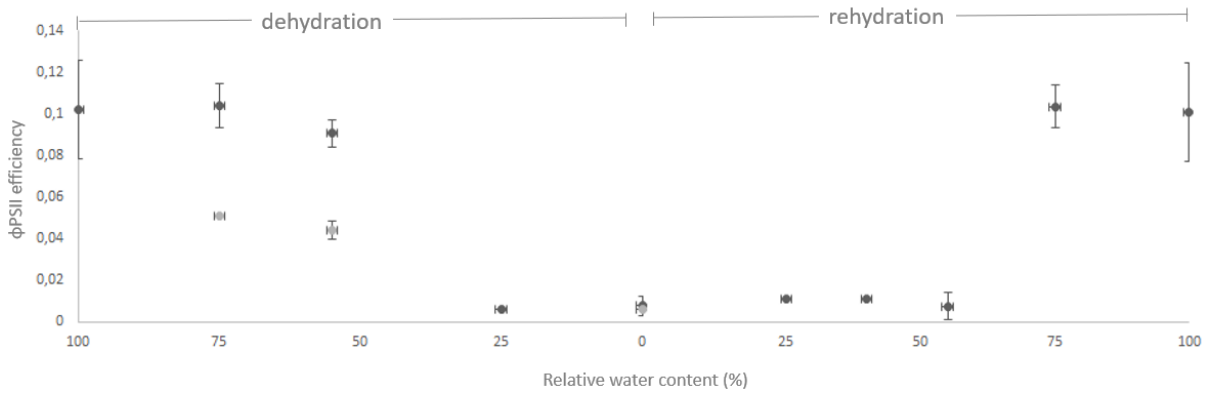

Figure 2.8: Maximum PSII efficiency (ΦPSII) between of desiccation tolerant, non-senescent tissue (NST, dark grey) and desiccation sensitive, senescent tissue (ST, light grey) of the resurrection plant *Eragrostis nindensis* upon severe water-deficit stress and recovery thereof (represented as relative water contents, RWC, %). The senescent tissue did not rehydrate beyond 20% RWC. Vertical bars represent standard errors.

Chlorophyll fluorescence (F_v/F_m) indicates the maximum quantum efficiency of PSII and is therefore an important indicator for physiological status. Since photosystems are major sites for ROS accumulation, PSII integrity is an important indicator for stress and is a good estimate of viability upon water-deficit stress (López-Pozo *et al.* 2019). The NST maintained healthy photosystems, indicated by relatively high F_v/F_m maintained until 50% RWC, and showed a slower decline in maximum quantum yield compared to the ST (Figure 2.9). The steady decline in F_v/F_m from 70% RWC in the ST showed a systematic shutdown of quantum efficiency and suggests that the ST responds earlier to stress. Photochemical activity ceased in the desiccated state in both tissue types, displaying desiccation-induced shutdown of electron flow. The variation in fluorescence observed in the desiccated state is a technical artefact of detecting such low fluorescence signals. This trend of relatively stable maximum efficiency of PSII continued until around 50% RWC, with a rapid decline by 20% RWC correlating with the shutdown of photosynthesis (Figure 2.7). The NST of *E. nindensis* showed recovery of the F_v/F_m to that of control plants once tissues reached 75% RWC, this correlates with all other photosynthetic measurements described above. After 75% RWC, photochemistry returned to that of control plants (100% RWC) and this correlated with the full return of gas exchange.

In summary, it is apparent that photosynthesis is slowed between water contents of 60-40% RWC but is shutdown thereafter in both tissue types. In addition, the efficiency of photosynthesis was lower in the ST than the NST.

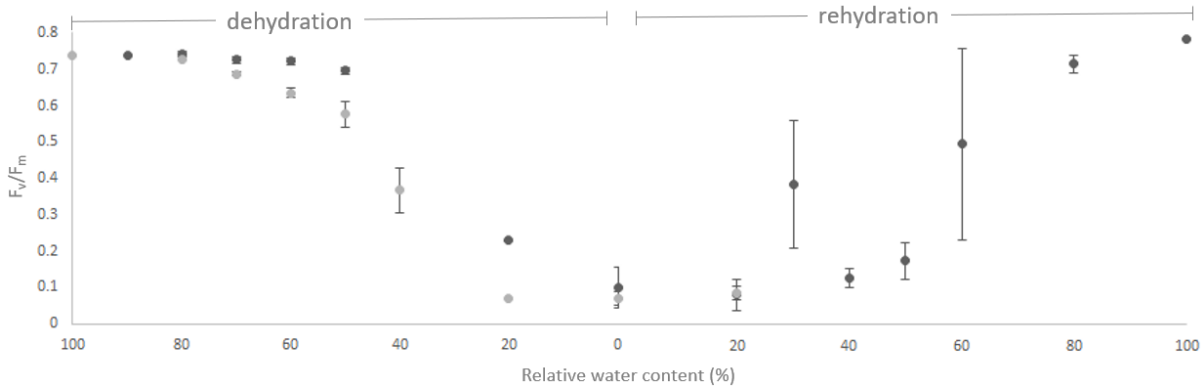

Figure 2.9: Maximum quantum efficiency of PSII (F_v/F_m) of desiccation tolerant, non-senescent tissue (NST, dark grey) and desiccation sensitive, senescent tissue (ST, light grey) of the resurrection plant *Eragrostis nindensis* upon severe water-deficit stress and recovery thereof (represented as relative water contents, RWC, %). The senescent tissue did not rehydrate beyond 20% RWC. Vertical bars represent standard errors.

Since *E. nindensis* displays poikilochlorophylly, it was anticipated that chlorophyll would decline during desiccation. Interestingly, the fully hydrated ST of *E. nindensis* had higher total chlorophyll content compared to the NST (Figure 2.10). Despite this, the rate of chlorophyll breakdown was much higher in the ST, where chlorophyll content at 75% RWC was a quarter of that in the NST. By 60% RWC, the NST had reduced chlorophyll contents by roughly 30% from 6.9 to 4.7 mg/ml/mgDW. There was a total loss of detectible chlorophyll at 40% RWC in both tissue types, correlating with the shutdown of photosynthetic parameters above. Chlorophyll contents remained unchanged in the desiccated state. During rehydration, the chlorophyll content was detectable at 40% RWC in the NST, with higher levels of chlorophyll a than b. This showed that the synthesis of chlorophyll precedes the initiation of photosynthesis (~75% RWC). The ST rapidly lost chlorophyll during drying and did not reassemble chlorophyll during rehydration.

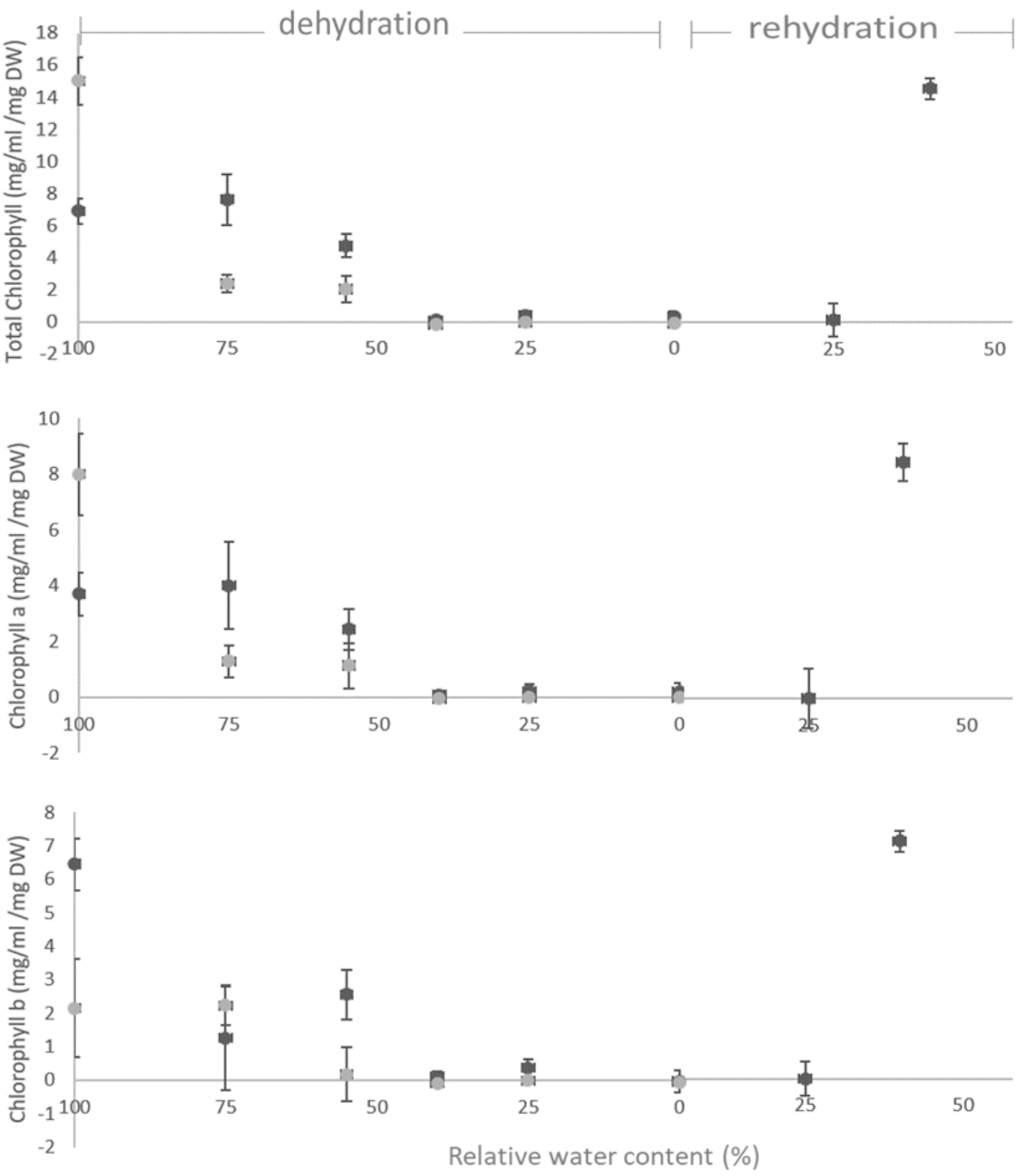

Figure 2.10: Chlorophyll contents of desiccation tolerant, non-senescent tissue (NST, dark grey) and desiccation sensitive, senescent tissue (ST, light grey) of the resurrection plant *Eragrostis nindensis* during drying and rehydration (represented as relative water contents, RWC, %). The senescent tissue did not rehydrate beyond 20% RWC. Vertical bars represent standard errors.

In addition to leaf curling and chlorophyll degradation, *E. nindensis* leaves accumulated anthocyanins in response to severe water-deficit stress in both tissue types (Figure 2.11). The rate of anthocyanin increase during drying was similar between the tissue types. The ST accumulated anthocyanins, especially at very low water contents. This is in contradiction to the trends found by Vander Willigen

et al. (2001b), were anthocyanins were only detected in the NST. This implies that anthocyanin accumulation is not a constitutive response to water-deficit stress, but rather determined by the environmental conditions and individual plant response. In support of this, anthocyanin accumulation in response to increased light stress due to chlorophyll degradation has been observed in developmental senescence, which increases flavonoid biosynthesis, such as anthocyanins (Buchanan-Wollaston *et al.* 2005).

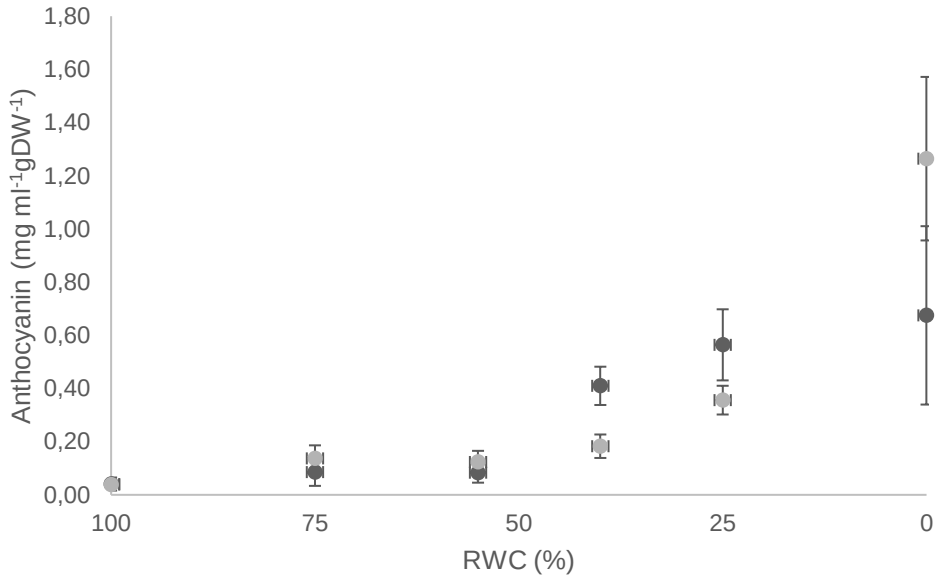

Figure 2.11: Anthocyanin content of desiccation tolerant, non-senescent tissue (NST, dark grey) and desiccation sensitive, senescent tissue (ST, light grey) of the resurrection plant *Eragrostis nindensis* upon severe water-deficit stress (represented as relative water contents, RWC, %). Vertical bars represent standard errors.

2.3.4. Cellular ultrastructure

2.3.4.1 Non-senescent tissue – bundle sheath cells

E. nindensis is a C4 grass and displays typical Kranz anatomy of having bundle sheath cells associated with vascular tissues, surrounded by palisade mesophyll cells (Vander Willigen *et al.* 2001b). Bundle sheath cells from fully hydrated leaves showed a typical centrifugal arrangement of starch filled chloroplasts with stacked grana (Figure 2.12, A). Being a C4 species, starch was only present in the bundle sheath cells. At moderate water-deficit stress (60% RWC), bundle sheath cells maintained their fully hydrated shape, with chloroplasts arranged proximal to the vascular bundles (Figure 2.12, B). Chloroplasts were surrounded by mitochondria, however, there was a noticeable depletion in starch, albeit still present. There was an increase in ordered vacuolation and the thylakoid membranes remained intact. A few small, regularly sized osmophilic bodies, which were confirmed as lipid droplets (LDs) (see **Chapter 5)**, began accumulating along the plasma membrane on the periphery of the bundle

sheath cell walls. By 40% RWC the chloroplasts showed less tight congregation near the vascular bundles and appeared more spread out, occupying most of the cellular space along with fragmenting vacuoles (Figure 2.12, C). Large osmophilic bodies, potentially polyphenols or enlarged LDs, accumulated amongst the starch-containing chloroplasts at around 40% RWC, but were less frequently observed at lower water contents. These bodies are structurally different to the smaller LDs observed at the cells' periphery and are potentially the breakdown products of thylakoid membranes, which result in excess fatty acids. Photosynthesis shut down below 40% RWC and the concurrent accumulation of large LDs is likely as a result of the temporary storage of thylakoid lipids, however, this needs to be confirmed. Starch and lipid biosynthesis are competing pathways, with starch dominating over lipid synthesis unless carbon supply exceeds the uptake capacity of starch synthesis (Fan *et al.* 2012). The flow of carbon towards lipids as a complex storage reserve coincides with the reduction in photosynthetic carbon assimilation by 40% RWC (Figure 2.7), thus suggesting that when photosynthesis is shutdown, excess lipids form lipid bodies. The accumulation of lipids appeared to coincide with a decrease in starch and could indicate that the dominant complex reserve source switched from starch to lipids during drying. *E. nindensis* contains comparatively lower concentrations of phenols (10.5 mg GAE/gDW) compared to other resurrection plants, such as *M. flabellifolia* (247.1 mg GAE/gDW), *X. viscosa* (39.6 mg GAE/gDW) and *X. schlechteri* (45.8 mg GAE/gDW), indicating that phenol accumulation is not the chief strategy to mitigate water-deficit induced damage (Farrant *et al.* 2007; Tuba *et al.* 2011).

Under severe water-deficit stress (25% RWC) the bundle sheath cells of the NST dramatically deviated from their fully hydrated ultrastructure (Figure 2.12, D). The cell was dominated by tightly packed vesicles and dismantled, yet intact, organelles. Chloroplasts showed complete thylakoid disassembly, characterised by the presence of thylakoid vesicles and clustered plastoglobuli. Interestingly, starch was still present, although the lack of the "halo" indicates no metabolic activity. The starch is potentially an early energy source upon rehydration. LDs seen at 40% RWC remained accumulated at large densities along the cell wall and congregated around the plasmodesmata (Figure 2.12). The plasmalemma was clearly intact and well preserved, and the congregation on both sides of the plasmodesmata by LDs suggests that this cell is actively communicating with neighbouring cells or has the potential to do so. The significance of these LDs and the plasmodesmata is discussed in **Chapter 5**.

In the desiccated state (<5% RWC) chloroplasts remained disassembled as seen in 25% RWC, indicating that by 25% RWC the reorganisation of ultrastructure required for the desiccated state has mostly been achieved. Despite the critically low water content, the cytoplasm was well preserved with intact endoplasmic reticulum (ER), plastoglobuli, electron dense cytosol and distinct (unfused) vacuoles

(Figure 2.12, E). Chloroplasts from bundle sheath cells regularly contained starch molecules accumulated near the vascular bundle. Small clusters of dense matter in the cytoplasm (Figure 2.12, E) looked similar to what Tymms *et al.* (1982) described as polyribosomes. The authors stated that protein synthesis occurs during early rehydration, and the presence of dense polyribosomes near the ER could be an indication that the NST is prepared for protein synthesis during rehydration, however, this needs to be confirmed. During rehydration, bundle sheath cells resembled their fully hydrated state within 12h (Figure 2.12, F). Vacuoles had mostly coalesced and LDs previously dominating the cell walls were no longer present. Chloroplasts showed signs of thylakoid membrane assembly. Again, starch showed an interesting trend, as some bundle sheath cells contained large starch molecules apparently being actively metabolised (halo present). The hydrated starch is likely an early energy source for recovery of metabolism since photosynthesis has not yet reactivated by 12h. In addition, the disappearance of LDs correlated with thylakoid reassembly and suggests that they are potentially involved in membrane repair along with energy storage during rehydration (see **Chapter 5**).

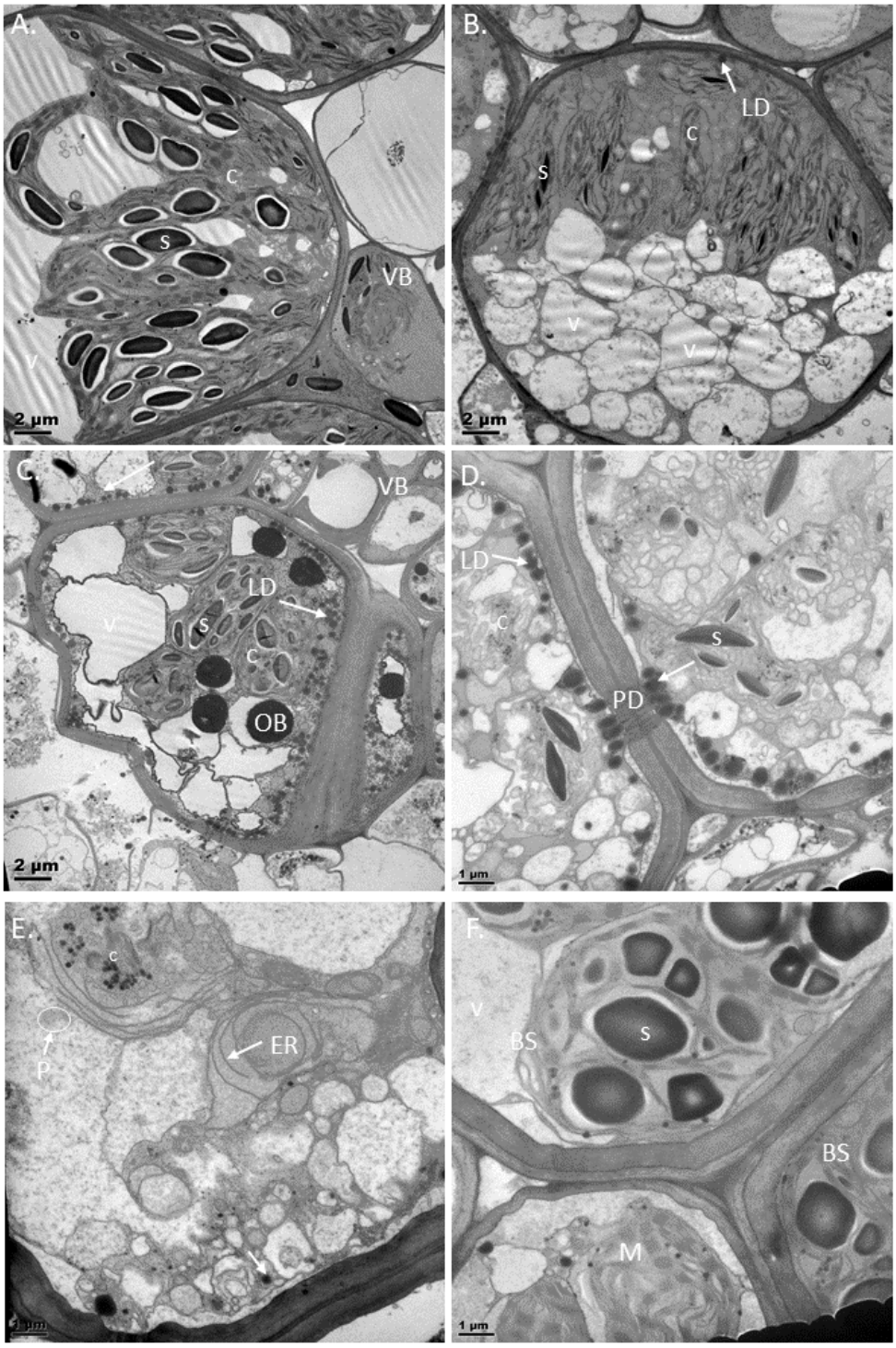

Figure 2.12: Transmission electron microscopy of the bundle sheath (BS) cells of desiccation tolerant, non-senescent tissue (NST) of the resurrection plant *Eragrostis nindensis* during drying (represented as relative water contents, RWC, %) and rehydration (12h). (A) when fully hydrated (100% RWC), chloroplasts (c) were fully formed and were actively photosynthesising and producing starch (s). (B) at 60% RWC vacuoles (v) become fragmented and lipid droplets (LDs) accumulated at low densities around the plasmalemma (arrow). (C) at 40% RWC the bundle sheath cells reduced in size but maintained their shape. Large osmophilic bodies (OB) appeared and small LDs accumulated along the cell wall (arrow). (D) at 25% RWC, chloroplasts were dismantled but cell communication was intact via preserved plasmodesmata (PD). The accumulation of the LDs was a distinctive feature. (E) at the desiccated state (<5% RWC) darkly stained clusters not dissimilar to polyribosomes (p) were present. (F) after 12h of rehydration chloroplasts were mostly reassembled and starch molecules were present. M = mesophyll cell.

2.3.4.2 Non-senescent tissue – mesophyll cells

The mesophyll cells in the NST showed gradual but complete degradation of thylakoid membranes within chloroplasts from fully hydrated to <10% RWC. By 60% RWC, chloroplasts appeared swollen and thylakoids were being dismantled and contained plastoglobuli (Figure 2.13, B). Cell walls showed some compression and cellular debris and vesicles were present. At 40% RWC, mesophyll cells underwent cell wall folding reducing mechanical injury, whereas the bundle sheath cells did not (Figure 2.13, C). At this water content, thylakoids were completely dismantled and contained numerous plastoglobuli. Some peripheral osmophilic bodies, possibly small LDs, were present, but at very low densities compared to bundle sheath cells at the same water content. Where visualised, the nucleus containing darkly-stained nucleoli-like bodies (arrowed, Figure 2.13, C), which could indicate densely stacked, untranslated RNA, possibly for translation during rehydration as seen in *X. humilis* (Dace *et al.* 1998; Luo *et al.* 2018b). Mesophyll cells had a reduced volume (due to cell wall folding) and showed some vacuolation, but not to the extent of the bundle sheath cells. Cell-to-cell communication via plasmodesmata that appeared to be intact was evident at 25% RWC (Figure 2.13, D) much like in the bundle sheath cells. Desiccated mesophyll cells showed a high degree of cell wall folding but did not show signs of plasmalemma rupturing (Figure 2.13, E). After 12h rehydration the mesophyll cells had regained cell volume and the thylakoids had reformed (Figure 2.13, F).

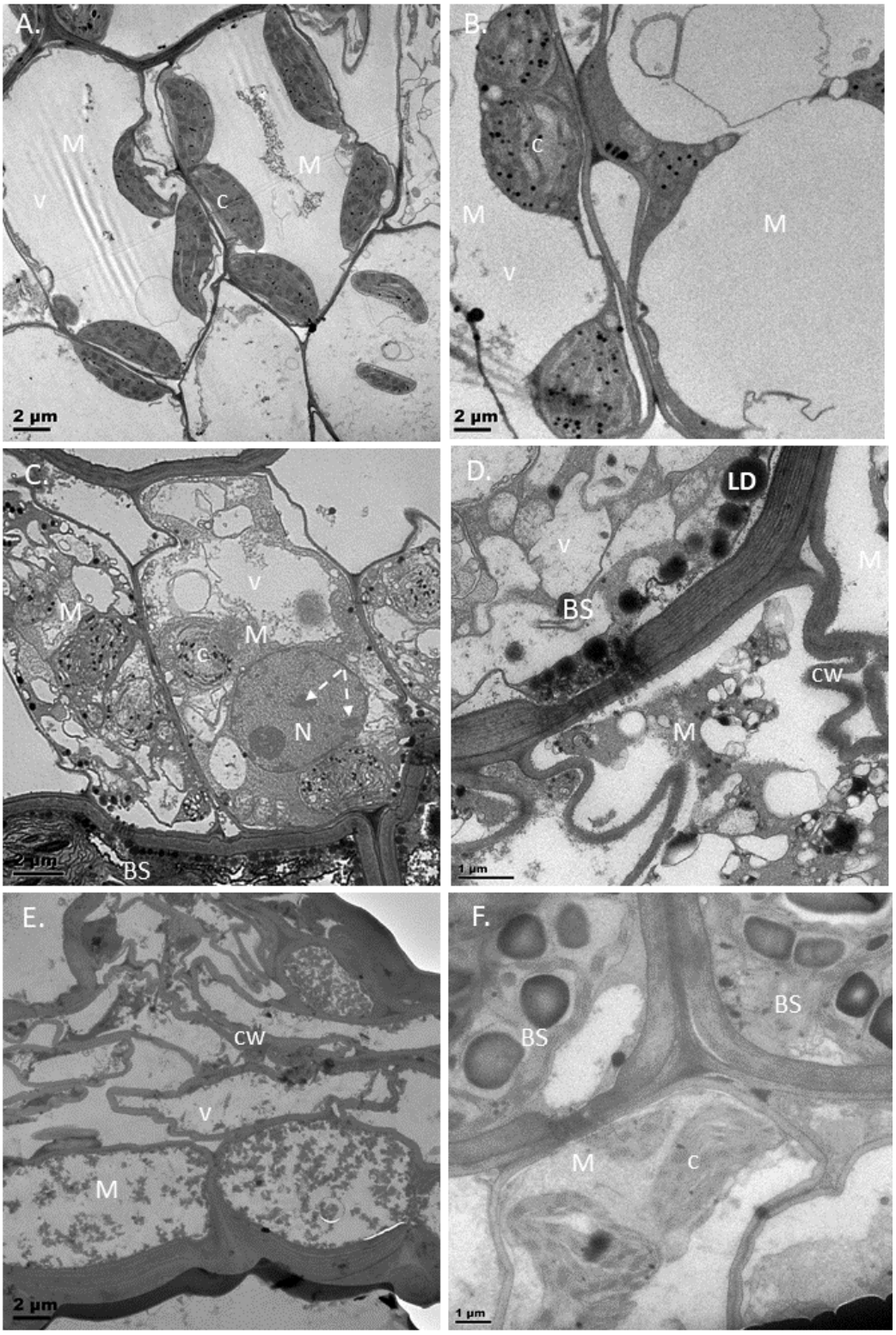

Figure 2.13: Transmission electron microscopy of the mesophyll (M) cells of desiccation tolerant, non-senescent tissue (NST) of the resurrection plant *Eragrostis nindensis* during drying (represented as relative water contents, RWC, %) and rehydration (12h). (A) when fully hydrated (100%), chloroplasts (c) were arranged along the cell wall. (B) at 60% RWC chloroplasts appeared swollen and plastoglobuli appeared (dark circles within chloroplasts). (C) at 40% RWC the mesophyll cells reduced in size, vacuoles (v) became fragmented, thylakoids were disassembled and the nucleus (N) showed nulcleoli-like bodies (dashed arrows). (D) at 25% RWC no chloroplasts were distinguishable and cell walls (cw) were folded. (E) at the desiccated state (<5% RWC) mesophyll cells were compressed but cell membranes remained intact. (F) after 12h of rehydration, thylakoids in the mesophyll cell (M, bottom) were mostly reassembled and cell volume reached fully hydrated size. BS = bundle sheath cell.

2.3.4.3 Senescent tissue – bundle sheath cells

There were distinct ultrastructural differences between the tissue types upon water-deficit stress, with the most predominant being the visible deterioration of cellular organisation and architecture during drying below 25% RWC in the ST (Figure 2.14). Like the NST, fully hydrated leaves had chloroplasts with distinguishable thylakoid membranes dominated with starch (Figure 2.14, A). During drying to 60% RWC, the ST was characterised by large starch-filled chloroplasts. Although the chloroplasts have a more amyloplast appearance due to the absence of distinguishable thylakoid membranes, the cells were actively photosynthesising (Figure 2.7) and were clearly producing starch (Figure 2.14, B), illustrating their function as source tissues. Mitochondria with densely stained cristae, indicative of active respiration, clustered around the chloroplasts (Figure 2.14, F). There were no organised vacuole-like structures as seen in the NST. Large osmophilic bodies had accumulated, often in somewhat electron-opaque structures between chloroplasts. The bundle sheath cells at 25% RWC were characterised by the continued presence of large, irregularly sized osmophilic bodies, with a notable absence of small LDs surrounding the cell wall as observed in the NST (Figure 2.14, C). This prompted the hypothesis that the osmophilic bodies in the ST lack oleosin, a protein regulating the size of LDs (Siloto *et al.* 2006), explored further in **Chapter 5.** The ST produced starch and large osmophilic bodies, however, it failed to lay down protective mechanisms, such as vacuolation, or peripheral LDs as in the NST. The subcellular organisation of bundle sheath cells at this RWC showed little sign of plasmalemma withdrawal from the cell walls, despite the aqueous fixation, which exacerbates this in desiccated tissue (Wesley-Smith 2001), suggesting some degree of mechanical stabilisation in these tissues. However, in the desiccated state the bundle sheath cells showed major signs of subcellular attrition (Figure 2.14, D). No distinguishable organelles were present and cell-to-cell communication was compromised. Large circular lipid-like bodies, although not as darkly staining as in other images, were present in some cells. Where remaining cellular debris was visualised, this appeared clumped and in places was darkly stained, indicating potential polyphenols or cell debris (Figure 2.14, E). The disappearance of most osmophilic bodies (possibly lipid) in the desiccated state could indicate potential transportation to sink tissues, making the ST functional more like classical senescence, however, this can only be confirmed through trace studies beyond the scope of this thesis. The bundle sheath cells showed compression upon lack of water and even the characteristically thick cell walls were folded, which is not observed in the NST, indicating mechanical injury. During rehydration, the cells collapsed further, showed no distinguishable organelles, and showed no signs of recovery (Figure 2.14, E.). The bundle sheath cells of the ST did not survive rehydration.

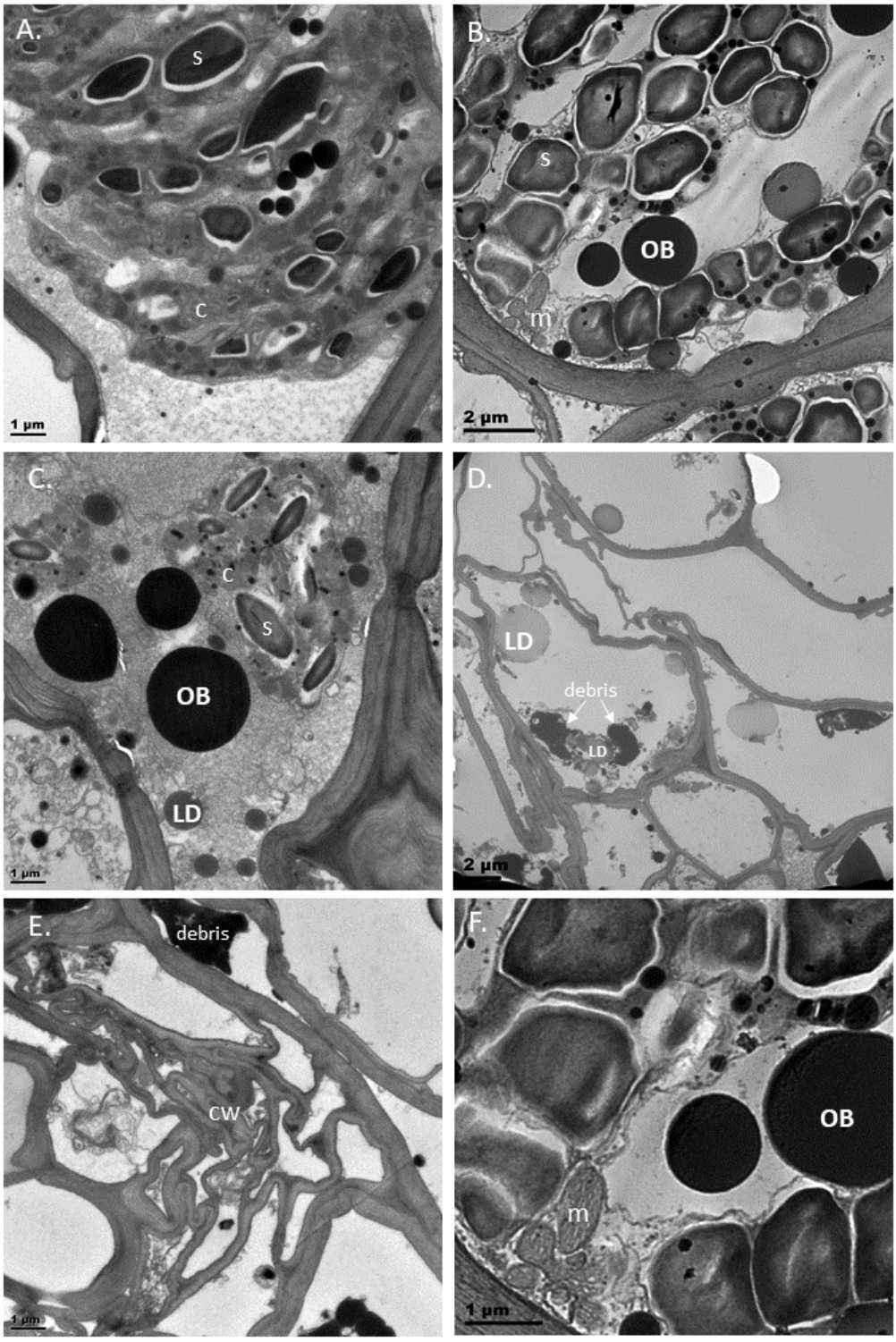

Figure 2.14: Transmission electron microscopy of the bundle sheath cells of desiccation sensitive, senescent tissue (ST) of the resurrection plant *Eragrostis nindensis* during drying (represented as relative water contents, RWC, %) and rehydration (12h) (A) when fully hydrated (100% RWC), chloroplasts (c) are fully formed and were actively photosynthesising and produced starch (s). (B) at 60% RWC, chloroplasts were indistinguishable and large starch grains, lipid droplets (LD) and osmophilic bodies (OB) accumulated, which were surrounded by mitochondria (m) that appeared to be active. (C) at 25% RWC chloroplasts were dismantled, starch was reduced, but still present, and large osmophilic bodies appeared alongside dispersed and infrequent lipid droplets. (D) at the desiccated state (<5% RWC) cell walls (cw) are collapsed and large lipid droplets and cell debris was evident. (E) after 12 hours of rehydration bundle sheath cell walls had collapsed and cells did not recover. (F) a magnified view of (B) detailing the mitochondria and the size of OB and starch.

2.3.4.4 Senescent tissue – mesophyll cells

The mesophyll cells of the ST were similar in ultrastructure compared to the NST mesophyll cells at 100% RWC (Figure 2.15, A). At 60% RWC the plasmalemma had withdrawn from the cell wall, yet remained intact, surrounding the chloroplasts containing dismantled thylakoids and enlarged plastoglobuli (Figure 2.15, B and F). This correlated with the low gas exchange measurements in the ST (Figure 2.7 – 2.9). Nevertheless, the similarities between tissue types at 60% RWC disappeared by 25% RWC, where considerable cytoplasmic dissolution and plasmalemma rupture was evident (Figure 2.15, C, double arrow). Thereafter, in the desiccated state (Figure 2.15, D), the mesophyll cells appeared dead; membranes were torn, no distinguishable organelles were present and there was no evidence of a controlled disassembly of chloroplasts. Cell debris and some remaining osmophilic bodies remained. Interestingly, senescence is not a spatially uniform process and occurs in local patches before spreading to neighbouring cells (Lim *et al.* 2007). It is therefore the overall ratio of healthy to damaged cells within a leaf that determines the survival of the leaf. Mesophyll cells collapsed during rehydration and showed a striking difference to their NST counterparts (Figure 2.15, E).

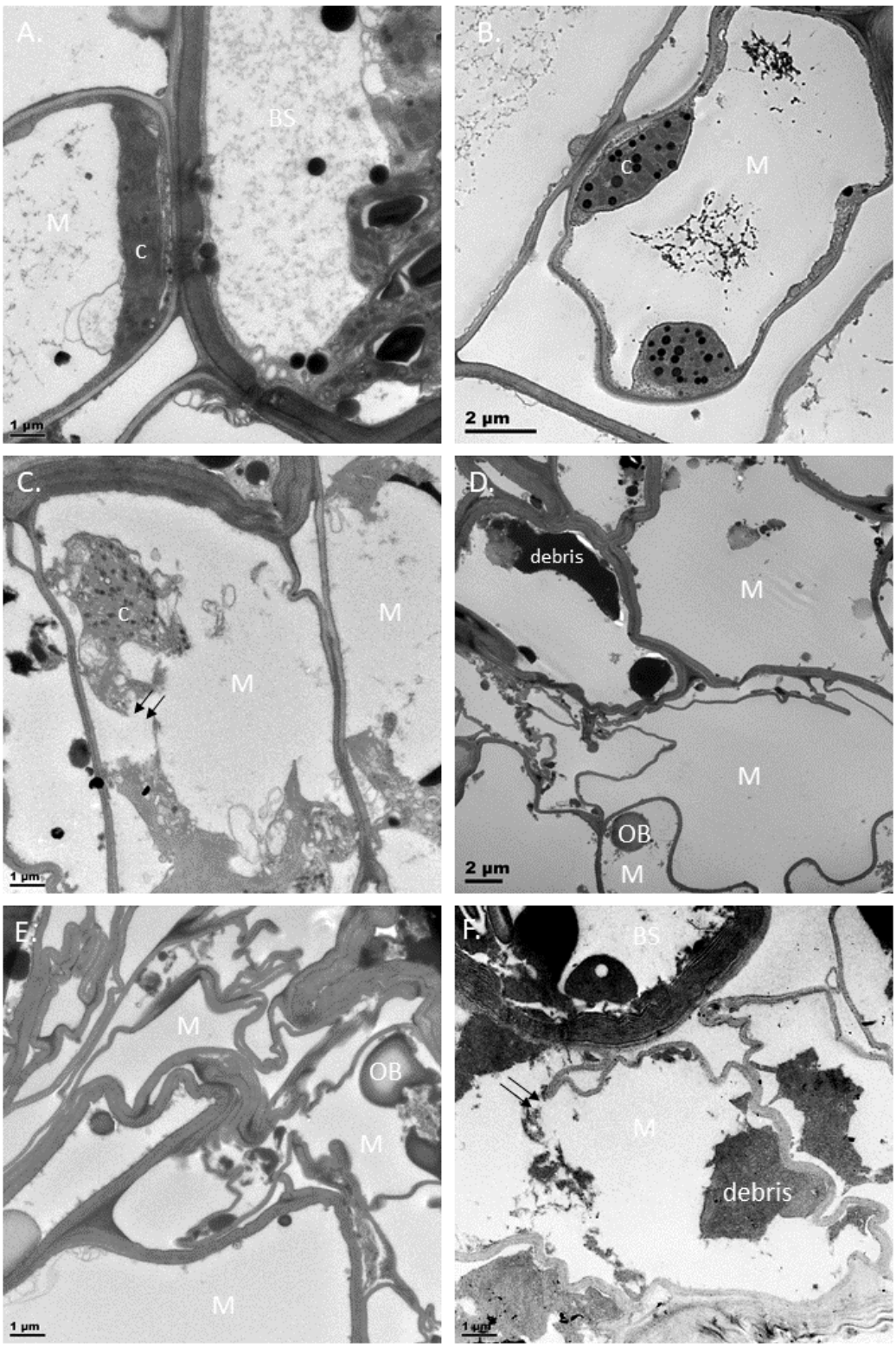

Figure 2.15: Transmission electron microscopy of the mesophyll (M) cells of desiccation sensitive, senescent tissue (ST) of the resurrection plant *Eragrostis nindensis* during drying (represented as relative water contents, RWC, %) and rehydration (12h) (A) when fully hydrated (100% RWC), chloroplasts (c) were fully formed and aligned against the cell wall. (B) by 60% RWC the plasmalemma had withdrawn and enlarged plastoglobuli appeared. (C) at 25% RWC cellular disorganisation and plasmalemma rupturing (double arrow) became apparent. (D) in the desiccated state (<5% RWC) only osmophilic bodies (OB) remained recognisable and cell walls (cw) were extensively folded. (E) after 12h rehydration no recognisable organelles existed apart from some osmophilic bodies. Cell walls were collapsed. (F) in the desiccated state (<5% RWC) plasmalemma rupturing was evident (double arrow). BS = bundle sheath cell.

2.4. GENERAL DISCUSSION AND CONCLUSION

The purpose of this **Chapter** was to physiologically characterise the differences between the NST and the ST in *E. nindensis* under different RWCs. The data showed that in the fully hydrated state, both the NST and the ST behave similarly in terms of photosynthetic efficiency (Figure 2.7, Figure 2.9, Figure 2.10, Figure 2.3) and leaf ultrastructure (Figure 2.12 – 2.15). Yet, differences arose in these parameters during drying, suggesting differences in the regulation of metabolic activity in these tissue types. This could be a consequence of a lack of induction of desiccation tolerance mechanisms in the ST, ultimately causing death and uncontrolled senescence of this tissue. Alternatively, this could be a deliberate induction of senescence in the more mature tissues of this species, which in turn could provide energy to surviving (NST) tissues for early recovery before photosynthetic efficiency is restored.

During drying, the reduction in surface area (leaf rolling) and increased UV-radiation reflection (silica, hairs) occurred in both tissue types, indicating that these morphological responses are constitutive and therefore independent of tissue type. However, drying below 40% RWC resulted in inadequate rolling of some of the ST leaves (Figure 2.4), which could have resulted in light and photosynthetic stress at lower water contents.

The rate of drying has been proposed to be an important factor in determining the desiccation tolerance in angiosperm resurrection plants, where the induction of protection mechanisms during dehydration is crucial for their survival (Gaff *et al.* 1976; Farrant *et al.* 1999; Griffiths *et al.* 2014). There was no difference in the drying rate between tissue types (Figure 2.3), which precludes the suggestion that insufficient protection might have been laid down in the ST. However, inadequate protection of the photosynthetic apparatus (regardless of the drying rate) could affect viability. Griffiths *et al.* (2014) have proposed that regulation of desiccation-induced senescence is determined by the rate of drying and the age of leaf tissues. If the rate of drying is high, cell death will also occur as there is insufficient time for metabolic re-programming and cellular processes to combat severe water stress. The similar rate of drying suggests that the rate of water loss is a controlled process, and that drying itself does not induce senescence in the ST, but rather the regulated changes in transcript abundance and resulting metabolic and physiological changes determine which tissues are destined for senescence.

The cessation of photosynthesis during drying is a desiccation tolerance trait, regardless of whether plants retain chlorophyll (homoiochlorophyllous) or not (poikilochlorophyllous) (Farrant *et al.* 2017). Both tissue types show a controlled reorganisation of the subcellular structure upon moderate water-deficit stress (60% RWC), which is potentially a general response to drought. Whether this

reorganisation is in response to the initiation of senescence or desiccation tolerance, is unconfirmed, as decoupling senescence from desiccation tolerance is difficult. Indeed, the shift from stacked grana to thylakoid disassembly and the corresponding formation of plastoglobuli is both a poikilochlorophyllous and senescence trait (Lim *et al.* 2007; Charuvi *et al.* 2019), however, the outcomes of such processes are very different (survival vs death). This is evident as only the NST copes with further drying, as seen by a higher F_v/F_m (Figure 2.9), showing a general protection of membrane integrity, coupled with ordered subcellular ultrastructure (Figure 2.12 – 2.15). Although quantum efficiency of PSII remains largely uncompromised until around 60% RWC in the NST (Figure 2.8), photosynthesis is reduced (Figure 2.7). This suggests that electron transfer is possible, but that the amount of light absorbance has been reduced, as seen in changes in the leaf morphology (Figure 2.4). The ST experienced stress earlier and to a greater degree than NST, showing a steeper decrease in photosynthetic and maximum quantum efficiency (thus indicating compromised membrane integrity), and failed to develop mechanical stabilisation to the extent of the NST, as seen by the lack of vacuolation (Figure 2.14). The lack of TIP3;1 expression in the ST (Vander Willigen *et al.* 2004) also suggests the failure of the ST to accumulate solutes into the vacuoles during drying, thereby incurring mechanical stress. By 75% RWC, the ST had severely compromised photosynthesis, and the observed lack of stacked thylakoid membranes at 60% RWC and low chlorophyll contents support this notion (Figure 2.14, B). Photosynthesis is therefore reduced during desiccation in *E. nindensis,* losing efficiency at 75% RWC (more so in the ST) and is completely shut down by 40% RWC in both tissue types.

One of the strongest patterns emerging from the ultrastructural study was the accumulation of small, regular LDs surrounding the bundle sheath cell walls exclusively in the NST (Figure 2.12, D and 2.13, D). LDs were more apparent in the bundle sheath cells presumably due to these cells being the sites of carbon fixation and are therefore sites of carbon and lipid biogenesis and storage, which can provide energy upon rehydration and repair membranes (Deruyffelaere *et al.* 2015; Juergens *et al.* 2016; Pyc *et al.* 2017). Furthermore, due to the lack of cell wall folding these cells require mechanical stabilisation, which the LDs partially provide, including stabilising plasmodesmata to maintain cell-to-cell communication (see **Chapter 5**, Hoekstra *et al.* 2001; Pintó-Marijuan *et al.* 2014; Seiwert *et al.* 2017). The ST had increased starch content at higher water contents, followed by the accumulation of osmophilic bodies during drying (Figure 2.14). It is possible that the osmophilic bodies in the ST are LDs that are enlarge due to the lack of oleosin, which is discussed in **Chapter 5**, and are referred to further as enlarged LDs for clarification. After 25% RWC these enlarged LDs became less prominent, potentially as a result of the cessation of lipid production due to metabolic arrest or as a result of being exported to sink tissues. Regardless, the enlarged LDs in the ST were starkly different to the small LDs

in the NST. The ability of the NST to resynthesise lipids and proteins is largely dependent on functional endoplasmic reticulum (ER) organelles (Williams *et al.* 2014; Eichmann *et al.* 2012). The ER also acts as a molecule transporter to and through the plasmodesmata and thus plays a critical role in cell communication (Wright *et al.* 2006). In the NST, the ER was well-preserved, along with other key organelles, and showed tight reorganisation upon desiccation and recovery therefrom. In addition, the increase in larger lipid bodies, coupled with the simultaneous preservation of starch granules, reflects the high energy status of the cell. This might explain the lack of observed autophagy-related vesicles. The breakdown of chlorophyll and the accumulation of complex reserves (both starch and lipids) from broken-down membranes could lessen the need for nutrient redistribution through autophagy (Avila-Ospina *et al.* 2014; Asami *et al.* 2018). *E. nindensis* therefore appears to opt towards the synthesis of high-energy complex reserves in the form of lipids during drying. Desiccation tolerance is energetically expensive and the efficient use of complex reserves during drying is critical (Paul *et al.* 2018). However, the role of these lipid bodies as an energy source does not appear to be the sole function. The ordered distribution of these small LDs around the cell wall during drying, especially at 25% RWC (Figure 2.12, D and 2.13, D), and their congregation around the plasmodesmata, suggests a more prominent role. Plasmodesmata are intercellular pores, connecting distant regions of the plant through which nutrients (sugars, amino acids), macromolecules (proteins), mRNAs (including transcription factors) and hormones (including important signalling hormones like ABA) are transported (Lough *et al.* 2006; Thieme *et al.* 2015). Therefore, these lipid bodies likely have a membrane stabilising, trafficking or repairing role, which is exclusively observed in the NST. The distinct absence of these lipid bodies in the ST highlights the importance of these subcellular structures in conveying desiccation tolerance. This observation was intriguing and resulted in an in-depth look into the lipid composition changes during drying and rehydration in *E. nindensis* and is discussed further in **Chapter 5**.

Upon rehydration the differences in the tissue types become obvious, where the NST showed drastic reorganisation towards recovery within 12h. Physiological changes upon rehydration were quicker than during drying (72h vs 10 days) in *S. stapfianus* as noted by Blomstedt *et al.* (2018). In the bundle sheath cells of the NST chloroplasts appear almost fully formed and large, swollen starch grains appear. This starch is most likely from stored reserves, not photosynthetically synthesised, as photosynthesis only resumes after ~72h. This drastic change strongly coincided with the disappearance of small LDs and indicates the role of these LDs functioning as high-energy sources for repair upon rehydration.

In conclusion, it is difficult to differentiate between the induction of desiccation tolerance and the onset of senescence, as both processes invoke similar processes of cessation of gas exchange and

ultrastructural reorganisation (particularly photosynthetic shutdown, chlorophyll breakdown and thylakoid dismantling). Despite this, clear physiological differences were present, and the NST and ST displayed two distinctly different phenotypes in response to water-deficit stress. Only the NST of *E. nindensis* achieved the necessary reorganisation and physiological adjustments required to protect the cell and prevent senescence. The NST underwent ordered subcellular restructuring, accumulated small LDs and maintained membrane viability and intercellular communication. The NST therefore avoided the termination stage of senescence through strategic mitigation of cell rupturing through vacuolation and lipid accumulation (amongst others), which is demonstrably less evident in the ST. The ST also underwent subcellular reorganisation, but the order and control required for desiccation tolerance was not maintained, and the cells succumbed to stress and died. This **Chapter** confirmed that the sampling strategy of the two different tissue types was consistent. Scrutinising the different phenotypes upon desiccation minimised the confounding effects of species or growth conditions, and this study therefore provided an appropriate model for senescence processes in resurrection plants. How the NST of *E. nindensis* regulates changes at a molecular level is discussed in **Chapter 3**, and the differences in transcript abundance between the NST and ST are discussed in **Chapter 4**.

Chapter 3

GLOBAL TRANSCRIPTOMIC ANALYSIS UNDERLYING DESICCATION TOLERANCE IN *E. NINDENSIS*

3.1. INTRODUCTION

Plants are sessile organisms and therefore need to adapt to constant changes in their ecological niche. Surviving adverse environmental conditions, such as prolonged drought, depends on the plant's ability to adjust their physiology, alter their metabolism and metabolic products, and modify the underlining gene expression that regulates biological processes. It is crucial to identify the transcripts and genes and related traits that contribute to desiccation tolerance to understand how resurrection plants cope with extreme water loss (Mohanta *et al.* 2017). Whole transcriptome analyses is a powerful tool to identify which transcripts are regulated and how the changes in transcript abundance translate to the gene expression that conveys tolerance (Trapnell *et al.* 2012; Ma *et al.* 2015; Peng *et al.* 2018). Genes involved in similar biological processes are often co-expressed, and the relationship between these causal genes and their regulation can help decode complex biological processes in the context of abiotic stress (Righetti *et al.* 2015; Serin *et al.* 2016; Mohanta *et al.* 2017). Therefore, by subjecting plants to desiccation and rehydration and analysing changes in RNA abundances, the changes in transcript abundance under severe abiotic stress can be explored.

Resurrection plants have fine-tuned the balance of preventing cell death whilst simultaneously supplying organs and tissues with the energy required to induce the necessary gene expression as well as allowing for the metabolic and ultrastructural changes needed for the acquisition of desiccation tolerance (Munné-Bosch *et al.* 2004; Gaff *et al.* 2013; Griffiths *et al.* 2014; Williams *et al.* 2015). Through the transcriptomic analysis of multiple resurrection plants, key features of desiccation tolerance have been identified that are common during desiccation: photosynthesis is shut down, metabolism is reprogrammed, protective metabolites are accumulated, and senescence is inhibited (Ramanjulu *et al.* 2002; Liu *et al.* 2019b). It is also important to recognise that transcription is one developmental step ahead of the proteome (Silva *et al.* 2016). Through transcriptome analysis, it has been hypothesised that resurrection plants co-opt seed-related mechanisms to convey vegetative tolerance (Costa *et al.* 2017a; VanBuren *et al.* 2018; Hilhorst *et al.* 2018a).

In this **Chapter**, whole transcriptomes of hydrated, dehydrated, desiccated and rehydrated *E. nindensis* are analysed by focusing on the changes in transcript abundance in desiccation tolerant NST. A parallel analysis with the processes operating in desiccation sensitive ST is provided in **Chapter 4**. Traits related to desiccation tolerance of *E. nindensis* have not been characterised at the molecular level before, therefore this study will provide the foundation for future molecular work in this species.

Desiccation tolerance requires an ordered metabolic arrest resulting in a quiescent state that resembles dormancy in orthodox seeds. Links between these similar processes are discussed. The main findings of this **Chapter** indicate that the NST of *Eragrostis nindensis* undergo highly-regulated and well organised metabolic reprogramming. Core traits identified here are similar to those that have been documented in other resurrection plants. Overrepresented GO terms coupled with clustering analysis provide insights into how this resurrection plant copes with severe abiotic stress, and how these DEGs translate into desiccation tolerance.

3.2. METHODS

3.2.1. Total RNA extraction

Plant material was collected, maintained, dehydrated and rehydrated as described in **Chapter 2**. Total RNA was extracted in triplicate from both leaf tissue types (NST and ST) for sequencing analysis (see Appendix, Table A2). Due to financial constraints, the ST was sequenced at 100%, 60%, 25% and 18% RWC only. These RWCs were chosen due to the distinct physiological and ultrastructural changes observed in **Chapter 2**. To capture transcript abundance changes in the ST, a RWC of 18% was chosen in an attempt to get transcript abundance changes at low RWCs but aim to avoid sequencing completely degraded tissue, which could be the case at very low RWCs. Snap frozen samples (between 50 -100 mg) were ground in liquid nitrogen and homogenised in 750 µl of TRIzol© reagent (Sigma-Aldrich, St. Louis, Mo, USA) by vortexing for 5 minutes, thereafter incubated for a further 5 minutes on ice. Samples were always kept on ice unless otherwise stated. Following the addition of 200 µl of chloroform, samples were mixed by inversion for one minute, thereafter incubated for three minutes, with a brief inversion every minute following centrifugation for 15 minutes at 12000 x g at 4°C. Samples were chloroform extracted, and 350 µl of aqueous phase was transferred to new microtubes. RNA was precipitated in 500 µl cold isopropanol for 20 minutes, thereafter centrifuged for 10 minutes at 12000 x g at 4°C. The RNA pellet was washed twice with 500 µl of freshly made 75% ethanol (EtOH), and air-dried for 10 minutes in a fume hood at 55°C. The RNA pellet was resuspended in 50 µl RNase-free water (Qiagen). Samples were DNase-treated using DNase 1 (NEB), and further purified using the Qiagen RNeasy® MiniKit columns according to the manufacturer's instructions. Polymerase chain reaction (PCR) amplification was used to test for genomic DNA, where each sample was run in triplicate using a chloroplast barcoding marker (psb_AF and trn_HR) as a primer. Samples with genomic DNA contamination were further treated with DNase 1 and the PCR repeated to ensure complete removal of genomic DNA.

3.2.2. RNA quality control and cDNA library preparation

RNA quality was verified by assessing the purity, integrity, and concentration of each sample through bioanalysis (Sigma), nanodrop and gel electrophoresis. Each sample was aliquoted into four microtubes - two for bioanalysis (5µl), one for RNA-sequencing (5 µl of 2.5 µg), and one for quantitative real-time PCR (RT-qPCR) (5 µl) - in a sterilised lamina flow room for transportation to Queensland University of Technology (QUT), Australia for sequencing. Samples were express shipped to QUT on dry ice and immediately stored at -80°C. To assess whether the transit caused any RNA

degradation, the samples were again sent for bioanalysis (Agilent) and Q-bit analysis to quantify their RIN (RNA integrity numbers). Higher quality RINs were chosen for the paired-end sequencing (between 7.1 and 8.3), while the single-end sequencing RIN ranged between 6.5 and 8.3 (Appendix, Table B1).

3.2.3. RNA sequencing

A total of 30 samples, representing six water content categories, in the two tissue types were sequenced by the Central Analytical Research Facility at QUT to provide raw reads for RNA-seq analysis. cDNA libraries were prepared with bar-coding for paired-end (n= 10, 150 nt amplification) and single-end (n = 20, 75 nt amplification) samples, which were sequenced with Illumina HighSeq 2000 in accordance with the manufacturer's protocol. Paired-end reads produce longer contigs (referred to in this thesis as transcripts, i.e. RNA molecules) and thus generate a higher quality dataset needed for *de novo* assembly construction (sequencing commenced prior to the knowledge of a genome, see **Appendix 2**). Due to funding constraints one sample per triplicate biological replicate was sequenced for paired-ends. Forward (left) and reverse (right) reads were properly aligned with the same number of reads. Both paired-end and single-end reads were used, in combination, for the RNA-seq analysis throughout the thesis. This produced an RNA-seq library per sample that reflected the relative transcript abundance, as the number of reads from each transcript is proportional to the relative abundance of that transcript within the sample (Trapnell *et al.* 2012).

Sequenced reads were processed and visualised using the standard tool FASTQC (http://www.bioinformatics.babraham.ac.uk/projects/fastqc/) as described in (Chen *et al.* 2016). Adapters were removed, and reads were trimmed using Trimmomatic v.033 (Bolger *et al.* 2014) with the following parameters: HEADCROP – 12, CROP – 149, SLIDINGWINDOW 4, 24 and MINLEN 50. Reads were trimmed when the average quality fell below 25 PHRED score across nucleotide bases (Appendix, Table B1). All reads below 50 base pairs were cut and the range of sequence lengths were 50-139 for paired-end reads. This produced a set of high quality raw FASTQ files used for downstream abundance estimation and differential transcript abundance.

3.2.4. RNA-seq genome-based assembly

The genome of *E. nindensis* was sequenced and annotated by the VanBuren Lab from Michigan State University, USA (Pardo *et al.* 2019). The constructed d*e novo* assembly and raw reads from NST at 60%

RWC and <10% RWC were used to train the genome. The following RNA-seq analysis was conducted using the *E. nindensis* genome v1.0.

The RNA-seq raw reads were processed using the tuxedo pipeline (Pertea *et al.* 2016). Reads were aligned to the reference genome using HISAT2 to determine transcript level alignment. StingTie assembled and quantified alignments into transcripts for each sample. Transcripts belonging to the same gene were merged in StringTie Merge and abundance was re-estimated per sample. Read counts were normalised for each library using three different methods in edgeR (McCarthy *et al.* 2012) to produce counts per million (CPM), transcripts per million (TPM) and fragments per kilobase per million (FPKM). Transcript abundances were then $\log_2$ transformed ($\log_2$/(FPKM+1)). Fold changes were calculated through pairwise comparisons, by comparing each treatment (RWC + tissue type) to the control (100% RWC, NST). Transcripts were considered significantly expressed (differentially expressed genes, DEGs) when their abundances were significantly different to the control (Benjamini & Hochberg (1995) False Discovery Rate (FDR) correction, q-value ≤ 0.05) after a threshold cut-off of 2.0 $\log_2$ fold change. The term transcript is used when describing those sequences constructed through RNA-seq (e.g. accumulating transcripts), whereas DEGs and genes refer to those transcripts that have annotations (e.g. senescence associated genes (SAGs)).

3.2.5. Transcriptome validation through RT-qPCR

Once the DEGs were constructed, 10 genes of interest (GOI) were chosen for RT-qPCR validation of the transcriptome. However, since the library prep for cDNA synthesis used for RNA-seq differed from that of RT-qPCR, it was first necessary to clone the PCR products into *E. coli* and subsequently confirm the product amplicon through sequencing. First, primers were designed based on the RNA sequences for housekeeping genes (F-Box, GAPDH, ubiquitin) and DEGs of interest to desiccation tolerance (drought recovery, trehalose phosphatase, LEA3, RUBISCO) and senescence (SAG, WRKY, WRKY70, Table 3.2). Total RNA was then used as a template for cDNA library construction using SuperScript IV Reverse Transcriptase (Invitrogen). Oligo(dT) primers annealed to the template RNA thus separating messenger RNA (mRNA) from the total RNA. The success of cDNA synthesis was validated by conducting a PCR using 18S primers from *Musa acuminata* (banana). Primers were tested on 1 µl of pooled cDNA from the three biological replicates per RWC. RT-qPCR was performed using a two-step profile of 45 cycles of 10 seconds at 95°C, followed by 30 seconds at 60°C. PCR amplification of cDNA was confirmed through separation of PCR product on polyacrylamide gel through electrophoresis. Bands of each GOI was excised for PCR product extraction and purification using Bio-Rad Freeze ‘n Squeeze™. Purified products were ligated into pGEM-T Easy Vector System I (Promega) according to

the manufacturer's protocol using a 1:3 vector to insert (100 bp) ratio. After transformation into *Escherichia coli*, the culture was plated onto Luria-Broth-agar containing 100 µg/ml ampicillin. Bacterial transformation was confirmed using blue-white colony screening. Colony PCR products were re-amplified and run on polyacrylamide gels through electrophoresis. Two PCR product bands from each GOI were excised, cleaned and sequenced to confirm the amplicons.

Primer efficiency using a standard curve was analysed in triplicate using the following primer serial dilutions (1:1, 1:2, 1:10, 1:20, 1:40). Once the performance of each primer was established, the relative RNA abundance of each GOI was assessed through RT-qPCR using pooled cDNA from the three biological replicates per RWC. A two-step profile of 30 cycles of 15 seconds at 95°C, followed by 60 seconds at 60°C, was used. To ensure pipetting accuracy, an Eppendorf epMotion® 5075 automated pipetting machine was used to pipette the Sybr Green I master mix (5µl 2 x Sybr Green, 0.3 µl of 10µM Primer F and R, 3.4 µl dH_2O) with 1 µl of 90 µg cDNA template. Data analysis was performed on BioRad CFX Manager™ software using the housekeeping genes as internal standards. The RT-qPCR expression intensity (fold-change) of each GOI was calculated using the $2^{-\Delta\Delta Ct}$ method and compared to the patterns derived from the RNA-seq analysis.

Table 3.2: Primer pairs for cDNA targets for the *Eragrostis nindensis* transcriptome validation using quantitative real-time polymerase chain reaction (RT-qPCR).

cDNA target	association	5' primer sequence	3' primer sequence
RUBISCO	desiccation tolerance	CGACAAAGGAACAATTCATGG	CATCAGCTTCATCGCCTACA
LEA3	desiccation tolerance	CAACCTTTGCTTCGTTTTCC	GGCCTGGTAGCTAGCCTTGT
trehalose phosphatase	desiccation tolerance	ACCTGCTCGTGACTGGAGTT	TACGCTGGTAGCCATGGAAT
ERD7	desiccation tolerance	GTGATGCCATGACTGTGGAC	GAATTCAGGTGGGGAGTCCT
DROUGHT RECOVERY	desiccation tolerance	GATGGAGGATGCTTTTGCTC	TTTCGACCGCAATAATGATG
WRKY70	senescence	GCTCACTCGCACACACTCTC	CCTCTCTGCAACCACCACTT
WRKY DNA -binding	senescence	TCAGGTTCTCCAGGAGGTTG	GACGCTCTTCGACGTCTTCT
SAG	senescence	CCAAGGCAGTGGCTAAAGAG	GAAGTCCCATTCGACCAGAA
SAG21	senescence	GCAATGCATCCCACTATCCT	TAAATTGCCGGATACCTTGG
F-box	housekeeping	ATGCTGATAGAGGGGGACCT	GGCGTCTTGGAGCTGATACT
GAPDH	housekeeping	CATCTTTGCTAGGGGCAGAG	CGAGTCCACTGGTGTCTTCA
Ubiquitone	housekeeping	CTGTCAGATCCGATCCTGCT	CAAAACAGCAAAGGTGCAAA

3.2.6. Annotation

Multiple annotation tools were used to increase the number of transcripts annotated, as each database or tool predicts slightly different annotations. This was also used to evaluate existing annotations and thus increased confidence in the predicated annotations. Sequence predictions by

Interpro Scan (EBI) identified conserved Pfam domains, GO annotations and BLAST hits. The best hit was determined as the lowest e-value with a threshold score of $<1e^{-10}$. In addition, *E. nindensis* sequences were aligned against the Arabidopsis genome using BLAST to identify Arabidopsis homologues. In addition, only when more than ten *E. nindensis* reads were mapped to the same homologue was the annotation assigned. The tool Mercator was used to generate Mapman ontologies for the gene sequences (Thimm *et al.* 2004). Mercator performs BLAST searches against the Arabidopsis TAIR 10 database, SwissProt and Uniref90. The BLAST cut-off was set at the default bit-score of 80 (Lohse *et al.* 2014). This generated categories that grouped transcripts into bins according to functional plant categories (e.g. lipid metabolism, RNA regulation of transcription, PSII etc.).

Assembly completeness was assessed using Benchmarking Universal Single-Copy Orthologs (BUSCO, Simão *et al.* 2015) using the plant ortholog database Embryophyta odb9 (http://busco.ezlab.org/). This quantified the assembly quality based on the presence and composition of expected genes known to be evolutionarily conserved across plants.

3.2.7. Functional enrichment analysis

Metabolic reprogramming in response to stress, such as severe water loss or recovery upon rehydration, requires the intricate coordination of gene expression. This reprogramming is likely orchestrated by thousands of transcripts changing in abundance (accumulating or diminishing). Making biological sense of this extensive dataset is complex and requires the interactions between transcripts and their respective biological functioning to be known (Trapnell *et al.* 2013; Conesa *et al.* 2016). To interpret this, the Biological Networks Gene Ontology (BiNGO) tool within Cytoscape (version 3.5.1) was used to visualise the overrepresented GO categories in each sample. BiNGO calculates which GO terms are statistically overrepresented (i.e. enriched) in a set of transcripts, based on the composition of the GO terms from the entire dataset (Maere *et al.* 2005). BiNGO uses hypergrometric statistical tests to correct for multiple testing (Maere *et al.* 2005) and functional categories were considered to be enriched when the FDR was <0.05. BiNGO takes the composition of the entire transcriptome into account and is a powerful tool to tease out trends that would otherwise be difficult to detect by looking at the transcript abundance trends alone.

Due to the hierarchical nature of GO terms, multiple GO terms can be assigned to each transcript. To reduce this redundancy, the platform REViGO (reduce and visualise GO) was used to eliminate semantically-similar GO terms (Supek *et al.* 2011). Redundant categories describing the biological processes or metabolic functions were therefore removed. A ratio of the expected to observed number of transcripts was calculated and this represented the degree to which each category was

overrepresented. A similarity index of 0.7 was used, and redundant transcript categories were removed using the dispensability index threshold of $p < 0.05$, unless otherwise stated.

3.2.8. K-means clustering (KMC)

Transcripts from NST were grouped into clusters using Genesis (ver 1.8.1, Sturn *et al.* 2002) based on the similarity of their expression profiles. First, to evaluate the performance (i.e. homogeneity of transcripts clustered), Figure of Merit (FOM) analysis was used to determine an appropriate number of clusters (Olex *et al.* 2011). Highly homogenous clusters, i.e. clusters with low within-cluster variation, increase the predictive power of the algorithm, thus forming biologically meaningful groups. Expression values were "normalised to experiment" before running k-means clustering (KMC) analysis. Each cluster was analysed separately for the overrepresentation of GO term categories using BiNGO in Cytoscape as described above. The ratio of the observed versus expected frequency of the category compared to the entire dataset was used to indicate the contribution of each category within a cluster. Biological categories had a threshold cut-off of a dispensability index of 0.5.

3.3. RESULTS AND DISCUSSION

3.3.1. Assessment of transcriptome quality

The *E. nindensis* genome is octoploid, possibly from an allotetraploid event followed by an autotetraploid event and exhibits a clear 4:2 synteny pattern with *Eragrostis tef* (Pardo *et al.* 2019). The estimated total assembly size using cytometry is 1.0 Gb, and after filtering out redundant haplotypes, a total haploid assembly of 986 Mb across 4368 contigs (with an N50 of 520 kb) was yielded (Pardo *et al.* 2019). This thesis is based on the first *E. nindensis* genome construction (v1.0), which produced 118,201 gene constructs. This is a much larger genome in comparison to that of *E. tef*, which has a total haploid assembly size of 576 Mb with 1344 contigs with an N50 of 1.55 Mb, and 68,255 gene constructs (VanBuren *et al.* 2019b). Similarly, several other resurrection plants have comparatively smaller genome sizes, such as *Oropetium thomaeum* (245 Mb), *Lindernia brevidens* (270 Mb) and *Xerophyta schlechteri* (295.5 Mb), whereas *Boea hygrometrica* (1448 Mb) is much larger (Costa *et al.* 2017a; VanBuren *et al.* 2015; Xiao *et al.* 2015; VanBuren *et al.* 2018). Furthermore, *E. nindensis* has 40 chromosomes compared to the 20 in *E. tef* and 48 in *X. schlechteri* (Costa *et al.* 2017a; Pardo *et al.* 2019; VanBuren *et al.* 2019b). The average GC-content for *E. nindensis* is 45.96%, compared to 34.86%, 36.51%, and 42.30% for *O. thomaeum*, *X. schlechteri* and *B. hygrometrica* respectively (Costa *et al.* 2017a). This high GC-content is not uncommon in grasses or other

resurrection plants, and it has been suggested that GC-rich DNA can be advantageous for cell regulation during environmental stress (Beck *et al.* 2007; Šmarda *et al.* 2014), although this is not a determinant of desiccation tolerance (Costa *et al.* 2017a). Furthermore, the *E. nindensis* genome had a BUSCO score of 96%, indicating that this is a well-annotated genome (see **Appendix 2**, Table B1). Overall, 69% of all transcripts and 88% of the DEGs were annotated using various annotation tools (Table 3.2). This high coverage of annotated transcripts allowed for dominant trends to be detected in the enrichment analyses based on known-gene functions.

Table 3.2: Various annotation tools were used to increase the identification of transcripts derived from the transcriptome. Combining these tools resulted in the majority (69%) of sequences having an assigned annotation. *At*= *Arabidopsis thaliana*, GO = Gene Ontology.

Annotation Method	Number	%	E-value threshold
Mercator	56051	47%	80*
Swissprot	44871	38%	$1E^{-10}$
GO	32585	28%	$1E^{-10}$
At homologues	58076	49%	$1E^{-10}$
Pfam	44871	38%	$1E^{-10}$
Annotated	81159	69%	-
Unannotated	36850	31%	-
Total transcripts	118009		

*BLAST cutoff

RNA-seq libraries were mapped against the genome with an overall alignment rate of 90% (Appendix, Table A2). A principle component analysis (PCA), consisting of all samples normalised relative to the control, illustrated that the observed variability was associated with RWC (PC1, 27%, Figure 3.16). This suggested that each RWC category had distinct transcript abundance patterns. The second principle component (PC2, 17%) separated the samples according to their sequencing depth (paired-end vs single-end samples).

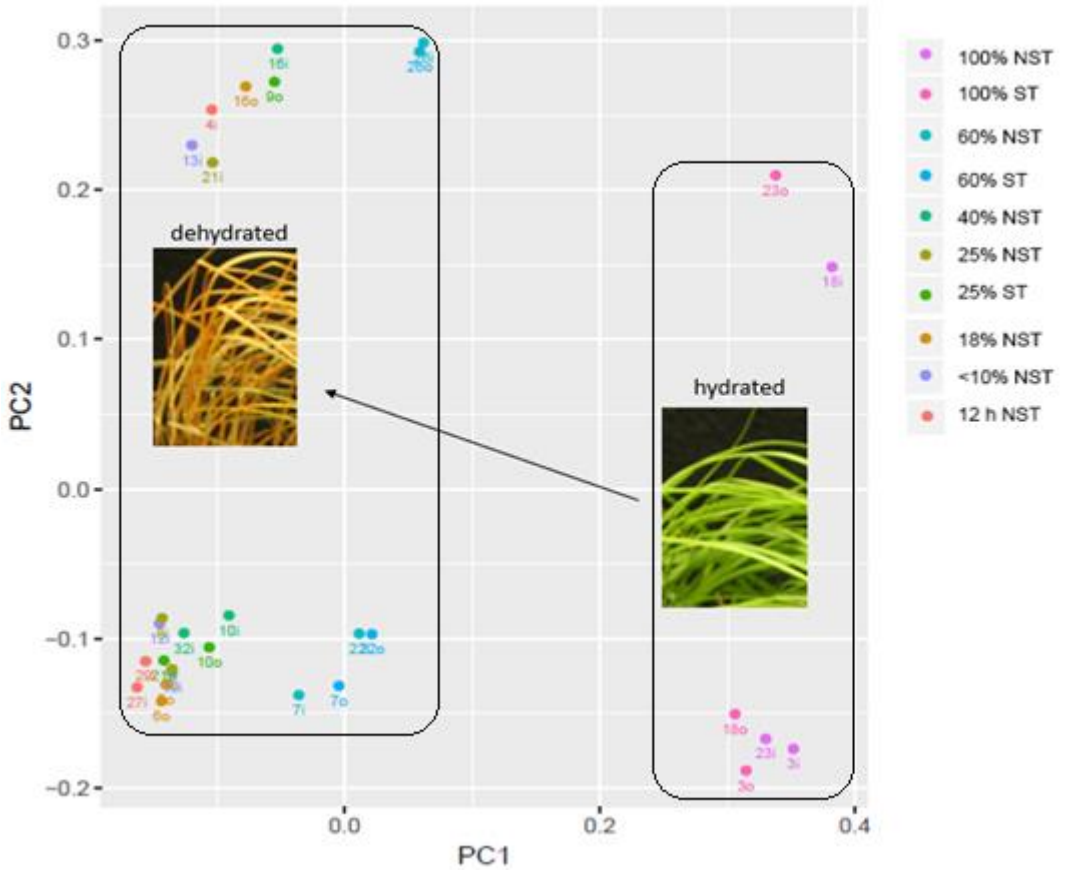

Figure 3.16: Principle component analysis (PCA) showed a distinction between hydrated (100% relative water content, RWC, %) and desiccated plants (<10% RWC), as highlighted by the boxes, showing a clustering of samples across the water gradient of desiccation tolerant, non-senescent tissue (NST) and desiccation sensitive, senescent tissue (ST) of the resurrection plant *Eragrostis nindensis*. Principal Component (PC) 2 indicates the separation of library depth of the sequences (paired vs single-end). The numbering refers to the plant number (Appendix, Table A2), where 'i' is the NST and 'o' is the outer (ST) leaf.

3.3.2. RT-qPCR transcriptome validation

Transcriptional changes were analysed from the independent RT-qPCR analysis across the GOI at various water contents (Figure 3.17). The normalised fold change ($2^{-\Delta\Delta Ct}$) trends generally mimicked the expression levels derived from the RT-qPCR, indicating that the *in silico* constructed transcript abundance trends reflected the mRNA abundances. This demonstrated the reproducibility of the transcript abundance trends derived from the transcriptome. LEA3 and trehalose phosphatase transcript abundances increased during drying, whereas WRKY and drought recovery transcripts appeared stable in the NST but diminished in abundance in the ST. RUBISCO transcript abundances diminished during drying, which was expected due to the poikilochlorophyllous nature of *E. nindensis*. Trehalose phosphatase abundances differed at 25% RWC in the ST, where this enzyme increased in abundance from 60% RWC in the transcriptome but diminished at 25% RWC in the RT-qPCR. This is likely due to the low abundance of this enzyme (Grennan 2007). Nevertheless, the trends observed validated the transcriptome. Correlation analysis are depicted in Appendix, Table A13.

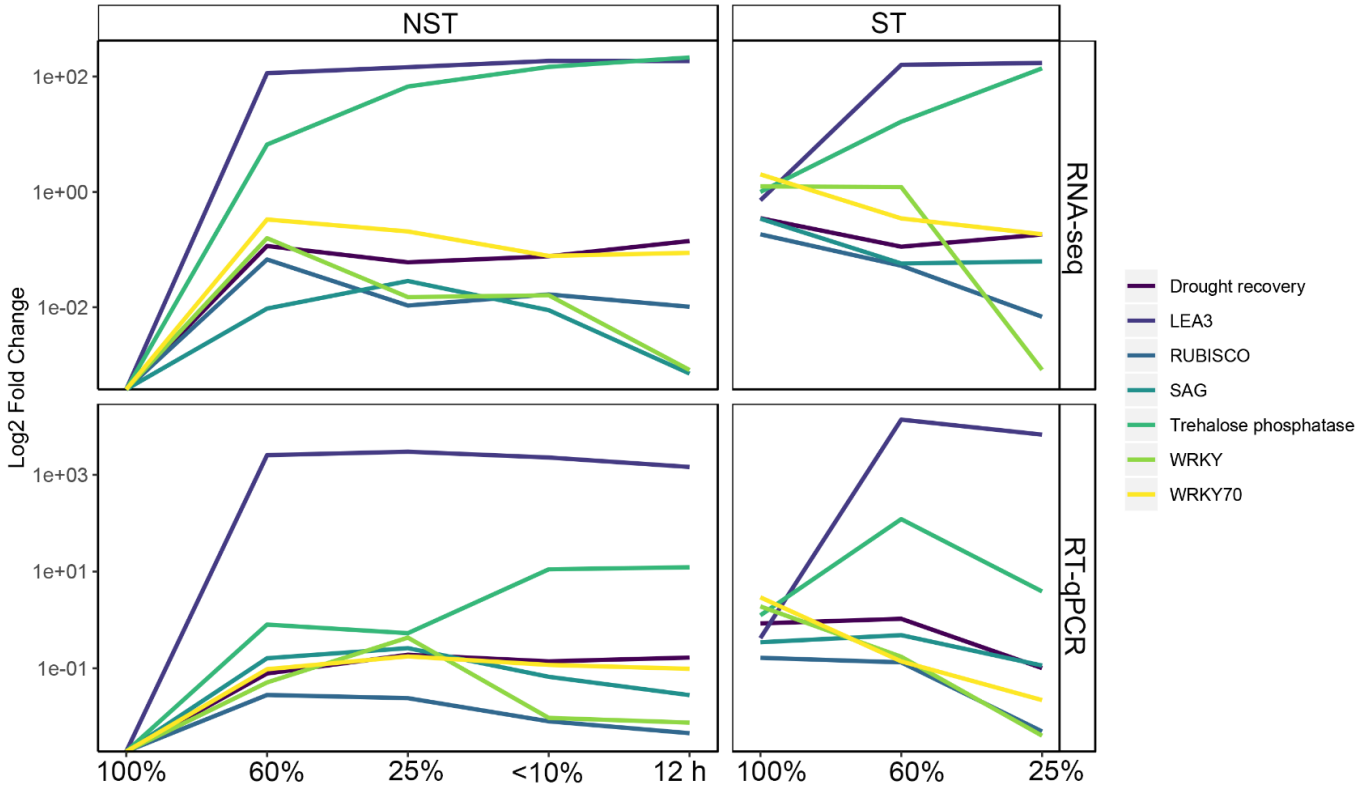

Figure 3.17: Transcriptome expression patterns were validated through quantitative real-time PCR (RT-qPCR) of selected genes of interest (GOI) during drying (represented as the relative water content, %) and rehydration (12h) in desiccation tolerant, non-senescent tissue (NST) and desiccation sensitive, senescent tissue (ST) of the resurrection plant *Eragrostis nindensis*. Transcript abundance profiles (normalised fold change ($2^{-\Delta\Delta Ct}$)) of GOI relating to desiccation tolerance (drought recovery, trehalose phosphatase, LEA3 (late embryogenesis abundant protein), RUBISCO (ribulose-1,5-bisphosphate carboxylase/oxygenase)) and senescence (senescence associate gene (SAG), WRKY, WRKY70) showed similar trends during drying and therefore validated the transcriptome. GOI expression patterns were normalised to the internal controls (GAPDH, F-Box and ubiquitin). Correlation analysis are presented in the Appendix (Table A13).

3.3.3. Functional enrichment analysis of co-expressed transcripts

Tolerance to desiccation requires a plethora of genes acting in synchronisation to lay down the protective measures necessary for survival. This involves suites of transcripts that are co-expressed as the plant dehydrates. *E. nindensis* has a clear desiccation tolerance strategy that must be, at least partially, characterised by changes in transcript abundance in the NST that reflect distinct biological processes at different stages of drying. Since desiccation tolerance is a process, the functional categories enriched throughout these stages are transient and each RWC stage had characteristic dominant trends that remained enriched throughout drying. These stages were described as mild (60% RWC), moderate (40% RWC), severe (<25% RWC) water-deficit stress and desiccation (<10% RWC) and are the focus of this section.

3.3.3.1 Water-deficit stress-induced accumulating transcripts

Of the 7643 DEGs in the NST, 68.5% (2246 transcripts) were common amongst all RWC stages and this implies that the core traits required to convey desiccation tolerance are within this group of co-expressed transcripts (Figure 3..1). Biological processes relating to the response to desiccation and the concomitant functional categories (‘*response to ABA’, ‘response to heat’* etc.) were enriched throughout desiccation. Enriched categories included those relating to solute metabolism and transport (‘*raffinose catabolism’, ‘amino and folic acid transport’, ‘nitrogen fixation’*), photosynthetic shutdown (‘*regulation of chlorophyll metabolic process’, ‘cellular respiration’*), ‘*reproduction*’, cell wall metabolism (‘*arabinogalactan protein metabolic process’, ‘cell wall macromolecule catabolic process’*) and accumulation of metabolites (‘*lipid storage’* and ‘*hexokinase dependent signalling’*). These processes represent the core traits required for desiccation tolerance (Farrant *et al.* 2017; Costa *et al.* 2017b) and the consistently high transcript abundances associated with those processes in the NST upon desiccation illustrated this. Regulation of cellular metabolism (‘*TOR signalling’*) and protein processing (‘*protein unfolding’, ‘vacuolar protein processing’*) were also commonly enriched across RWC stages during drying and suggest an active metabolic role of detoxification during desiccation (Gechev *et al.* 2012; Farrant *et al.* 2017). There was enrichment of ‘*TOR signalling’* upon desiccation, and while it has been reported that TOR is activated under energy surplus and suppresses autophagy while promoting growth and anabolism (Schepetilnikov *et al.* 2017; Asami *et al.* 2018), the *E. nindensis* transcripts in the ‘*TOR signalling’* category belong to the TAP42-like family, which negatively regulates TOR (Jacinto *et al.* 2001). This therefore implies that metabolism is arrested below RWCs of 60% (Figure 3..1). Some transcripts were categorised with cell wall degradation (*‘cell wall macromolecule catabolic process’*) and several transcripts within this category are annotated as the enzyme endo-β-mannanase (AT5G66460). This enzyme hydrolyses cell wall polysaccharides during germination and promotes both cell wall loosening and breakdown of reserves (Kigel *et al.* 1995), demonstrating the cessation in growth.

Resurrection plants are hypothesised to have co-opted typically found in orthodox seeds to convey vegetative desiccation tolerance (Costa *et al.* 2017a; VanBuren *et al.* 2017) and *E. nindensis* is no exception. Several DEGs accumulating in abundance across all RWC stages during drying were enriched with transcripts associated with ‘*seed development*’, ‘*dormancy*’ and ‘*germination’*, such as small hydrophilic seed proteins (AT2G40170), LEAs and proteins expressed in seed-related lipid bodies, such as oleosin (AT4G25140) and caleosin (AT4G26740) (Figure 3..1, dashed box). These transcripts were all highly significant (corrected p-value <0.001) and are representative desiccation

tolerance traits in *E. nindensis*, supporting the co-option hypothesis raised by Costa *et al.* (2017c) and VanBuren *et al.* (2017). In orthodox seeds, dormancy is a critical mechanism that controls the timing of germination and is associated with delay in growth and implied metabolic arrest (Baskin *et al.* 2014). Resurrection plants require an ordered metabolic arrest to prevent energy consuming processes and start the desiccation tolerance shift in metabolism towards the accumulation of protective metabolites under sever water-deficit stress. The accumulation of dormancy-related transcripts is indicative of the metabolic arrest observed in several resurrection plants and is indicative of a strong drought response signal (Costa *et al.* 2016).

The category '*reproduction'* was highly enriched throughout the different stages of drying (Figure 3..1). These transcripts are associated with the reproductive organs, such as seeds and hence overlap with seed related genes. For example, a gene thought to be almost exclusively expressed in seeds, 1-CYSTEINE PEROXIREDOXIN 1 (AT1G48130), but also reported in the *X. viscosa* (Mowla *et al.* 2002), was highly enriched throughout drying. Other transcripts related to sucrose metabolism in developing seeds in Arabidopsis (SUS3, AT4G02280) were also highly enriched, illustrating the association of seed development and reproduction with desiccation tolerance. However, the ecological life history strategy should be taken into molecular context. Stress has a compelling effect on the timing of flowering, and can either enhance or inhibit flowering, depending on the life history trait of the species (Takeno 2016). Flowering represents the transition from vegetative to reproductive growth (Kazan *et al.* 2016). Resurrection plants also exhibit this developmental shift as they inhibit growth and promote seed-related genes (which are inherently developmentally or reproductive-related) during drying. It is therefore difficult to decouple whether transcript abundances are accumulating for protection during drying or for the signalling for flowering during rehydration. However, this category is likely to relate to flowering and suggests that there is more to this than simply attributing this enrichment to seed-related desiccation tolerance traits. *E. nindensis* flowers upon rehydration (personal observation). In Afrikaans, an official language in South Africa, the common name for this species is *Agtdaepluimgras*, literally translated as "eight-day plume grass" illustrating that this species takes roughly eight days to flower following rain (van Outshoorn 2012)**.** The enriched '*reproduction*' related transcripts are therefore apt and reflect the ecology and observed phenotypic flowering-response post rehydration. This trait has been reported in *X. humilis* (Myers *et al.* 2010) and has been observed in *Craterostigma* species (Scott 2000) and illustrates that stress is a negative-regulator of flowering in these resurrection plants, where stress prevents flowering in favour of survival. As in several other xeric plant species, these desiccation tolerant species have altered their flowering life history trait to invest in flowering when environmental conditions are favourable (i.e. with rainfall), and the transcriptome reflects this.

Upon moderate water-deficit stress (<40% RWC) accumulating transcripts were enriched for processes relating to vacuolation and autophagy (‘*protein ubiquitination’, ‘vacuolar sequestering’*). These traits were supported by ultrastructural studies in **Chapter 2**, where the bundle sheath cells were dominated by vacuolation at these RWCs (Figure 2.12). At this stage of dehydration, leaf tissues are likely to be accumulating metabolites (such as sugars, lipids and proteins) and experience subcellular alterations (such as thylakoid dismantling and vacuolation). These processes minimise macromolecular denaturation and undesirable interactions due to the lack of water (Gechev *et al.* 2012). The dominant enriched categories, e.g. *‘positive regulation of ribosome biogenesis’, ‘protein modification’, ‘ubiquitination folding’*, reflect the ability of *E. nindensis* to maintain protein structure and function. This maintenance is critical to ensure proper cellular functioning, and the enriched categories clearly reflect maintenance of protein integrity upon desiccation in the NST. This is similar to major transcript abundance shifts seen in *X. schlechteri,* where transcripts related to ‘*protein folding’, ‘protection and translation control’* were enriched between 60% and 40% RWC (Costa *et al.* 2017a). The enrichment of ‘*proline biosynthetic process’* related transcripts was experimentally validated by Vander Willigen *et al.* (Vander Willigen *et al.* 2004), where proline accumulated in conjunction with proteins and sucrose in *E. nindensis.* The enriched categories from 40% RWC suggest a shift in metabolism towards maintenance and protection of proteins and mechanical stabilisation, highlighting that the desiccation tolerance programme is geared towards protecting those proteins that are necessary for the acquisition of desiccation tolerance.

DEGs common to both the NST and ST upon severe water-deficit stress (<25% RWC) were heavily enriched with transcripts associated with transcription and gene regulation (‘*mRNA processing’, ‘RNA splicing’, ‘dephosphorylation of RNA polymerase’*). Transport of solutes involved in central pathways (‘*triose phosphate transport’, ‘electron transport chain’*) and sugars (‘*glucose-6-phosphate’*) were enriched, which alludes to these transcripts being highly relevant for the quick resumption of metabolic activity upon rehydration (Figure 3..1). This suggests that these transporting processes are critical to ensure rapid recovery. The RNA encoding of these genes must therefore be stored and protected from degradation during drying, potentially in processing bodies (P-bodies), which is discussed in **Chapter 4**. This process is similar to seeds, where stored reserves are mobilised after germination to provide energy and building blocks to sustain growth while the plant becomes photoautotrophic (Silva *et al.* 2016; Rajjou *et al.* 2004; Bai *et al.* 2017). A more detailed look into which transcripts might be important for rehydration (and are thus protected as suggested here) is discussed later in this section.

A total of 72 transcripts (2.2% of all accumulating transcripts in the NST) accumulated in abundance at <10% RWC. They were enriched for transcripts relating to DNA replication (‘*G1/S transition of*

mitotic cell cycle'), '*protein translation'*, '*amino acid biosynthesis'* and cell cycle ('*mitotic interphase'*) (Figure 3..1). Since these enriched categories are related to growth and synthesis of proteins, and growth is inhibited during desiccation, these transcripts are potentially being stored, and thus protected, for translation upon rehydration, as described above. Stable storage of transcripts associated with recovery of photosynthesis has been reported (Dace *et al.* 1998; Oliver 1991; Collett *et al.* 2003; Bajic 2006; Juszczak *et al.* 2017) and has been invoked for *X. schlechteri* (Costa *et al.*, 2017a). The accumulation of growth-related transcripts at such low water contents can therefore reflect the storage of RNA for recovery. Transcripts of an α-amanitin gene (AT5G45690), which is a transcriptional inhibitor that targets RNA polymerase II and is associated with mRNA storage (Rajjou *et al.* 2004; Sajeev *et al.* 2019), consistently accumulated in *E. nindensis* from 60% RWC through to <10% RWC in both the NST and ST (Figure 3..1). This transcription inhibitor plays an important role in seed-biology, where it actively degrades unprotected mRNA (i.e. transcripts not needed for seed maturation) and therefore plays an important role in transcriptional regulation of seed development (Rajjou *et al.* 2004; Sajeev *et al.* 2019). The phenomenon of storing mRNA for future expression has been shown in Arabidopsis, where mRNA is stored during seed maturation for expression during germination (Rajjou *et al.* 2004). Given that vegetative desiccation tolerance could be re-wired through pre-existing pathways from orthodox seeds (VanBuren *et al.* 2019a), it is reasonable to suggest that mRNA is also being stored in *E. nindensis* during late dehydration for expression upon rehydration similar to seed related processes. This is discussed further in **Chapter 4**.

The increase in transcript accumulation between 25% and <10% RWC is interesting as it is unlikely that protein synthesis and metabolism are active in the desiccated state, although increase in transcript abundance has been observed in *X. schlechteri* at low water contents (Costa *et al.* 2017a)**.** The '*shikimate pathway'* was highly enriched, which forms chorismate, a precursor to aromatic amino acids (phenylalanine, tyrosine, and tryptophan) that are key secondary metabolites (Herrmann *et al.* 1999). For example, phenylalanine is used to synthesise salicylic acid. This is an important growth hormone and has been associated with the induction of leaf senescence if programmed cell death is triggered (Rottet *et al.* 2015; Woo *et al.* 2018). In addition, salicylic acid is also associated with the acquisition of desiccation tolerance, as this hormone triggers signal transduction cascades that induce ROS scavenging and boosts cellular of protein and DNA (He *et al.* 2002; Parkhey *et al.* 2014). Another amino acid formed through the enriched shikimate pathway is tryptophan, an amino acid which synthesises the essential growth hormone auxin (Zhao 2012). This illustrates the enrichment of growth-related transcript abundance in the desiccated state, probably in anticipation of rehydration. Of the three chorismate synthase Arabidopsis homologues that were differentially expressed in *E. nindensis*, two (AT2G45300, AT4G39980) were highly expressed during drying and rehydration in the

NST as well as in the ST (**Chapter 4**). The enrichment of '*protein transport into the nucleus'* in the desiccated state indicates signalling or translation of proteins (DNA polymerase or lamins), and this is supported by the enrichment of '*heterochromatin organisation'*. Even at such low water contents, mRNAs are being transcribed that are essential for cell growth and repair. These processes are energy demanding and several transcripts relating to hexose and glucose catabolism also accumulated in abundance. This reiterates the importance of sugar accumulation upon desiccation for the dual role of stabilisation and in providing the energy required for the biosynthesis of essential transcripts.

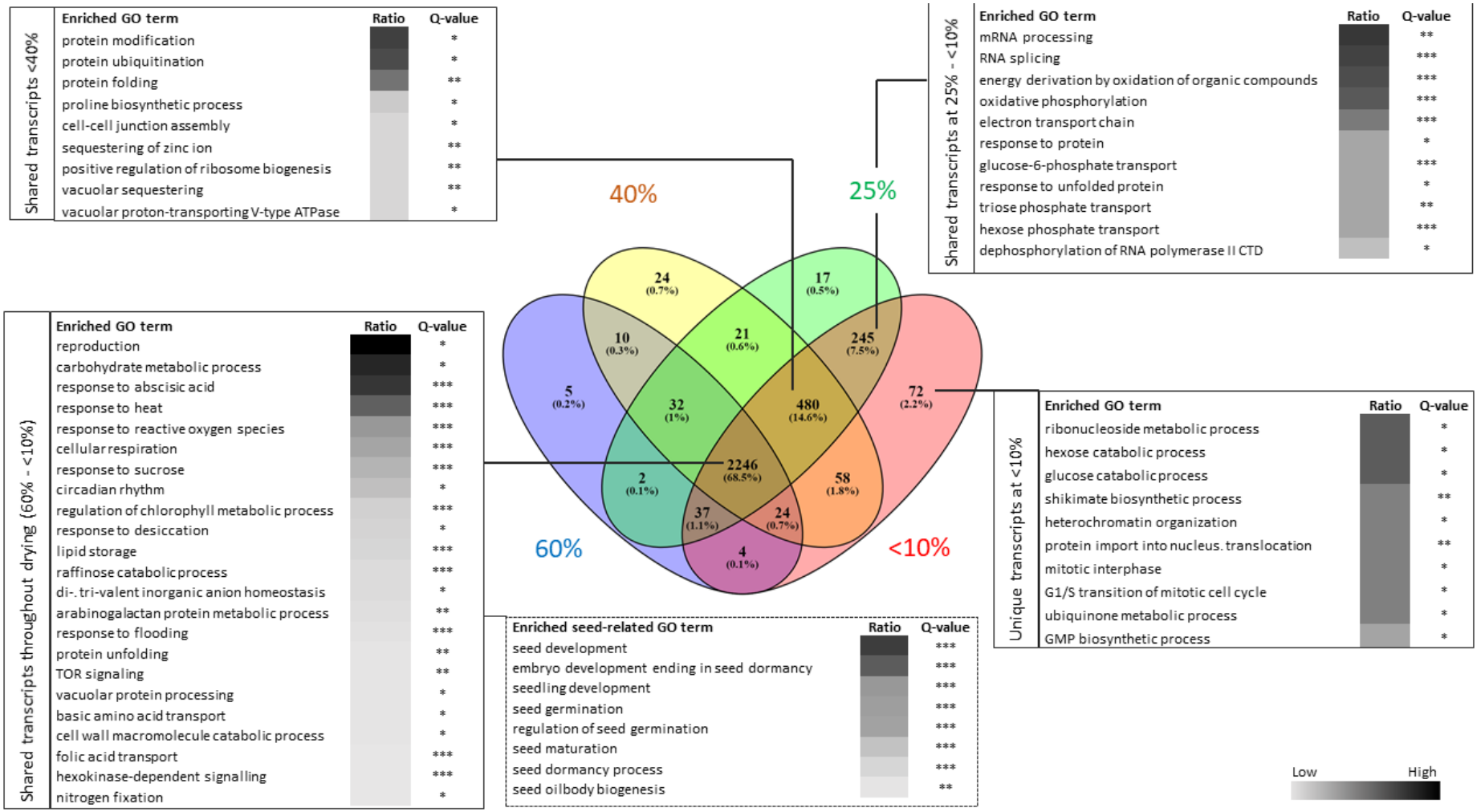

Figure 3.4.1: Water-deficit stress-induced accumulating transcripts, represented by enriched gene ontology (GO) categories, show distinct metabolic shifts in the desiccation tolerant, non-senescent tissue (NST) of the resurrection plant *Eragrostis nindensis* and embody core traits of desiccation tolerance. The number of DEGs are relative to fully hydrated leaves (100% RWC, NST). Boxes summarise the most enriched GO categories of transcripts expressed throughout drying at different stages of water-deficit stress (shared transcripts), or only expressed in the desiccated state (unique transcripts). Dotted box shows the seed-associated enriched GO categories that were expressed throughout drying. Significance was derived from BiNGO using FDR correction (q-value <0.05). Ratio (of expected to observed number of transcripts) represents the degree to which each category is overrepresented.

3.3.3.2 Water-deficit stress-induced diminishing transcripts

Overall there were fewer categories enriched during drying that showed diminishing transcript abundances (Figure 3.4.2). These transcripts indicated a general cessation of metabolism. Overall trends showed that metabolism was reduced during drying and was generally geared towards protective and repair mechanisms (as discussed above). The categories '*photosynthesis', 'carbon fixation', 'growth'* and '*gluconeogenesis'* had diminishing transcript abundances during drying. In support of this, chlorophyll a/b binding transcripts diminished in abundance during drying (Appendix, Figure A2), as has been shown in other resurrection plants (Challabathula *et al.* 2016; Yobi *et al.* 2017). Metabolism that is either dangerous (ROS producing photosynthesis) or energy consuming (growth) was systematically shutdown in favour of biological processes that induce survival (cellular protection and repair, as seen in Figure 3.4.2). For example, cell wall-related transcripts that were diminishing in abundance were composed of several cellulose synthase genes (AT1G02730, AT1G32180, AT1G55850, AT4G32410, AT5G05170, AT5G16910, AT5G17420, AT5G44030, AT5G64740), thus suggesting inhibition of growth. The reduction in metabolism coupled with the accumulation of dormancy related transcripts supports the established core traits resurrection plants employ to engage desiccation tolerance through metabolic arrest (Costa *et al.* 2017b; VanBuren *et al.* 2017).

Transcripts involved in '*leaf senescence'* also diminished in abundance. This is an important confirmation that senescence is a regulated process that is actively being suppressed in the NST during drying. This is discussed further in **Chapter 4**.

Of note was the category termed '*drought recovery*', as the diminished transcript abundances related to this category was unexpected. However, the eight transcripts involved in this category (consisting of two Arabidopsis homologues, AT1G70670 and AT2G37040) were exclusively related to lignin biosynthesis (Endo *et al.* 2018). The decline in transcripts associated with synthesis of secondary cell wall structure as the plant undergoes desiccation compliments the notion that cell growth was halted in favour of survival.

During moderate water-deficit stress (below 40% RWC), transcripts diminishing in abundance were related to the GO category *'chloroplast relocation'* (i.e. photosynthesis) and transcripts involved in protein degradation and signalling ('*stomatal complex development', 'protein chromophore linkage', 'circadian rhythm'*) (Figure 3.4.2). Transcripts relating to 'm*etabolite transporters and system development'* diminished in abundance. This category is composed of multiple genes relating to ATP binding, RNA transcription, signalling and protein degradation. The enriched categories relating to protein and transcriptional changes in abundance observed at 40% RWC (Figure 3.4.1) were diminished at 25% RWC (Figure 3.4.2). This demonstrates a metabolic shift associated with a reduction

in protein turnover at lower water contents. The coordinated expression reduction of a considerable number of transcripts associated with protein production indicates the maintenance of protein integrity, as protein protection and detoxification are associated with reduced molecular crowding (Farrant *et al.* 2015; Artur *et al.* 2019). Transcripts in the AUXIN RESPONSE FACTOR family were also enriched in this category. Two ATP synthase transcripts (in the '*proton transport ATP synthase complex biogenesis'* category) diminished in abundance below 40% RWC. Similarly, upon severe stress (<25% RWC) within the transcripts representing diminishing transcript abundances, categories relating to translation and signalling were predominantly enriched. This is a common theme and overall there is a general shutdown of transcripts involved in metabolism (lipid, secondary), signalling, translation and transport upon desiccation in the NST of *E. nindensis*.

There were 108 DEGs exclusively diminishing in abundance at <10% RWC, despite this, it was statistically insufficient to produce enriched categories. This suggests two things: firstly, that the majority of DEGs in the desiccated state are expressed at higher water contents (i.e. are common) and secondly, large-scale transcript abundance does not occur in the desiccated state, which represents the shift towards quiescence. Metabolic reprogramming at lower water contents has been observed in other resurrection plants, however, most studies report on accumulating transcripts, or look at general trends at lower water contents rather than exclusively diminishing in the desiccated state. It is therefore difficult to compare these results. Nevertheless, the top 40 transcripts are shown (Figure 3.4.2, which represent the general shutdown of metabolism seen throughout desiccation.

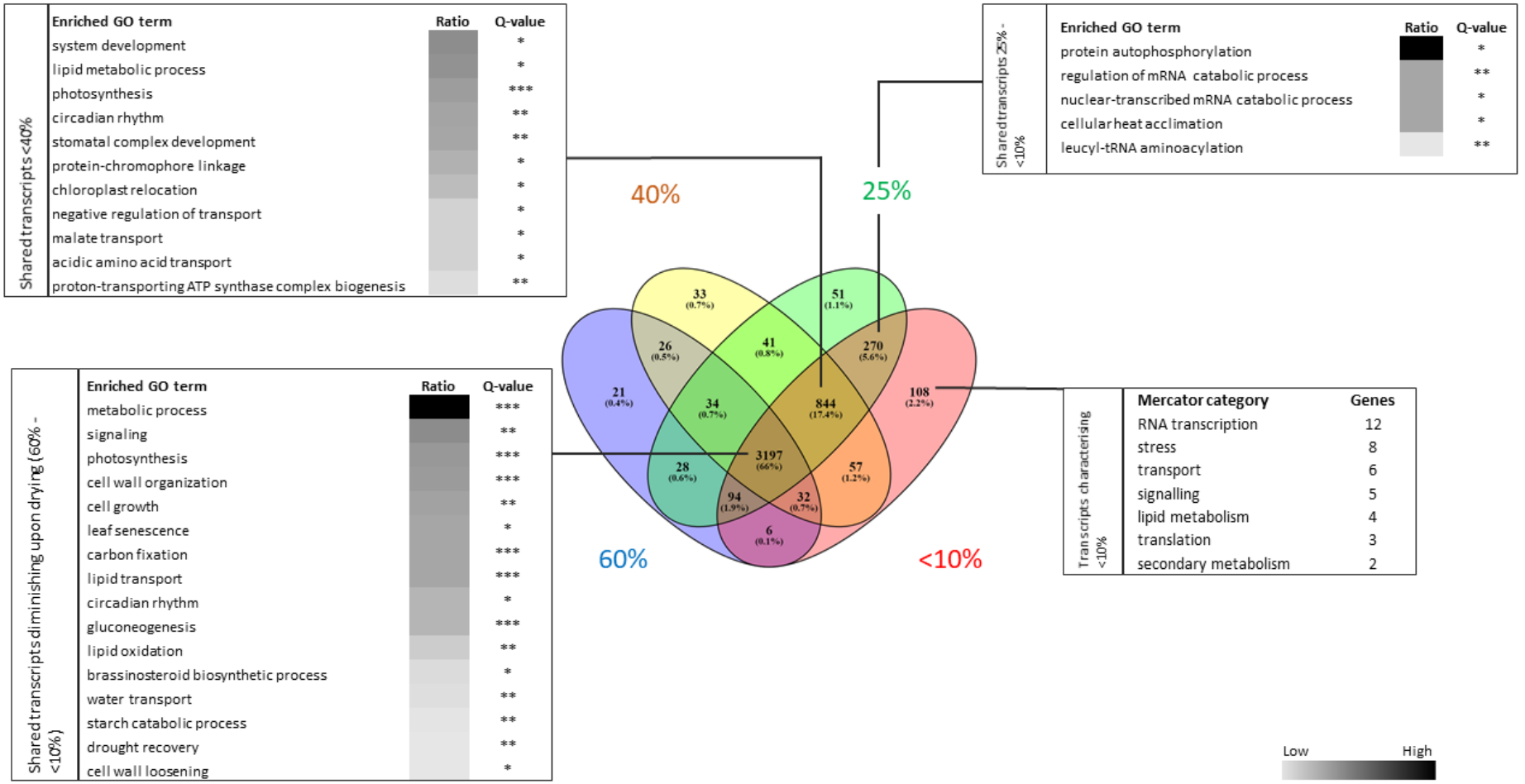

Figure 3.4.2: Water-deficit stress-induced diminishing transcripts, represented by enriched gene ontology (GO) categories, show distinct metabolic shifts in the desiccation tolerant, non-senescent tissue (NST) of the resurrection plant *Eragrostis nindensis.* The number of DEGs are relative to fully hydrated leaves (100% RWC, NST). Boxes summarise the most enriched GO categories of transcripts expressed during drying at different stages of water-deficit stress (shared transcripts). Mercator categories are shown for RWCs of <10%. Significance was derived from BiNGO using FDR correction (q-value <0.05). Ratio (of expected to observed number of transcripts) represents the degree to which each category is overrepresented.

3.3.3.3 Transcript abundance changes during rehydration

Since there is only one rehydration related timepoint, the changes in transcript abundance are discussed separately here. The DEG exclusively expressed during rehydration (relative to the 100% NST) with the highest fold change (relative to the control) of 14.4 was N-ACETYL-L-GLUTAMATE SYNTHASE 2 (NAGS2, AT4G37670, Appendix, Figure A4), which is putatively located in the chloroplast (Kalamaki *et al.* 2009). Over-expression of this gene in Arabidopsis showed an increased resistance to drought and salt stress due to altered nitrogen related biosynthesis (elevated ornithine levels, mild increases in arginine and citrulline, a hydroxyl scavenger) (Kalamaki *et al.* 2009). In another study, over-expression of NAGS2 delayed senescence and increased drought resistance by preventing chlorophyll loss (Capell *et al.* 1993). Since the chloroplast is a major site for carbon gain and nitrogen metabolism, and hence amino acid synthesis, the high transcript abundance of this gene represents metabolic reactivation upon recovery. The second highest fold change of 13.5 is a UDP-glycosyltransferase (AT5G49690) involved in flavonoid biosynthesis (such as anthocyanin), which was expressed during developmental senescence in Arabidopsis and is suspected to aid in the protection of light stress (Buchanan-Wollaston *et al.* 2005). Several of the DEGs accumulating upon early rehydration are unsurprisingly related to the protection of light induced stress as the chloroplasts begin to reform to become autotropic, which requires a controlled translational activity.

DEGs that were exclusively accumulating in the NST during rehydration showed a strong dominance of metabolic adjustment from quiescent to active metabolism (summarised in Appendix, Table A5). Seven GO categories below the dispensability threshold (<0.05) were enriched for DEGs relating to amino acid metabolism, protein synthesis, and RNA regulation. These were '*GMP metabolic process'*, '*mitotic interphase'*, '*nitrogen compound metabolic process'*, all of which are related to nucleotide synthesis (AT1G16350) and protein signalling (AT5G58590). The composition of the 103 transcripts within the '*nitrogen compound metabolic process'* category was interesting, as transcripts associated with RNA processing and regulation were dominant (31%, n = 31) as well as the biosynthesis of amino acids, nucleotides and synthesis of proteins. Enrichment included transcripts related to the maintenance of protein structure ('*cellular response to anoxia*', '*chaperone-mediated protein folding*', '*protein folding'*), and those related to chloroplasts ('*protein-heme linkage'*). This emphasises the importance of the unfolded protein response in resurrection plants.

Table 3.3 summarises the enriched functional categories accumulating during rehydration. Protein complexes, which included Fe-S clusters, associated with linear electron flow were enriched ('*protein-heme linkage'*). This indicates the quick resumption of energy generating processes in the absence of photosynthetic carbon gain. Transcripts enriched in rehydration were also involved in cellular

detoxification, as the Arabidopsis aldehyde oxidase multigene family oxidises toxic aldehydes and is comprised of Fe-S clusters and molybdenum cofactor domains (Srivastava *et al.* 2017), which were enriched in rehydration (‘*molybdenum incorporation into molybdenum-molybdopterin complex’*). Maintenance of cellular homeostasis during rehydration is critical as the influx of water alters the biochemical solution and hence biochemical reactions (Gao *et al.* 2017). This detoxification is further emphasised by the enrichment of ‘*aldehyde catabolic processes’*, as aldehydes are produced by oxidative stress, and the breakdown of these toxic by-products represent the reduction of cellular toxicity (Hou *et al.* 2015).

Some enriched GO terms diminishing during rehydration were associated with growth (‘*cellulose catabolic process’* and ‘*borate transmembrane transport’*), implying that although metabolism has activated (discussed above), growth has not yet resumed.

Table 3.3: Enriched gene ontology (GO) terms accumulating and diminishing in transcript abundance levels during rehydration (12h) in desiccation tolerant, non-senescent tissue of the resurrection plant *Eragrostis nindensis* indicate quick resumption of metabolism. Ratio (of expected to observed number of transcripts) represents the degree to which each category is overrepresented.

Term ID	Description	Ratio
Accumulating		
GO:0017003	protein-heme linkage	0.0136
GO:0071258	cellular response to gravity	0.0136
GO:0006089	lactate metabolic process	0.0204
GO:0009438	methylglyoxal metabolic process	0.0204
GO:0018315	molybdenum incorporation into molybdenum-molybdopterin complex	0.0136
GO:0042040	metal incorporation into metallo-molybdopterin complex	0.0136
GO:0046185	aldehyde catabolic process	0.0204
GO:0019243	methylglyoxal catabolic process to D-lactate via S-lactoyl-glutathione	0.0204
Diminishing		
GO:0030245	cellulose catabolic process	0.0135
GO:0035445	borate transmembrane transport	0.0101

3.3.4. K-means clustering (KMC)

Understanding the biological significance of these changes in transcript abundance is a challenge (Orlando *et al.* 2009). Co-expressed transcripts are often involved in similar biological processes (Orlando *et al.* 2009; Si *et al.* 2014). Therefore, grouping transcripts into clusters according to their expression patterns is an important tool for RNA-seq analysis, as this informs our understanding of which dominant transcript functional trends are activated or suppressed at different RWCs (Si *et al.* 2014). Desiccation tolerance is an ordered and systematic process, and these clusters therefore represent the transcriptomic shifts of similar biological categories being engaged during drying.

According to the Figure of Merit (FOM), 15 clusters would provide a good representation of the transcript abundance patterns present in the NST (Appendix, Figure A3) as they displayed a within-cluster variance that ranged from 0.05 - 0.33. There were clear waves of transcripts accumulating (Figure 3.5 1-3) and diminishing (Figure 3.5 4-8) in transcript abundance upon mild, moderate and severe water-deficit stress, desiccation and rehydration in the NST. Clusters with similar patterns will be discussed as superclusters (e.g. cluster 3 and 4).

Clusters 3 and 4 (containing 403 and 518 transcripts respectively) represented transcript abundances that accumulated at 60% RWC in the NST and were enriched with categories relating to initial drought responses. Enriched categories included important signalling processes upon moderate water-deficit stress ('*response to abiotic stimulus'*) and corresponding processes involved in maintaining cellular homeostasis ('*cation and anion homeostasis'*). Evidence of preparation for desiccation was shown, as '*lipid storage'*, '*reproduction*', and '*seed and seedling development*' were highly enriched and remained so throughout desiccation and early rehydration (Figure 3..1). These represented the initial responses of *E. nindensis* in restoring homeostasis for cellular protection under abiotic stress, while engaging in lipid (i.e. energy) storage. Several transcripts implicated in cellular protection in seeds and vegetative tissues of resurrection plants upon desiccation were present in this cluster. For example, several LEA transcripts were included in this supercluster, illustrating the preparation for desiccation, as these proteins, *inter alia,* secure cellular protection through protein stabilisation, chaperoning and anti-aggregation (Artur *et al.* 2018, 2019a; Hilhorst *et al.* 2018). This supercluster was also enriched with the category '*senescence*' and depicted processes that are related to senescence-associated nutrient reshuffling in plants (Otegui 2018). The transcripts in this category were mainly involved in the process of vacuolar proteases to detoxify the cell (AT4G32940) and sugar transport (SUS3 and SWEET15), indicating nutrient-reshuffling. AT4G32940 is also involved in cell death and processing of seed storage proteins (Wang *et al.* 2019a). Similarly, DEGs involved in the enriched category '*senescence*' included GLUTAMINE SYNTHETASES, which are involved in nitrogen metabolism, converting ammonia from degraded amino acids into available nitrogen necessary for the biosynthesis of proteins (Avila-Ospina *et al.* 2014). These enzymes are associated with seed storage proteins and also play an important role in nutrient reshuffling during senescence (Avila-Ospina *et al.* 2014) and storage of nitrogen reserves for seed germination and longevity (Nguyen *et al.* 2015). DEGs clustered here that promote senescence were associated with chlorophyll breakdown and transport of solutes, which demonstrates the transcriptional preparation for the breakdown of chlorophyll in this poikilochlorophyllous species, rather than senescence as displayed in desiccation sensitive species.

Functional categories enriched in DEGs diminishing in abundance at 60% RWC onwards depicted in cluster 12 and 9 (containing 362 and 484 transcripts respectively, Figure 3.5.2) are related to '*cell*

growth' (including '*cell wall biogenesis', 'cell adhesion', 'cell communication'*) and '*photosynthesis*', which supports the physiological photosynthetic shutdown observed in **Chapter 2**. The category '*senescence*' was also enriched within the transcripts represented by diminishing transcript abundances. These transcripts are mostly involved in hormone regulation of jasmonic acid and lipoxygenases, WRKY transcription factors and cell death, all of which are known regulators that promote senescence (Costa *et al.* 2017a; Williams *et al.* 2015). The decline in transcript abundance levels of senescence-promoting transcripts is therefore indicative of senescence being actively suppressed in the NST of *E. nindensis*. SAG12, an enzyme that encodes a cysteine protease and is involved in plant programmed cell death (Solomon *et al.* 1999), was also enriched in this cluster. This demonstrates that transcripts associated with senescence are tightly regulated to evoke different roles required for protection or repair when undergoing desiccation. Transcripts promoting senescence were diminishing in transcript abundance, whereas those delaying senescence were accumulating from 60% RWC throughout drying.

Clusters 13 and 8 (containing 280 and 644 transcripts respectively) represented transcripts accumulating in abundance upon moderate water-deficit stress (40% RWC, Figure 3.5.3). Several transcripts accumulating in abundance were associated with '*response to heat'* and '*temperature stimulus'* (cluster 13, containing 280 transcripts). These included seven transcripts encoding for heat-shock protein 20 (HSP20), one HSP90 gene and two MULTIPROTEIN BRIDGING FACTOR 1 (MBF1) genes, all proteins that function in heat and osmotic stress tolerance (Farrant *et al.* 2017). In plants, MBF1 is a transcriptional co-regulator that controls several developmental processes (Fan *et al.* 2017; Mariotti *et al.* 2000) and is associated with stress tolerance, particularly oxidative stress, where knockout Arabidopsis mutants showed increased sensitivity to oxidative stress (Arce *et al.* 2010). This supercluster therefore provided strong evidence that *E. nindensis* directs metabolic processes towards protection under environmental stress.

Cluster 8 (containing 644 transcripts) was enriched in the category '*circadian rhythm'*, which was dominated by transcripts relating to RNA transcription regulators (Figure 3.5.3). Similarly, '*iron-sulphur cluster assembly'* was over-represented within the DEGs in this cluster, which is associated with the synthesis of Fe-S proteins involved in DNA-synthesis and repair and oxidation-reduction reactions (Lill *et al.* 2015). This shows the protective mechanisms needed to convey desiccation tolerance by 40% RWC in the NST and is strong evidence of *E. nindensis* gearing towards desiccation. In addition, several ASPARAGINE SYNTHETASE transcripts were associated with '*cellular response to sucrose starvation*' and had a similar nitrogen metabolic role to GLUTAMINE SYNTHETASES that accumulated at 60% RWC in the NST, thus reiterating the role of controlled nutrient reshuffling upon

water-deficit stress for the continuation of protein synthesis and repair in the absence of photosynthetic carbon gain.

'*Photosynthesis', 'metabolic processes'* and '*regulation of hydrogen peroxide and ROS*' categories were over-represented in the DEGs diminishing in abundance at 40% RWC and were represented by cluster 10 and 6 (Figure 3.5.4). Transcripts associated with metabolite transport ('*membrane disassembly*') were diminishing in abundance. Again, these categories indicate metabolic arrest.

Accumulating transcripts associated with drying below 25% RWC in clusters 2 (containing 315 transcripts) and 5 (containing 392 transcripts) were enriched with biological functions relating to '*cellular respiration', 'protein folding', 'glucose transport', 'regulation of lipoprotein lipase activity'* and included several transcripts related to RNA transcription (Figure 3.5.5). The composition of enriched categories indicated that general maintenance is occurring in the desiccated state, or that they are cellular processes required for rehydration. For example, cellular respiration is one of the last processes to shut down upon desiccation and resume upon rehydration in resurrection plants (Farrant *et al.* 2007, 2017). The production of ATP is therefore stimulated to boost energy needed for the last few critical processes occurring at such low RWCs, particularly those processes related to maintaining protein folding. Similarly, the resumption of metabolism in an anhydrous, hypoxic state can be achieved through cellular respiration. Protein folding is required to maintain macromolecule integrity and reduce denaturing or mis-folded proteins that can be deleterious in the cell. Furthermore, the regulation of glucose transport and lipase activity suggests that these transcripts are accumulating in anticipation of the hydrolysis of complex reserves, such as starch or lipids throughout the desiccated state or upon rehydration. The accumulating transcripts associated with 25% RWC therefore shows a distinct shift towards the preservation of energy metabolism.

Clusters 14 and 7 (containing 334 and 382 transcripts respectively) showed that transcript abundance patterns that diminished in abundance below 25% RWC were involved in '*response to stimulus' and* defence *('multicellular organismal process', 'defence response'*) as well as representing a general arrest in metabolism and transport ('*protein phosphorylation', 'organic ion transport'* and *'transmembrane transport'*, Figure 3.5.6). This metabolic arrest was echoed in cluster 15, which represented transcripts diminishing in abundance in the desiccated state (Figure 3.5.7). DEGs in this supercluster were enriched with categories relating to metabolism *('secondary'* and '*amino acid'*), development *('root cap'* and *'vasculature'*) and *'response to stimulus'*. Few transcripts clustered into a single RWC category, except for those transcripts in cluster 11 (containing 375 transcripts), which exclusively diminished in abundance during rehydration and were associated with *'defence response'* and *'cellulose catabolic process'* (Figure 3.5.8).

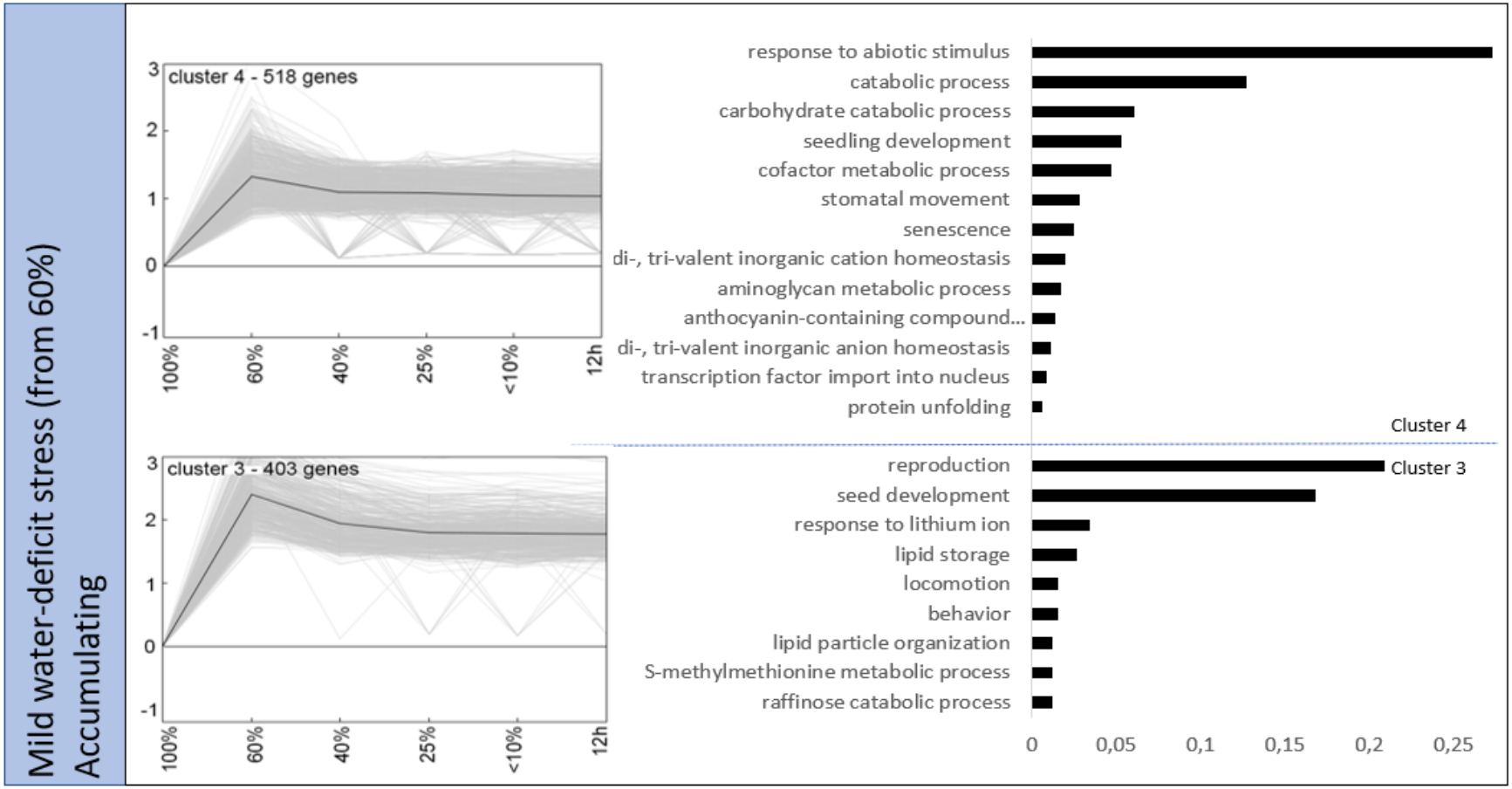

Figure 3.5.1: Clustering of DEGs with similar expression patterns and their corresponding over-enriched gene ontology (GO) categories show distinct changes in biological processes in the desiccation tolerant, non-senescent tissue (NST) of the resurrection plant *Eragrostis nindensis* upon mild (60% relative water content, RWC, %) water-deficit stress. K-means clustering (KMC) was performed in Genesis and shows two clusters with transcripts accumulating from 60% RWC throughout desiccation (<10% RWC) and rehydration (12h). Horizontal bar graphs represent the ratio of the observed versus expected frequency of the category compared to the entire dataset, indicating the contribution of each category within a cluster. DEG = differentially expressed genes. RWC = relative water content.

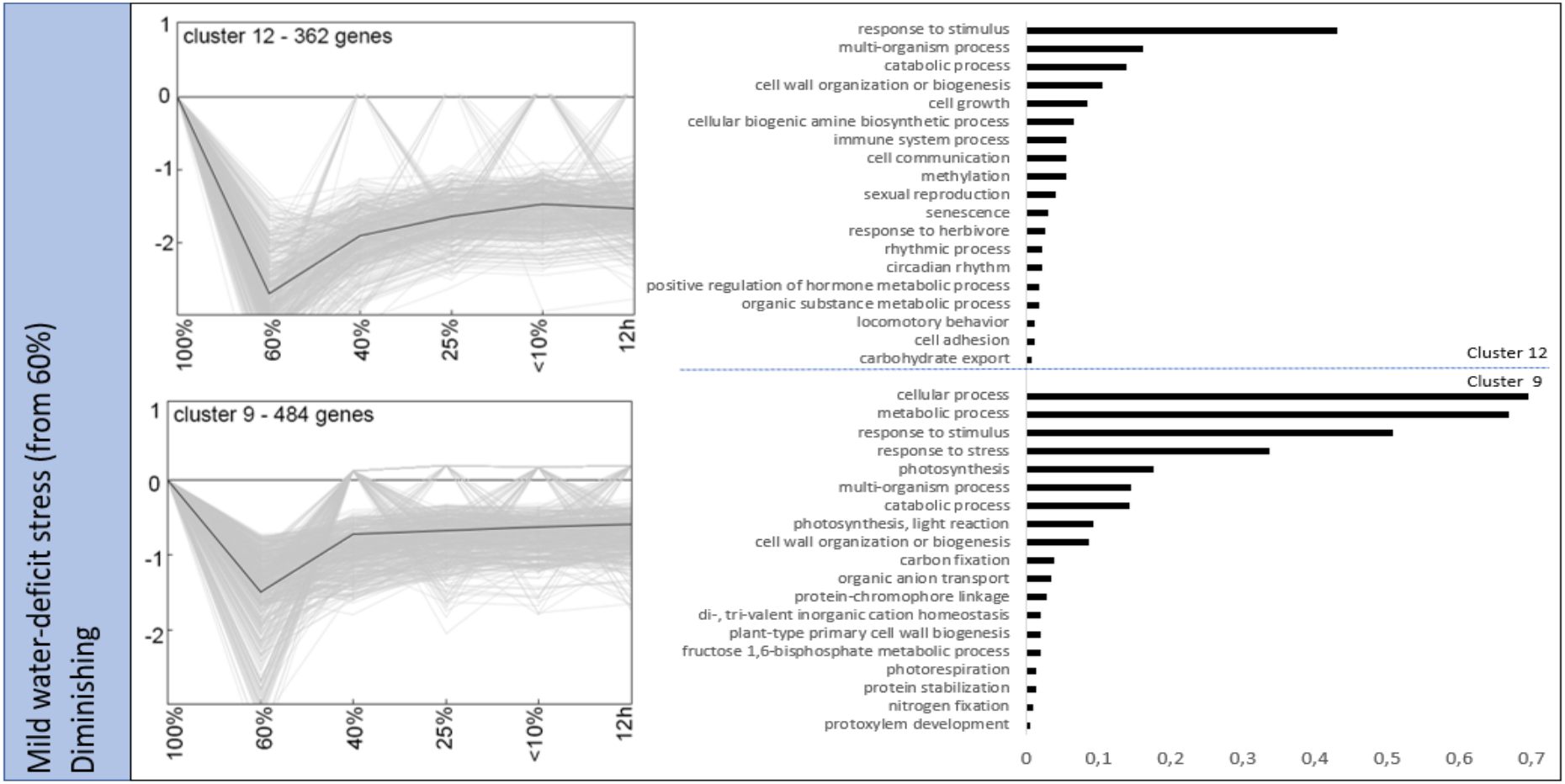

Figure 3.5.2: Clustering of DEGs with similar expression patterns and their corresponding over-enriched gene ontology (GO) categories show distinct changes in biological processes in the desiccation tolerant, non-senescent tissue (NST) of the resurrection plant *Eragrostis nindensis* upon mild (60% relative water content, RWC, %) water stress. K-means clustering (KMC) was performed in Genesis and shows two clusters with transcripts diminishing from 60% RWC throughout desiccation (<10% RWC) and rehydration (12h). Horizontal bar graphs represent the ratio of the observed versus expected frequency of the category compared to the entire dataset, indicating the contribution of each category within a cluster. DEG = differentially expressed genes. RWC = relative water content.

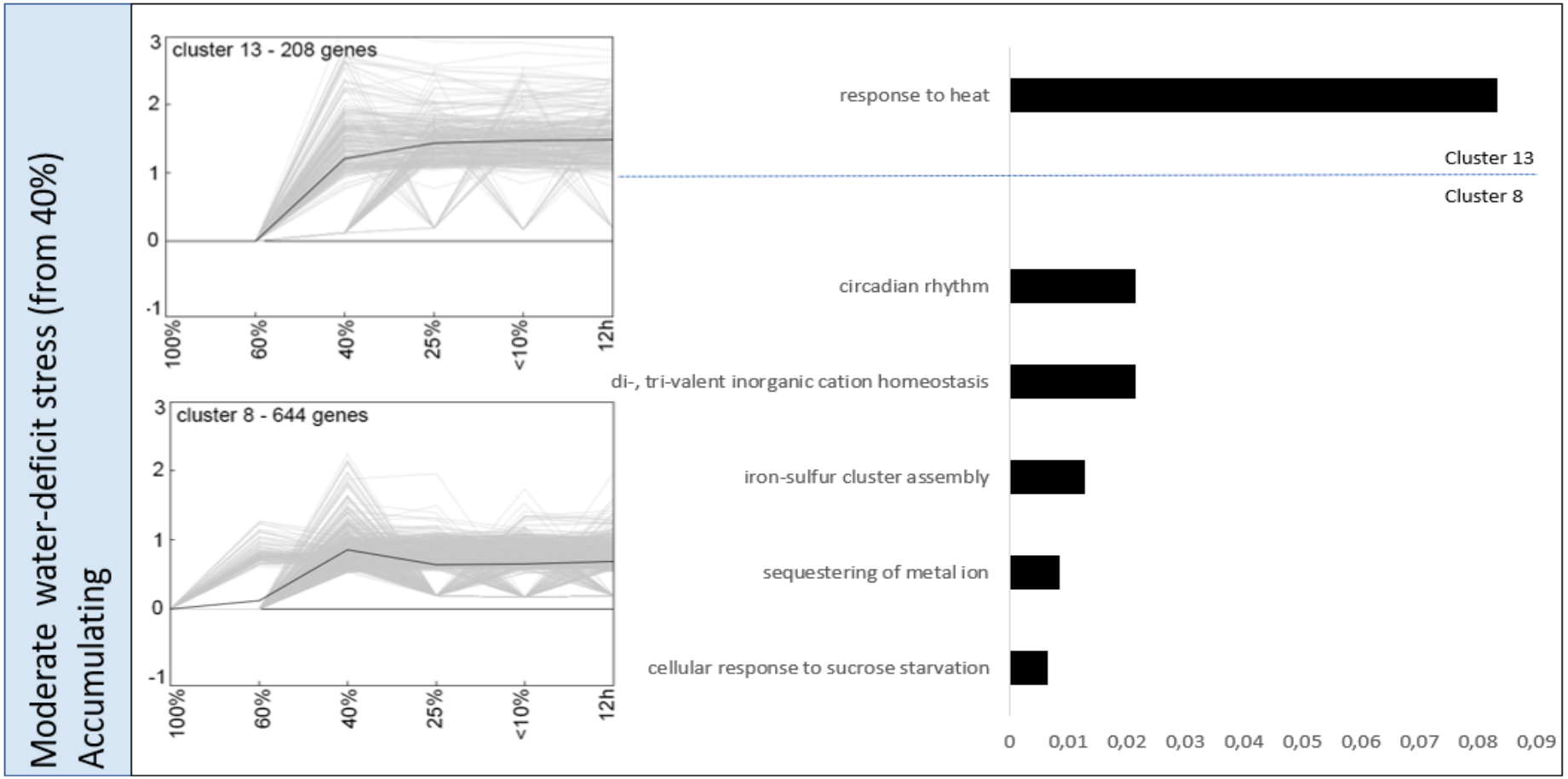

Figure 3.5.3: Clustering of DEGs with similar expression patterns and their corresponding over-enriched gene ontology (GO) categories show distinct changes in biological processes in the desiccation tolerant, non-senescent tissue (NST) of the resurrection plant *Eragrostis nindensis* upon moderate (40% relative water content, RWC, %) water-deficit stress. K-means clustering (KMC) was performed in Genesis and shows two clusters with transcripts accumulating from 40% RWC throughout desiccation (<10% RWC) and rehydration (12h). Horizontal bar graphs represent the ratio of the observed versus expected frequency of the category compared to the entire dataset, indicating the contribution of each category within a cluster. DEG = differentially expressed genes. RWC = relative water content.

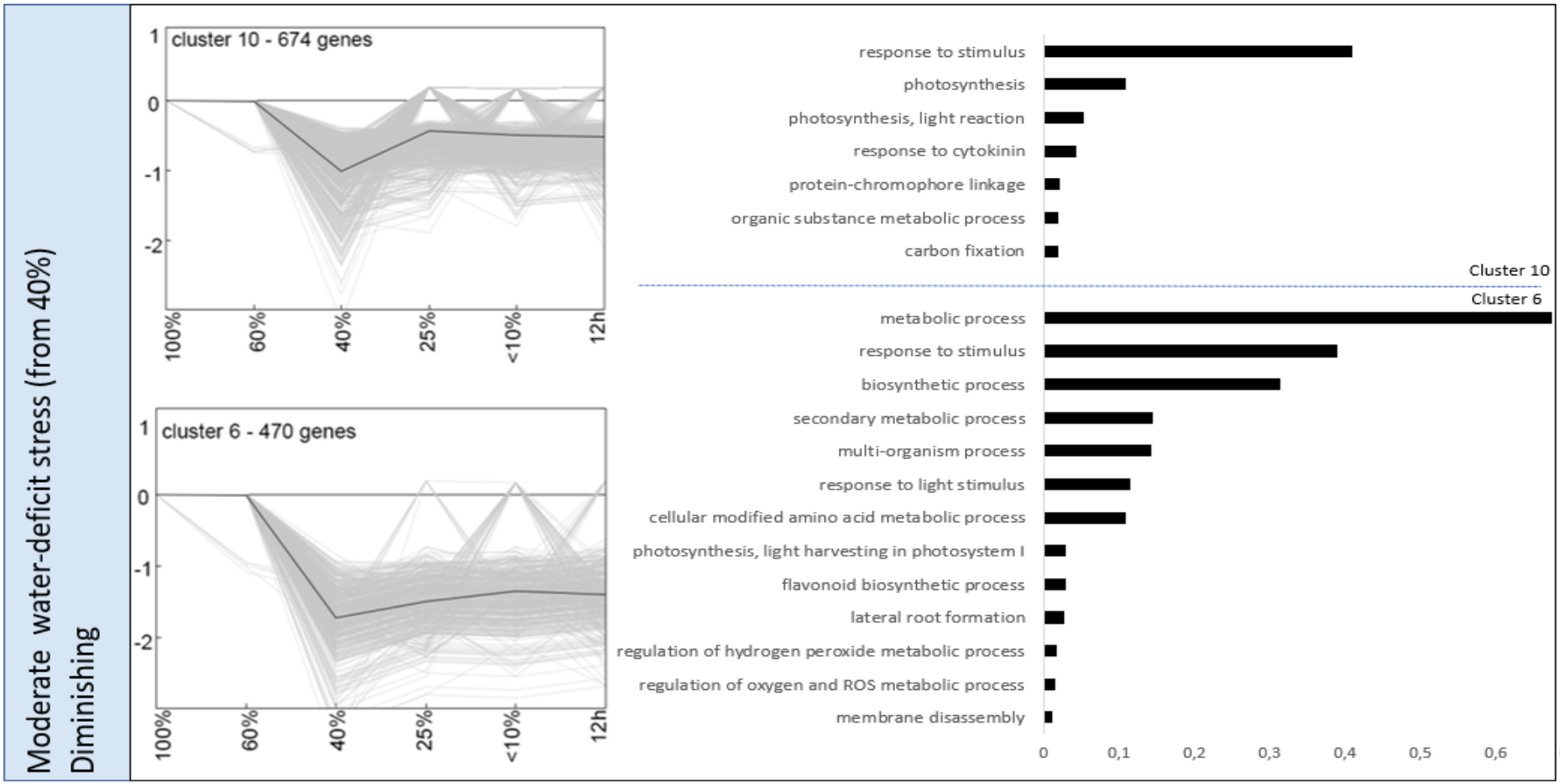

Figure 3.5.4: Clustering of DEGs with similar expression patterns and their corresponding over-enriched gene ontology (GO) categories show distinct changes in biological processes in the desiccation tolerant, non-senescent tissue (NST) of the resurrection plant *Eragrostis nindensis* upon moderate (40% relative water content, RWC, %) water-deficit stress. K-means clustering (KMC) was performed in Genesis and shows two clusters with transcripts diminishing from 40% RWC throughout desiccation (<10% RWC) and rehydration (12h). Horizontal bar graphs represent the ratio of the observed versus expected frequency of the category compared to the entire dataset, indicating the contribution of each category within a cluster. DEG = differentially expressed genes. RWC = relative water content.

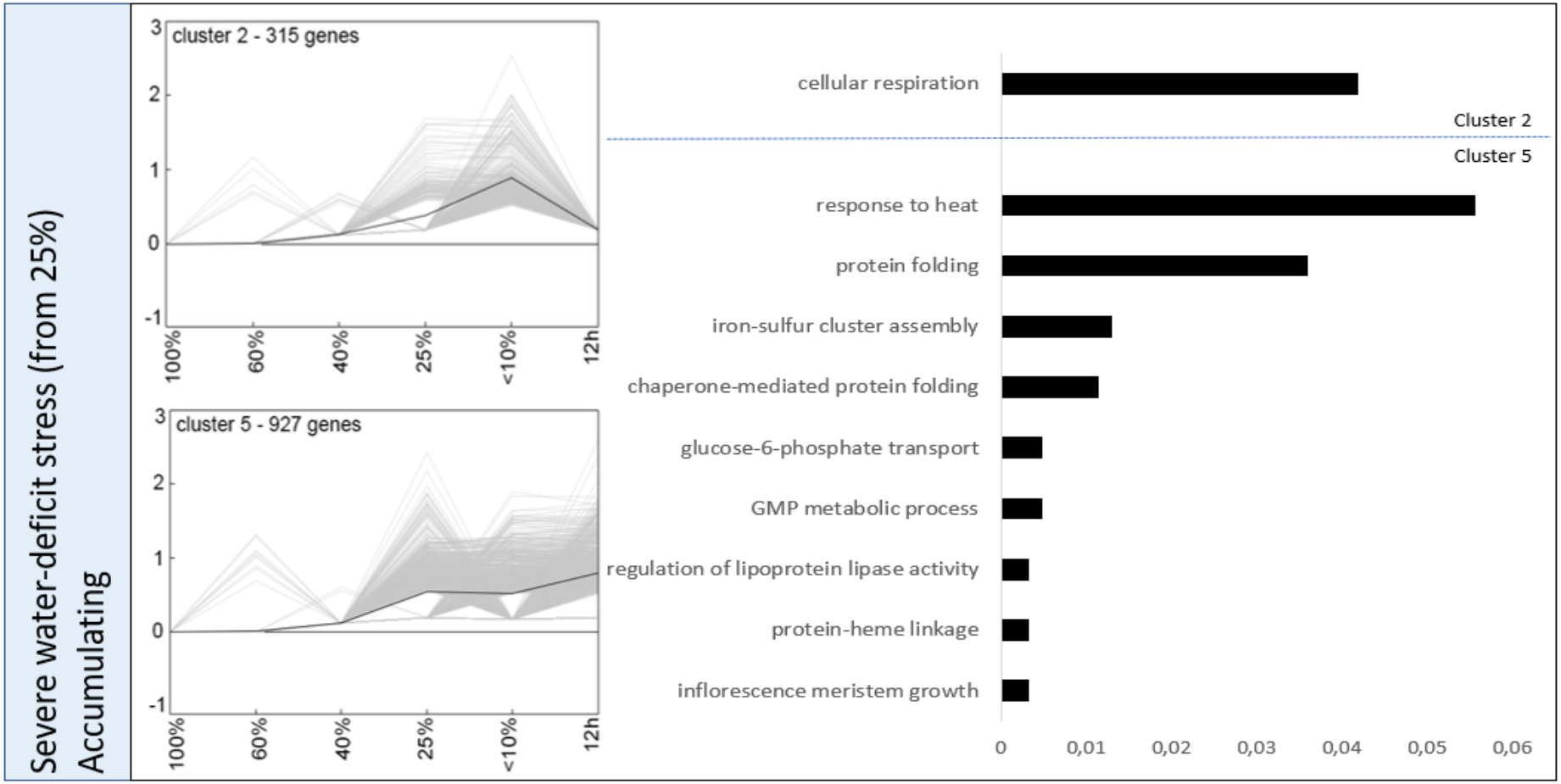

Figure 3.5.5: Clustering of DEGs with similar expression patterns and their corresponding over-enriched gene ontology (GO) categories show distinct changes in biological processes in the desiccation tolerant, non-senescent tissue (NST) of the resurrection plant *Eragrostis nindensis* upon severe (25% relative water content, RWC, %) water-deficit stress. K-means clustering (KMC) was performed in Genesis and shows two clusters with transcripts accumulating from 25% RWC throughout desiccation (<10% RWC) and rehydration (12h). Horizontal bar graphs represent the ratio of the observed versus expected frequency of the category compared to the entire dataset, indicating the contribution of each category within a cluster. DEG = differentially expressed genes. RWC = relative water content.

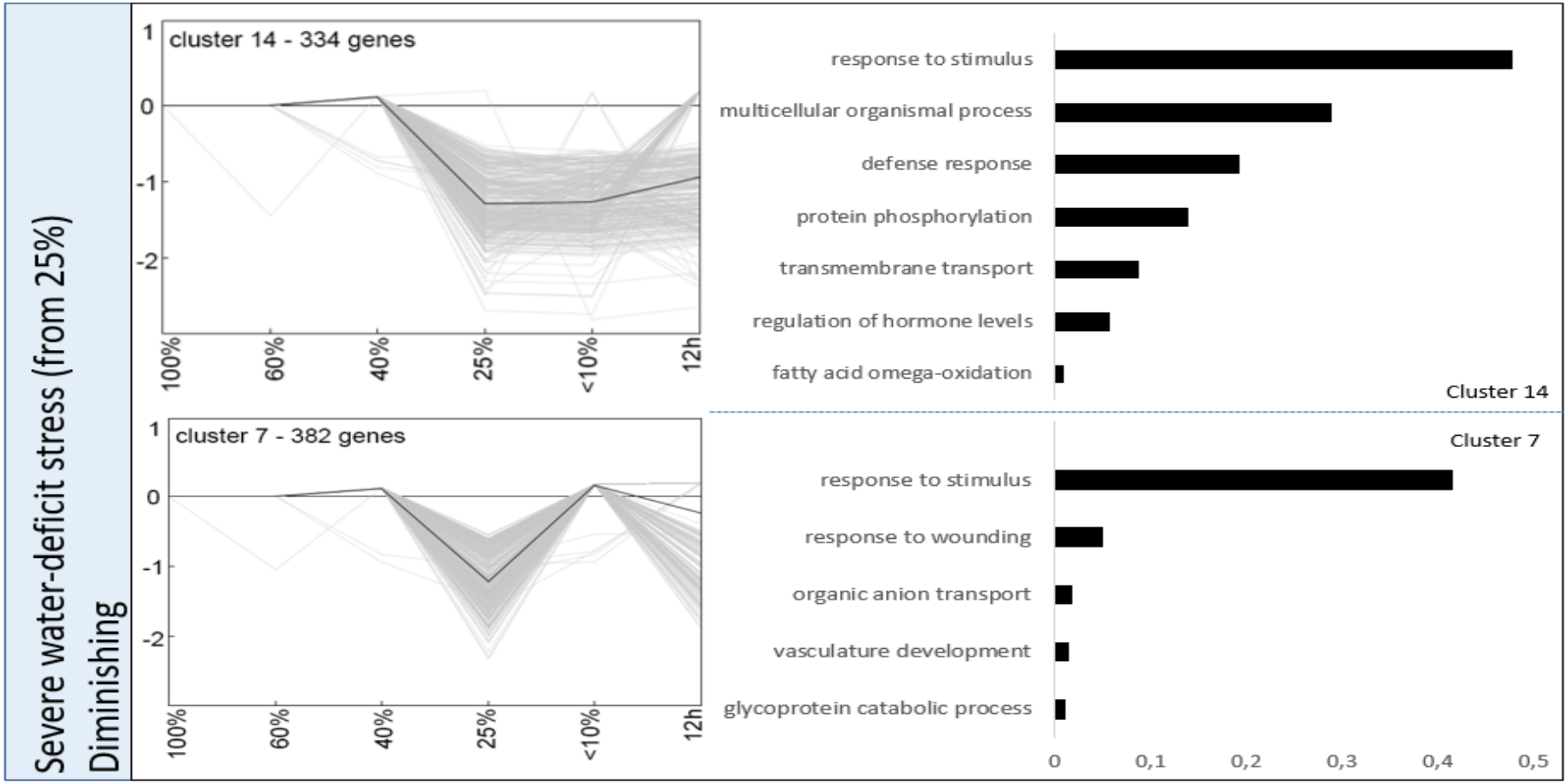

Figure 3.5.6: Clustering of DEGs with similar expression patterns and their corresponding over-enriched gene ontology (GO) categories show distinct changes in biological processes in the desiccation tolerant, non-senescent tissue (NST) of the resurrection plant *Eragrostis nindensis* upon severe (25% relative water content, RWC, %) water-deficit stress. K-means clustering (KMC) was performed in Genesis and shows two clusters with transcripts diminishing from 25% RWC throughout desiccation (<10% RWC) and rehydration (12h). Horizontal bar graphs represent the ratio of the observed versus expected frequency of the category compared to the entire dataset, indicating the contribution of each category within a cluster. DEG = differentially expressed genes. RWC = relative water content.

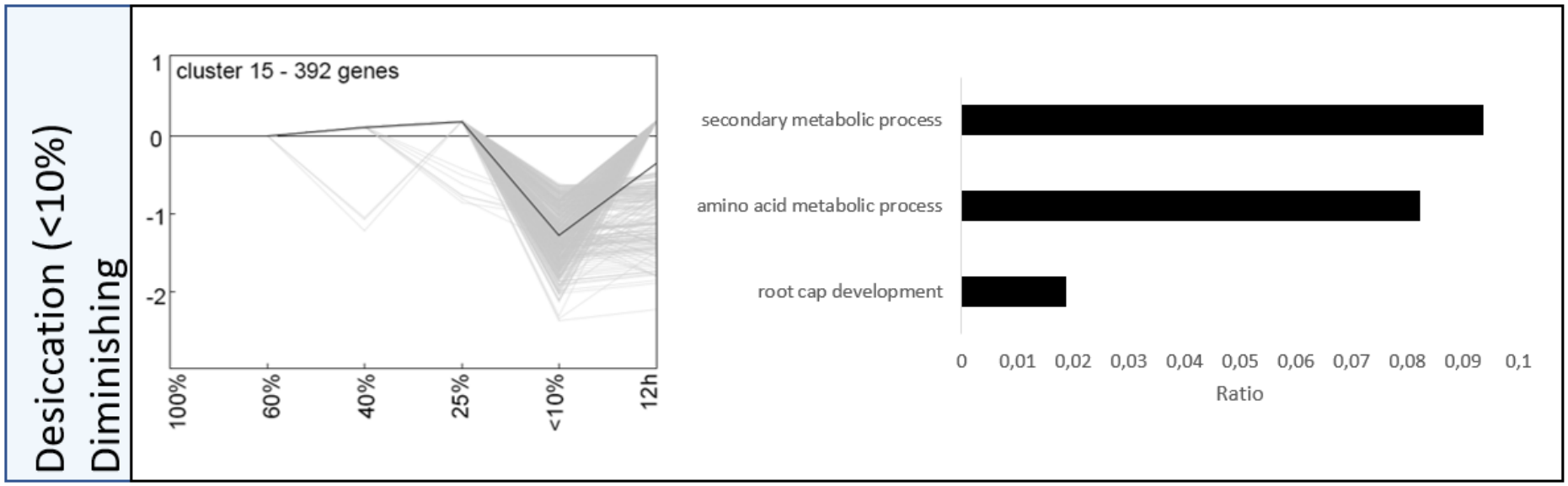

Figure 3.5.7: Clustering of DEGs with similar expression patterns and their corresponding over-enriched gene ontology (GO) categories show distinct changes in biological processes in the desiccation tolerant, non-senescent tissue (NST) of the resurrection plant *Eragrostis nindensis* upon desiccation (<10% relative water content, RWC, %). K-means clustering (KMC) was performed in Genesis and shows one cluster with transcripts diminishing from in the air-dry state (desiccation, <10% RWC) and rehydration (12h). Horizontal bar graphs represent the ratio of the observed versus expected frequency of the category compared to the entire dataset, indicating the contribution of each category within a cluster. DEG = differentially expressed genes. RWC = relative water content. RWC = relative water content.

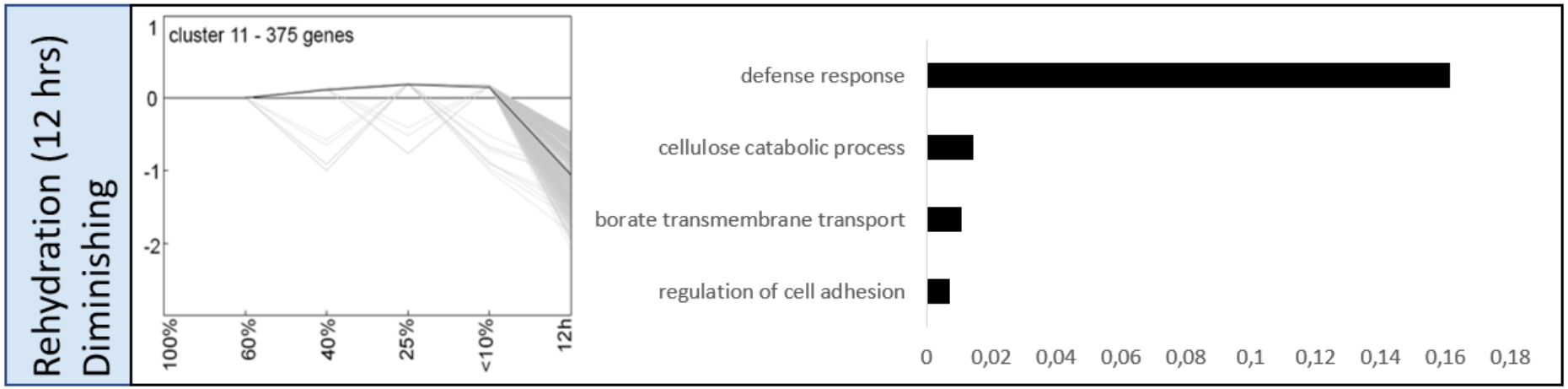

Figure 3.5.8: Clustering of DEGs with similar expression patterns and their corresponding over-enriched gene ontology (GO) categories show distinct changes in biological processes in the desiccation tolerant, non-senescent tissue (NST) of the resurrection plant *Eragrostis nindensis* during rehydration (12h). K-means clustering (KMC) was performed in Genesis and shows one cluster with transcripts diminishing from during rehydration (12h). Horizontal bar graphs represent the ratio of the observed versus expected frequency of the category compared to the entire dataset, indicating the contribution of each category within a cluster. DEG = differentially expressed genes. RWC = relative water content.

3.4. CONCLUSION

Eragrostis nindensis displays true vegetative desiccation tolerance that is genetically determined in the younger leaves upon desiccation. In the NST, the desiccation tolerance programme is dominated by core traits involved in broad biological processes that are common across all RWCs in the NST. These include well-known responses to desiccation (response to ABA, ROS, heat, sucrose, etc.), the accompanying reshuffling in metabolism (especially the shutdown of photosynthesis and growth arrest, and the accumulation of lipid storage, sucrose, RFO and nitrogen metabolism, and carbon partitioning/energy metabolism), and the transport of the metabolic intermediates and by-products of said metabolism. These processes are the same as described in other resurrection plants (Farrant *et al.* 2017, 2015; Dinakar *et al.* 2018). Some interesting features were apparent, such as starch catabolism diminishing (Figure 3.4.2) coupled with the simultaneous increase in lipid metabolism and storage (Figure 3.4.1), which might suggest that starch is not the primary energy store and emphasises the crucial role of lipids in the energy metabolism of *E. nindensis*. This is supported by starch granules being observed in the desiccated leaves and the distinct accumulation of lipid bodies in the NST (**Chapter 2,** Figure 2.12). *E. nindensis* appears to be using lipid bodies as a dominant storage for energy reserves, as reflected in the TEM (**Chapter 2**) and the transcriptomic signature (Figure 3.5.1). Furthermore, the observed enrichment in RNA transcription at lower water contents highlights the important role of organised and complex regulation upon severe abiotic stress. RNA related transcripts are overrepresented at 25% RWC (e.g. cluster 5) and the reoccurring trend of transcripts involved in RNA transcription (e.g. MBF1) reiterates this. This regulatory control is similar to that observed in seeds during maturation and development (Sajeev *et al.* 2019).

Parallels between *E. nindensis* and seed development have been previously drawn (Costa *et al.* 2017b; VanBuren *et al.* 2017), which is the foundation of desiccation tolerance in resurrection plants. In *E. nindensis,* seed-related transcripts are associated with metabolic arrest in preparation of seed dormancy. This, coupled with these transcripts significantly accumulating in abundance from 60% RWC throughout drying, suggests that at least some component of these transcripts could be a general drought response and might be common across all angiosperms. Recently, Pardo *et al.* (2019) have shown that non-resurrection plants also increase the transcript abundance of some seed-related transcripts in response to water-deficit stress, however, the authors state that transcript expression is insufficient or too late to prevent cellular damage and fails to prevent cell death. To investigate this further, the seed-related signature between the NST and ST needs to be compared, which is analysed in **Chapter 4**. Nevertheless, in *E. nindensis* common DEGs were enriched with seed-related GO

categories and represent the evolutionary redirection of seed associated metabolic pathways towards the acquisition of desiccation tolerance in vegetative tissues in a controlled manner.

Distinct biological processes act in concert and reflect the shifts in metabolism at different stages of water-deficit stress. These shifts are reflected in the KMC analysis, reinforcing the ordered shifts in metabolism from a photosynthesising, active plant to a quiescent metabolic state. These stages showed broad transitions accompanying different stresses; with general photosynthetic and growth shutdown (from mild water-deficit stress at 60% RWC), protection of cellular structure through unfolded protein responses and redirection towards protein maintenance and protection (from moderate water-deficit stress 40% RWC), to regulation of transcription (from severe water-deficit stress <25% RWC), and transcription towards DNA repair in the desiccated state (<10% RWC).

A transcriptomic desiccation tolerance signature in *E. nindensis* was identified and contributes to the broader understanding of desiccation tolerance in grasses (Poaceae) to inform future engineering of drought resistant crops. A comprehensive overview of desiccation tolerance traits in the NST of *E. nindensis* was established and how this species functions upon severe water-deficit stress is now better understood. It has been shown that *E. nindensis* conforms to the known desiccation tolerance traits in its NST.

How the molecular processes differ between desiccation tolerant and desiccation sensitive leaves is discussed in the following **Chapter**, which delves into the molecular regulation of senescence in *E. nindensis*.

Chapter 4

MOLECULAR PROCESSES REGULATING NST AND ST IN *E. NINDENSIS*

4.1. INTRODUCTION

Senescence is genetically regulated through developmental and environmental signals and ultimately ends in cell death (Balazadeh *et al.* 2010; Guo 2018). It can be a mitotic process, characterised by the inability to properly replicate (e.g. cell division upon aging), or a post-mitotic process, described as a degenerative process (e.g. degrading organelles, proteins, chlorophyll etc. for nutrient remobilisation) after cellular maturation that results in cell death (Lim *et al.* 2003; Griffiths *et al.* 2014). Senescence induced by stress acts on existing cells and is therefore mostly post-mitotic (Lim *et al.* 2003). In resurrection plants, stress-related degenerative processes also resemble post-mitotic senescence, such as the dismantling of chlorophyll and photosynthetic components in poikilochlorophyllous resurrection plants. However, senescence-related cell death is mitigated in desiccation tolerant leaves through the extraordinary redirection of metabolism from growth towards the synthesis of protective compounds and eventual metabolic shutdown (Farrant *et al.* 2017). Metabolic arrest has been linked with delayed senescence, potentially due to a reduction in oxidative stress, as shown in an *ore4-1* Arabidopsis mutant that exhibits only partially functional chloroplasts and displayed a delay in the senescence phenotype (Munné-Bosch *et al.* 2002; Lim *et al.* 2003). Resurrection plants engage in cellular protection by shutting down the processes resulting in excessive ROS, as seen in *Sporobolus stapfianus,* where transcripts associated with carbon fixation and photosynthesis were significantly reduced during dehydration, indicating the regulated shutdown of photosynthesis (Yobi *et al.* 2017). The transition of *E. nindensis* from hydrated, metabolically active NST to a quiescent metabolic state upon desiccation was described in **Chapter 3.** This demonstrated the general metabolic arrest and accompanied accumulation of protectants during drying for protection in the desiccated state, however, how senescence itself is regulated has not yet been explored.

It has been shown, to some degree, that the desiccation tolerant tissues of resurrection plants inhibit senescence by co-ordinating the different processes that trigger senescence in desiccation sensitive species (Griffiths *et al.* 2014). This ability to avoid stress-induced senescence is a key feature of desiccation tolerance. Other than a few key studies (e.g. Griffiths *et al.* 2014; Christ *et al.* 2014; Williams *et al.* 2015) research into senescence in resurrection plants has not been adequately explored. SAGs have been observed to decrease in desiccation tolerant leaves (Griffiths *et al.* 2014) and inferences have been made about how tolerant tissues mitigate senescence. For example, the elevated cytokinin levels in *S. stapfianus* is thought to be implicated in the suppression of senescence upon desiccation as this hormone is attributed to the onset of senescence in desiccation sensitive species (Munné-Bosch *et al.* 2004; Griffiths *et al.* 2014). Yet, senescence is a complex phenomenon that cannot be explained by suppressing SAGs or hormones alone (Woo *et al.* 2013; Yolcu *et al.* 2018). Comparison of NST and ST in the same species can give insight into what other processes are involved. To date, there has been no published study conducted, in which comparative characterisation of the changes in genetic control between young, desiccation tolerant tissues that prevent senescence (i.e. NST) and older tissues that succumb to stress-associated damage (i.e. ST). In *Eragrostis nindensis,* the fact that the older leaves die during drying suggests that senescence is developmentally programmed (Woo *et al.* 2013; Griffiths *et al.* 2014; Guo 2018). However, these leaves would grow normally in the absence of abiotic stress and show a premature death induced by water-deficit stress (i.e. post-mitotic senescence). The ST in *E. nindensis* is therefore regulated by environmental cues. This **Chapter** explores how the genetic programme of the tissue destined to senesce differs from the surviving NST.

In this **Chapter**, the differences in transcript abundance patterns of NST and ST are examined. A transcriptomic analysis is presented, which focusses on how *E. nindensis* responds to desiccation and, additionally, how these processes differ to those in tissues that fail to prevent cell death. Overrepresented GO categories in each RWC showed general trends and biological processes involved in desiccation tolerance. Common biological pathways and their underlying transcripts were identified in NST and ST upon desiccation. Finally, a targeted approach looking at known desiccation tolerance associated transcripts encoding for LEAs, HSPs, stabilising sugars and their transports, antioxidants, aquaporins, and senescence was explored. This is followed by an in-depth analysis of transcripts exclusively being expressed in either tissue type. This is based on the premise that those transcripts present in NST, but absent in ST, are critical for desiccation tolerance and represent the key transcripts that regulate desiccation tolerance and senescence. Furthermore, the role of RNA regulation and protein metabolism were identified as key traits differentiating the NST from the ST in *E. nindensis*.

4.2. METHODS

The procedures for seedling germination, plant growth and dehydration/rehydration of plants as described in **Chapter 2**, RNA extraction, quality control, transcriptome assembly through the bioinformatic pipeline, annotation and analysis (BiNGO and functional enrichment) were the same as described in **Chapter 3.** DEGs were condensed into over-represented GO categories. In a few instances transcript composition in a category was discussed. These specific transcripts are not reported in the text because they consist of hundreds of transcripts, however, when specifically mentioned, are listed in the Appendix, page 229 onwards. ST was sampled from the same plants utilised for NST studies, such that the samples were as closely matching as possible. Since this **Chapter** investigates whether the desiccation tolerance programme in the NST is transcriptionally engaged in the ST (or not), a targeted analysis of the core set of transcripts involved in desiccation tolerance associated metabolic pathways was undertaken for both tissue types. Analysis of DEGs occurring only within one tissue type is referred to as "exclusive" and includes the subset of DEGs present in one tissue type only (e.g. accumulating or diminishing exclusively in NST). Hidden Markov Models generated by Pfam were used to identify proteins of interest. Metabolic pathways relating to sugars and cell wall metabolism were interpreted using Mercator version 4.0 (Schwacke *et al.* 2019) and Mapman (Thimm *et al.* 2004).

4.3. RESULTS AND DISCUSSION

4.3.1. Transcriptome overview of senescence

A total of 8185 transcripts were considered differentially expressed compared to the control (100% RWC, NST). The majority of these DEGs occurred in the NST (7643 transcripts), however, many of these were shared with the ST, which had 5494 DEGs shared across all water contents (Figure 4.1). There were more DEGs exclusive to the NST (2690 transcripts) compared to only 542 transcripts that were exclusive to the ST, demonstrating that the desiccation tolerance programme in the NST was evident. The differences in the number of DEGs alone indicated that the NST was under a more complex regulatory control.

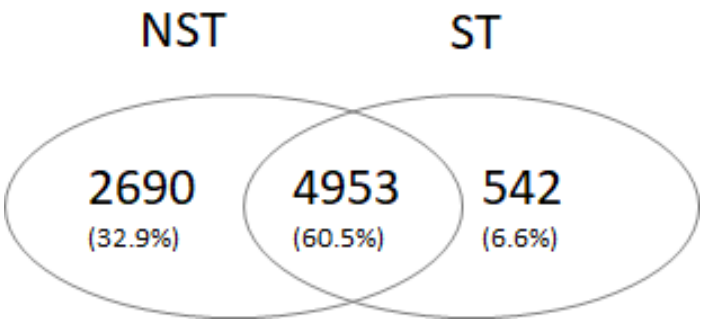

Figure 4.1: The desiccation tolerant, non-senescent tissue (NST) of the resurrection plant *Eragrostis nindensis* contained more differentially expressed genes (DEGs, n = 7643), and more exclusively present DEGs (n = 2690) when compared with the desiccation sensitive, senescent tissue (ST). DEGs were defined as having statistically significant differences in transcript abundance (>2.0 or <-2 log_2 fold change, FDR <0.05) compared to the control (fully hydrated NST).

Three DEGs were identified as being differentially expressed in the ST at 100% RWC, where one transcript was accumulating (Eni_004103, fold change (FC) = 8.8, FDR = 0.032) and two transcripts diminishing (Eni_011626, FC = -8.9, FDR = 0.004, Eni_064039, FC = -11.1, FDR = 0.032) in abundance (Appendix, Figure A4). Since these tissues have not been subjected to abiotic stress, these DEGs are likely to represent developmental senescence and signify the first significant change in transcript abundance. The low number of DEGs when fully hydrated validates that the transcript abundance in the NST and ST was similar before the onset of water-deficit stress and reiterates that changes in transcript abundances during dehydration, desiccation and rehydration were stress-induced. The only DEG that accumulated in abundance at 100% RWC in the ST compared to the NST was a xylase (AtXYN1, AT1G58370), which is associated with cell wall degradation (Suzuki *et al.* 2002; Endo *et al.* 2018). Xylem cell wall organisation is important for solute transport and transcription and regulates the relationship between cell wall formation and stress signalling (Endo *et al.* 2018; Gao *et al.* 2018; Jeong *et al.* 2018). This might indicate nutrient reshuffling associated with a mature leaf. Two DEGs were diminished in abundance at 100% RWC in the ST when compared to the NST. One of these DEGs (Eni_011626) is associated with metal handling, binding, chelation and storage (AT5G49940) and is a NifU-like protein required for the biosynthesis of ferredoxin, a major electron carrier in PSI (Yabe 2004). Knock-out mutants of this gene in Arabidopsis were dwarfed, showed impaired PSI, and exhibited chlorotic leaves (Yabe 2004). This gene is therefore associated with the functioning of chloroplasts and hence photosynthesis. The other DEG (Eni_064039, AT5G50740) is predicted to be located in the plasma membrane and cytoplasm, and is involved in heavy-metal iron transport and detoxification (De Abreu-Neto *et al.* 2013). This gene has been implicated in maintaining metal homeostasis and plays a role in the regulation of the transcription response to cold and drought (Barth *et al.* 2009; De Abreu-Neto *et al.* 2013). It is interesting to detect evidence of transport and shutdown

of photosynthesis in the hydrated ST, as these are two major biological processes associated with senescence. These relatively minor changes suggest that developmental leaf senescence has been initiated. Senescence is a slow process and can start even before leaf maturation (Breeze *et al.* 2011) and might be an important signal to determine if the leaf will undergo processes to protect and survive abiotic stress (NST), or if the leaf is doomed to senesce (ST).

Transcript abundance changes were observed at 60% RWC in both tissue types and continued throughout drying and rehydration (Figure 4.2). Interestingly, there were new transcripts differentially abundant at 25% RWC in both tissue types, at 18% RWC in the ST and <10% RWC and 12h rehydration in the NST. This suggests that *E. nindensis* is still actively transcribing RNA at very low water contents between 25% and 10% RWC, and by 12h after re-watering when RWC has returned to ~ 20% RWC. In this tissue most transcripts remained differentially expressed during rehydration, with 210 DEGs exclusively accumulating and 393 DEGs exclusively diminishing in the NST (discussed in Table 3.3). Overall, there were more transcripts diminishing than accumulating in abundance, hinting at evidence of metabolic arrest upon desiccation, a well-documented desiccation tolerance trait (Challabathula *et al.* 2016; Costa *et al.* 2017b). The number of both accumulating and diminishing DEGs consistently increased upon water-deficit stress, indicating a corresponding metabolic shift.

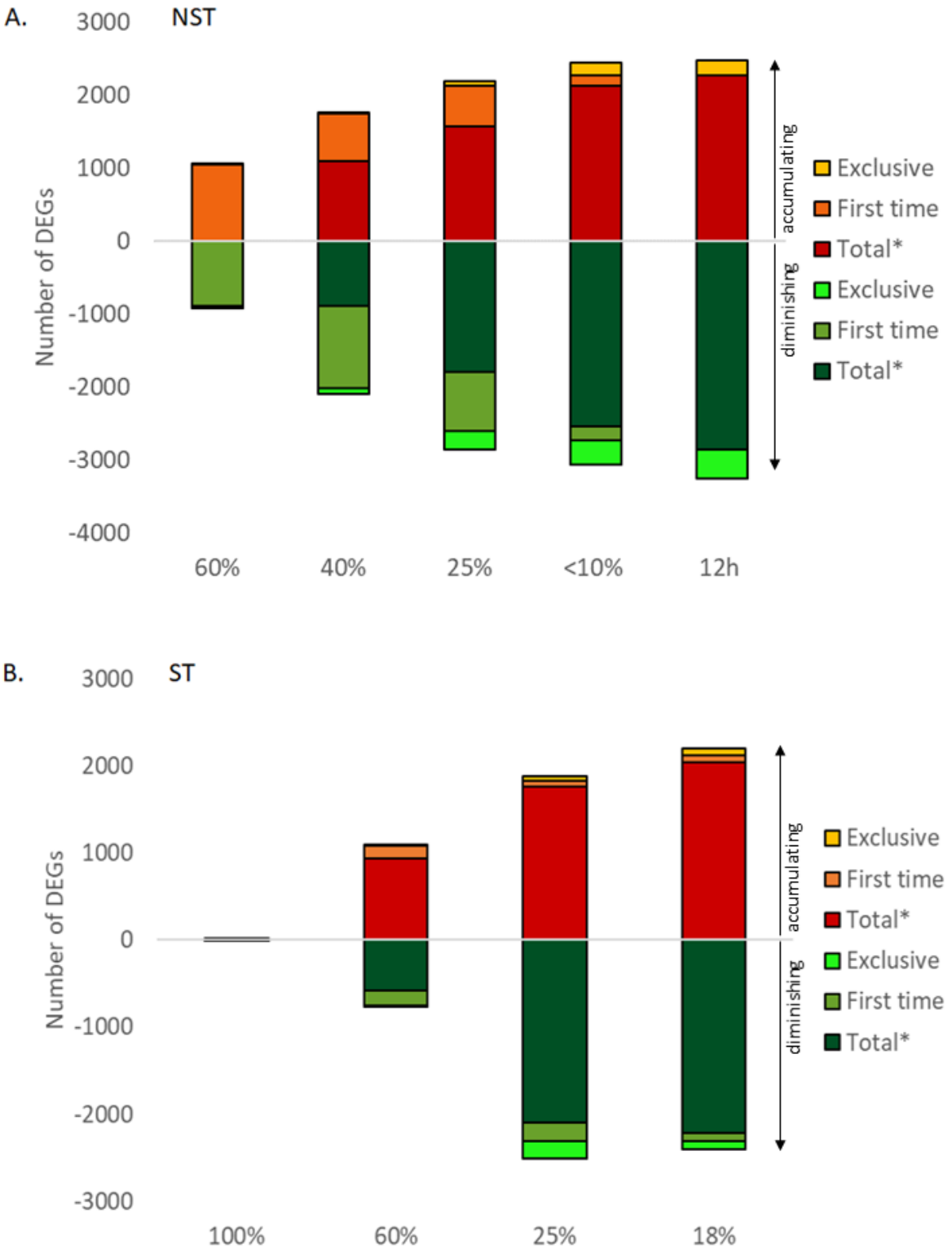

Figure 4.2: Changes in transcript abundance patterns during drying (represented as relative water content, RWC, %) and rehydration (12h) showing differentially expressed genes (DEGs) accumulating and diminishing in transcript abundance compared to the fully hydrated control (NST) in the (A) non-senescent tissue (NST) and (B) senescent tissue (ST) of the resurrection plant *Eragrostis nindensis*. There were only three DEGs in the ST when both leaves were hydrated (100% RWC), however, this number increased with further drying. Total* transcripts excludes transcripts that are expressed exclusively or for the first time. First time transcripts do not include exclusive transcripts. RWC = relative water contents, DEG significance was defined as >2 or <-2 $\log_2$ fold change and FDR <0.05. DEGs are derived from both paired- and single-end reads.

4.3.2. Insights into known important traits of desiccation tolerance: a targeted analysis

Resurrection plants have captured the fascination of researchers since the 1970s and the accumulation of desiccation tolerance traits characterised in several species has revealed a core set of conserved desiccation tolerance responses (recently reviewed in Giarola *et al.* 2017; Farrant *et al.* 2017; Blomstedt *et al.* 2018). This core set includes LEAs, HSPs, osmoprotectants, antioxidants and ROS scavengers, and the accumulation of compatible solutes with the onset of osmotic adjustments, particularly sugars (sucrose, trehalose, raffinose family oligosaccharides (RFOs)). These metabolites need to be transported, and several transporter proteins are implicated, such as the 'SUGARS WILL EVENTUALLY BE EXPORTED TRANSPORTER' (SWEET) (Chen *et al.* 2012; Eom *et al.* 2015), sugar transporters (Jameson *et al.* 2016) and ATP-binding cassette (ABC) transporter genes (Vanderlinde *et al.* 2010).

4.3.2.1 Protective proteins: LEAs and HSPs

LEA proteins encompass the majority of stress-responsive proteins and are highly conserved across organisms (Bartels *et al.* 2005; Artur *et al.* 2018). LEAs are peculiar proteins as they are unfolded in aqueous solution and change structural conformation when dried, which allows them to have multiple functions and contributes to the formation of the "glassy state" (Shih *et al.* 2004; Tunnacliffe *et al.* 2007; Covarrubias *et al.* 2017). Intriguingly, their intrinsic disorder allows them to bind to several substrates within numerous biochemical solutions (formed under cellular desiccation) and are tightly associated with desiccation tolerance in seeds and vegetative tissues of resurrection plants (Leprince *et al.* 2010; Farrant *et al.* 2017; Artur *et al.* 2018). These stress-induced proteins are heat-stable and accumulate during the acquisition of desiccation tolerance, temperature stress (hot and cold), and salinity (Zhang *et al.* 2000; Hoekstra *et al.* 2001; Stevenson *et al.* 2016). As their name suggests they also become highly abundant during the late stages of embryo development. They are proposed to function in cellular protection upon water-deficit stress through their detoxifying and cell damage alleviating properties, prevent freezing or desiccation induced aggregation, promote vitrification, act as water-substitution molecules, and play a role in chaperoning or heat-shielding, amongst other functions (Bartels *et al.* 2005; Goyal *et al.* 2005; Umezawa *et al.* 2006; Oliver *et al.* 2009). Previously thought to be seed-specific proteins, transcript abundance of LEAs has been confirmed in several resurrection plant leaves, such as *Craterostigma plantagineum* (Giarola *et al.* 2015), *Boea hygrometrica* (Xiao *et al.* 2015), *S. stapfianus* (Le *et al.* 2007), *Xerophyta humilis* (Collett *et al.* 2004), *X. schlechteri* (Costa *et al.* 2017a) and *Myrothamnus flabellifolia* (Ma *et al.* 2015). The presence of LEAs in *E. nindensis* has also recently been confirmed (Pardo *et al.* 2019).

Due to their complexity and largely unknown functions, several classification systems have been utilised over time. However, as most LEA proteins can be grouped into eight families in the Pfam database according to their primary sequences, namely dehydrin (DHN), LEA_1, LEA_2, LEA_3, LEA_4, LEA_5, LEA_6, and seed maturation protein (SMP), this system has been applied in this work. LEA proteins from all eight families were identified according to the most commonly used method (as seen in Hilhorst *et al.* 2018; Artur *et al.* 2018). A total of 83 LEA, 14 DHN and 11 SMP motif-containing transcripts are present in the genome, of which 28, 12 and 5 respectively were differentially expressed upon desiccation and/or rehydration (Figure 4.3). This finding is proportionately similar to Costa *et al.* (2017a) where 126 LEA motif-containing transcripts were identified in the *X. schlechteri* genome, with 90 being differentially expressed. Transcripts for LEA proteins strongly accumulated at 60% RWC in both the NST and ST and maintained a constant expression throughout drying and rehydration, peaking slightly at 25% RWC (Figure 4.3, B). There appears to be little differences in the expression patterns between the tissue types, and this suggests that the ST is also engaging in a desiccation tolerant programme by accumulating LEA transcripts, or that these LEAs are important for other processes. Recently, Pardo *et al.* (2019) have shown a similar trend, where a non-resurrection plant *Eragrostis tef* showed an increase in LEA proteins upon water-deficit stress, and suggested that such seed desiccation related pathways might be engaged in grasses regardless of their tolerance to desiccation. However, the authors mention the ability to accurately express the proteins is impaired or is ineffective in mitigating the damage.

Only LEA_2 transcripts both accumulated and diminished during drying, a pattern observed in both tissue types (Figure 4.3). This is unsurprising given that LEA_2 has over 3,126 associated genes, by far the largest LEA family (Artur *et al.* 2018). Costa *et al.* (2017a) found similar trends in *X. schlechteri*, where LEA_2 transcript abundance decreased during late dehydration, suggesting the proteins from this family are not essential in conveying desiccation tolerance in this species. However, Magwanga *et al.* (2018) reported that overexpressing LEA_2 proteins lead to increased drought tolerance in upland cotton (*Gossypium hirsutum*) due to increased root length, higher antioxidants and lower oxidants, thus illustrating that the precise function of LEAs are unknown. The only LEAs that exclusively occurred during rehydration in the NST were two LEA_2 transcripts, and one HSP20 that diminished after rehydration. This suggests that large transcriptional changes in transcripts encoding these proteins have not occurred by 12h rehydration. In addition, there was slight variation amongst the tissue types with respect to expression patterns (Figure 4.3, A). Nevertheless, *E. nindensis* conforms to the current understanding of LEAs in resurrection plants, where the majority of LEA, DHN and SMP transcripts accumulated upon desiccation, surprisingly in both tissue types.

HSPs have predicted chaperone functions in that they assist in protein folding, aid protein and membrane stabilisation, and prevent aggregation by binding to proteins (Wang *et al.* 2004; Zhang *et al.* 2013). They are heat-stable, disordered like LEAs, accumulate upon desiccation and seed maturation, and show increased expression in transcripts and proteins upon desiccation in several resurrection plants and seeds (Buitink *et al.* 2006; Oliver *et al.* 2009; Farrant *et al.* 2017). In *E. nindensis* HSPs strongly accumulated upon desiccation in both the NST and ST (Figure 4.3, A). Three classes (HSP20, n = 21; HSP70, n = 15; and HSP90, n = 5) significantly increased in abundance. Of the 41 accumulating transcripts annotated as HSPs in *E. nindensis*, the most abundant belongs to a small heat shock protein (sHSP) with a molecular weight between 15-22 kDa (Waters 2013). A similar amount of sHSPs (n = 25) transcripts were identified as accumulating in desiccated *B. hygrometrica* leaves (Zhang *et al.* 2013). Previous studies have shown that sHSPs do not directly fold proteins, but rather initiate stabilisation by strongly binding to denatured substrates and passing them downstream to other chaperonins/HSPs that aid in protein folding (Wang *et al.* 2004; Sun *et al.* 2012). Furthermore, sHSPs do not require ATP to function, and are therefore energetically viable at low water contents, such as desiccation and the early stages of rehydration, when energy producing processes are limited (Bondino *et al.* 2012; Farrant *et al.* 2017). This might explain the high abundance of sHSP transcripts in *E. nindensis* upon desiccation and implies their importance in acquiring desiccation tolerance. However, the overall similarities in expression patterns in the NST and ST implies that the desiccation associated transcriptome is activated in STs, unless the HSPs have another function other than simply desiccation tolerance.

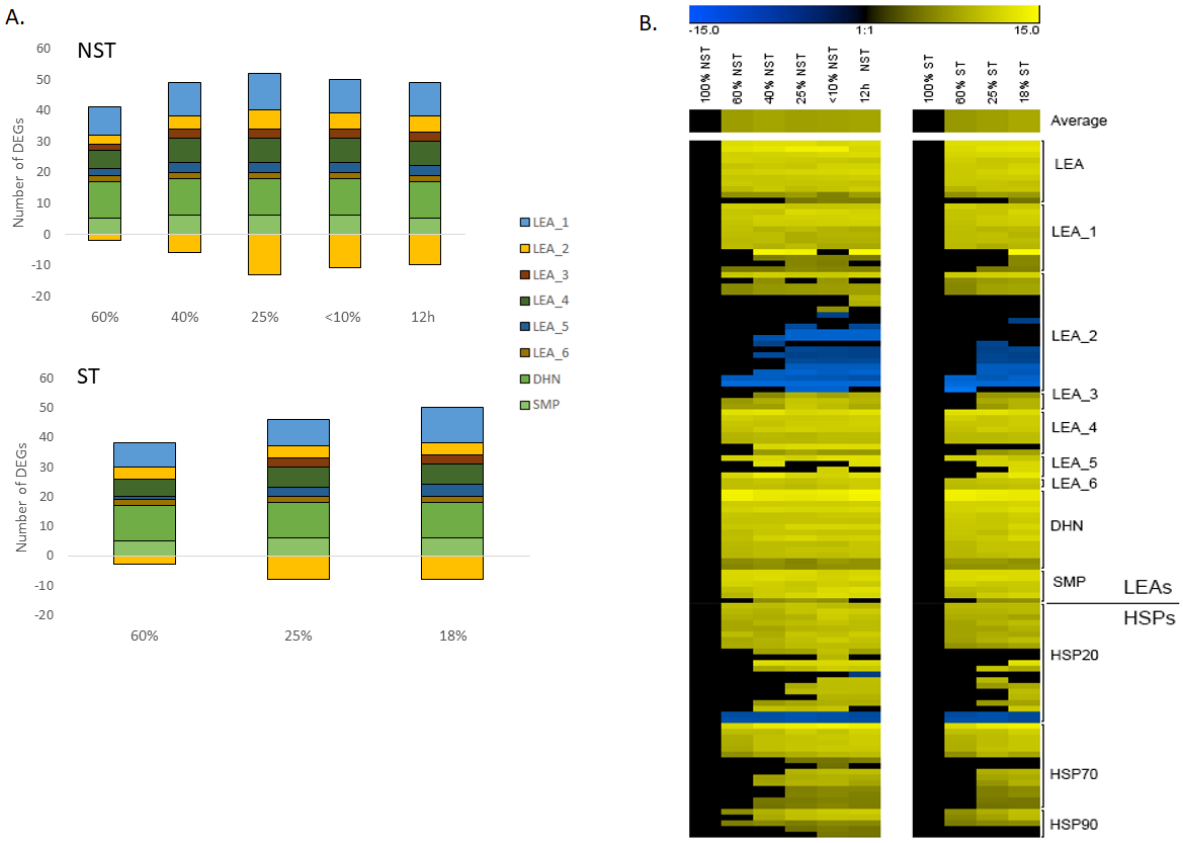

Figure 4.3: Expression profiles of LEAs (late embryogenesis abundant proteins) and HSPs (heat-shock proteins) at different relative water contents (RWC, %) in the desiccation tolerant, non-senescent tissue (NST) and desiccation sensitive, senescent tissue (ST) of the resurrection plant *Eragrostis nindensis* during drying and rehydration (12h). (A) Number of LEAs accumulating or diminishing in transcript abundance relative to the hydrated control (NST, 100% RWC). Top panel represents changes in the NST and bottom panel those in the ST. Colours represent the different LEA families described in the associated legend. Only differentially expressed genes (DEGs) are depicted, derived from the statistically significant change (>2 or <-2 log_2 fold change, FDR <0.05) in transcript abundance compared to the control (NST, 100% RWC). (B) Heatmap showing differential transcript abundance trends. The colour scale represents log_2 fold change values. Average bar indicates the mean expression trends during drying.

4.3.2.2 Sucrose and trehalose

Sucrose is a well-known key-player in desiccation tolerance as it not only acts as an energy source, but can stabilise cellular structures, counteract the reduction in osmotic potential during water-deficit stress, and potentially scavenge ROS (Hoekstra *et al.* 2001; Zhang *et al.* 2016a). Accumulation of sucrose is associated with the vitrification of cells upon desiccation in several resurrection plants, and is a mechanism to stabilise cells at low water contents (Buitink *et al.* 2004; Farrant *et al.* 2015, 2017). Furthermore, compounds, such as sugars can be preferentially excluded from proteins, keeping them preferentially hydrated and thus preventing denaturing or unfolding (Hoekstra *et al.* 2001). During drying, the absence of water requires vacuoles, organelles and cytoplasm to substitute water with such metabolites to provide an alternative medium that allows minimal, yet essential, macromolecular functioning, such as transcription and transport. These sugars also act as

osmoprotectants and help maintain cell turgor (Tang *et al.* 2017). In addition, sucrose can act as a signalling molecule that triggers downstream gene expression changes (Zwack *et al.* 2016). Given the importance of sugars in desiccation tolerance, their transcriptomic signatures in metabolic regulation and transport are discussed.

In the NST of *E. nindensis* leaf sucrose levels increase upon desiccation (Vander Willigen *et al.* 2004; Illing *et al.* 2005). Preliminary data suggests that sucrose accumulates in similar quantities in the ST (Dace, *unpublished*). This supports the notion that sucrose (and other sugars) accumulation is a general response to stress amongst all plants (Ruan 2014). Interestingly, *E. nindensis* does not accumulate sucrose to the extent of other resurrection plants, as illustrated by the percentage change in sucrose between hydrated and dry leaves in *X. humilis* (~90%), *M. flabellifolia* (~130%) and *S. stapfianus* (~100%), whereas *E. nindensis* has a ~7% change in sucrose upon desiccation (Illing *et al.* 2005). However, in an alternative study, Ghasempour *et al.* (1998) reported a comparatively similar increase in sucrose in *E. nindensis* compared to *S. stapfianus* and other resurrection plants, and this, coupled with the observed increase in sucrose from published sources (Vander Willigen *et al.* 2004; Illing *et al.* 2005), confirms that sucrose accumulates during drying in *E. nindensis*. It is possible that the total amount of sucrose might be underrepresented, as there could be differential sucrose locations in *E. nindensis*, in which bundle sheath cells, which displayed a greater degree of vacuolation and less wall folding, could have proportionately more sucrose than mesophyll cells, which mechanically stabilise through cell-wall folding (Figure 2.12). However, very low sucrose to RFO ratios in desiccated leaves were found in *Borya constricta, Microchloa kunthii* and especially in *E. nindensis* (Farrant *et al.* 2017), indicating that sucrose is not the dominant protective sugar in these species. It is possible that these species accumulate other complex reserves as storage compounds during drying along with sucrose, as is proposed for *E. nindensis*. This suggests that different solutes are accumulated during drying that provide a protective and/or energy storing role, in combination with sucrose. It is possible that lipids are playing an important additional energy storage role, as lipid accumulation was highly regular and abundant in the NST (Figure 2.12).

There is also no definitive evidence of autophagy upon desiccation (**Chapter 2**) and this, coupled with a potentially high nitrogen content potentially due to the breakdown of chlorophyll and photosynthetic constituents (due to the poikilochlorophyllous nature of this plant), suggests that the leaves would not experience energy starvation. In combination, this might explain the increase in sucrose during drying, but at comparably lower levels to other resurrection plants due to alternative sugars accumulating, and potentially the alternative energy storage mechanism of lipids. Nevertheless, sucrose did accumulate and this increase is likely derived from conversion of stored polysaccharides, such as stachyose, 2-octulose or starch, as sucrose accumulated after photosynthetic

shutdown (Illing *et al.* 2005). The conversion of reserves that accumulated in the hydrated state has been observed in *C. plantagineum, C. wilmsii* and *Lindernia brevidens*, where stored 2-octulose was converted into sucrose during drying, this being a feature of desiccation tolerant Linderniaceae (Bianchi *et al.* 1991; Cooper *et al.* 2002; Phillips *et al.* 2008; Oliver *et al.* 2011). Preliminary unpublished metabolome data on *E. nindensis* shows that 2-octulose is not present in *E. nindensis* and furthermore, few other sugars are present in high abundance in the hydrated tissues (Dace, *unpublished*). This suggests that sucrose is accumulated via other metabolic pathways.

Sucrose is synthesised in the cytosol by the enzymes SUCROSE-PHOSPHATE SYNTHASE (SPS) and SUCROSE PHOSPHATE PHOSPHATASE (SPP) (Ruan 2014). Despite the accumulation of sucrose in *E. nindensis*, SPP transcripts diminished in abundance during drying below 25% RWC in the NST and remained unchanged during drying in the ST (Figure 4.4). Furthermore, no SPS transcripts were differentially expressed. Thus, sucrose formation in *E. nindensis* might be generated via other enzymes. The increase in sucrose and other sugars might be a consequence of the initial breakdown in starch, and the combination of the cessation of growth (observed in **Chapter 3**) coupled with the continuation (although low) of photosynthesis upon mild water-deficit stress (observed in **Chapter 2**). Muller *et al.* (2011) demonstrated that photosynthesis continues in non-resurrection plants upon water-deficit stress, whereas growth is affected earlier and to a greater degree, thus resulting in a net carbon gain upon mild dehydration. The increase in sucrose cannot be attributed to the low, but functional, photosynthetic rates in *E. nindensis,* however, they could contribute to the increase in the sugar pool when growth is inhibited**.**

SUCROSE SYNTHASE (SUS) has been invoked in sucrose synthesis (Angeles-Núñez et al. 2010; Baroja-Fernandez et al. 2012; Yobi et al. 2017), where, along with INVERTASE (INV), it cleaves sucrose to form UDP-glucose and fructose (Figure 4.4, A). SUS3 was highly expressed in the transcriptome of *E. nindensis*. SUS3 showed a strong accumulation in abundance upon desiccation, with overall expression being highest at 40% RWC in the NST and 25% RWC in the ST, with a fold change of 4.85 and 4.90 respectively (Figure 4.4, B). SUS is a more energy efficient sucrose-cleaving enzyme compared to INV and is thus a biomarker for sink strength (Xu *et al.* 2012). It has also been shown that while INV is essential for normal growth in Arabidopsis, SUS is a more important enzyme under stressed conditions as it requires little ATP and therefore functions under non-photosynthetic conditions (Barratt *et al.* 2009). It has been suggested that INV plays a regulatory role in seed development, whereas SUS plays a stronger role in cellulose, starch, lipid and protein biosynthesis in late seed development (Ruan 2014). In *E. nindensis*, sucrose CELL-WALL INV (SINV(cw)) was differentially expressed in the ST, whereas transcript abundance remained mostly unchanged in the NST (Figure 4.4, Figure 4. B and Figure 4.5). Whether the accumulation of INV transcripts in the ST plays a regulatory role in promoting

the breakdown of sucrose for the remobilisation under senescence is unknown. In light of this, Blomstedt *et al.* (2018) remark that sucrose loading from the senescing leaves to the younger (desiccation tolerant) leaves in *S. stapfianus* is critical for the switch to desiccation tolerance during drying. Nevertheless, the accumulation of SUS3 in *E. nindensis* reflects the ability of this enzyme to remain active under low energy conditions and indicates a change in metabolism under severe water-deficit stress.

In *E. nindensis,* SUS4 transcripts diminished upon water-deficit stress (Figure 4.4, B). Different SUS isoforms have distinct responses to different abiotic stresses, which denote their various roles (Bieniawska *et al.* 2007; Fallahi *et al.* 2008). In Arabidopsis*,* SUS3 transcripts accumulate with the onset of seed maturation (coinciding with the onset of desiccation tolerance) and are strongly linked with seed development (Baud *et al.* 2004; Fallahi *et al.* 2008). Furthermore, transcript expression of SUS3 was induced through dehydration and was observed to behave like an osmoticum (rather than sucrose-responsive) in Arabidopsis (Baud *et al.* 2004). Two SUS transcripts were also highly expressed in the roots and leaves of the resurrection plant *C. plantagineum* upon desiccation, and emphasised the importance of sugar metabolism in desiccation tolerance (Kleines *et al.* 1999). The high expression of SUS3 in *E. nindensis* supports the co-option of seed-related pathways to obtain desiccation tolerance hypothesis. However, the shared expression across both tissue types reinforces the notion that this might be a general response to drying in grasses, as suggested in Pardo *et al.* (2019). In addition, SUS4 is induced through hypoxia and the diminishing transcript abundances of SUS4 transcripts, with the corresponding accumulation of SUS3 transcripts in *E. nindensis,* suggests a metabolic re-direction towards pathways that are known to aid desiccation tolerance, such as seed development and maturation.

Although SUS3 is a reversible enzymatic reaction, this is usually in the sucrose cleaving direction, thus producing UDP-glucose and fructose (Geigenberger *et al.* 1993; Verbančič *et al.* 2018). The association with seed maturation and desiccation tolerance might be due to the products of SUS3 (mainly UDP-glucose) being substrates for trehalose or the re-synthesis of sucrose, both important sugars associated with autophagy and desiccation tolerance. Like sucrose, trehalose is a non-reducing protective sugar, which mitigates protein denaturation and has chaperoning properties (Tapia *et al.* 2014). Trehalose has been found to increase in low concentrations in several resurrection plants and has been implicated in playing a role in desiccation tolerance (e.g. *M. flabellifolia* (Phillips *et al.* 2002), *S. stapfianus* (Yobi *et al.* 2017), *T. loliiformis* (Williams *et al.* 2015), *Oropetium thomaeum* (Zhang *et al.* 2018). How trehalose induces desiccation tolerance is unknown (Blomstedt *et al.* 2018), and it has been suggested that trehalose itself is not implicated in water-deficit stress tolerance, but rather it is the regulatory role of trehalose or its synthesis intermediates that induce changes that result in

increased stress tolerance (Grennan 2007). In light of this, Williams *et al.* (2015) found that trehalose triggered autophagy during dehydration of *T. loliiformis* and concluded that trehalose played an important role in preventing programmed cell death (PCD) and senescence by detoxifying the cell and reshuffling nutrients during dehydration-induced caloric deficiency. Trehalose also acts as a stress signalling molecule by regulating the SUCROSE NON-FERMENTING 1–RELATED KINASE (SnRK1) gene, which triggers autophagy and negatively regulates starch synthesis (Dobrenel *et al.* 2013; Asami *et al.* 2018). Trehalose is hydrolysed into two glucose molecules by TREHALASE (Grennan 2007). In general, the transcript abundance of the enzymes responsible for the synthesis of trehalose (TPP and TPS, TREHALOSE-PHOSPHATASES and TREHALOSE-6-PHOSPHATE (T6P) SYNTHASE, respectively) diminished in both tissue types during drying, except for two isoforms, which were exclusively accumulating in the ST (Figure 4.4,Figure 4. B). This suggests that trehalose breakdown is being favoured by both tissue types, and that trehalose synthesising transcripts are induced in the ST only. This might indicate that the ST is experiencing stress differently to the NST.

Changes in trehalose contents during drying is unknown for *E.* nindensis, however, preliminary results do show the presence of trehalose in both desiccated NST and ST (Dace, *unpublished*). In *T. loliformis,* trehalose accumulates upon desiccation, however, at significantly lower levels than sucrose (~60 mg g^{-1} dry mass vs ~0.448 µg g^{-1} dry mass, William *et al.* 2015). This demonstrates that small amounts of trehalose are sufficient to trigger metabolic processes (such as autophagy) and therefore require tight regulation. Indeed, the low micromolar concentrations of trehalose suggest its role in regulation rather than metabolism (Paul *et al.* 2018). The presence of both trehalose catabolic (TREHALASE) and anabolic (TPP) enzymes in *E. nindensis* illustrates this subtle regulation. Overall, this analysis shows that sucrose levels increase, yet only SUS3 showed a significant accumulation in abundance upon desiccation. SUS3 is key in controlling the breakdown of sucrose into intermediates used for both trehalose production and the synthesis of sucrose. Trehalose requires less UPD-glucose than sucrose, suggesting a potential role of SUS3 in sucrose reshuffling, via the intermediate UDP-glucose, towards trehalose metabolism, whilst recycling most of the glucose back towards sucrose synthesis, maintaining high sucrose levels. This could indicate the role of trehalose in acting as a stress signalling molecule, and its role in desiccation tolerance and senescence needs to be experimentally validated.

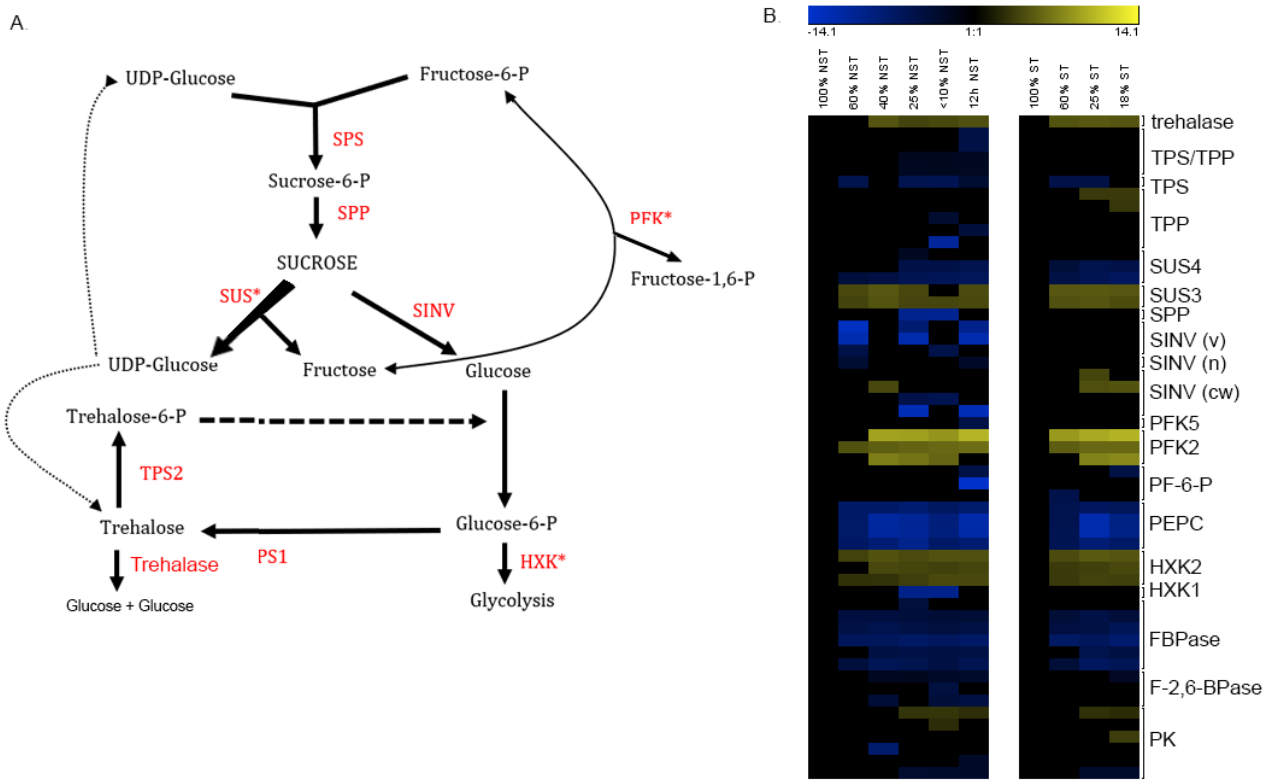

Figure 4.4: Changes in sugar metabolism during drying (represented as relative water content, RWC, %) and rehydration (12h) in the resurrection plant *Eragrostis nindensis* in desiccation tolerant, non-senescent tissue (NST) and desiccation sensitive, senescent tissue (ST). (A) Pathway illustrating the synthesis and breakdown of sucrose, and (B) the corresponding transcript abundance changes represented in a heatmap of key sugar transcripts involved in sugar metabolism. Enzymes are depicted in red, * represent accumulating transcripts. Only differentially expressed genes (DEGs) are depicted, derived from the statistically significant change (>2 or <-2 log_2 fold change, FDR <0.05) in transcript abundance compared to the control (NST, 100% RWC). The colour scale represents log_2 fold change values. v = vacuolar, n = neutral, cw = cell wall.

4.3.2.3 Cell wall invertases

The flow of sucrose into and within a cell and the associated cell wall related enzymatic processes are described in Figure 4.5. Most sucrose transporter transcripts diminished during drying (Figure 4.8) and this, coupled with the accumulation of sucrose symporters, suggests that sucrose is transported into the cell via sucrose H+ transporters and/or through plasmodesmata (Figure 4.5). In general, there were few differences in the transcript abundance patterns between the NST and ST, except for CELL WALL SUCROSE INVERTASES (SINV(cw)). SINV(cw) transcripts were highly expressed in the ST, but not in the NST, during drying (Figure 4.4). This enzyme plays an essential role in development and primary metabolism by converting sucrose into glucose and fructose, an irreversible conversion (Ruan *et al.* 2010; Jameson *et al.* 2016). The expression of SINV(cw) has been linked to cell growth via cell wall expansion resulting from the increased osmotic effect of fructose and glucose compared to sucrose (Ruan *et al.* 2010). However, this is unlikely to promote expansion due to the lack of water as a result

of dehydration. Furthermore, growth-related and cellulose synthase transcripts diminished (Figure 4.5, Figure 3.4.1 and Figure 3.5.2), which reflects the observed cessation of cell growth in resurrection plants during drying. The accumulation of these transcripts in the ST might indicate a breakdown of sucrose into transportable units for the reshuffling of nutrients to the NST associated with senescence.

Transcripts of sucrose vacuolar INV (SINV(v)) are associated with sucrose-storing organs (Yau *et al.* 2003; Ruan 2014) and were exclusively diminishing in the NST during desiccation. This decrease in sucrose-storage organs reinforces the hypothesis that *E. nindensis* does not use sucrose as its primary energy source, but rather alternative complex reserves, such as lipids, or chloroplast-derived nitrogen. SINV(cw) are activated upon pathogen attack or wounding, and are highly active during early seed development (Weber *et al.* 1995). Invertases break down sucrose (Yau *et al.* 2003) and accumulated more in the ST than the NST, potentially for the export to sink tissue (e.g. NST and roots).

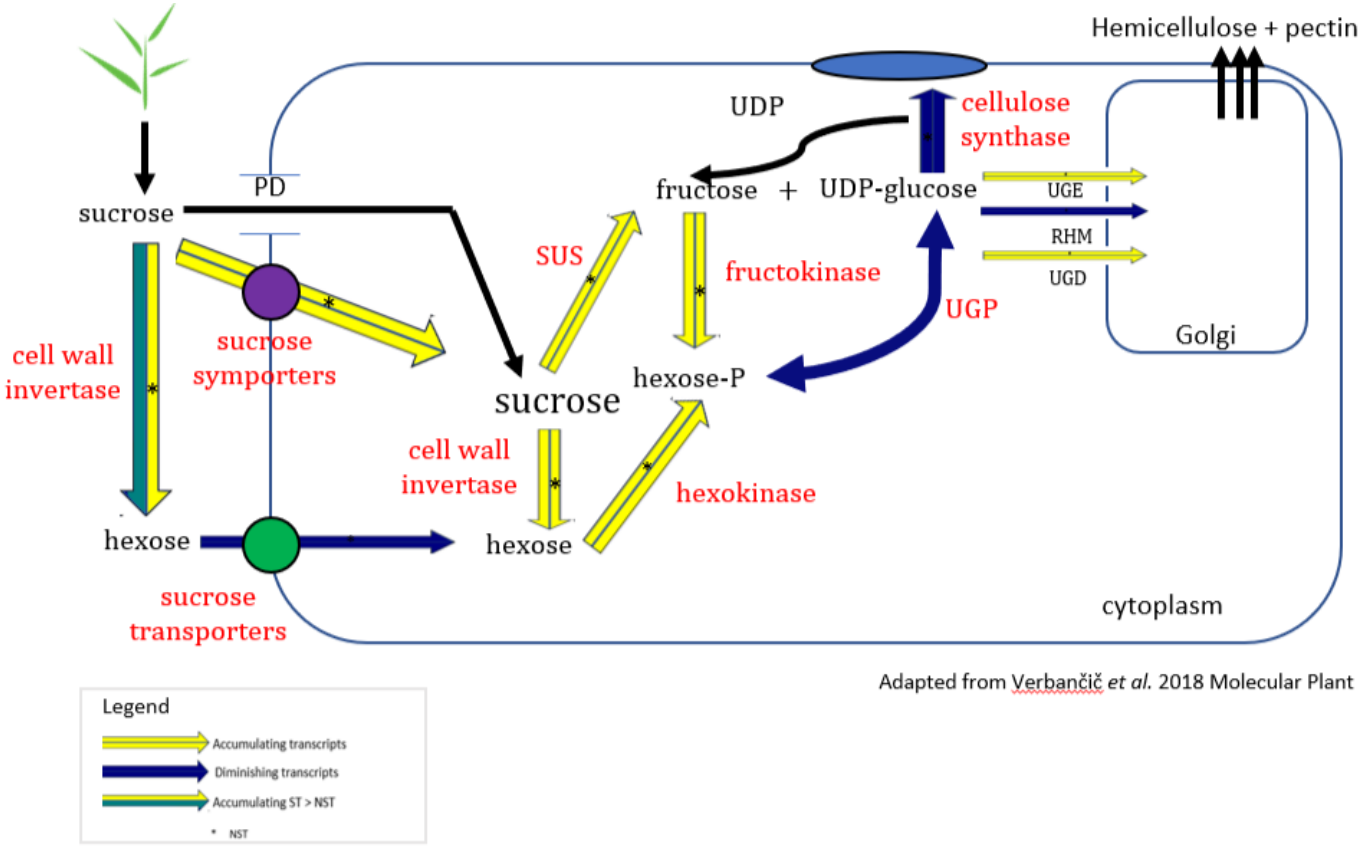

Figure 4.5: Model inferred from transcript abundance data showing the hypothesised flow of sucrose import into a cell, and subsequent synthesis and breakdown, resulting in cell wall metabolism. Yellow arrows indicate accumulating transcript abundances during drying in *Eragrostis nindensis*, while blue arrows indicate diminishing transcript abundances. The arrow is divided into desiccation tolerant, non-senescent tissue (NST) indicated by *, and desiccation sensitive, senescent tissue (ST). Sucrose is transported to the cell and imported via plasmodesmata (PD) or imported via sucrose symporters or, after hydrolysed into hexose by cell wall invertases, imported by sucrose transporters. Intracellular sucrose is then broken down by cell wall invertases or sucrose synthase (SUS). SUS increases the fructose and UDP-glucose pool, both precursors for cellulose, hemicellulose and pectin. Transcript abundances for cellulose synthase are diminishing upon water-deficit stress in *Eragrostis nindensis* suggesting that growth has been arrested and that there has been an increase in the hexose pool during drying. Diagram has been adapted from Verbančič *et al.* (2018).

4.3.2.4 Raffinose family oligosaccharides (RFOs)

RFO accumulation is a desiccation tolerance trait that is common among seeds and resurrection plants (Peters *et al.* 2007; Oliver *et al.* 2011; Giarola *et al.* 2017; VanBuren *et al.* 2017; Farrant *et al.* 2017). Their accumulation in desiccation tolerant tissues upon severe water-deficit stress is well-documented (e.g. *S. stapfianus* and *O. thomaeum* (Oliver *et al.* 2011; VanBuren *et al.* 2017)). Peters *et al.* (2007) established that raffinose acts as both a protective sugar and carbon storage for rehydration in *X. viscosa*. Raffinose is also a signalling molecule and a key component of carbon partitioning (Nishizawa *et al.* 2008; Elsayed *et al.* 2014). RFOs therefore play an important role in vitrification during desiccation and are stabilising sugars (Buitink *et al.* 2004; Farrant *et al.* 2017).

The accumulation of RFO transcript abundances was observed in *E. nindensis* (Figure 4.6, B). Unpublished data from the PhD thesis of Halford Dace show that raffinose and stachyose contents increased during drying, the former starting at a higher RWC (~80% RWC) and reaching higher levels, the latter accumulating below 50% RWC. Galactinol was not accumulated. In contrast, the transcriptome of *E. nindensis* showed a general accumulation of galactinol, raffinose and stachyose synthases, but to a greater extent in raffinose and stachyose synthases (Figure 4.6, B), supporting the metabolite data. The decrease in galactinol (Dace, *unpublished*) upon desiccation in *E. nindensis*, coupled with the high expression of raffinose synthases (Figure 4.6, B), suggests that galactinol is converted into raffinose and RFOs. The large increase in raffinose during drying in *E. nindensis* (Farrant *et al.* 2017, Dace, *unpublished*), coupled with the transcriptomic signature of RFO synthases (Figure 4.6), implies that these sugars are key vitrification solutes, enabling cellular protection under desiccation. This is also observed in *E. nindensis* with other protective sugars (other than sucrose) accumulating, seen by the low sucrose to RFO ratios, as discussed earlier (Farrant *et al.* 2017). In addition, raffinose can acts as a ROS scavenger, further implicating its role in desiccation tolerance, and unlike other antioxidants, such as tocopherols and ascorbate, is not destroyed in the process and can therefore be recycled (Foyer *et al.* 2011). Again, the similarity between the NST and ST is intriguing, as the ST clearly experiences irreparable water-deficit induced damage, showing no evidence of the potential protective function of raffinose. Nevertheless, accumulating transcript abundances of RFOs during desiccation is indicative of *E. nindensis* engaging in a desiccation tolerance programme, but contributing to tolerance only in the NST.

As outlined above, *E. nindensis* accumulates sucrose during drying, however, this accumulation is comparatively low compared to other resurrection plants. Asami *et al.* (2018) proclaim that the total sugar is not as important as the ratio of the types of sugars in triggering metabolic responses. The ratios of sugars differ between the NST and ST in *E. nindensis*; levels of reducing sugars glucose and

fructose are much higher in the ST, whereas the non-reducing sugars raffinose and sucrose are higher in the NST (Dace, *unpublished*). Pourtau *et al.* (2006) found senescing Arabidopsis leaves to strongly accumulate both glucose and fructose. Metabolic data in *E. nindensis* showed that glucose levels more than doubled in the ST at 30% RWC compared to those in the NST at the same water contents (Dace *unpublished*). Glucose accumulation is associated with a senescence response (Pourtau *et al.* 2006; Wingler *et al.* 2009) and this, coupled with low glucose concentrations observed in desiccation tolerant leaves (e.g. *S. stapfianus* in Oliver *et al.* 2011), implies that the ST is displaying a senescent phenotype detected through metabolism, rather than the transcriptome.

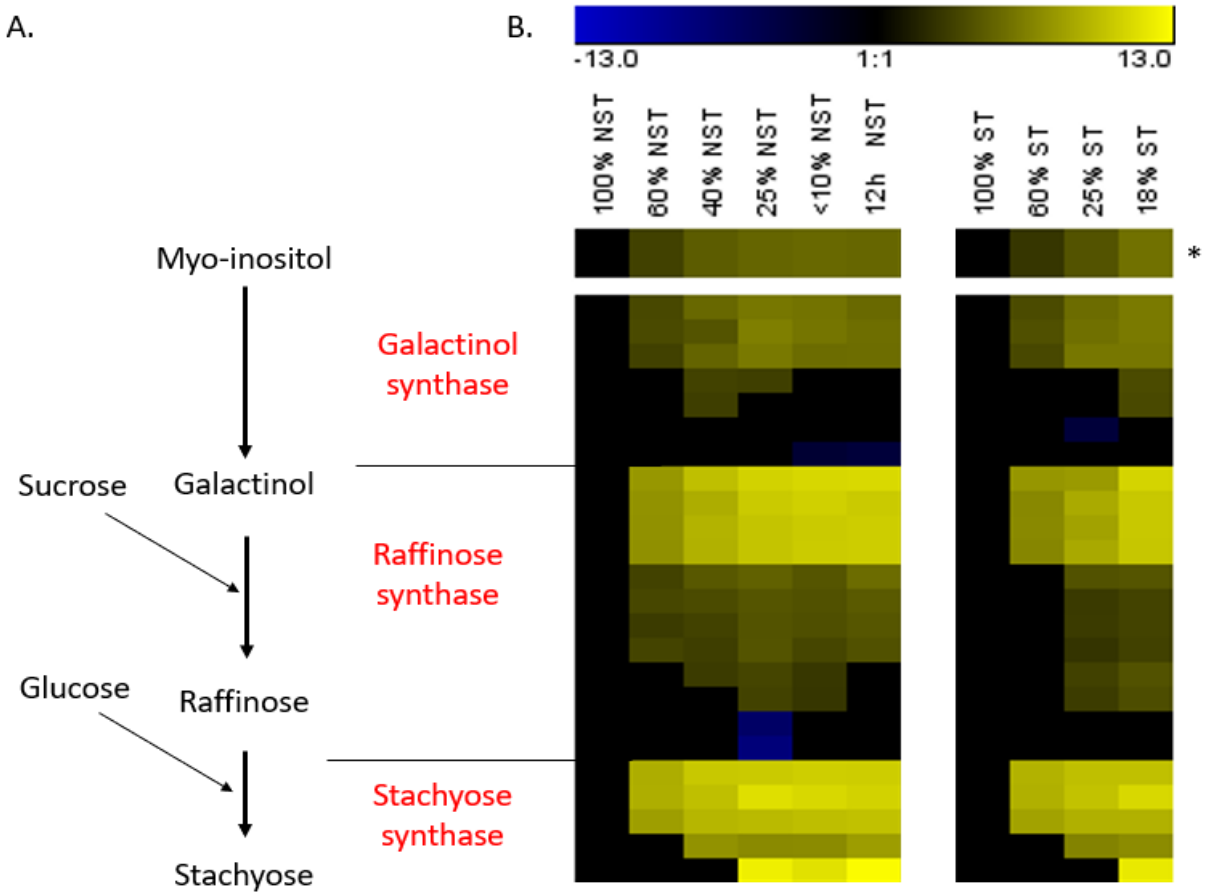

Figure 4.6: Changes in transcript abundance of raffinose family oligosaccharides (RFOs) during drying (measured as a relative water content, %) and rehydration (12h) in the resurrection plant *Eragrostis nindensis* between desiccation tolerant, non-senescent tissue (NST) and desiccation sensitive, senescent tissue (ST). (A) The metabolic pathway of RFOs is indicated in the flow diagram (black arrows), corresponding with the RFO enzymes (depicted in red). (B) Heatmap showing RFO-related differentially expressed genes (>2.0 or <-2 log_2 fold change values, FDR <0.05), denoted in yellow and blue indicating accumulating and diminishing transcripts compared to the NST hydrated control (100% RWC). The colour scale represents log_2 fold change values. * indicates the average bar showing the mean expression trends during drying.

4.3.2.5 Starch

Starch is commonly broken down in response to stresses, and this is true for many resurrection plants (Zhang *et al.* 2018; Blomstedt *et al.* 2018). However, starch granules were observed in *E. nindensis* in the desiccated state, in both tissue types, although there was a reduction in starch granules during drying (Figure 2.12, Figure 2.14). This suggests that starch is not completely broken down and can act as a complex storage reserve during drying. The transcriptome showed a trend of starch synthesis and breakdown with the transcript abundance of ADP-GLUCOSE PYROPHOSPHORYLASE (AGPase) accumulating in both tissue types (Figure 4.7, B). AGPase is involved in the first step of starch biosynthesis (Figure 4.7, A), in which glucose-6-P is converted into ADP glucose and ultimately starch. This induction is seen early (at 60% RWC), prior to the shutdown of photosynthesis (at 40% RWC, Figure 2.7), and could either suggest the ongoing, albeit inefficient, production of starch until photosynthetic shutdown, or, more likely, the storage of these transcripts in anticipation of rehydration. The latter is supported by the expression of AGPase being unchanged, compared to the control, at very low water contents in the ST but remaining highly expressed in the desiccated and rehydrated states of the NST (Figure 4.7, B). In seeds, starch mobilisation is enhanced through amylase activation to provide energy for germination (Paul *et al.* 2018), supporting the transcript-storing hypothesis for rehydration. Furthermore, STARCH SYNTHASE transcripts that catalyse the conversion of ADP-glucose into amylose (linear) diminished at lower water contents, from 40% RWC in the NST and 25% RWC in the ST, indicating that starch accumulation is slowed, if not halted, during desiccation. It is therefore unlikely that starch is being accumulated at lower water contents, but rather suggests that this complex carbohydrate is (at least partially) stored for breakdown and energy use in recovery for rehydration.

Transcripts of STARCH SYNTHASE 1 (SS1), the enzyme responsible for the synthesis of amylopectin (branched), accumulated in <10% RWC and 12h in the NST only. The branched crystalline structure makes starch insoluble in water (Green *et al.* 1975), and therefore stabilises starch in the presence of water. The accumulation of SS1 during desiccation and rehydration is therefore presumably to stabilise stored starch during rehydration, in conjunction with the anticipation of starch production upon photosynthetic re-activity. There was no change in the transcript abundance of glycogen branching enzymes.

There is evidence of starch degradation in both tissue types upon desiccation (Figure 4.7, B), which supports the observed reduction in starch (Figure 2.12, Figure 2.14). Transcript accumulation of chloroplastic located α-AMYLASE (n = 1) and β-AMYLASE (n = 7) in both tissues suggests that starch is being broken down into glucose and maltose (Figure 4.7, B). Several β-AMYLASE transcripts were

diminishing, particularly in the ST, however, this is expected given that regulation requires both catabolic and anabolic components. In general, transcripts converting starch to glucose-1-P (STARCH PHOSPHORYLASE) diminished or remained unchanged, whereas those converting starch to glucose and maltose (amylases) accumulated upon desiccation. This suggests a metabolic flow towards an increased sugar pool. If glucose (via amylases) is produced, these molecules appear not to be transported out of the chloroplast, as starch transporter transcripts were diminished in both tissue types (Figure 4.7, A). It is possible that the products of starch breakdown are being converted into other storage units, potentially lipids, as lipid accumulation has been observed in the ultrastructural studies in **Chapter 2** (Figure 2.12). The composition and structure of the lipids differ between the NST and ST during drying, and the lipid and associated transcriptome changes are briefly reported in **Chapter 5**.

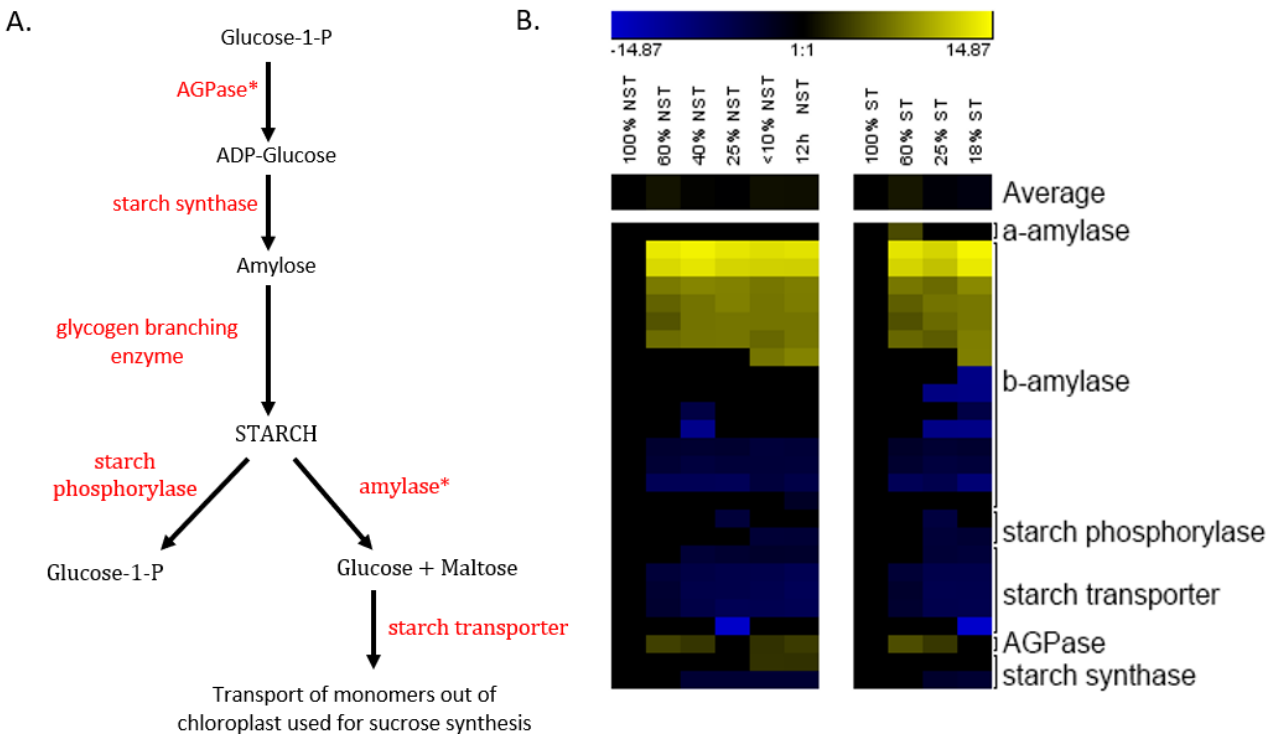

Figure 4.7: Summary of changes in starch metabolism during drying (measured as a relative water content, %) and rehydration in the resurrection plant *Eragrostis nindensis* in desiccation tolerant, non-senescent tissue (NST) and desiccation sensitive, senescent tissue (ST). (A) Metabolic pathway illustrating the synthesis and breakdown of starch, and (B) the corresponding transcript abundance changes represented in a heatmap of key starch transcripts. Enzymes are depicted in red, * represents accumulating transcripts. Only differentially expressed genes (DEGs) are depicted, derived from the statistically significant change (>2 or <-2 log_2 fold change values, FDR <0.05) in transcript abundance compared to the control (NST, 100% RWC). The colour scale represents log_2 fold change values. Average bar indicates the mean expression trends during drying.

4.3.2.6 Sugar transporters and SWEETs

Sugars are the primary source of carbon and energy in organisms and their synthesis and subsequent transport is essential for growth, development, and response to stresses (Chen *et al.* 2010). Specialised transporter proteins translocate sugars from photosynthetic tissues (source) across plasma membranes into non-photosynthetic tissues (sinks) and play a critical role in source to sink dynamics through phloem loading (Walmsley *et al.* 1998; Jameson *et al.* 2016). Three main sugar transporter families perform this function and play a key role in sucrose efflux; monosaccharide transporters (MSTs), sucrose transporters (SUTs) and SWEETs (Eom *et al.* 2015). MSTs and SUTs form a collective superfamily referred to in this thesis collectively as SUTs. SUTs translocate sugars from the apoplast into sink cells where they are specifically expressed (Rottmann *et al.* 2016). SWEETs are structurally different to SUTs and are membrane-bound proteins that assist in transmembrane sugar translocation (Eom *et al.* 2015). Each transporter protein plays a different physiological role, although only a handful have been characterised (Durand *et al.* 2016).

Six SWEETs were differentially expressed in *E. nindensis* (Figure 4.8), with only two of these (SWEET7 and SWEET15) accumulating in transcript abundance upon desiccation, in both the NST and ST. The specific role of SWEET7 is unknown, although it is a known bidirectional sugar transporter (Chen *et al.* 2012). SWEET15 is also known as SAG29, a senescence-associated gene, and is also a bidirectional sugar transporter (Seo *et al.* 2011b). SWEET15/SAG29 responds to environmental stresses, is regulated by drought, salinity, ABA and other osmotic stresses, and is often used as a marker of senescence (Gepstein *et al.* 2003, Seo *et al.*, 2011b). In Arabidopsis, SWEET15/SAG29 expression increased in senescing tissues but also in developing seeds and reproductive tissues, suggesting that SWEET15/SAG29 might play a role in controlling sink strength (Chen *et al.* 2015; Durand *et al.* 2016). Seo *et al.* (2011b) suggest SWEET15/SAG29 plays a role in membrane permeability, transporting sugars in senescing tissues, and this supports the dual role of SAG29 as a transporter (SWEET15). SWEET11, SWEET12 and SWEET15 are involved in seed development, and knockout mutants in Arabidopsis produced defected seeds, showing reduced weight and lipid content, retarded embryo development and wrinkled seeds (Chen *et al.* 2015). Lipid content reduction of the double mutant of SWEET11;12 was significantly less (34% vs 71%) than the triple mutant (Chen *et al.* 2015), suggesting that SWEET15 is an important sugar translocator for the downstream synthesis of lipids. This is interesting as the conversion of sugars into lipid bodies has been supported by the ultrastructural observation of lipid accumulation in **Chapter 2** (Figure 2.12) and will be further examined in **Chapter 5**. Nevertheless, the transcript abundance accumulation of SWEET15 and SWEET7 in both the NST and ST indicates that sugar transport is transcriptionally regulated in both tissue types. The direction of sugar flow is unclear and needs to be experimentally validated.

The remaining four SWEETs (SWEET11, SWEET12, SWEET14, SWEET17) diminished in transcript abundance upon desiccation in both tissue types. SWEET11 has been reported to be co-expressed with SPS to transport sucrose from mesophyll or bundle-sheath cells into the phloem apoplasm (Chen *et al.* 2010). Since photosynthetic carbon gain has largely shut down by 40% RWC, the corresponding diminishing transcript abundance of SWEET11 is expected. However, the accumulation of SWEET transcripts in other resurrection plants have been documented (e.g. SWEET12 – 15 in *T. loliiformis* by Asami *et al.* (2019)). In general, there were few differences in the abundance patterns between the NST and ST.

Of the 161 SUT motif-containing transcripts in the genome, six were DEGs and a further two were annotated as hexose-H(+)-symporters (Figure 4.8). SUTs have been implicated in the fine-tuning of the regulation of sugar efflux in sink tissues during development or response to environmental stresses (Rottmann *et al.* 2016) and are predominantly responsible for sugar import into cells via the cell wall (Eom *et al.* 2015). In *E. nindensis,* transcript abundance trends are similar between the NST and ST, except for the two hexose symporters, which are significantly induced at 40% RWC in the NST but only at 18% RWC in the ST (Figure 4.8). Two SUTs accumulated upon water-deficit stress in both tissue types, which indicates that they play a role in sugar transport and/or stress signalling in response to water-deficit stress, as implied by Xu *et al.* (2018a). The RNA of the one DEG (AT1G11260) is cell-to-cell mobile and could indicate storage for sugar translocation during rehydration (Figure 4.8) (Thieme *et al.* 2015). The other DEG (AT1G50310) is expressed in pollen tubes in Arabidopsis (TAIR 2019a) (Figure 4.8). Rottmann *et al.* (2016) remark on the importance of this specialised SUT in fine-tuning energy supply into the gametophyte, and the expression of this SUT appears to be a critical adaptation as pollen tip growth is one of the fastest plant growth processes. The accumulation of these previously identified pollen-specific transcripts in *E. nindensis* vegetative tissues might indicate a novel acquired role in desiccation tolerance, as the efficient sugar uptake in cells needing energy for the metabolic readjustments during drying is critical. Given that water-loss can be rapid in resurrection plants, an efficient energy supply is needed to ensure that protection mechanisms are laid down before desiccation.

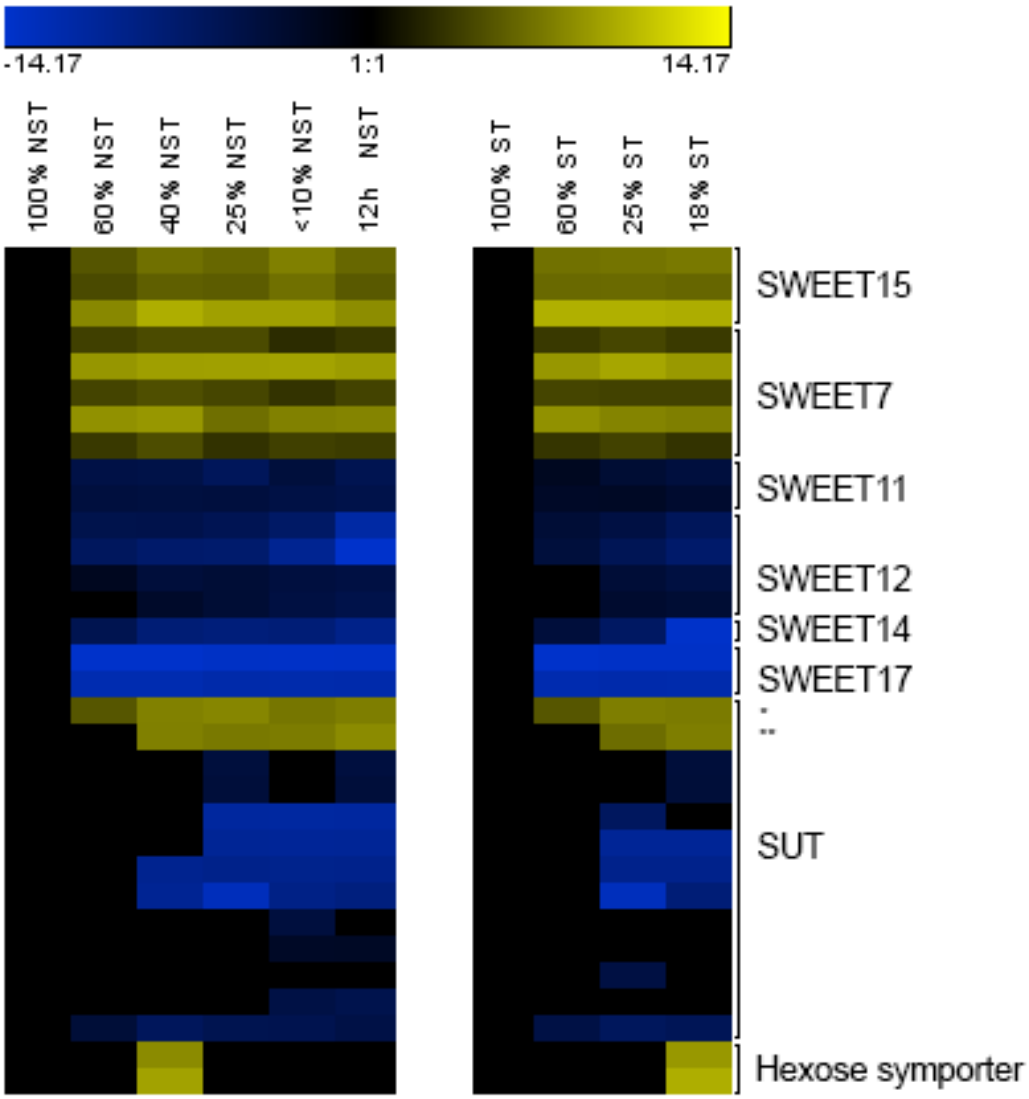

Figure 4.8: Sucrose transporter changes in transcript abundances during drying (measured as a relative water content, %) and rehydration (12h) in the resurrection plant *Eragrostis nindensis* in desiccation tolerant, non-senescent tissue (NST) and desiccation sensitive, senescent tissue (ST). SWEETs = sugars will eventually be exported transporter, SUT = sucrose transporters. Asterix refers to two SUT transcripts specifically mentioned in the text (* = AT1G11260, ** = AT1G50310). Only differentially expressed genes (DEGs) are depicted, derived from the statistically significant (>2 or <-2 log_2 fold change values, FDR <0.05) change in transcript abundance compared to the control (NST, 100% RWC). The colour scale represents log_2 fold change values.

4.3.2.7 ABC transporters

ATP-binding cassette (ABC) transporters translocate sugars, amino acids, lipids, ions and hormones (amongst other solutes) across plasma membranes using cellular energy (Jones *et al.* 2004b). These transporters occur in all living organisms and are key players in several cellular process including cellular detoxification, maintaining osmotic homeostasis and nutrient uptake, and are crucial for plant growth, development, pathogen resistance and response to abiotic stresses (Martinoia *et al.* 2002; Kang *et al.* 2011). In the leaves of *E. nindensis* 55 ABC transporters were differentially expressed during drying (Figure 4.9), 12 of which were accumulating in transcript abundance and correspond to eight Arabidopsis homologues. These transporters are purportedly localised in various tissues, such as in chloroplasts, vacuoles, membranes and are involved in the transport of solutes during flowering, seed and expansion (growth) (Kang *et al.* 2011; Dinakar *et al.* 2013). The remaining 43 transporters diminished in transcript abundance, which demonstrates that their role in transporting solutes during drying is complex and requires the regulation of different transporters in various organelles and tissues.

Three *E. nindensis* transcripts (corresponding to the Arabidopsis homologue AT2G47800, ABC-C4, n=5) had a consistently higher fold change during drying in the NST when compared to the ST (red box in Figure 4.9). According to TAIR (2019b), this ABC-C4 gene is involved in response to water deprivation and was found to transport RNA from root to shoot (Thieme *et al.* 2015). Those authors postulated that metabolism in some cells (e.g. leaves) can be affected by distant cells (e.g. roots) through the transport of mobile RNA encoding key enzymes or regulators thereof. The transport of RNA, mediated by ABC transporters, could change the energy status in the cell, and therefore affect processes (such as growth) in response to stresses detected in the roots (such as water deprivation).

Another significant difference between the NST and ST could be seen in three transcripts namely ABC-B26 (AT1G70610), ABC-G40 (AT1G15520) and ABC-1-LIKE KINASE (AT1G79600) (shown in red boxes in Figure 4.9), hinting at some transcriptional differences in the regulation of senescence between the tissue types. These ABC transporter transcripts were significantly diminished in abundance below 25% RWC in the NST, yet remained unchanged in the ST (Figure 4.9). The corresponding Arabidopsis homologue ABC-B26 and ABC-G40 has been reported to play a role in transmembrane transport from the chloroplast and is expressed in reproductive structures and vascular leaf senescence stages, amongst others (TAIR 2019c). Its suppression in the NST might be related to the lack of senescence in this tissue. The other homologue (ABC-1-LIKE KINASE) acts like a chaperone-like protein and modulates chlorophyll content, plays a role in the antioxidant vitamin E metabolism and is expressed upon nitrogen starvation, photo-oxidative stress and water deprivation (Yang *et al.* 2012). It is unclear

why there is an active suppression of this ABC transporter (AT1G79600) in the NST and not the ST, since both tissue types *inter alia* breakdown chlorophyll.

Export of nutrients from a leaf indicates the function of that leaf as a source and can either reflect carbon-fixing (energy generating) tissue or senescing tissue (Buchanan-Wollaston *et al.* 2005). Since photosynthetically-driven carbon fixation has ceased below 40% RWC in *E. nindensis*, the increase in ABC transporter transcripts could indicate the movement of solutes required for energy sources for metabolically active processes from ST sources, or through carbohydrate anabolic processes in NSTs. The direction of solute flux is unknown, but the large increase in the 12 ABC transporters may indicate a role in protection under osmotic stress and transport of solutes for energy and storage.

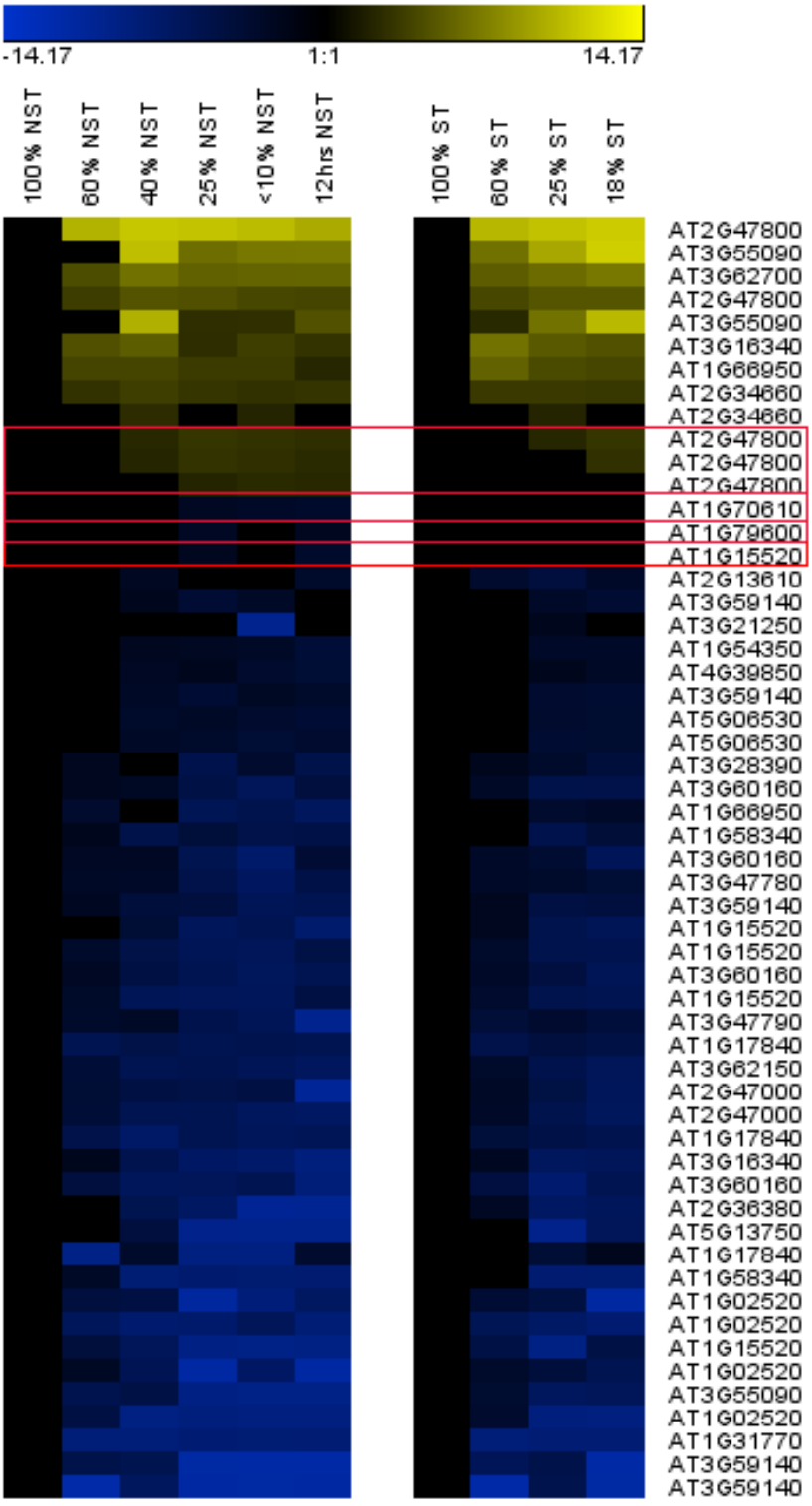

Figure 4.9: Heatmap showing transcript abundance trends of ATP-binding cassette (ABC) transporters depicting differential transcript expression trends during drying (measured as a relative water content, %) and rehydration (12h) in the resurrection plant *Eragrostis nindensis* in desiccation tolerant, non-senescent tissue (NST) and desiccation sensitive, senescent tissue (ST). Only differentially expressed genes (DEGs) are depicted, derived from the statistically significant (>2 or <-2 log_2 fold change values, FDR <0.05) change in transcript abundance compared to the control (NST, 100% RWC). The colour scale represents log_2 fold change values. The red boxes indicate transcripts that show fold change differences between the two tissue types; AT2G47800 is ABC-C4, accumulating in transcript abundance more in the NST than the ST, and AT1G70610 (ABC-B26), AT1G79600 (ABC-1-LIKE KINASE) and AT1G15520 (ABC-G40) are exclusively diminishing in the NST.

4.3.2.8 Aquaporins

Turgor loss in response to drying can cause irreparable membrane damage if the cell volumes reduce beyond a critical threshold (Meryman 1974; Forterre 2013). In order to mitigate this instability, cells need to either replace water with compatible solutes or reduce cell volume through folding (Farrant *et al.* 2007, 2017). *E. nindensis* employs cell wall folding in mesophyll cells, while maintaining cell volume in the bundle-sheath cells through vacuolation (Figure 2.12, Figure 2.14) also reported by Vander Willigen *et al.* (2004). The movement of water and solutes across membranes is regulated by specialised protein channels called aquaporins, which are localised in the plasmalemma, endoplasmic reticulum, vacuole and plastid membranes (Maurel *et al.* 2015). Aquaporins play a critical role in fine-tuning the mechanical properties of cells by controlling the efflux of water and solutes. This is particularly important in resurrection plants during both dehydration, where subcellular occupation of non-aqueous solutes are needed to maintain volume, and on rehydration, where the sudden influx of water can cause membrane tearing (Pammenter *et al.* 1999).

Aquaporins are divided into five categories; plasma membrane intrinsic proteins (PIPs), tonoplast intrinsic proteins (TIPs), nodulin26-like intrinsic protein (NIPs), small basic intrinsic proteins (SIPs) and uncharacterised intrinsic proteins (XIPs, Danielson *et al.* 2008). Vander Willigen (2004) found a TIP3;1 aquaporin (which was previously thought to be exclusively localised in seeds) in bundle sheath cell vacuoles in desiccated *E. nindensis* leaves. The authors alluded to its role in increasing membrane permeability, thus aiding in rapid water influx during rehydration. Furthermore, in the absence of water to fill vacuoles, TIP3;1 was found to regulate the influx of non-aqueous solutes (proline, sugars and proteins) into the vacuole during desiccation, thus aiding mechanical stabilisation. In addition, only the desiccation tolerant leaves of *Sporobolus stapfianus* accumulated TIP transcripts in the desiccated state, with little to no expression in the hydrated state, suggesting that TIPs aid to accommodate the large changes in osmotic potential during drying, as well as facilitate rehydration by increasing membrane permeability (Neale *et al.* 2000). Similarly, PIPs identified in *Craterostigma plantagineum* also accumulated in transcript abundance during drying (Mariaux *et al.* 1998).

Thirty-one aquaporin DEGs were identified in *E. nindensis* (Figure 4.10). Of these, the majority showed transcripts diminishing in abundance in both the NST and ST during drying. Exceptions are some transcripts of TIPS1, 2 and 3 (discussed below) and one sieve cell differentiation transcript (AT1G31880), belonging to the NIP family, which accumulated exclusively in the NST at 40% RWC. Furthermore, its transcript abundance was maintained during desiccation and rehydration in this tissue. Sieve elements play a major conductive role in the phloem by transporting carbohydrates, proteins, RNAs, small RNAs and hormones (Walz *et al.* 2002; Batailler *et al.* 2012). Although the specific

role of this gene in desiccation tolerance is unknown, its accumulation represents one of the few differences in the transcriptomic signature between the NST and ST upon desiccation. Here, the distinct accumulation of transcript abundance of an important phloem loading transporter in only the NST shows a difference in regulation between STs and NSTs.

Apart from the TIP4 family, which declined during drying, several TIPs, namely TIP1;1, TIP2, TIP3;1, TIP3;2, accumulated in *E. nindensis* (Figure 4.10). The transcript abundance accumulation of TIP3;1 validated the observation by Vander Willigen *et al.* (2004) of protein expression of TIP3;1 in desiccated NSTs. Although the transcriptome is a developmental step before the proteome, it is still interesting to see the presence of these transcripts at 60% RWC when the TIP3;1 protein was only detected below 10% RWC in the NST. Additionally, these transcripts were also found to be significantly accumulating in abundance in the ST despite this protein not being detected by western blotting (experiment conducted by Vander Willigen *et al.* (2004), and repeated here, data not shown).

TIP3;1 is also implicated in autophagy by moving protein (possibly denatured) into the vacuole (Moriyasu *et al.* 2003). The observed vacuolation and organised cellular structure in the NST (Figure 2.12) compared to the ST (Figure 2.14) potentially verifies the role of TIP3;1. Here, the NST increases mechanical stability through vacuolation (predominantly in the bundle sheath cells), coupled with the influx of potentially denatured proteins, thereby reducing oxidative stress. TIP3;2 is thought to be seed-specific and is highly abundant during seed maturation (Mao *et al.* 2015), although lessons from TIP3;1 and this *E. nindensis* transcriptome provide strong evidence that this aquaporin is expressed in the vegetative tissues of *E. nindensis*. These findings suggest that vacuolar aquaporins (i.e. TIPs) are important for the acquisition of desiccation tolerance and are regulated under water-deficit stress in *E.* nindensis. This highlights the need to conduct a full proteomic study on *E. nindensis* to confirm the expression of proteins to infer any differences between NST and ST.

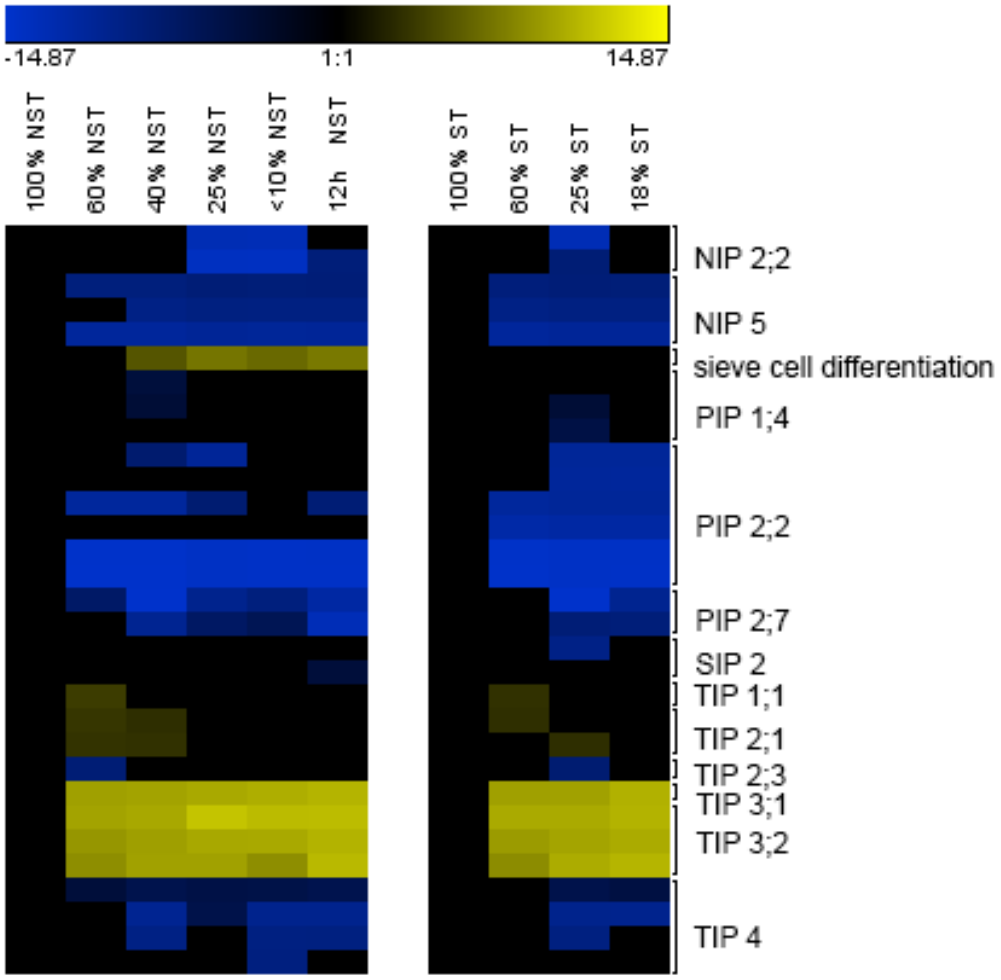

Figure 4.10: Heatmap representing the expression of aquaporin transcripts during drying (measured as a relative water content, %) and rehydration (12h) in the resurrection plant *Eragrostis nindensis* in desiccation tolerant, non-senescent tissue (NST) and desiccation sensitive, senescent tissue (ST). Only differentially expressed genes (DEGs) are depicted, derived from the statistically significant change (>2 or <-2 log_2 fold change values, FDR <0.05) in transcript abundance compared to the control (NST, 100% RWC). The colour scale represents log_2 fold change values. Abbreviations correspond to the following: plasma membrane intrinsic proteins (PIPs), tonoplast intrinsic proteins (TIPs), nodulin26-like intrinsic protein (NIPs), and small basic intrinsic proteins (SIPs).

4.3.2.9 Antioxidants

Resurrection plants employ multiple enzymatic and non-enzymatic antioxidants to mitigate oxidative damage and ROS accumulation during water-deficit stress (Dinakar *et al.* 2018). During late response to drying, the lack of water surrounding macromolecules increases their concentrations, resulting in an increased likelihood of harmful molecular interactions through protein aggregation that could denature macromolecules or damage membranes (Hoekstra *et al.* 2001; Berjak *et al.* 2013; Farrant *et al.* 2015). Antioxidants are ubiquitous in all plants, however, resurrection plants both strongly maintain and protect these ROS scavenging systems under severe abiotic stress, thereby maintaining redox homeostasis (and low ROS concentrations) and preventing excessive damage leading to cell death (Illing *et al.* 2005; Farrant *et al.* 2015; Georgieva *et al.* 2017b; Wang *et al.* 2018b). One hundred and fifty-five DEGs annotated as having antioxidant properties were found to be differentially expressed in *E. nindensis* during drying and rehydration, with 55 of these accumulating (Figure 4.11). Of those 55, nine were exclusively present in the NST, especially upon 12h rehydration, and included PEROXIDASES, FERREDOXIN, LACTOYLGLUTATHIONE LYASE and THIOREDOXIN. These are well-known antioxidants and have been identified in other resurrection plants. For example, LACTOYLGLUTATHIONE LYASE was one of the most highly expressed transcripts upon severe dehydration in *C. plantagineum* (Rodriguez *et al.* 2010). Ferredoxin is also a critical component of linear electron transfer flow in the thylakoid membrane (Lyska *et al.* 2013). Three DEGs where exclusively accumulating in the ST: GLUTATHIONE S TRANSFERASE (Eni_019294, AT3G62760), PEROXIDASE (Eni_091037, AT4G11290) and TOCOPHEROL CYCLASE (Eni_105533, AT4G32770). The former two DEGs belonged to multiple other transcripts with the same Arabidopsis homologue that were present in both tissue types, and therefore do not represent exclusive antioxidants in the ST. Eni_105533, however, was the only transcript relating to TOCOPHEROL CYCLASE, which is involved in vitamin E biosynthesis (Lundquist *et al.* 2012). Vitamin E prevents non-enzymatic lipid oxidation and is important for seed longevity (Sattler *et al.* 2004). This gene is also the main lipid antioxidant in plastoglobuli (Dłużewska *et al.* 2016), however, it is unclear why the ST would engage in tocopherol (vitamin E) synthesis and not the NST. This might indicate the preference towards other (unidentified) antioxidant systems in the NST.

Amongst transcripts expressed in both tissue types, the most highly abundant differentially expressed antioxidant (Eni_100318) was GLUTATHIONE PEROXIDASE (AT4G11600), a phospholipid peroxidase also found to be highly expressed at >30% RWC in *X. viscosa* (Illing *et al.* 2005), and accumulated during drying in *M. flabellifolia* (Kranner *et al.* 2002). This antioxidant has been implicated in oxidative signalling as well as providing a general protective role by keeping the ROS concentration below harmful levels (Wang *et al.* 2018b). However, this antioxidant was present at high levels in the

hydrated (control) plants in *M. flabellifolia* and is therefore both constitutively expressed and induced upon water-deficit stress (Kranner *et al.* 2002; Leprince *et al.* 2010). The high expression in both the NST and ST in *E. nindensis* illustrates this induced expression. Furthermore, when comparing seed antioxidants with vegetative tissues of resurrection plants to identify desiccation-specific antioxidants, Illing *et al.* (2005) found that 75% of antioxidants are expressed in the control plants and are therefore ubiquitous (termed housekeeping). Illing *et al.* (2005) also found that antioxidant activity remained at higher levels in *E. nindensis* compared to its desiccation sensitive sister-species *E. tef.* The heatmap illustrates that most antioxidant-related transcripts that were accumulating in abundance are constitutively expressed and elevation occurred on mild water-deficit stress (from 60% RWC) through to desiccation (<10% RWC) in both tissue types. This shows the maintenance and protection of these systems under severe abiotic stress. In summary, the transcriptomic antioxidant signature of the NST is similar to that of ST and does not show a clear trend towards greater antioxidant potential in the NST.

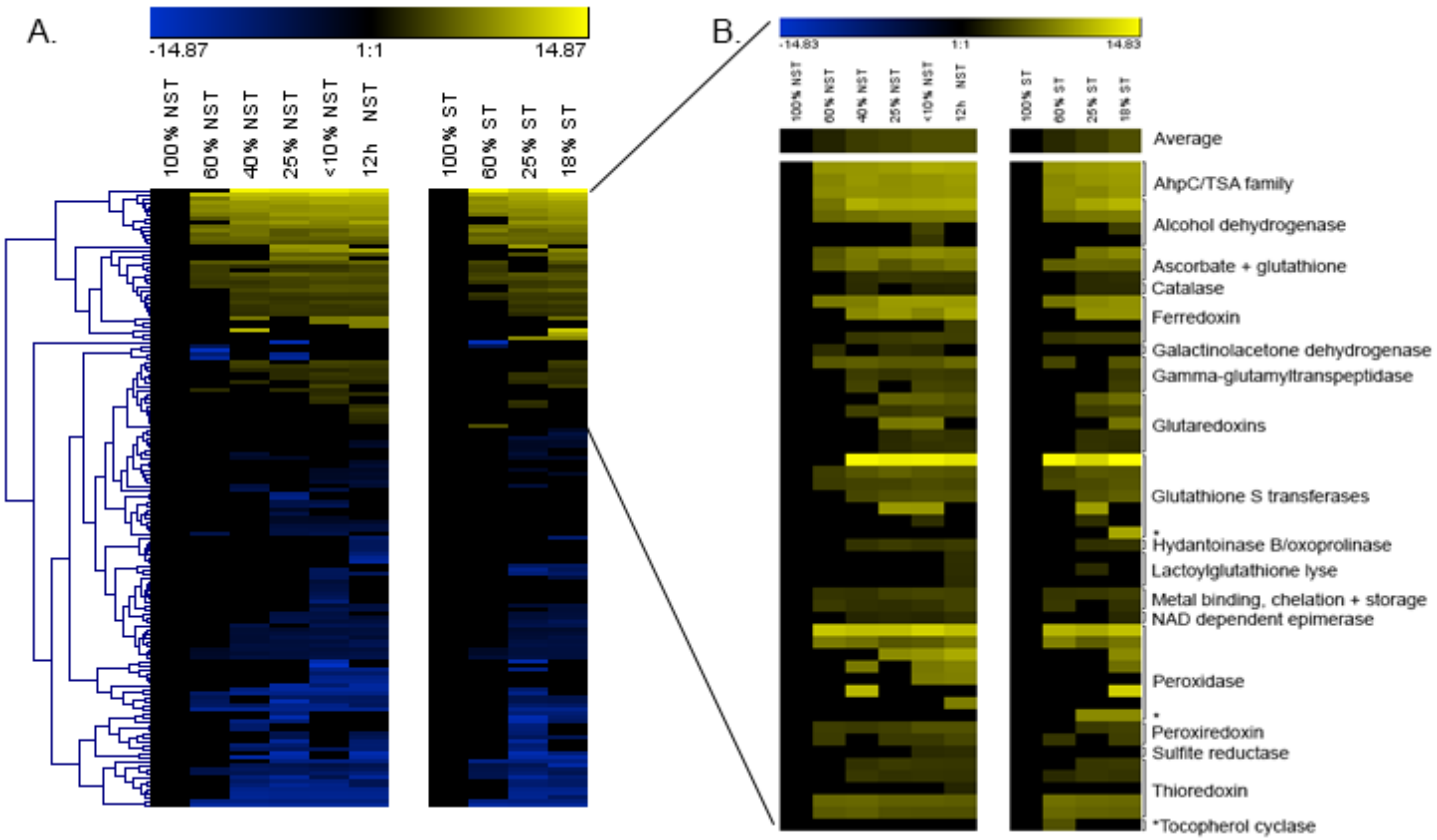

Figure 4.11: Antioxidant changes in transcript abundance in desiccation tolerant (non-senescent, NST) and sensitive (senescent tissues, ST) leaves of the resurrection plant *Eragrostis nindensis* upon severe water-deficit stress (%) and rehydration (12h). Only differentially expressed genes (DEGs) are depicted, derived from the statistically significant (>2 or <-2 log_2 fold change values, FDR <0.05) change in transcript abundance compared to the control (NST, 100% RWC). The colour scale represents log_2 fold change values. (A) Hierarchical clustering of DEGs showing several transcripts accumulating and diminishing in abundance. (B) Only transcripts accumulating during drying are shown, where * indicates transcripts that are exclusively accumulating in the ST. Average bar indicates the mean expression trends during drying.

4.3.2.10 Transcripts associated with senescence

A total of 59 DEGs with annotations associated with senescence were found to be differentially expressed during drying and rehydration in *E. nindensis*. The majority of these (n = 50) were diminishing in transcript abundance during desiccation (Figure 4.12). Several RUBISCO-related DEGs were diminishing during drying, demonstrating that chlorophyll breakdown upon abiotic stress is generally seen as a senescence-associated trait. In addition, two glutamine synthetases were accumulating in both tissue types, indicating that these DEGs are implicated in the nutrient reshuffling associated with both senescence and desiccation-response in resurrection plants. The response of these DEGs showed the same trend across both tissue types, thus making it difficult to decouple the effect of senescence from that of desiccation tolerance.

Interestingly, most of these (n = 28) were exclusively diminishing in transcript abundance in the NST, showing a strong shutdown of the senescence pathway in this tissue (Figure 4.12, red box). The DEGs diminishing in transcript abundance included well-known transcription factors that are positive regulators of senescence, such as NAC and WRKY (Woo *et al.* 2018; Yolcu *et al.* 2018). NAC transcription factors increased in expression upon salt-stress in Arabidopsis (Balazadeh *et al.* 2008), showing the activation of salt-induced senescence. *E. nindensis* showed the opposite relationship. Furthermore, other than SAG21 (SWEET15) discussed above, the only other SAG differentially expressed during drying was SAG12, a senescence-specific cysteine protease, which also diminished in abundance (Figure 4.12) and in cluster 9 and 12 (Figure 3.5.2), as reported in **Chapter 3**. This suppression of SAGs and their regulators (NAC/WRKY) highlights the differences in regulation between desiccation tolerant (resurrection plants) and desiccation sensitive species, such as Arabidopsis. Senescence is controlled by a complex network and involves the activation of signalling cascades mediated by transcription factors (Woo *et al.* 2018; Bresson *et al.* 2018). This strongly suggests that there is a difference in the regulation of senescence between tolerant and sensitive species, also reflected here between the NST and ST, where the NST actively suppressed senescence processes that would result in cell death. This is the first evidence of confirmed senescence associated transcripts being differentially regulated between the two tissue types. Similarly, in *X. schlechteri* and *T. loliiformis*, other senescence promotors are also inhibited upon desiccation, such as SAGs and pro-apoptosis genes (Williams *et al.* 2015; Costa *et al.* 2017). This hints that senescence is actively regulated in resurrection plants, however, coupling this with the similar global trends in the NST and ST revealed in this transcriptome shows that senescence is not simply controlled by a reduction in senescence-related transcripts. Furthermore, resurrection plants require an ordered metabolic arrest

ending in a quiescent, dormant state upon desiccation. The suppression of transcripts associated with senescence and their regulators in the NST, coupled with the cessation of metabolism, reflects this ordered reprogramming of metabolism in desiccation tolerant leaves.

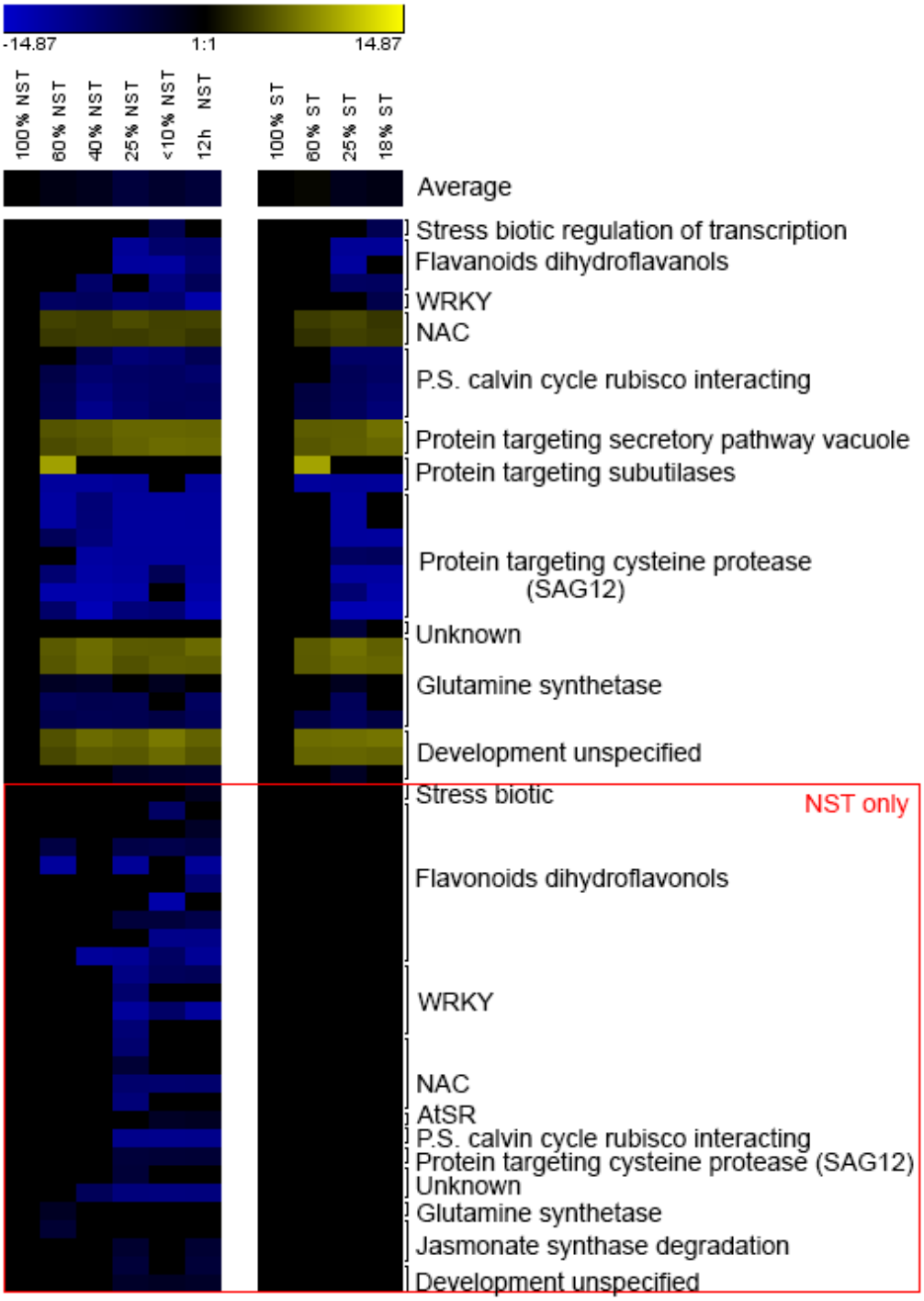

Figure 4.12: Changes in senescence associated transcript abundances during drying (measured as a relative water content, %) and rehydration (12h) in the resurrection plant *Eragrostis nindensis* in desiccation tolerant, non-senescent tissue (NST) and desiccation sensitive, senescent tissue (ST). Several senescence-related transcripts were exclusively diminishing in the NST (red box). Only differentially expressed genes (DEGs) are depicted, derived from the statistically significant (>2 or <-2 $\log_2$ fold change values, FDR <0.05) change in transcript abundance compared to the control (NST, 100% RWC). The colour scale represents $\log_2$ fold change values. Average bar indicates the mean expression trends during drying.

4.3.3. Enrichment associated with desiccation tolerance: An overview

In general, enriched categories showed similar trends in both tissue types, but key differences were also seen (Table 4.3). Both tissue types accumulated transcripts relating to '*seed and seedling development and dormancy*' (a proxy for desiccation tolerance), '*nutrient transport*', '*cellular homeostasis*' and *'cell communication'* (Table 4.3, A). Evidence of transcript accumulation in the '*signalling*' category and active '*protein processing'* in both tissue types suggests that metabolism is active, albeit slowed, and that protein turnover is potentially occurring throughout drying. Transcripts relating to the *'protein import into nucleus'* category showed accumulation during the desiccation and rehydration phases, possibly in anticipation of the translation of important transcripts upon rehydration. This category consists of transcripts predominantly involved in signalling cascade and RNA-binding, such as CYTOKININ RESPONSE FACTOR 4 (AT4G27950) and RAN BINDING PROTEIN-1 (AT5G58590). These transcripts are involved in the G-protein signalling pathway and are therefore important cellular signalling molecules during abiotic or biotic stress (Nilson *et al.* 2010; Muller *et al.* 2011; Kushwah *et al.* 2017). This accumulation of signalling and RNA-binding transcripts in the NST implies tighter transcriptional and translational regulation and could be an important factor differentiating desiccation tolerant and sensitive tissues. Furthermore, cytokinin regulates growth, stabilises photosynthetic machinery and has been linked to senescence inhibition and increased resistance to drought (Weaver *et al.* 1998; Prerostova *et al.* 2018). Cytokinins are also induced by stresses, such as drought (Prerostova *et al.* 2018) and have been shown to increase stress tolerance in transgenic tobacco by stimulating cytokinin production (Rivero *et al.* 2007). Transgenic Arabidopsis with enhanced cytokinin levels exhibited faster recovery and growth upon re-watering, however, it also exhibited increased water loss, which can be disadvantageous during long-term drought. The regulation of cytokinin is therefore more important than the abundance. CYTOKININ RESPONSE FACTOR 4 is induced by abiotic stress and not transcriptionally regulated by cytokinin, therefore playing a role in cytokinin modulation during stress (Zwack *et al.* 2016).

At severe-water stress (below 25% RWC), the '*GMP biosynthetic process'* category was overrepresented and accumulated in the NST only. Since GMP is essential for RNA, the NST might be investing into transcripts that will aid rapid translation of transcripts required for protection or recovery upon rehydration. This is commonly seen in seeds, where transcripts accumulate upon seed maturation and are stored for germination after imbibition (Sajeev *et al.* 2019).

Response to sugar transcripts (*'response to glucose'*, *'response to hexose'*) also had a dominant trend of accumulating in the NST (Table 4.3, A). Sugar metabolite accumulation is a trademark of desiccation tolerance, although most species accumulate sugars in the form of sucrose rather than glucose

(Hoekstra *et al.* 2001; Illing *et al.* 2005; Farrant *et al.* 2007) . There is a clear dominance of sugar-related transcripts enriched in the NST compared to the ST (glucose and hexose related categories, Table 4.3, A). Other non-reducing polysaccharides accumulated upon desiccation, and the category *'RFO biosynthesis'* showed extensive accumulation in the NST. The overrepresentation of RFOs exclusively in the NST, despite RFO-related transcript expression in the ST (Figure 4.6), suggests that the overall RFO metabolism is enriched in the NST, and emphasises the importance of RFOs in the NST. This enrichment analysis confirms the importance of these sugars in desiccation tolerance. As mentioned above, RFOs are key players in important cellular processes including acting as osmoprotectants and antioxidants, are compatible solutes and signalling molecules (Elsayed *et al.* 2014), and have been implicated in vitrification of tissues in the desiccated state (Hoekstra *et al.* 2001; Costa *et al.* 2017b; Farrant *et al.* 2017). Given the roles of raffinose, the over enrichment of RFOs exclusively in the NST of *E. nindensis* (in Figure 4.6 and Table 4.3), suggests that there are some differences in sugar regulation between the tissue types. It is possible that insufficient protection in the ST could contribute to water-deficit induced cell death.

Most of the GO categories showed similar trends in both the NST and ST (Table 4.3, A, B). One category is of particular interest: '*embryo development ending in seed dormancy*'. This category included 81 DEGs and was predominantly comprised of several LEAs (n = 31), and contained important regulators, such as bZIP transcription factors, RNA transcription, sugar related synthases and calcium signalling, as well as several unannotated transcripts. Upon seed maturation, various protective molecules (such as lipids, oleosins, LEAs and HSPs) and transcripts are accumulated and stored for germination. This is followed by metabolic arrest and ultimately leads to seed dormancy (Bai *et al.* 2018). The links between seed dormancy and desiccation tolerance have been discussed above (see also Figure 3.4.1). The fact that these dormancy transcripts are constitutively expressed throughout drying in both tissue types suggests that they play a general role in response to water-deficit stress and might reveal a general response to drought. However, the ST does not recover and failed to adequately engage in cellular protection, which suggests a general system failure in the ST. Again, this supports the notion that desiccation sensitive species or tissues engage in seed-related pathways upon severe stress, although the ST experiences some failure and results in cell death (Pardo *et al.* 2019).

The enriched categories of '*Leaf senescence*' and '*aging*' were exclusively diminishing upon desiccation in the NST (Table 4.3, B). To clarify, this does not represent exclusive transcripts diminishing in the NST but rather that transcripts in these categories are disproportionately represented in the NST only. Looking into the individual transcripts revealed that there were far more WRKY, NAC and MYB transcription factors relating to senescence diminishing in abundance, as depicted previously in Figure 4.12. The overrepresentation of senescence across the entire transcriptome in the NST only reinforces

the results seen in Figure 4.12, where major transcription factors regulating senescence processes were actively suppressed in the NST. This is a strong confirmation that senescence related transcripts were suppressed predominantly in the NST as opposed to the ST.

'*Lipid storage'* transcripts accumulated in abundance in both tissue types and this corresponded with diminishing *'lipid transport'* transcript abundances (Table 4.3, B). This suggests that lipids are being formed as energy stores during drying. Lipids play a pivotal role in desiccation tolerance, particularly in seeds, which is discussed in detail in **Chapter 5**. Plastoglobuli, the breakdown components of chloroplasts, function as lipid storage units and are known to increase upon water-deficit stress in poikilochlorophyllous species (Farrant 2000; Ingle *et al.* 2008), as well as in senescence or excessive oxidative stress on the photosynthetic machinery (Pressel *et al.* 2010; Charuvi *et al.* 2019). Lipid droplets were observed in both tissue types, although they appeared to differ in size, shape and distribution (Figure 2.12 - Figure 2.15). Lipid metabolism was therefore altered in both the NST and ST upon water-deficit stress, although the final products might differ between the tissues, as suggested by the ultrastructural observations in **Chapter 2**.

Transcripts associated with '*photosynthesis*' declined in both tissue types, which is unsurprising as this species exhibits the poikilochlorophyllous phenotype. However, a decline in photosynthesis is also a senescence-induced response and therefore attributing this decline to poikilochlorophylly alone cannot be stated with certainty. '*Growth*' enriched categories were diminishing in the NST only, although '*cell growth'* and '*cell wall biogenesis'* transcripts diminished in both tissue types (Table 4.3, B). The category enriched with '*cellulose biosynthesis'* diminished in the NST. This suggests that transcript abundance changes related to growth were highly overrepresented and implies that this category has greater transcriptomic redirection than in the ST. Overall, both tissue types responded to '*osmotic stress'* from water deprivation and accumulated a series of transcripts relating to seed development, protection (sugar metabolism), and solute transport and storage.

'Drought recovery' was an overrepresented category diminishing in both tissue types (Table 4.3B). However, looking at the composition of the category showed that these transcripts were mostly related to lignin biosynthesis. Six *E. nindensis* transcripts were annotated as the enzyme PHENYLALANINE AMMONIS-LYASE (AT2G37040), which is involved in polyphenol and lignin biosynthesis (Liu *et al.* 2018). The transcripts involved were identified as caleosins (AT1G70670), which are related to lipid structure and play a role in lipid degradation (Brocard *et al.* 2017). These DEGs were diminishing exclusively in the NST, which shows a strong suppression of lipid body breakdown during desiccation. This might be a growth suppression response under stress, as lignin deposition would be halted, and lipids stored for energy requirements, on rehydration.

Table 4.3: Overrepresented gene ontology (GO) categories accumulating (A) or diminishing (B) during drying (relative water content, %) and rehydration (12h) in the desiccation tolerant, non-senescent tissue and desiccation sensitive, senescent tissue of the resurrection plant *Eragrostis nindensis*. Biological process categories were determined in BiNGO (Biological Networks Gene Ontology) and REViGO (reduce and visualise gene ontology). Q-values were derived from BiNGO using FDR correction (q-value <0.05) with a >2 or <-2 log_2 fold change. The ratio (of expected to observed number of transcripts) represents the degree that each category is overrepresented, darker values represent high ratio and indicate their enrichment.

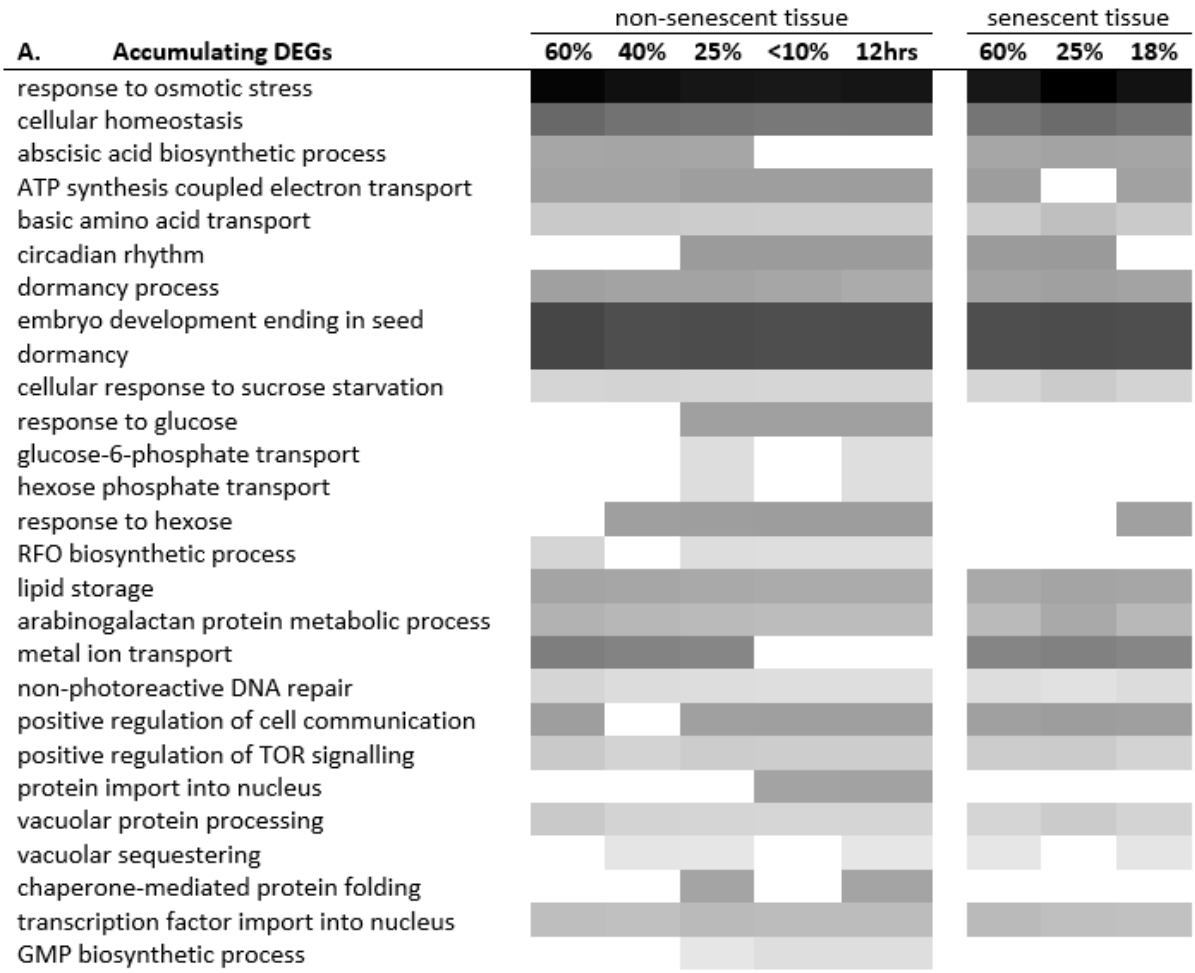

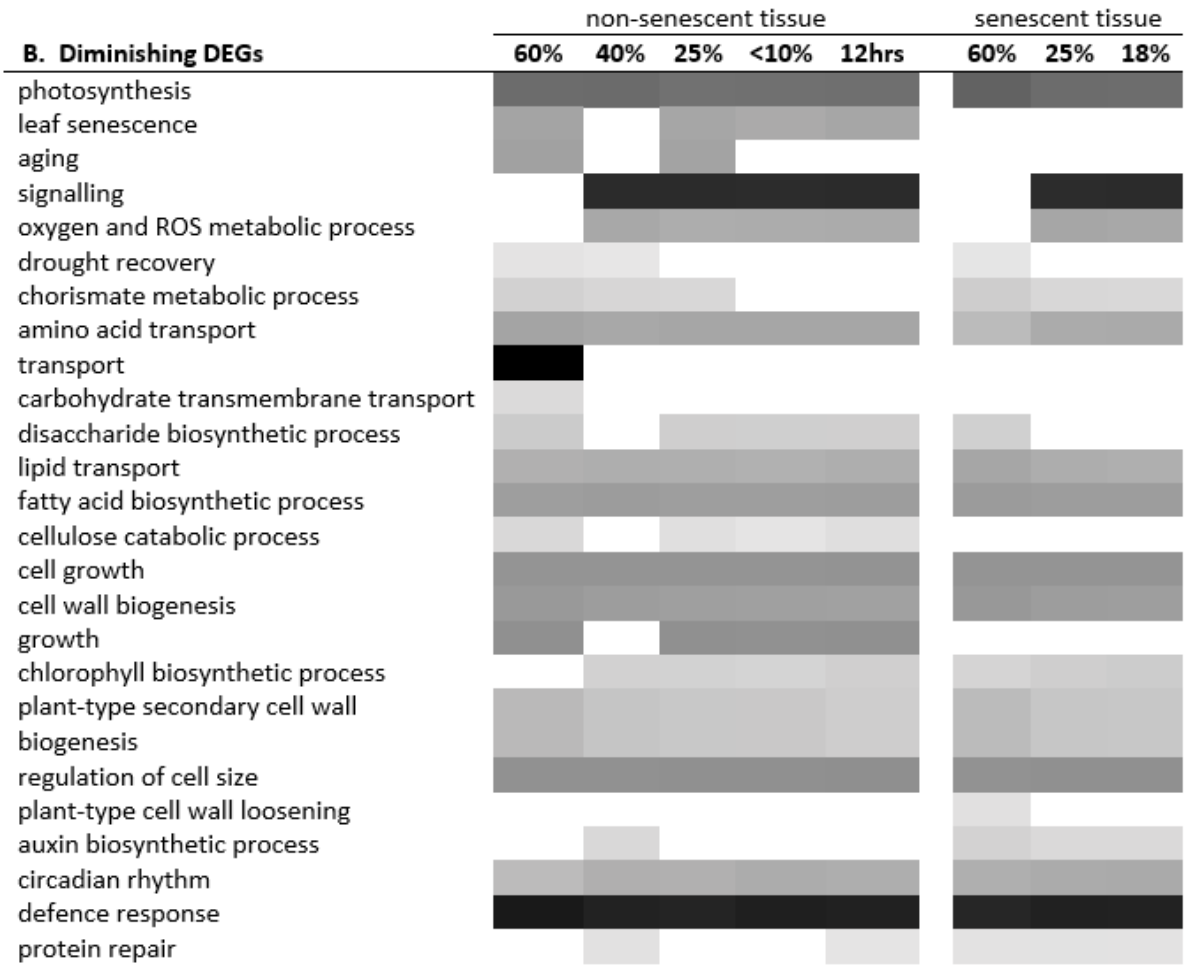

4.3.4. Regulation of senescence: differences between the NST and ST

One the of most intriguing results from the transcriptome is the mirrored transcript abundance patterns between the NST and ST, suggesting that, in general, the ST is responding similarly to the NST and is engaging some of the desiccation tolerant responses. Although *E. nindensis* clearly has a different senescence phenotype (shown in **Chapter 2**), this difference was not overtly obvious in the transcriptome. Some differences exist but the overwhelming trends in the NST were paralleled in the ST. To investigate this (non-)senescence phenomenon further, DEGs exclusively co-expressed in the NST and ST were analysed to help identify the core set of transcripts that differentiate the two tissue types. Exclusive transcripts were identified, and each subset subjected to an enrichment analysis to determine the overrepresentation of biological processes exclusively present (or absent) in each tissue type. Since there is no 12h ST timepoint, these DEGs were removed from this analysis. For biological processes overrepresented during rehydration see Table 3.Table 3.3.

4.3.4.1 DEGs exclusively accumulating

In the NST, 39 GO categories were enriched with 633 accumulating transcripts that were exclusively present in the NST (Figure 4.13.1). Of these categories, five were below the <0.05 dispensability threshold: '*amino acid biosynthetic process*' (GO:0009082), '*response to heat*' (GO:0009408), '*chaperone-mediated protein complex assembly*' (GO:0051131), '*regulation of seed germination*' (GO:0010029), and '*glucose-6-phosohate transport'* (GO:0015760) (Appendix, Table A5). The first four categories are known drivers of protein metabolism and are related to the synthesis and refolding of proteins under abiotic stress and include 10 HSPs. Furthermore, several of the DEGs relating to these enriched categories are also involved in signalling, protein degradation and post-translational modification, or transport. In addition to this, '*RNA processing'* (GO:0006396) and related overlapping categories (GO:0008380, GO:0016071, GO:0006397, GO:0010467, GO:0032006) were investigated further due to the dominance of DEGs enriched in this category.

In the ST, the 222 transcripts exclusively accumulating showed an over-representation in *'mitochondria-nucleus signalling*' and '*mitochondrial ATP synthesis'* (Figure 4.13.1, Appendix, Table A6). Three DEGs belonging to the '*mitochondria nucleus signalling'* category were annotated as alternative oxidases (AOX, AT3G22370). In C4 plants, such as *E. nindensis*, AOX were found not to play a photoprotective role of PSII as in C3 plants (Zhang *et al.* 2017b), but rather is an important signalling system from mitochondria to nucleus in response to stress, particularly carbon and nitrogen starvation (Butow *et al.* 2004). This mitochondrial retrograde response could therefore be an important factor regulating senescence in response to water-deficit stress, as there is an acute enrichment of the AOX and ATP synthesis pathways exclusive to the ST during drying. Since the nucleus controls metabolism through the regulation of transcription, the role of mitochondrial signalling on the nucleus might be an important factor determining whether a cell survives or senesces and should be explored in future studies. The enrichment of these GO categories indicates a general response to maintaining energy supply through ATP and indicates an important role of mitochondria-nucleus signalling in response to water-deficit stress and a lack of transcripts affiliated with protection as seen in the NST.

4.3.4.2 Post-transcriptional and translational regulation influences senescence

The NST had more DEGs exclusively accumulating (20.5%, n= 633) compared to 7.2% (n = 222) in the ST (Figure 4.13.1). This suggests that the NST exhibits a tighter control of transcription regulation under abiotic stress. The differences between the NST and ST become apparent at the lower water contents, represented by the average bar in Figure 4.13.1, where transcript accumulation steadily increased at lower water contents. A striking feature of the exclusive analysis revealed that the DEGs

exclusively accumulating in the NST were strongly over-represented into two broad categories: regulation of transcription (*'RNA processing'* and related categories) and protein metabolism (*'amino acid metabolism'*, *'response to heat'*, protein folding *'response to unfolded protein'*, chaperoning *'chaperone-mediated protein complex assembly',* import into nucleus *'protein localisation in nucleus'* and several overlapping transcripts from '*regulation of seed germination'*) (Figure 4.13.1). These two biological processes, albeit broad, dominated the DEGs enriched exclusively in the NST, but showed a clear absence of enrichment in the ST (Figure 4.13.1). To investigate the suspected role of RNA storage, the category '*RNA processing'*, and associated categories, were explored.

4.3.4.3 The role of transcriptional control in the NST: RNA processing

Of the 93 DEGs belonging to the enriched '*RNA processing'* and related categories, 28 are involved in the regulation of transcription and are comprised of several stress-related transcription factors (e.g. bZIP, NAC) or transcripts involved in post-translational modification (protein synthesis and degradation, Appendix, Table A9 – Table A12). The capacity to adjust the transcriptome through transcript synthesis and degradation upon abiotic stress is essential to ensure correct RNA turnover of stress related transcripts and thus ensures the appropriate downstream transcriptional activity (Perea-Resa *et al.* 2016). RNA degradation processes through decapping therefore play a critical role in stress response (Anderson *et al.* 2009; Ivanov *et al.* 2018). Amongst the enriched '*RNA processing'* category, the highest fold changes of 11 and 10.7 (in 40% and 25% RWC, respectively; Appendix, Table A9) is a SMALL NUCLEAR RIBONUCLEOPROTEIN FAMILY PROTEIN (AT3G14080) involved in the LSM1-7 decapping activator complex, shown to play a major role in mediating abiotic responses in Arabidopsis (Wawer *et al.* 2018; Chantarachot *et al.* 2018). The distinct presence of transcripts required for the fine-tuning of RNA turnover and transcription in the NST, coupled with the absence of these transcripts in the ST, suggests that the translational apparatus is not only functional, but also discerning.

4.3.4.4 The role of transcriptional control in the NST: Post translational modification

The transcriptome of *E. nindensis* showed more '*post-transcriptional modification'* DEGs (n = 15) exclusively accumulating during drying in transcript abundance in the NST compared to the ST (n = 3) (Appendix, Table A10). A further 7 DEGs were exclusively accumulating during rehydration, with 11 DEGs exclusively diminishing during rehydration. Several studies have shown a disassociation between the abundance of RNA and protein translation (Sablok *et al.* 2017; Bai *et al.* 2017). This is largely due

to important or stress-related RNAs selectively undergoing post-transcriptional modifications that play a role in translation under stress (Bai *et al.* 2017). RNAs can affect translation as their GC-content, motif enrichment, transcript length and secondary structure affect the binding of RNA to the ribosome and hence exhibit translational control (Bai *et al.* 2017; Sablok *et al.* 2017; Sajeev *et al.* 2019). In Arabidopsis seeds, RNA undergoes changes in their association to ribosomes based on the abovementioned attributes of the RNA, and are thus undergoing selective translation during seed germination (Bai *et al.* 2017; Sajeev *et al.* 2019). The genes under translational control play a role in protection and are associated with desiccation tolerance: LEAs, HSPs, seed storage proteins, cell wall-related genes, ribosomal genes and ABA-auxin related genes, *inter alia*, showing the importance of post-transcriptional regulation on translation control (Bai *et al.* 2017).

DEGs relating to translation were dominant in the NST (Figure 4.13.1). The NST also exhibited higher transcript accumulation (Figure 4.1) and survives post-desiccation. Taken together, this implies that transcripts are stored in NST of *E. nindensis* during drying. This is a critical step in desiccation tolerance: the ability to stabilise and store RNA during severe drying for the recruitment of these RNAs for protein synthesis during recovery (Wood *et al.* 1999; Blomstedt *et al.* 2018). The notion that desiccation tolerant leaves show higher RNA accumulation has been identified in other species (Bartels *et al.* 1990; Oliver 1991). The accumulation of RNA is not a desiccation tolerance trait *per se* as desiccation sensitive species also accumulate transcripts upon stress, however, these are transcriptionally impotent (Jang *et al.* 2019). Oliver (1991) has shown that the transcribed RNA of a desiccation tolerant moss *Syntrichia ruralis* increased upon slow drying. This RNA is stably bound to ribonucleoprotein (RNP) complexes that protect the structural integrity of the RNA until initiating protein translation (Luo *et al.* 2018b; Wang *et al.* 2018a). Like *S. ruralis,* other resurrection plants accumulate transcripts required for rapid re-synthesis of the photosynthetic apparatus during rehydration, and it has been postulated that these RNAs are maintained and stably stored for up to a year in the desiccated state (Dace *et al.* 1998; Bajic 2006). Juszczak and Bartels (2017) observed that desiccation tolerant species recruited RNAs into polysomes more efficiently than desiccation sensitive species, stabilising the RNA and delaying its degradation during drying. However, in *E. nindensis,* the decline in ST protein turnover cannot be attributed to the reduction in mRNA transcripts as similar expression patterns were found in key traits of desiccation tolerance, as described above (LEAs, HSPs, antioxidants etc.).

All organisms have mechanisms to regulate post transcriptional processing, and this translational regulation enables cells to rapidly and reversibly respond to endogenous and environmental signals (Sajeev *et al.* 2019). Once RNA is exported from the nucleus it is intricately regulated to determine whether it is translated, degraded or stored (Weber *et al.* 2008; Chantarachot *et al.* 2018). RNAs typically have short half-lives (measured in minutes) and if not translated in the cytoplasm by

polysomes, are aggregated into membrane-less bodies that contain ribonucleoprotein (RNP) complexes (Chantarachot *et al.* 2018; Sajeev *et al.* 2019). These bodies are identified as stress granules (SGs) or processing bodies (P-bodies) and play a role in the storage of non-translatable RNAs or are sites for RNA degradation (Jang *et al.* 2019; Luo *et al.* 2018b). The rate of RNA degradation is as important as transcription, as both of these determine the amount of RNA in the steady state pool (Bremer *et al.* 2014). How RNAs are selected for storage or degradation and how this process is regulated is still unknown (Wang *et al.* 2018a). Whether P-bodies or SGs form in *E. nindensis* is unknown, as they are detected through immunofluorescence localisation studies, which was beyond the scope of this thesis. Nevertheless, evidence suggests that there is transcribed RNA in leaves of *E. nindensis* that is repressed/stabilised and safely stored during the desiccated state and recruited into the polysome for protein synthesis during rehydration. This is based on the following two factors. Firstly, the high RNA transcription observed at lower water contents suggests that transcripts are stored, including several which are associated with recovery. For example, the transcript abundance accumulation of early light-induced proteins (ELIPs) during drying in both tissue types (Appendix, Figure A4) suggest that these transcripts are stored for rehydration, as ELIPs play a role in the early recovery of poikilochlorophyllous species (Xiao *et al.* 2015; Dinakar *et al.* 2018; VanBuren *et al.* 2019a). Secondly, the exclusive analysis highlighted the role of RNA regulation and protein metabolism as the main differences separating the NST from the ST. In addition, Dace *et al.* (1998) argue that RNAs for PSII components must be stored in the desiccated leaves in *X. humilis* and that protein synthesis is re-established during rehydration (Tuba *et al.* 2011). Still, no study has investigated the storage of RNAs in resurrection plants despite the large possibility that the absence of RNA storage is unlikely. The transcriptome of *E. nindensis* has shed light on this, as the data imply that there is a failure in adequate RNA regulation in the ST that results in either insufficient storage (i.e. protection) of RNA or non-selective degradation of transcribed RNA.

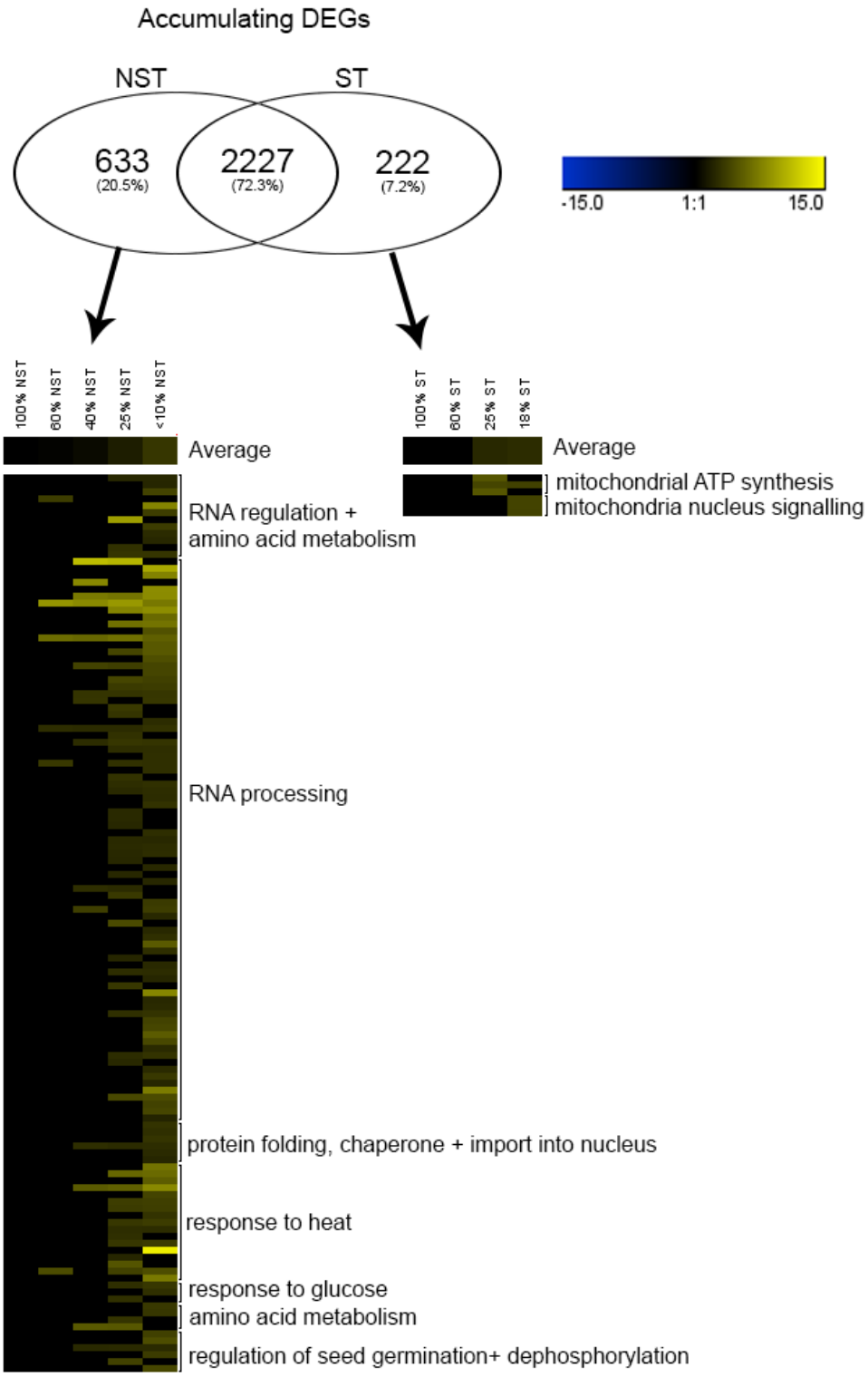

Figure 4.13.1: Dominant transcript abundance patterns of differentially expressed genes (DEGs) exclusively accumulating in desiccation tolerant, non-senescent tissue (NST) and desiccation sensitive, senescent tissue (ST) of the resurrection plant *Eragrostis nindensis* during drying (represented as relative water content, RWC, %). The dominant overrepresented gene ontology (GO) categories indicate the main differences between the NST and ST during drying. For a comprehensive list of enriched GO categories see the Appendix, Table A5 and Table A6. DEGs were derived from the statistically significant changes (>2 log_2 fold change, FDR <0.05) in transcript abundance compared to the control (NST, 100% RWC). The colour scale represents log_2 fold change values. Average bar indicates the mean expression trends during drying.

4.3.4.5 Annotated transcripts imply translational control in the NST

Cellular response to stress results in rapid proteome adjustments through the regulation of RNA transcription and translation (Wang *et al.* 2018a). Gene expression is a complex process and requires the controlled regulation of transcription, post-transcription modification and/or processing, RNA stability, protein synthesis and protein degradation as well as metabolite production and/or degradation (Dutt *et al.* 2015). Translation of RNA is under tight regulatory control and begins with the initiation of protein synthesis, which is the most rate-limiting, regulated and complex step (Dutt *et al.* 2015; Sesma *et al.* 2017). Although translational control was not investigated *per se* (beyond the scope), the annotated transcripts that are exclusively accumulating in abundance suggest greater translational control in the NST compared to the ST. Transcripts relating to ribosomal proteins of 40S and 60S are both highly over-represented from <10% RWC in the NST (Appendix, Table A11). These proteins carry out the initiation and elongation stage and are regulated by other proteins (mTOR, eIF4E and eIF2α) that control transcript expression (Sesma *et al.* 2017). Neale *et al.* (2000) showed an increased expression in eIF1 (elongation factor1) protein translation initiation factor during drought stress in desiccation tolerant leaves of *S. stapfianus*, which is in contrast to Bremer *et al.* (2014) and Giarola *et al.* (2015), who used eIF4E as a reference gene due to its stable expression. There was no significant increase in transcript abundance of the elongation factors eIF4E and eIF2α in *E. nindensis* and their consistent expression during drying indicates their ubiquitous roles as housekeeping genes, and not stress-response genes. However, three elongation factor transcripts were differentially expressed in the transcriptome, of which all are exclusively present in the NST at <10% RWC, however, only one is accumulating (Eni_062202, Appendix, Table A11). Furthermore, the NST had a higher presence of transcripts related to *'initiation'*, '*elongation*', *'ribosome biogenesis pre-rRNA processing and modifications'* and '*ribosome biogenesis'* compared to the ST (Appendix, Table A11). The enrichment of several initiation and elongation transcripts, as well as a significant increase in the translation machinery (e.g. ribosomes) portray a flow in transcript abundance towards protein metabolism. In addition, the exclusive NST analysis depicted the maintenance and protection of existing proteins in the NST, as the categories of '*protein folding'* and '*chaperone*' were highly over-represented in accumulating DEGs (Figure 4.13.1). However, the absence of these over-represented categories in the ST, coupled with the paralleled transcription patterns between the NST and ST shown in the targeted analysis (Table 4.3) suggest that either protein synthesis is deactivated in the ST, or that the transcribed RNA in ST is not being protected, and hence degraded, or potentially, both.

Protein transcription and translation is a response to stress in desiccation tolerant plants (Oliver 1991; Gaff *et al.* 1997, 2009; Blomstedt *et al.* 2010). One key feature of desiccation tolerance is that the translational machinery of desiccation tolerant species remains functional at low water contents,

whereas translation is severely compromised in desiccation sensitive species, and other than a few SAG products, is essentially shut down (Bartels *et al.* 1990; Griffiths *et al.* 2014). Recently, Pardo *et al.* (2019) have shown that transcripts annotated as "seed related genes" accumulate during drying, regardless of their tolerance to desiccation (highly accumulated in both desiccation tolerant *E. nindensis* and *O. thomaeum* and desiccation sensitive *E. tef, Sorghum bicolour, Zea mays*). A similar pattern was depicted in *E. nindensis,* where the desiccation tolerant and sensitive tissues both accumulated seed-related genes during drying (embryo development ending in seed dormancy, Table 4.3, A). This suggests that these genes represent a general drought response in plants, but that only desiccation tolerant tissues survive due to their ability to regulate transcription and translation at critical water contents. The dominant transcriptomic signature identified in the exclusively accumulating DEGs in the NST reinforces this notion. In addition, several accumulating transcripts in lower water contents, especially in rehydration, are related to protein synthesis (initiation and ribosomal synthesis) and protein degradation (mostly ubiquitin-like processes), which validates the potential efficacy of the translational machinery at low water contents during rehydration in *E. nindensis* (Appendix, Table A11). The presence of several DEGs related to ubiquitination and degradation also demonstrates the importance of maintaining a selective degradation system to lessen the harmful consequences of mis- or unfolded proteins (Appendix, Table A11 and Table A12). Furthermore, of the 89 *'protein synthesis'* DEGs in the transcriptome, 50 of these are absent in the ST and are mostly involved in ribosome biosynthesis, which is a component critical to translation (Appendix, Table A11). The over-representation of transcripts in the NST, suggests a tighter control of metabolic readjustment into, and recovery from, the quiescent desiccated state, and the over-representation of processes relating to transcription (especially RNA storage) and translation indicate better control compared to the ST. These processes, coupled with the ordered accumulation of known desiccation tolerance traits during drying, separate the surviving, desiccation tolerant leaves from the senescing desiccation sensitive leaves in *E. nindensis.*

4.3.4.6 DEGs exclusively diminishing

Like the exclusively accumulating DEGs, the abundance of exclusively diminishing DEGs was greatest at lower water contents (below 40% RWC, represented by the average bar, Figure 4.13.2). Similarly, the NST showed greater transcriptional flux illustrated by the number of exclusively diminishing DEGs (32.3%, n = 1454) compared to the ST (10.1%, n = 452). Several GO categories were enriched with DEGs diminishing in abundance (Appendix, Table A7 and Table A8). Amongst the DEGs with exclusively diminishing transcripts in the NST, the category '*senescence*' was highly over-represented (Figure

4.13.2). This finding is consistent with Table 4.3, B, where the senescence category is only over-represented in the NST. The transcripts in this category are predominantly well-known transcription factors WRKY and NAC (n = 8), and flavonoids involved in secondary metabolism (n = 9). The flavonoid transcripts belong to two Arabidopsis homologues: AT5G24530 (which is associated with the biosynthesis of salicylic acid) and AT1G17020 (a senescence-related gene involved in redox reactions) (Zhang *et al.* 2017a). Previous studies have found a decline in SAGs during drying in resurrection plants (Griffiths *et al.* 2014), and this analysis both validates and expands on those findings. Here, it is shown that senescence was actively suppressed in the NST, and this, coupled with the maintenance of the proteins and transcriptional apparatus, is a dominant factor that prevents senescence and cell death in the NST of *E. nindensis*.

The *'signalling'* and '*protein phosphorylating'* categories had several overlapping DEGs and were over-represented within the DEGs diminishing exclusively in the NST (Figure 4.13.2). The majority of these DEGs are identified as leucine-rich protein kinases involved in broad signal transduction, from perceiving signals to transducing them via autophosphorylation (Liu *et al.* 2017). This phosphorylation plays a critical role in the regulation of downstream gene expression by affecting the activation of transcription factors (Joshi *et al.* 2016). The enrichment of '*protein phosphorylating*' related DEGs illustrates tight post-translational control in the NST. Also, 50% of these were cell-to-cell mobile, a feature that is an important regulator of development, implying a shutdown of long-distance signalling mechanisms (Luo *et al.* 2018a). This, coupled with diminishing transcripts of '*photosynthesis*' and '*growth*' (Table 4.3) reflects the general shutdown of metabolism observed in **Chapter 3** and represents the controlled readjustment of the translational machinery.

In the ST, most transcripts strongly diminished at 25% RWC with very few changes at 18% RWC (Figure 4.13.2). Nine GO categories were enriched (Appendix, Table A8), with the top three showing transcript abundances diminishing in '*photosynthesis*', '*stomatal complex morphogenesis'* and '*regulation of cell adhesion',* indicating a general cessation in regulation related to photosynthesis and growth. Although the shutdown of photosynthesis was observed in both tissue types, these DEGs represent those that are unique to the ST. However, how these DEGs contribute to senescence (if they do), is unclear. Identifying whether the outcome of chlorophyll restructuring, and breakdown is reversible (i.e. whether the chloroplasts reform and recover, or whether they degrade and senesce), is difficult, and requires the identification of a specific biomarker to differentiate the senescence from the desiccation tolerance process.

In summary, there were more DEGs exclusively diminishing in abundance in the NST (n = 39, excluding DEGs in rehydration only) compared to the ST (n = 9), and these showed a suppression of senescence

in the NST only. Coupled with this, the transcripts exclusively accumulating in the NST showed an over-representation of DEGs related to RNA processing and translational machinery (Figure 4.13.1). This indicates a greater control of translation in the NST under severe water-deficit stress. These changes became apparent at lower water contents (25% RWC), demonstrating the inability of non-desiccation tolerant tissues to survive below 30% RWC, as originally proposed for seeds by Vertucci and Farrant (1995) and implicated for resurrection plants (Farrant *et al.* 2012). The paralleled acquisition of desiccation tolerance in the vegetative leaves of resurrection plants can be extended to the seed-like mechanism of RNA stabilisation, protection and storage, and this transcriptome reflects this concept.

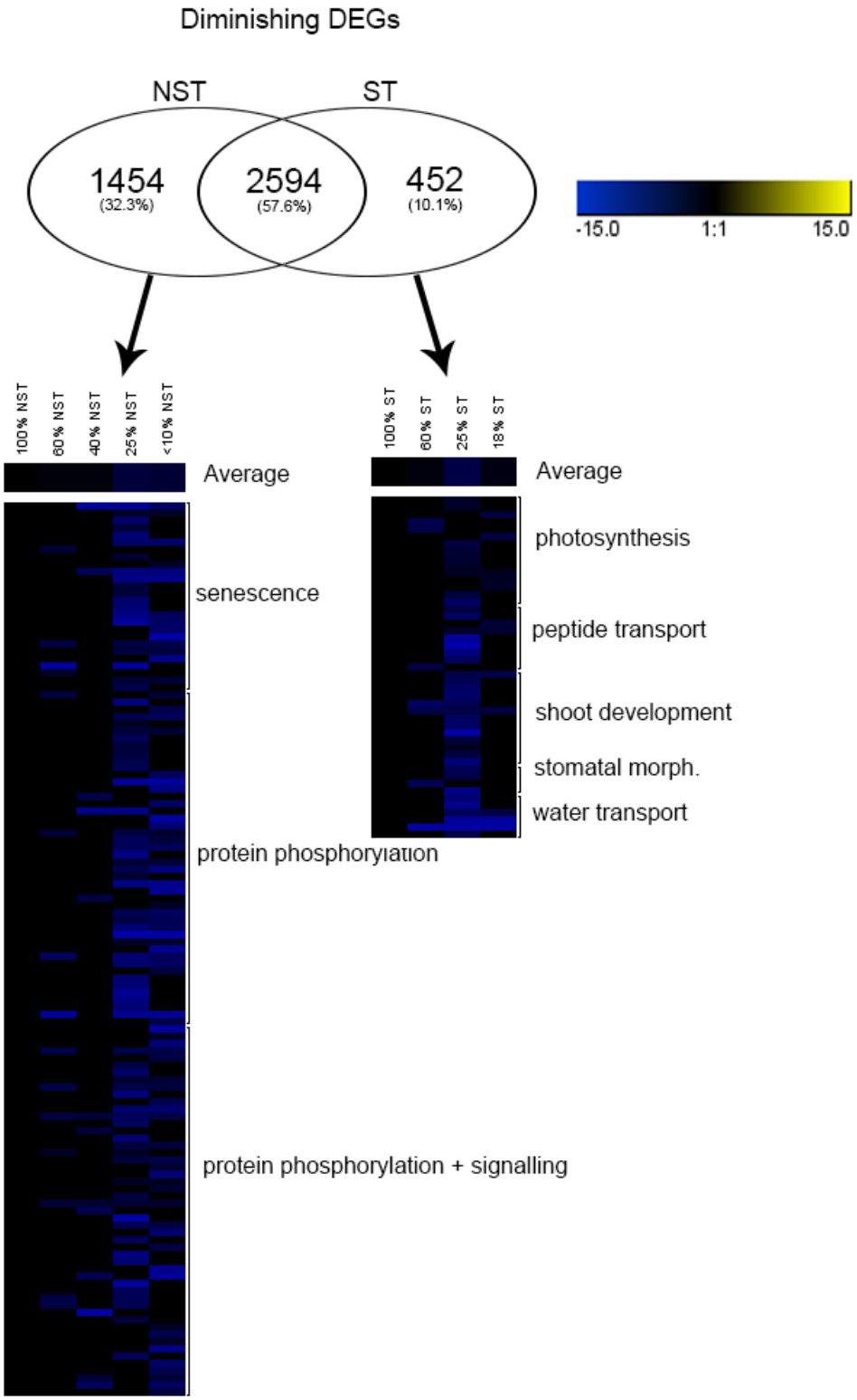

Figure 4.13.2: Dominant transcript abundance patterns of differentially expressed genes (DEGs) exclusively diminishing in desiccation tolerant, non-senescent tissue (NST) and desiccation sensitive, senescent tissue (ST) of the resurrection plant *Eragrostis nindensis* during drying (represented as relative water content, RWC, %). The dominant overrepresented gene ontology (GO) categories indicate the main differences between the NST and ST during drying. For a comprehensive list of enriched GO categories see the Appendix Table A7 and Table A8. DEGs were derived from the statistically significant changes (<-2 log_2 fold change, FDR <0.05) in transcript abundance compared to the control (NST, 100% RWC). The colour scale represents log_2 fold change values. Average bar indicates the mean expression trends during drying.

4.4. CONCLUSION

This **Chapter** has attempted to understand how the NST differs from the ST in *E. nindensis* by exploring the main differences in transcript abundances between the tissue types. The hypothesis of this thesis was that those transcripts not differentially expressed in the ST, but differentially expressed in the NST, must be key for desiccation tolerance. These transcripts could also shed light into the different regulatory processes of senescence. Delving into those transcripts exclusively expressed or suppressed in each tissue type identified strong trends.

The findings from this **Chapter** show that in the ST there is a general failure in RNA processing and translation coupled with the inability to suppress senescence. The significant transcriptional reprogramming in the NST as shown by suppressing known key-players of senescence is not detected in the ST. The senescence programme therefore seems to sit in between a desiccation tolerant and desiccation sensitive response. Senescence in *E. nindensis* can therefore be classified as a resurrection plant specific trait, where the transcriptional programme is generally maintained (resurrection plant response), however, translation is dysfunctional (non-resurrection plant response). Although translation continues in non-resurrection plants, this is limited to senescence-related genes and does not include the reprogramming of transcription (Bartels *et al.* 1990; Griffiths *et al.* 2014), as seen in the ST during drying. Furthermore, the key traits differentiating the NST from the ST were observed at lower water contents (below 25% RWC), demonstrating that only desiccation tolerant tissues can survive below 25% RWC (Vertucci and Farrant 1995; Farrant *et al.* 2012).

It is not the amount of RNA that differentiates the NST from the ST, as the levels of RNA were comparable between the two tissue types (Appendix, Table A). Juszczak and Bartels (2017) suggested lower RNA levels as one reason for the inability of desiccation sensitive species to survive severe stress. Similarly, VanBuren *et al.* (2018) observed lower oleosin RNA levels in the desiccation sensitive species *Lindernia subracemosa* compared to its desiccation tolerant sister species *Lindernia brevidens*, implying that transcriptional inefficiencies, resulting in lower RNA abundances, were a cause of insufficient protein turnover rather than translational failure, as observed in *E. nindensis.* It is known that desiccation tolerant plants suppress SAGs under severe-water stress (Griffiths *et al.* 2014), however, this has never been explored on a transcriptome-wide scale. Furthermore, there is a noticeable absence of adequate protection of the transcriptional and translational machinery in the ST (TEM images **Chapter 2**). Again, the NST showed substantial transcript abundance trends towards the protection of RNA and proteins. It has been suspected that resurrection plants alter their UPR

system and it has been speculated that resurrection plants store transcripts for translation upon recovery, however, further exploration into this has not yet been undertaken. Based on the annotation of the transcripts, this transcriptome has shown the transcriptional shifts towards protein folding, chaperoning and general protein metabolism and maintenance. Evidently, desiccation tolerance traits need to be appropriately laid down before the water content falls below a critical level to ensure whole-leaf survival. The NST mitigates the consequences of an anhydrous environment on the sub-cellular structure, membranes, and proteins, whereas the ST does not (**Chapter 2**). This might be explained by, *inter alia*, the insufficient regulation of RNA, and hence inadequately protected and unstable RNA in the ST.

This research suggests that it is the overarching process of translation that is a major determinant of whether a tissue survives or senesces in *E. nindensis*. Without the adequate maintenance of fundamental proteins, irreparable damage will eventually cause cell death. Since transcript abundance patterns are similar for the key desiccation tolerance traits, it is possible that *E. nindensis* engages in a regulation of senescence at the translational level, rather than a fine-tuning of transcriptional regulation. Transcript abundance is higher in the NST than the ST, suggesting a more complex regulation. Senescence in *E. nindensis* can therefore be characterised as being post-transcriptionally determined (i.e. RNA is protected in the NST but degraded in the ST) and translationally regulated (the machinery is maintained in the NST, whereas it is non-functional in the ST). Senescence therefore appears to be acting on the translational machinery. Transcription is cheaper than translation, and resurrection plants may have co-opted RNA storage and protection systems from seeds, just as angiosperm resurrection plants have acquired desiccation tolerance traits. Seeds are a known model to study the translational control from a quiescent to active metabolic state (Sajeev *et al.* 2019), and this thesis indicates that resurrection plants are also excellent models to investigate this developmental switch.

Chapter 5

LIPID COMPOSITION REFLECTS A CRUCIAL COMPONENT OF DESICCATION TOLERANCE OF *E. NINDENSIS*

5.1. INTRODUCTION

One of the key features differentiating desiccation tolerant from desiccation sensitive plant species is the irreparable membrane damage causing cell death in desiccation sensitive plants upon desiccation (Hoekstra *et al.* 2001; Rascio *et al.* 2005; Quartacci 2002; Bresson *et al.* 2018). Lipids form the basis of membranes and as such are fundamental to life (Ruiz *et al.* 2018). Found across all life forms, lipid metabolism is a vital process and is a conserved strategy of desiccation tolerance (Costa *et al.* 2016). Furthermore, lipids are crucial biomolecules in plants; they are vital energy stores, important signalling molecules, and are involved in membrane trafficking. Hence, they are essential for biochemical reactions, such as photosynthesis (van der Schoot *et al.* 2011; Fahy *et al.* 2011; Pyc *et al.* 2017; Huang 2018). Lipids play an active role during abiotic stress response and are promptly activated through stress stimuli, as seen by their accumulation and high turnover rates upon abiotic stress (Hou *et al.* 2016; Liu *et al.* 2019a). Changes in lipid conformation during drying are known to be involved in the acquisition of desiccation tolerance (Shimada *et al.* 2018). How lipid classes change and their role in desiccation tolerance strategies of *Eragrostis nindensis* is unknown. However, the ST of *E. nindensis* showed higher electrolyte leakage compared to the NST during drying and indicated ruptured plasmalemma membranes upon desiccation (Vander Willigen *et al.* 2001b). The desiccation tolerant leaves of *E. nindensis* can therefore prevent such rupturing through, *inter alia*, stabilising proteins and conformational changes in lipid structure upon desiccation, whereas the ST fails to achieve this protection, and dies. These changes in lipid composition during drying in *E. nindensis* are currently unknown.

Fatty acids (FAs) are the building blocks for membrane and neutral lipids (Aid 2019). They are synthesised in the plastids and are exported to the endoplasmic reticulum (ER), where they undergo diversification into different lipid classes, which exhibit diverse structures and functions (Moore *et al.* 2016; Shimada *et al.* 2018). For example, triacylglycerol (TAG), the simplest form of lipid, consists of three FAs with a glycerol head (Guo *et al.* 2017; Wang *et al.* 2017). FAs are converted into diacylglycerol (DG), which is either imported into the chloroplast for the synthesis of galactolipids

(MGDG, DGDG, SQDG; see Table 5.1 for details), or diversified into TAG or phosphatidylcholine (PC) in the ER (Mongrand *et al.* 1998; Wang *et al.* 2012a; Hu *et al.* 2012; Sato *et al.* 2017). Lipid classes are comprised of several combinations of molecular species, which vary in carbon chain length as well as the number and position of double bonds (Benning 2009). Lipid species are typically referred to by the length of their carbon chains and the number of double bonds they have. Amongst TAG species, for example, TAG 54:8 has 54 carbons with 8 double bonds in its FA chains (comprising of 18:2/18:3/18:3). The ability of plants to modify lipid species composition (i.e. the desaturation level of lipid acyl chains) is well established, however, these changes are minor when compared to changes in lipid classes upon environmental changes (Benning 2009). This **Chapter** will therefore focus on lipid classes, rather than identifying changes in lipid species.

Table 5.1: The abbreviation and category of the fifteen lipid classes identified in the resurrection plant *Eragrostis nindensis* show a dominance of glycerolipids.

Abbreviation	Class	Category
CE	cholesteryl ester	Sterol lipid
Cer-NS	ceramide non-hydroxyfatty acid-sphingosine	Sphingolipid
DGDG	digalactosyldiacylglycerol	Glycerolipid
MGDG	monogalactosyldiacylglycerol	Glycerolipid
DGTS	diacylglyceryl hydroxymethyl-n,n,n-trimethyl-β-alanine	Glycerolipid
SQDG	sulfoquinovosyl diacylglycerol	Glycerolipid
HBMP	hemibismonoacylglycerophosphate	Glycerophospholipid
HexCer-NDS	hexosylceramide non-hydroxyfatty acid-dihydrosphingosine	Sphingolipid
MG	monoacylglycerol	Glycerolipid
DG	diacylglycerol	Glycerolipid
TAG	triacylglycerol	Glycerolipid
PC	phosphatidylcholine	Glycerophospholipid
PG	phosphatidylglycerol	Glycerophospholipid
-	triphenyl phosphate	-
-	pheophorbide A	-

Plants can be classified into two groups based on their lipid biosynthetic pathway, namely C16:3 or C18:3 (Wang *et al.* 2012b; Liu *et al.* 2019a). In C16:3 plants, such as Arabidopsis*,* FA synthesis and lipid diversification occurs within the chloroplasts, where FAs are assembled into thylakoid membranes *de novo* (Mongrand *et al.* 1998). The alternative pathway, producing predominantly α-linolenic acid (C18:3), such as in pea (*Pisum sativum*) and wheat (*Triticum aestivum*), involves FA synthesis in the chloroplasts, which are exported into the ER where they are assembled into glycerolipids and are either diversified in the ER and cytosol, or re-imported into the plastid for membrane lipids (Wang *et*

al. 2012b; Sato *et al.* 2017). These C18:3 plants therefore utilise both plastid and ER organelles for the synthesis of lipids. Li *et al.* (2015) showed that the C18:3 pathway is favoured upon elevated temperature stress in three species (Arabidopsis*, Atriplex lentiformis* and wheat) and hypothesised that increasing C18:3 permits a higher degree of unsaturation, thus exhibiting growth advantages under high temperature stress. However, Mongrand *et al.* (1998) state that the ecosystem does not determine the C16:3/C18:3 phenotype. Which pathways *E. nindensis* uses is unknown, nevertheless, maintaining membrane integrity is vital to cellular functioning regardless of the plant's lipid biosynthetic pathway. During drying, cellular crowding increases the risk of macromolecular denaturation and membrane fusion or rupture, and membranes are one of the first cellular structures to be degraded upon stress (Gasulla *et al.* 2013). Excessive damage to the membrane causes cells and organelles to rupture releasing nucleases and proteases, which degrade the cytoplasm, and can result in cell death (Gasulla *et al.* 2013; Perlikowski *et al.* 2016; Tshabuse *et al.* 2018; Dinakar *et al.* 2018; Bresson *et al.* 2018).

Resurrection plants successfully employ multiple strategies to minimise oxidative and mechanical damage to the membranes during drying (Hoekstra *et al.* 2001; Farrant *et al.* 2015). This is achieved by chemical quenching of peroxides, increasing lipid-stabilising proteins, increasing cell wall folding, and altering membrane composition to convey membrane fluidity, all of which prevent water-deficit induced membrane tearing (Hoekstra *et al.* 2001; Pintó-Marijuan *et al.* 2014; Seiwert *et al.* 2017). During drying, the ability to withstand deleterious oxidation depends on the biophysical properties, and functionality, of membranes. These properties are determined by the degree of saturation, chain-length, polarity and lipid composition (Millar *et al.* 1998; Páli *et al.* 2003). One of the initial signs of stress are changes in membrane lipid composition (Quartacci *et al.* 1997; Gasulla *et al.* 2013; Tshabuse *et al.* 2018). Resurrection plants, such as *Xerophyta humilis* (Tshabuse *et al.* 2018)*, Craterostigma plantagineum* (Gasulla *et al.* 2013)*, Boea hygroscopica* (Navari-Izzo *et al.* 1995) and *Paraisometrum mileense* (Li *et al.* 2014), avoid mechanical stress on the plasmalemma by decreasing the degree of FA saturation in the lipid membranes, thus increasing membrane fluidity. This fluidity phenomenon, due to the increased poly-unsaturation of phospholipids, is well documented (Shivaraj *et al.* 2018), and although the nature of saturation, degree of changes in the total lipid content, and compositional changes of lipids upon desiccation is species-dependant, these traits are ubiquitous in resurrection plants and are therefore important mechanisms for desiccation tolerance (Li *et al.* 2014).

TAGs are neutral lipids and therefore act as repositories for carbon and energy (Lin *et al.* 2008; Pyc *et al.* 2017; Michaud *et al.* 2019), fuelling energy requirements when photosynthesis is inactive, such as during germination. Both DG and acyl-CoenzymeA (CoA) can form TAG, however, TAG can be catabolised back into DG, which can be converted into phospholipids or re-synthesised into thylakoid

membranes (Vance *et al.* 2004; Li-Beisson *et al.* 2013). Specifically, the degradation of TAGs, and the subsequent β-oxidation of FAs, produces ATP and thus provides energy (Yang *et al.* 2018). In addition, oils in seeds are constituted from TAG and therefore determine their economic value in many crops (Baud *et al.* 2010; Horn *et al.* 2016). Disruption in lipid metabolism, for example as a consequence of abiotic stress, can result in excess acyl moieties when the ability of plants to produce (supply) and use (demand) FAs is unbalanced (Ohlrogge *et al.* 1997). Excess levels of acyls can be toxic, resulting in cell death (Schaffer 2003; Lockshon *et al.* 2007; Petschnigg *et al.* 2009). Once synthesised in the ER, TAGs are stored in lipid droplets (LDs), which act as a "transient buffer" for these excess acyl moieties, as acyls can easily and stably be sequestered into LDs, thus preventing their potentially toxic effects (Murphy 2012; Chapman *et al.* 2012b, 2013; Turnbull *et al.* 2017). This is particularly important for highly unsaturated FAs, as ROS preferentially targets unsaturated FAs (Paliyath *et al.* 1992; Yang *et al.* 2009).

Under normal conditions, TAGs are lowly-abundant in leaves as they are constantly recycled to and from LDs and the ER, or β-oxidised (degraded) for energy release (Murphy 2012; Chapman *et al.* 2013). However, under stress (such as heat, drought, nutrient deficiency, salinity and chilling, reviewed in Higashi *et al.* 2019), or in oil seed and senescing leaves (Kaup *et al.* 2002; Lin *et al.* 2008; Slocombe *et al.* 2009; Watanabe *et al.* 2013), TAG can accumulate. TAG accumulation is therefore both developmentally regulated (such as in seeds and senescing leaves) and induced by exogenous environmental stimuli (Baud *et al.* 2010). For example, the de-esterified FAs from disassembled thylakoid membranes of chloroplasts in senescing leaves are a major source of TAG (Ohlrogge *et al.* 1997; Kaup *et al.* 2002; Fan *et al.* 2011; Tjellström *et al.* 2015). Kaup *et al.* (2002) demonstrated that the composition of TAGs in Arabidopsis are derived from thylakoid galactolipids (hexadecatrienoic acid (C16:3) and linolenic acid (C18:3)). Similarly, Quartacci *et al.* (1997) showed that the resurrection plant *Sporobolus stapfianus* synthesises TAG from DG derived from chloroplasts, as did Fan *et al.* (2011) with the microalgae *Chlamydomonas reinhardtii*. TAGs also increased in the NST of other resurrection plants (*C. plantagineum* and *B. hygroscopica*) during drying (Navari-Izzo *et al.* 1995; Gasulla *et al.* 2013). The accumulation of TAGs is therefore a common response to both desiccation tolerance and senescence, as both processes breakdown photosynthetic components, which can be stored as TAG within LDs. Thus, the accumulation of TAG has multiple proposed functions, including an efficient carbon and energy store, as well as a stable and safe form of excess acyl moiety storage in the form of LDs upon stress-induced lipid changes or senescence (Murphy 2012). However, stark phenotypic differences between the NST and ST observed in **Chapter 2** (Figure 2.12 - Figure 2.15) suggest that the structure of the LD packaging differs between senescent and desiccation tolerant tissues, which could be due to differences in TAG accumulation. In this **Chapter** the differences in TAGs between the NST

and ST in *E. nindensis* are investigated, which in turn could serve as biomarkers for desiccation tolerance based on the TAG compositional changes during drying.

The biophysical properties of lipids, such as TAG, have benefits over carbohydrates as a carbon store because lipids have more energy per unit mass (as they are more reduced) and take up less space (as they are hydrophobic being opposed to hydrated starch) (Chapman *et al.* 2013). They are therefore energy-rich and lightweight, which is advantageous in seeds because this facilitates dispersal (Heldt 1997; Subramanian *et al.* 2013). The regulation of TAG biosynthesis has not explicitly been documented for resurrection plants as it has in senescing leaves. For example, in senescing leaves of Arabidopsis, transcript abundance of the ER-localised protein that converts DG into TAG, called diacylglycerol acyltransferase 1 (DGAT1), showed increases in transcript and protein abundances (Boyle *et al.* 2012; Liu *et al.* 2015; Tjellström *et al.* 2015). Moreover, Arabidopsis DGAT1 knock-out mutants had reduced TAG accumulation (Slocombe *et al.* 2009), showing the importance of this enzyme in TAG biosynthesis. Degradation of TAG by lipases releases energy that supports energy-demanding metabolism, such as post-germinative growth (Deruyffelaere *et al.* 2015; Pyc *et al.* 2017). The biosynthesis and storage of TAG in LDs, and their subsequent degradation and release of TAG, therefore plays an important role in membrane remodelling (Wang *et al.* 2017) and hence potentially, desiccation tolerance. What needs to be determined is how TAG species composition differs between the NST and ST in *E. nindensis* and identify the hallmarks of TAG in desiccation tolerance.

Approximately 70-80% of the lipids in photosynthetic cells are constituents of thylakoid membranes (Heldt 1997). These membranes, including envelope membranes, consist of galactolipids in various proportions, namely MGDG (~49%) and DGDG (~30%), followed by SQDG (~5%) (Hölzl *et al.* 2019). The outer envelope, however, is comprised of 32% PC, which is otherwise absent from the thylakoid and inner membranes (Botella *et al.* 2017; Hölzl *et al.* 2019). This in turn has been linked to the biochemically similar composition of the ER, thus representing the ER-plastid contact site (Wang *et al.* 2012b). This contact site is important for the transfer of lipids (e.g. FAs, DG) between these organelles, as acyl chains are exclusively made in the plastid, but used in every subcellular component, thus requiring the tight regulation of lipid transfer (Ohlrogge *et al.* 1997; Wang *et al.* 2012b). Galactolipids are critical for photosynthesis and their compositional changes during drying have been a focus of research in both desiccation sensitive and tolerant species. Reduction in the most abundant galactolipid MGDG (Fan *et al.* 2011) has been observed in both homoio- and poikilochlorophyllous resurrection plants, where MGDG decreased in desiccated leaves (coupled with a simultaneous increase in DGDG) in *C. plantagineum* (Gasulla *et al.* 2013), *S. stapfianus* (Quartacci *et al.* 1997), *X. humilis* (Tshabuse *et al.* 2018) and *B. hygroscopica* (Navari-Izzo *et al.* 1995). Moreover, lipid remodelling in the chloroplasts upon desiccation-induced photosynthetic shutdown is a potential

source for lipids. For example, the increase in TAG in *S. stapfianus, C. plantagineum* and *B. hygroscopica* was attributed to the breakdown of MGDG with subsequent conversion into plastoglobuli (Navari-Izzo *et al.* 1995; Quartacci *et al.* 1997; Gasulla *et al.* 2013). Plastoglobuli are localised accumulations of LDs enclosed in the stroma of chloroplasts (Chapman *et al.* 2013). It is crucial to note that TAG that accumulates outside the plastid in cytosolic LDs is functionally different to plastoglobuli, as LDs have functions beyond the confines of plastids (discussed below). Furthermore, ultrastructural evidence of cytosolic LD formation is lacking, as cytosolic LDs have not been observed in resurrection plants (see Quartacci *et al.* 1997; Tshabuse *et al.* 2018; Charuvi *et al.* 2019). However, not all species are capable of converting chloroplast lipids into DGs for the conversion into TAGs (Turnbull *et al.* 2017), such as *P. mileense* where TAG concentrations remained unchanged (Li *et al.* 2014). Nevertheless, chloroplast lipids can break down upon water-deficit stress, which can be converted into TAG within plastids (i.e. plastoglobuli) for the reconversion into membranes during rehydration or stored in cytosolic LDs for various functions (discussed below).

The importance of lipids is demonstrated in their abundance, where approximately 5-10% of dry leaf weight is comprised of lipids, primarily through membranes, but also through the accumulation of LDs (Huang, 1992; Ohlrogge and Browse, 1995). In plants, TAG synthesised in the ER is sequestered into the interior of the phospholipid bilayer, which form a LD that buds off in the cytosol (Figure 5.1) (Paul *et al.* 2014; Sato *et al.* 2017; Huang 2018). These circular organelles contain a densely packed core of energy-rich TAGs, amongst other metabolites, surrounded by a phospholipid monolayer imbedded almost exclusively with specialised proteins called oleosins, but also caleosins and steroleosins (Leprince *et al.* 1998; Frandsen *et al.* 2001; Shimada *et al.* 2008; Chapman *et al.* 2012b; Huang 2018). Oleosins have a thumb-tack-like structure (Buchanan *et al.* 2015) and are amphiphilic: They contain a long hydrophobic hairpin (proline knot) that is inserted into the TAG core stabilising the LD, whereas the hydrophilic N and C-terminal peptides interact with the cytoplasm (Huang 1992; Leprince *et al.* 1998; Siloto *et al.* 2006; van der Schoot *et al.* 2011). Individual oleosins interlock, forming an "oleosin cage" and this contributes to their steric hinderance and negative charge, which repel other oleosin-coated LDs (Siloto *et al.* 2006; van der Schoot *et al.* 2011; Fang *et al.* 2014). This shields the LDs, and therefore stabilises them by preventing LD aggregation or coalescence (Hsieh *et al.* 2004; Siloto *et al.* 2006; Hsiao *et al.* 2011; Huang 2018). Furthermore, TAGs are the most energy-dense form of carbon storage (Durrett *et al.* 2008; Fan *et al.* 2012) and TAG-containing LDs therefore function primarily as energy storage for metabolic processes like membrane biogenesis, rather than providing a structural role like membrane glycero- or phospholipids (Ohlrogge *et al.* 1995; Hsieh *et al.* 2005; Huang 2018). LDs therefore differ from membrane lipids in their structure and function.

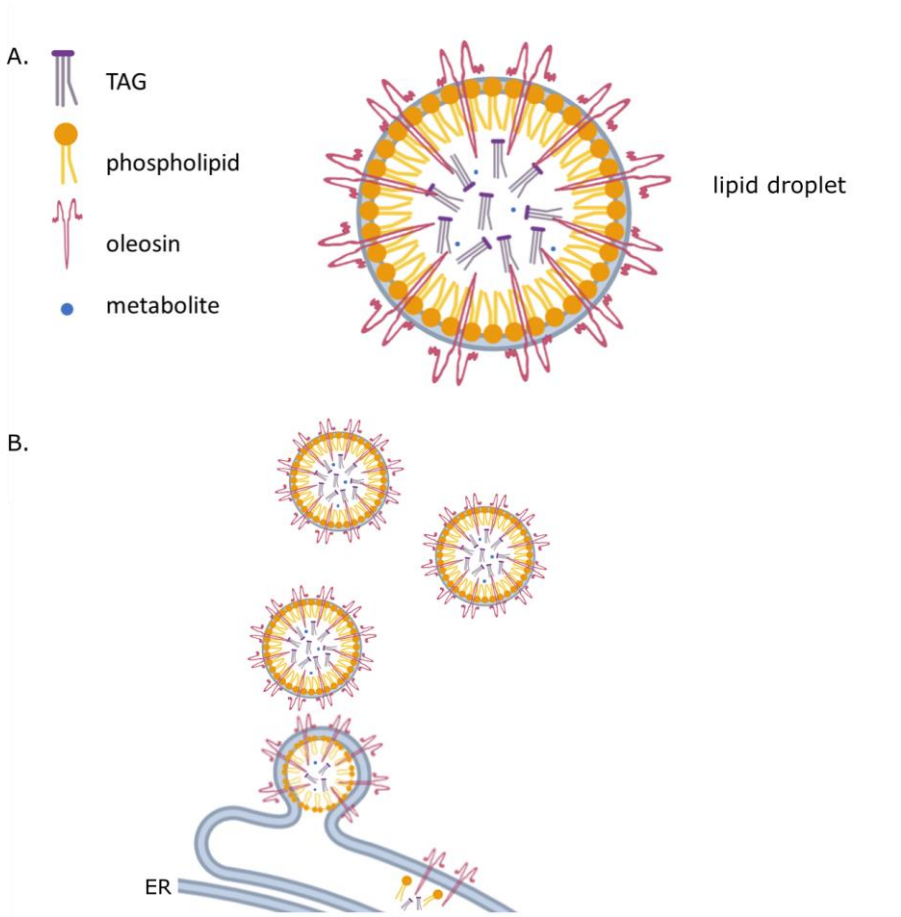

Figure 5.1: Lipid droplet (LD) composition (A) and formation (B). (A) A representation of a LD cross-section showing a phospholipid monolayer imbedded with oleosin, containing triacylglycerol (TAG) and other metabolites. (B) TAG is formed within the endoplasmic reticulum (ER) along with the secretory protein oleosin, which bud off from the ER, forming LDs. The diagram was constructed using BioRender (https://biorender.com/) and is a modified version of the diagram created by Siloto *et al.* (2006).

Oleosins regulate the size and shape of TAG-containing LDs, therefore stabilising them during desiccation and imbibition in seeds (Huang 1992; Hsieh *et al.* 2004; Siloto *et al.* 2006; Huang 2018; Shimada *et al.* 2018), and this characteristic has important implications for desiccation tolerance. Siloto *et al.* (2006) confirmed the role of oleosin in determining LD size, shape and stability, as oleosin accumulation was directly proportional to the LD size in Arabidopsis seeds. The authors prevented oleosin synthesis through RNA interference and T-DNA insertion. The seeds of the Arabidopsis mutants, devoid of oleosin protein expression, showed enlarged LDs and delayed germination, demonstrating the role of oleosins in the timeous remobilisation of energy-rich TAG, which are critical for germination. The small size of oleosin-coated LDs (0.5 - 2.0 µm) increases its surface to volume ratio, thereby facilitating lipase binding, and subsequent lipolysis for the quick release of TAG (Hsieh *et al.* 2004; Huang *et al.* 2015). Since lipase activity is proportional to the lipid substrate, this allows for the rapid mobilisation of lipids for use during germination in seeds (Leprince *et al.* 1998; Huang

2018). It follows that the role of oleosin in regulating the size of LDs could also be associated with the quick energy release needed for recovery during rehydration in resurrection plants. TAGs are rapidly converted into sucrose (Graham 2008) and therefore LD degradation is important for prompt energy mobilisation in germinating seeds. This is likely also true for the recovery from desiccation in resurrection plants. Furthermore, Leprince *et al.* (1998) postulated that the presence of oleosins in seeds is also related to the stabilisation of the LDs themselves during imbibition. Enlarged LDs are also a typical sign of senescence, where FA turnover is high (Siloto *et al.* 2006; Shimada *et al.* 2008; Slocombe *et al.* 2009; Li-Beisson *et al.* 2013; Miquel *et al.* 2014; Shimada *et al.* 2015), however, the expression of oleosin in senescence tissue is unknown. Thus, oleosins are critical proteins for LD development and are essential to maintain small sized LDs for the rapid mobilisation of TAG. LD development is thus crucial for germination and it is the size of the LDs that facilitate this benefit, which is determined by oleosin.

In addition to their role as storage organelles, recent studies have proposed that they are not merely inert (Pyc *et al.* 2017), but also function in signalling and membrane trafficking (van der Schoot *et al.* 2011; Rinne *et al.* 2011; Gasulla *et al.* 2013; Paul *et al.* 2014; Hou *et al.* 2016). Oleosin-coated LDs are synthesised in the ER, however, they accumulate along the plasmalemma in response to water-deficit or freezing stress, thus necessitating vesicle trafficking to the target site (Shimada *et al.* 2008; van der Schoot *et al.* 2011; Rinne *et al.* 2011; Paul *et al.* 2014). The signal responsible for LD targeting is unknown, however, Paul *et al.* (2014) hypothesised that oleosin could be a possible candidate. Secretory proteins are also made and matured in the ER, and LDs have been shown to function as an ER cargo delivery system, where opportunistic proteins and/or enzymes “hitch a ride” on the LDs that are destined for the plasmalemma (van der Schoot *et al.* 2011; Paul *et al.* 2014). Furthermore, Welte (2009) proposed that LDs could traffic signalling molecules that have difficulty moving through aqueous cytoplasm due to their hydrophobicity, thereby aiding their movements. LDs could therefore function as membrane traffickers of molecules from the site of synthesis (ER), to the site of response (plasmalemma). This can result in the change in conformation or activity of the regulating proteins or enzymes, which in turn alter the plasmalemma or plasmodesmata (Rinne 2011). These changes are critical as they influence cell-to-cell communication and affect membrane repair by providing membrane constituents (lipids and proteins) (Juergens *et al.* 2016). For example, in a *Populus* hybrid (*Populus tremula* x *Populus tremuloides*), a deciduous tree, plasmodesmata cell communication was re-opened after LDs delivered lipid-anchored proteins to the plasmalemma, which hydrolysed the stress-induced accumulation of callose, ending chilling-induced dormancy (Rinne *et al.* 2011). Cell-to-cell communication is essential for cells to perceive, receive and respond to extracellular signals, and the direct role of LDs in aiding the transport of signalling or regulatory enzymes to the plasmalemma

is crucial for plants to coordinate mechanisms in response to stress (van der Schoot *et al.* 2011; Bobik *et al.* 2015; Hou *et al.* 2016).

The presence of oleosins in seeds has been known since the 1980s, and Pammenter *et al.* (1999) included the presence of oleosins in seeds as a marker for the acquisition of desiccation tolerance. Oleosin transcript abundance increased during drying in the resurrection plant *Lindernia brevidens* and its desiccation sensitive sister-species *Lindernia subracemosa* (VanBuren *et al.* 2018), and the resurrection plants *Oropetium thomaeum* (VanBuren *et al.* 2017) and *Selaginella tamariscina* (Xu *et al.* 2018b). Although oleosin transcript abundance was seen in *L. subracemosa,* this was lowly expressed compared to the desiccation tolerant *L. brevidens* (VanBuren *et al.* 2018), which suggests that although oleosin expression can occur in non-desiccation tolerant tissues, it is too lowly expressed and inefficient to reap the desiccation tolerance benefits of this protein, as seen in the highly expressed oleosin in tolerant tissues. Despite the interest in oleosins, confirmation through immunoblotting of oleosin in vegetative tissues of resurrection plants has not been conducted, nor has ultrastructural evidence been given for their presence in desiccated tissues. Oleosin expression in *E. nindensis* was therefore investigated to understand the role of this lipid-specific protein in desiccation tolerance and senescence.

The role of LDs and global lipid changes in desiccation tolerance is unknown in *E. nindensis*. Furthermore, studies into the changes in the lipid composition in the NST and ST of *E. nindensis* are absent. General trends in the lipid profile were therefore assessed in this **Chapter**, including an investigation into the role of LD accumulation. In addition, the hypothesis that the lack of small, regularly sized plasmalemma located lipids in the ST is due to the lack of oleosin was tested by quantifying the changes in relative abundance of oleosin between tissue types during drying. Since conducting a proteomic analysis was beyond the scope of this thesis, and oleosin is highly relevant to LD formation, this protein is a suitable case study to observe how the changes in lipo-protein expression between tissue types can affect cellular structure and function upon water-deficit stress. LDs, and their oleosin protein coat, each have specific roles (Leprince *et al.* 1998) and are recognised in this thesis as distinct entities, separate to membrane lipids. In summary, global changes in lipids, including a lipo-protein (oleosin), were explored to investigate the metabolic differences between the NST and ST, as lipids were regarded as dominant ultrastructural features (**Chapter 2**). The importance of the role of lipids in desiccation tolerance was echoed in the transcriptome (**Chapter 3 and 4**), as lipid metabolism and storage were enriched during drying (Figure 3.4.1, Figure 3.5.1, Table 4.1). Lipids were therefore investigated as part of this thesis because of their consistent appearance throughout the transcriptome and their striking appearance in the microscopy images (Figure 2.12, Figure 2.14), coupled with their critical importance in desiccation tolerance.

5.2. METHODS

5.2.1. Lipid extraction and sample preparation

Targeted metabolic profiling was performed using Liquid-Chromatography High Resolution Mass Spectrometry (LC-HRMS) on three biological replicates of *E. nindensis* at 100% and 25% RWC in both the NST and ST. Additional desiccated (<10% RWC) samples were submitted for analysis, however, the samples were not weighed and were therefore excluded from the lipidomics analysis, however, these samples were used for determining the predominant biosynthetic pathway (C16:3 vs C18:3) of *E. nindensis*. Tissues were sampled as outlined in **Chapter 2** and freeze-dried whole leaves were sent to Université de Technologie de Compiègne, France, where the lipids were extracted using a modified Folch (1956) method and further analysed through mass spectrometry. 20 mg of freeze-dried leaves were transferred in a 2 mL screw cap tube. To prevent lipase activity, 400 µL of isopropanol at 70°C was added. Lipids were extracted using 1 mL of cold chloroform/isopropanol (2:1) with 1 mM butylated hydroxytoluene and 400 µL H_2O. After 1 hour of incubation on ice, the samples were centrifuged at 13,000 rpm for 5 minutes at 4°C. The organic layer (lower phase) was transferred into a new tube. The lipid extraction was repeated a second time and the lower phases were pooled, dried under a stream of nitrogen at 20°C, and resolubilised in 200 µl of isopropanol.

5.2.2. LC-HRMS analyses

LC-HRMS was used to identify various lipid species by providing structural information about the lipids (such as polar head group, length, unsaturation levels) as well as showing the presence of glycosyl units in lipid molecules by using exact mass, tandem mass spectrometry (MS/MS) and retention time (Murphy *et al.* 2001). Lipids were separated on a C18 Hypersil Gold column (100 x 2.1 mm, 1.9 µm, Thermofisher) at 50°C, using an elution gradient composed of a solution of 10 mM of ammonium formate and 0.1% formic acid (acetonitrile: H_2O = 60:40, v/v) (solvent A) and a solution of 10 mM of ammonium formate and 0.1% formic acid (isopropanol: acetonitrile: H_2O = 90:8:2, v/v) (solvent B). The gradient was as follows: solvent A: 0–2 minutes 68%, 2–8 minutes 60%, 8–10 minutes 55%, 10–16 minutes 50%, 16–22 minutes 40%, 22–28 minutes 30%, 28–35 minutes 20%, 35–40 minutes 0%. Finally, solvent B was returned to 40% over the next 0.1 minutes and equilibrated for 10 minutes before the next injection. The flow rate was set at 0.25 $ml.min^{-1}$ and the injection volume was set to 2 µL. LC-ESI-HRMS2 analyses were achieved by coupling the LC system to a hybrid quadrupole time-of-flight Ultra High Definition (QToF) mass spectrometer Agilent 6538 (Agilent Technologies) equipped with an electrospray ionisation (ESI) dual source. The source temperature, fragmentor and the

skimmer were set up respectively at 350°C, 150 V and 65 V. The acquisition was made in full scan mode between 100 m/z and 1700 m/z, with a scan of two spectra per second. Selected parent ions were fragmented with collision energy fixed at 35 eV. MS/MS scans were done on the six most intense ions above. Two internal reference masses were used for in-run calibration of the mass spectrometer: 121.0509, 922.0098 in positive ion mode and 112.9856, 1033.9881 in negative ion mode. The total LC-HRMS/MS run was 40 minutes with 10 minutes of equilibration. MassHunter B.07 software processed the data. The mass spectra were acquired using a dual electrospray ionisation in positive and negative-ion mode.

5.2.3. Data processing and annotation

Agilent generated files corresponding to samples were processed using MZmine 2 v2.37 (http://mzmine.github.io/). The mass detection was realised keeping the noise level at 2.0E3 for MS1 and 0.0E0 for MS2 in centroid. The chromatogram builder, using a minimum time span of 0.10 minutes, a minimum height of 1.0E3 and a m/z tolerance of 5 ppm, was used. Chromatogram deconvolution was used using the local minimum search algorithm. The chromatographic threshold was 30.0%, the search minimum in retention time range was 0.05 minutes with a minimum relative height of 5% and a minimum ratio of peak top/edge of 2. Peak duration range 0.05 - 3 minutes. MS/MS scans were paired using a m/z tolerance range of 0.05 Da and retention time tolerance range of 0.1 minutes. Isotopologues were grouped using the isotopic peaks grouper algorithm with a m/z tolerance of 0.008 and a retention time tolerance of 0.3 minutes. A peak alignment step was performed using the join aligner module (m/z tolerance = 0.008, weight for m/z = 50, weight for retention time = 50, absolute retention time tolerance 2 minutes). The peak finder module was used with an intensity tolerance of 10%, m/z tolerance of 0.008 and retention time tolerance of 1.0 minutes. The resulting peak list was filtered to include peaks with readings in at least two samples, a minimum peak isotope pattern of two, and by keeping only peaks with MS/MS. The peak list was annotated using a combination of three databases: lipid search (Taguchi *et al.* 2010), lipid blast (Kind *et al.* 2014) and lipid match (Koelmel *et al.* 2017). Non-annotated features were removed. The nomenclature used for lipid classes identified was according to Pauling *et al.* (2017).

5.2.4. Statistical Analysis

All statistical analysis was performed using MetaboAnalyst v3.0 (www.metaboanalyst.ca). To determine statistical significance, annotated features were first normalised using the weight of the

sample (mg dry weight (DW)), log_2 transformed, then "mean-centred and divided by the square root of the standard deviation" scaling of each variable (pareto data scaling). A PCA and a dendrogram were performed to detect trends and outliers. The PCA is an unsupervised analysis, where sample similarity within the data is identified without taking the sample type or class into account (Alonso *et al.* 2015). Comparisons between RWC and tissue type were then subjected to a Partial Least Squares-Discriminant Analysis (PLS-DA), a supervised analysis, where the analysis is informed by the sample classes, thereby maximising sample variation. The suitability of the model was confirmed through a permutation test of 1000 iterations. This was followed by a variable importance in projection (VIP) score analysis, which visualised which lipid classes were important in the model.

Pairwise comparisons were analysed to assess the changes in lipid classes during drying in the NST (i.e. 100% RWC vs 25% RWC), and between tissue types at hydrated (i.e. 100% RWC NST vs 100% RWC ST) and dehydrated (i.e. 25% RWC NST vs 25% RWC ST) timepoints. The peak intensities represent the comparative differences in lipid class abundances between two conditions only and are not quantitative methods. This is because ionisation yields and collision energies in the collision cell may not be specific from one class of lipids to another (e.g. PC vs TAG). However, one can compare lipid classes between two conditions (e.g. TAG vs TAG). Therefore, box plots depicting pairwise comparisons were used to identify changes in lipid classes upon water-deficit stress. The volcano plot and heatmaps were performed to test significant differences (<0.05) between the NST and ST to identify biomarkers for desiccation tolerance**.** Volcano plots incorporated both t-test and fold change statistics to identify significance between sample pairs.

Since lipid class changes represent the dominant changes in response to stress (Benning 2009), general trends in lipid classes were analysed, focussing only on TAG species compositional changes due to their observed accumulation. Therefore, for the purposes of this thesis, only the 15 annotated lipid classes were investigated, rather than a thoroughly detailed investigation into the full lipid compliment (i.e. unannotated) during drying. This was done to compliment the ultrastructural and transcriptomic observations in lipid accumulation identified previously. Key lipid-related DEGs are briefly discussed.

5.2.5. Protein extraction

Protein was extracted from the stored organic phase of the Trizol© extracted RNA from samples for RNA-seq discussed in **Chapter 3**. Three biological replicates were used per indicated RWC. The organic phase was extracted to a new microtube and 10 µl protease inhibitor (Sigma-Aldrich) was added to prevent protein degradation. After adding 300 µl of cold 100% ethanol (EtOH), the protein extract was

inverted approximately 25 times and incubated at room temperature for 5 minutes and thereafter centrifuged for 10 minutes at 2500 x g. The supernatant containing soluble proteins was transferred to a fresh 2 ml microtube containing 1 ml of cold isopropanol. After 10 minutes of incubation at room temperature the protein extract was centrifuged for 10 minutes at 10250 x g at 4°C. The precipitated protein formed a pellet, which was washed thrice with 2 ml of 0.1 M ammonium acetate prepared in 100% MeOH. The pellet was briefly vortexed, centrifuged for 3 minutes and the supernatant removed at each wash. After the last wash step the supernatant was removed and 2 ml of cold 100% acetone was added to the extract, vortexed briefly and centrifuged for 3 minutes at 10250 x g. The supernatant was carefully removed, and the pellet let to air dry for approximately 7 minutes at 10250 x g. The pellet was resuspended in 50 µl of 2% sodium dodecyl sulphate (SDS) buffer (w/v), inverted for 1 minute and left on ice overnight to resuspend. Protein extracts were stored at -80°C.

5.2.6. Protein quantification

The protein concentration was quantified using the Micro BCA™ Protein Assay Kit (Pierce, USA). Eight bovine serum albumin (BSA) standards were used with a range of 0 – 2000 µg/µl of BSA in 2% SDS. Using a 96-well plate, 5 µl of the blanks, BSA standards and samples were aliquoted in triplicate into the wells. Samples were both undiluted and diluted (1:10). 100 µl of the BCA Working Reagent was added to each well, incubated for 30 minutes at 37°C with gentle shaking, and measured at 562 nm (Thermo Scientific™ Multiskan™ GO Microplate Spectrophotometer, USA). Protein concentration was calculated based on the standard curve.

5.2.7. Western Blot

To separate the proteins based on their molecular mass a 1mm SDS-PAGE (SDS-polyacrylamide gel electrophoresis) was used (Lämmli 1970). Samples were denatured by adding Lämmli buffer, briefly centrifuging, and further denaturing the samples at 95°C for 5 minutes. Samples were immediately placed on ice and briefly centrifuged before being loaded onto the SDS-PAGE. The protein extracts were run on 15% resolving gel (3.65 ml 40% acrylamide/bis (19:1), 3.65 ml Milli-Q H_2O, 2.5 ml 1.5 M Tris-HCl pH 8.8, 100 µl 10% SDS, 100 µl 10% APS (ammonium persulphate), 5 µl TEMED), and 6% stacking gel (600 µl 40% acrylamide/bis (19:1), 2.36 ml Milli-Q H_2O, 1 ml 1.0 M Tris-HCl pH 6.8, 40 µl 10% SDS, 40 µl 10% APS, 4 µl TEMED) at 100 V for 2.5 hours using fresh tank buffer (0.2 M glycine, 25 mM tris, 0.1% SDS). Each gel had one lane of 3 µl protein standard ladder (Color Prestained Protein Standard, Broad Range (11–245 kDa), NEB) to determine the molecular weight of proteins.

The SDS-PAGE separated proteins were then transferred onto a polyvinylidene fluoride (PVDF) membrane, with a 0.22 µm pore size (Durapore®). First, the PVDF membrane was polymerised in 100% EtOH. Then, the sponges, filter paper, PVDF membrane and gel were soaked in cold transfer buffer (Towbin *et al.* 1979) for 15 minutes. The sponge, filter paper and membrane were placed on the positive electrode (white side of the cassette). Bubbles were carefully rolled out before placing the gel onto the membrane. Soaked filter paper was place over the membrane and bubbles were removed. After preparing the sandwich, the cassette was placed in the transfer tank with cold tank buffer and ice packs. The gel was electroblotted on the membrane overnight at 40 V at 4°C.

After the transfer, the membrane was rinsed in Milli-Q H_2O. To verify whether the proteins were transferred equally to the membrane, the gel was briefly stained with 1 mL Ponceau. The membrane was washed thrice with wash buffer (1x TBS with 0.2% v/v Tween-20) for 5 minutes each wash. The membrane was blocked with blocking buffer (5% skim milk, 100 mM Tris/HCl, pH 7.5, 0.2% v/v Tween-20) for 2 hours with gentle shaking at room temperature. The blocking buffer was discarded, and the membrane rinsed in wash buffer for 5 minutes. The membrane was incubated with the rabbit polyclonal antibody oleosin (OLE1, AT4G25140, PhytoAB) overnight at 4°C with gentle shaking. The antibody dilutions were 1:1000 in antibody buffer (5% skim milk, 100 mM Tris/HCl, pH 7.5, 0.05% v/v Tween-20). Horseradish peroxidase-conjugate goat anti-rabbit antibody (Sigma), diluted to 1:2000 in antibody buffer, was used as the secondary antibody. The membrane was incubated with the secondary antibody for 2 hours at room temperature with gentle shaking. The membrane was washed thrice with wash buffer (5 minutes each). Due to intellectual property the sequence of the OLE1 antibody was not received, however, PhytoAB used BLAST to assess sequence similarity to all the oleosin genes in the *E. nindensis* genome.

To visualise the antibody signal, the chemiluminescent ECL (WesternBright, Advansta) detection kit was used. Equal volumes (200 µl) of component A and B were added to 400 µl Milli-Q H_2O and placed directly onto the membrane. After incubating for 2 minutes in the dark, the membrane was visualised under UV with a Molecular Imager ChemiDoc system (Bio-Rad, Germany). The colourmetric and chemiluminescent images were merged**.**

5.3. RESULTS

5.3.1. Global changes in lipids

The glycerolipid composition of desiccated leaf tissues of *E. nindensis* is presented in Figure 5.2. Given the dominance of C18:3, which contributes to over 70% of all FAs, *E. nindensis* can be considered a C18:3 plant. The ST had a higher proportion of C18:3 and lower levels of C18:2 than the NST in the desiccated state.

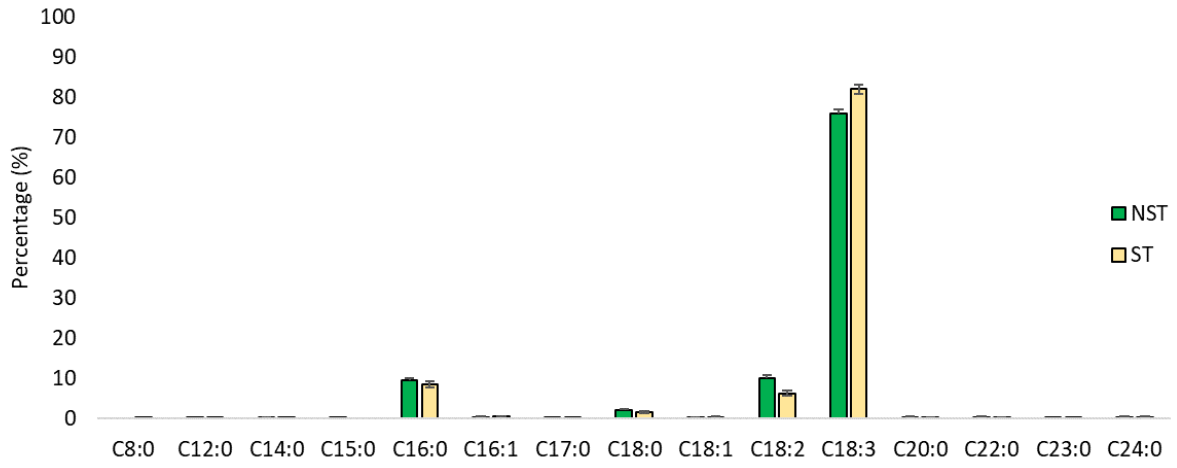

Figure 5.2: Glycerolipid moieties showing carbon length and saturation between the non-senescent tissue (NST) and senescent tissue (ST) of *Eragrostis nindensis* upon desiccation (<10% relative water content).

A total of 316 lipid species were identified (of which 205 were annotated), consisting of 15 lipid classes (Table 5.1). In order to visualise the groupings associated with changes in lipid composition during drying to 25% RWC, a PCA was performed (Figure 5.3, A.). The PCA showed clear separation between tissue types and RWCs (Figure 5.3, A.), with 83.0% of the variation explained by the first two principal components (PC1 = 49.2%, PC2 = 33.8%), indicating that RWC and tissue type were strong determinants of variation. This separation was echoed in the dendrogram (Figure 5.3, B.). This distinction allowed the analysis of the supervised PLS-DA analysis. The heatmap further demonstrated that there were differences between tissue types, even at full leaf hydration (100% RWC, Figure 5.3, C.), with distinct changes in peak intensities (representing abundances) during drying to 25% RWC. Relative peak intensities were depicted in Figure 5.4 to show representative changes in lipid classes between samples. In general, TAG and its intermediates (DG, MG), structural lipids (PC, PG), and total lipid content increased upon dehydration in the NST (Figure 5.4). Statistical associations were explored in pairwise comparisons between samples, discussed below.

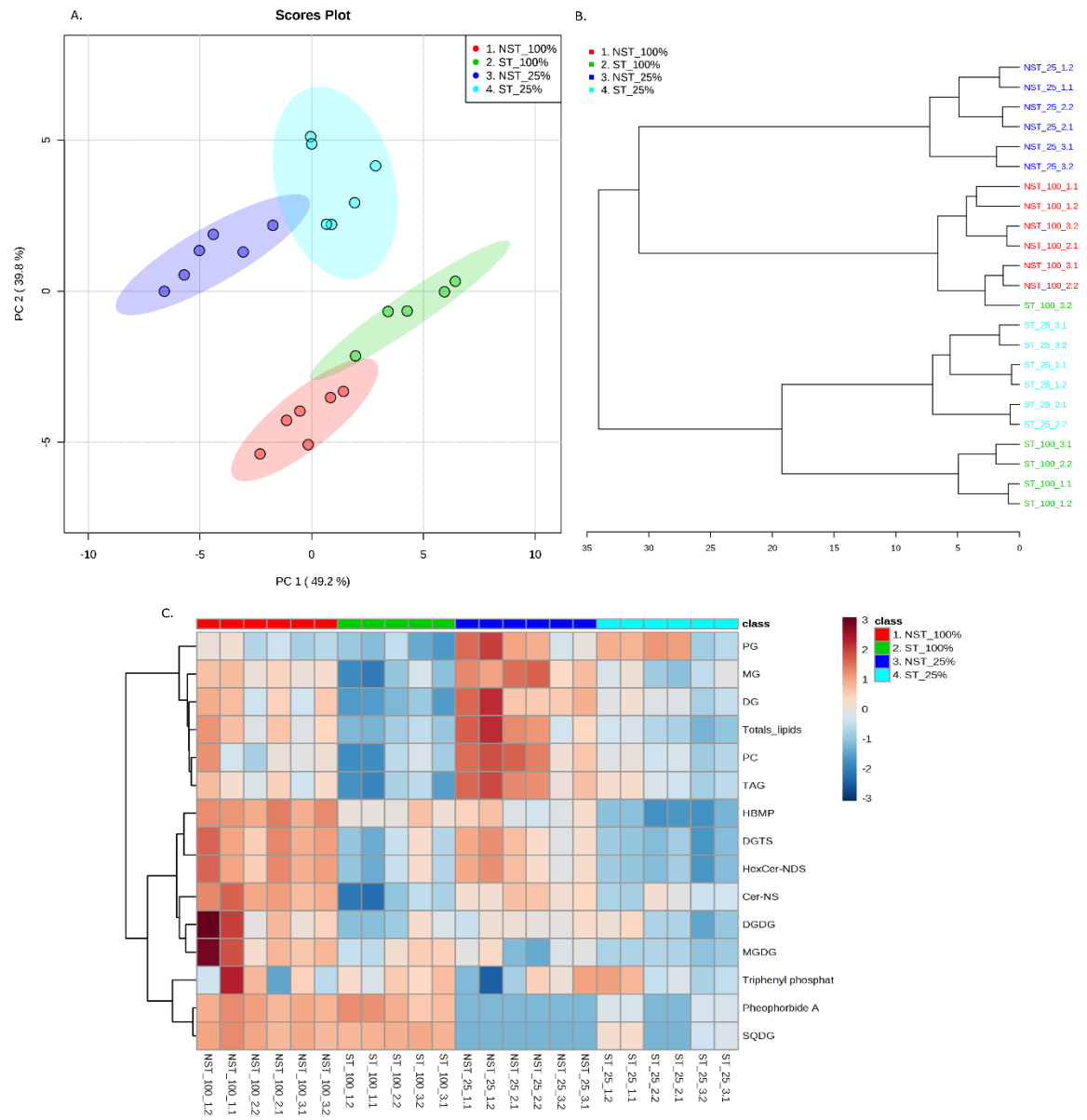

Figure 5.3: (A) PCA plot, (B) dendrogram and (C) heatmap of *Eragrostis nindensis* based on 15 lipid classes during drying from 100% to 25% relative water content (RWC) in desiccation tolerant, non-senescent tissue (NST) and desiccation sensitive, senescent tissue (ST). Samples are grouped according to their RWCs and tissue types. The explained variation for each component in the PCA is indicated in parentheses. Refer to Table 5.1 for abbreviations.

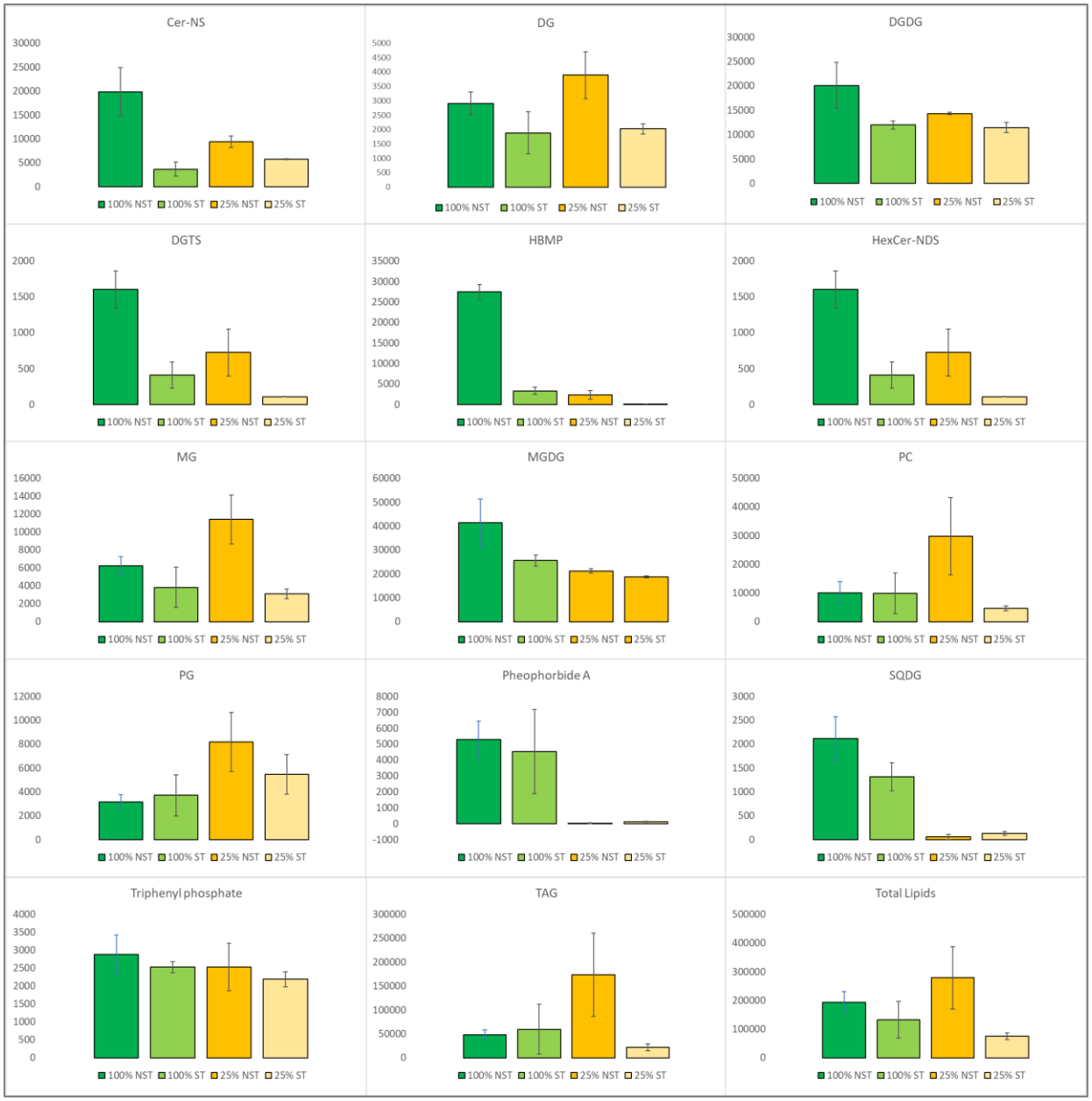

Figure 5.4: Average peak intensities of lipid classes between the desiccation tolerant, non-senescent tissue (NST) and desiccation sensitive, senescent tissue (ST) of the resurrection plant *Eragrostis nindensis* between hydrated (indicated in green, 100% relative water content (RWC)) and dehydrated (indicated in yellow, 25% RWC) conditions. The averages and standard error of three biological replicates is shown. The bar graphs serve as representative peak intensities to illustrate general trends. For statistical differences, see pairwise comparisons in Figure 5.5 – Figure 5.7.2. Refer to Table 5.1 for abbreviations.

Since the data separated according to RWC and tissue type in the unsupervised analysis (PCA), a supervised analysis (PLS-DA) was conducted to maximise the data separation between the groups. The VIP score analysis indicated that three lipid classes with the most significant differences across all 4 samples were HBMP (see Table 5.1), pheophorbide A and SQDG (Figure 5.5). HBMP had the greatest difference in abundances, where there were higher abundances in the NST at 100% RWC compared

to the other water contents and tissue types, whereas pheophorbide A and SQDG significantly decreased (to a barely detectable level) upon dehydration to 25% RWC in both tissue types. Three lipid classes were highest in the ST at 100% RWC (pheophorbide, SQDG and triphenyl phosphate). As reflected in Figure 5.4, the relative changes in lipid class abundances showed significant accumulation of TAG and its precursors (MG, DG), structural lipids (PG, PC) and total lipids upon dehydration to 25% RWC in the NST (Figure 5.5). These lipid classes represented the major changes in global lipid composition upon dehydration in *E. nindensis* and are reflected in the average peak abundance (Figure 5.4). MGDG, the most abundant lipid in the chloroplast (Fan *et al.* 2011), was highest in the NST at 100% RWC, as was DGDG. The ST had consistently lower abundances of lipids, regardless of class, in the dehydrated state.

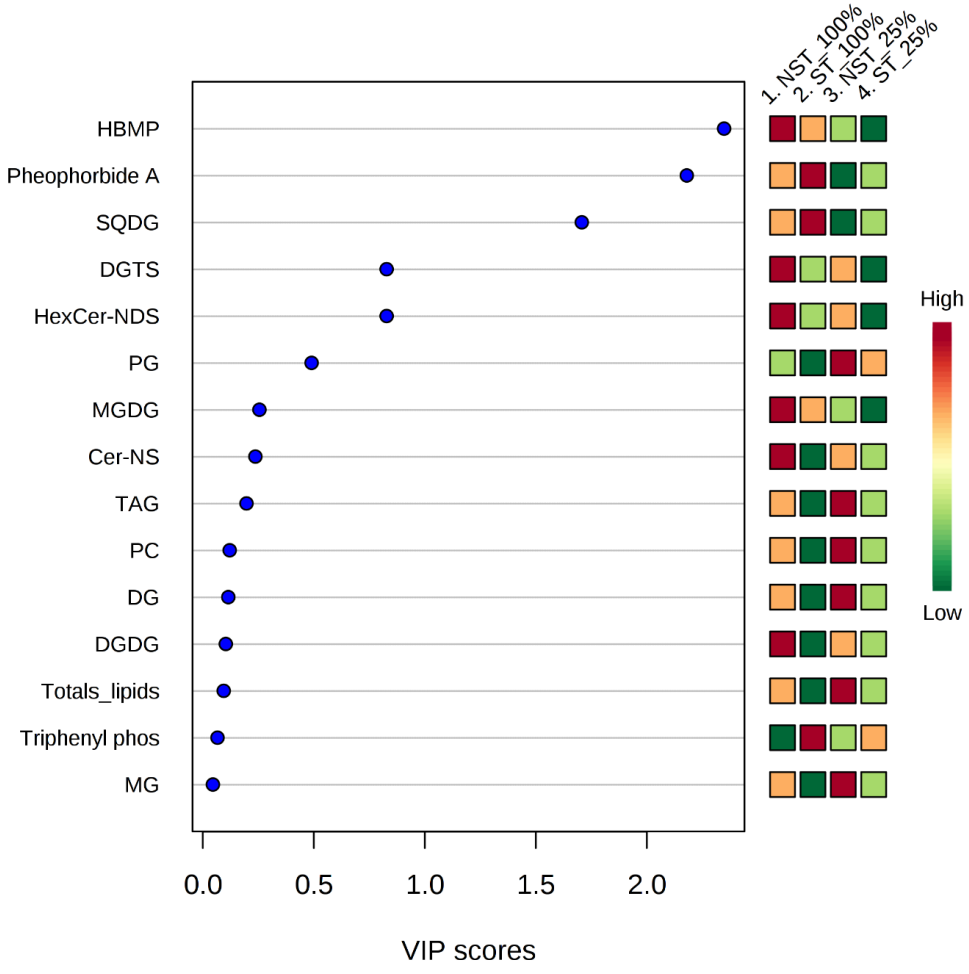

Figure 5.5: Variable importance in projection (VIP) plot displaying differences in lipid classes (including total lipids) across hydrated (100% relative water content (RWC)) and dehydrated (25% RWC) leaves (both non-senescent tissue (NST) and senescent tissue (ST)) in the resurrection plant *Eragrostis nindensis*. Differences in lipid classes were identified by PLS-DA. The coloured boxes (right) indicate relative abundances (peak intensities) of the corresponding lipid classes. Refer to Table 5.1 for abbreviations.

5.3.2. Changes in lipid class composition

5.3.2.1 Differences in hydrated leaves

The PCA and heatmap showed that the main driver of sample separation in hydrated leaves was tissue type, with PC1 of 90% (Figure 5.6.1). Although one ST sample showed inconsistencies in peak intensities compared to the other ST samples, clear differences in lipid classes between tissue types in hydrated leaves were evident (Figure 5.6.2, A and B). Pairwise comparisons between the tissue types revealed that eight lipid classes were significantly more abundant in the NST compared to the ST (Figure 5.6.2). This consisted of four glycerolipids (DG, TAG, DGTS, MG), two glycerophospholipids (PC, HBMP) and two sphingolipids (Cer-NS, HexCer-NDS, Table 5.). In addition, the NST had higher abundances of total lipids.

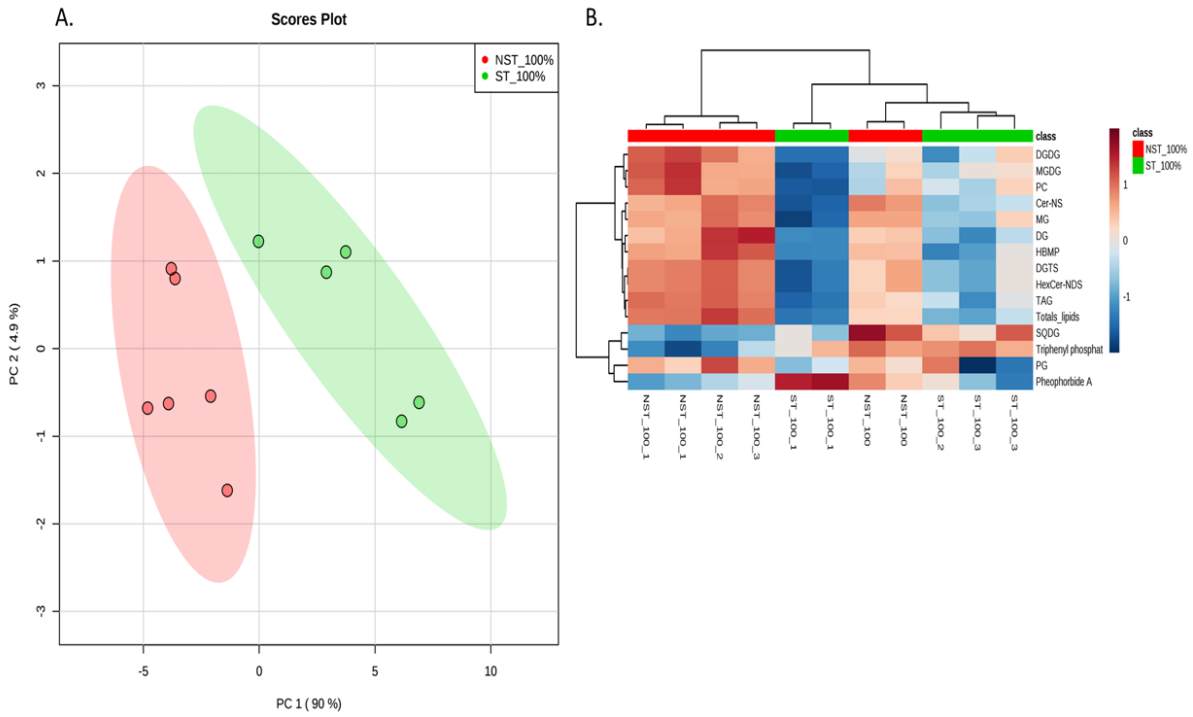

Figure 5.6.1: Differences in known (targeted) lipid classes in *Eragrostis nindensis* under hydrated (100% relative water content (RWC)) conditions between non-senescent tissue (NST), in red, and senescent tissue (ST), in green, represented by a (A) PCA plot and (B) heatmap. Refer to Table 5.1 for abbreviations.

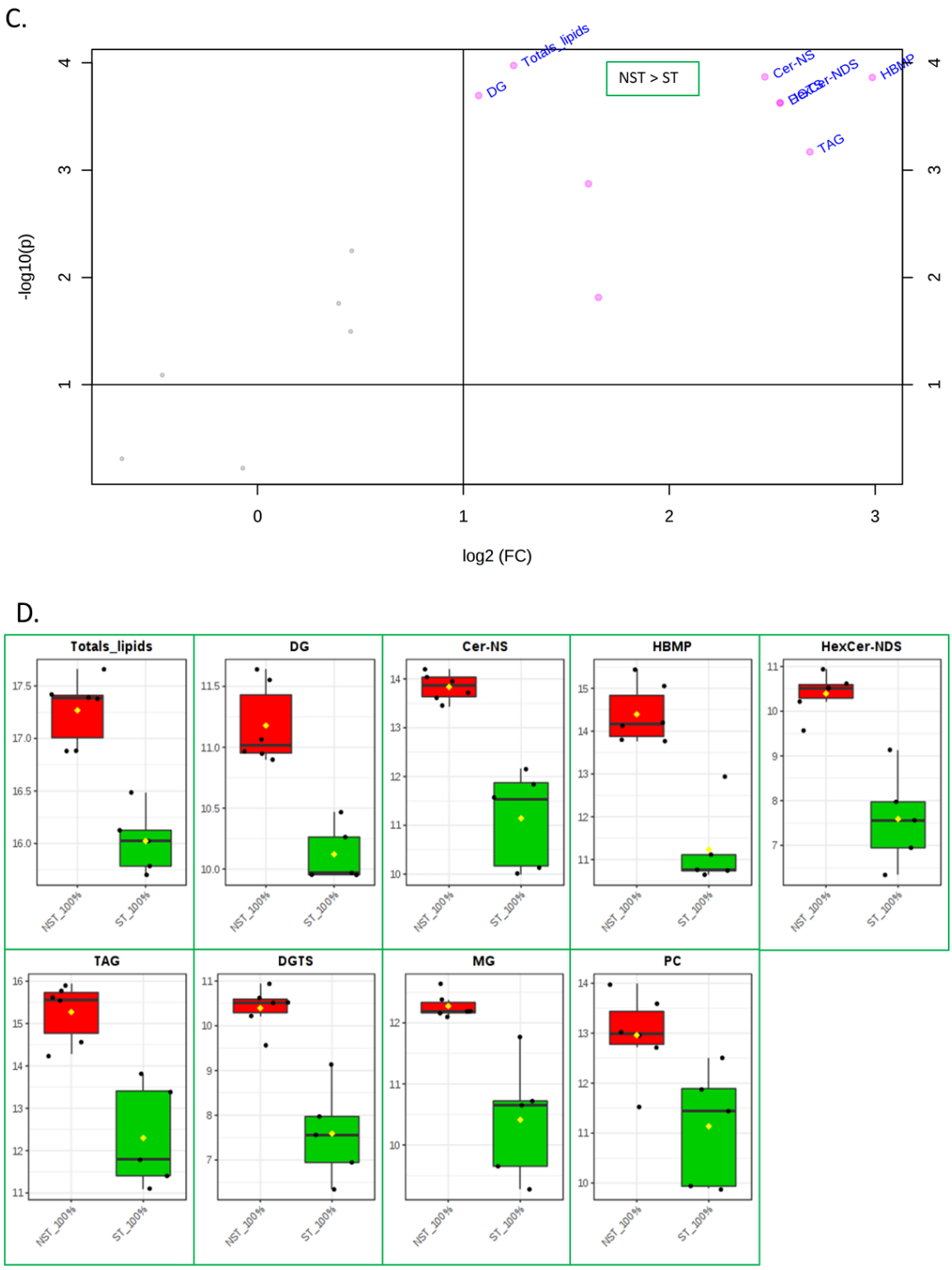

Figure 5.6.2: Differences in known (targeted) lipid classes in *Eragrostis nindensis* under hydrated (100% relative water content (RWC)) conditions between non-senescent tissue (NST), in red, and senescent tissue (ST), in green, represented by (C) volcano plot and (D) corresponding box plots. Statistically significant changes in lipid class fold change are represented as box plots (D), where a log_2 fold change of >1 represents significantly higher lipid class abundances in the NST compared to the ST at 100% RWC. Refer to Table 5.1 for abbreviations.

5.3.2.2 Differences in dehydrated leaves

There were differences between tissue types at 25% RWC, with 74.4% (PC1) of the data variation being explained by tissue type (Figure 5.7.1). Seven lipid classes were higher in abundance in the NST compared to the ST (Figure 5.7.2). There was a higher abundance of total lipids in the NST at 25% RWC. Two lipid classes (pheophorbide A, and SQDG) were present in the ST, but were undetected in the NST.

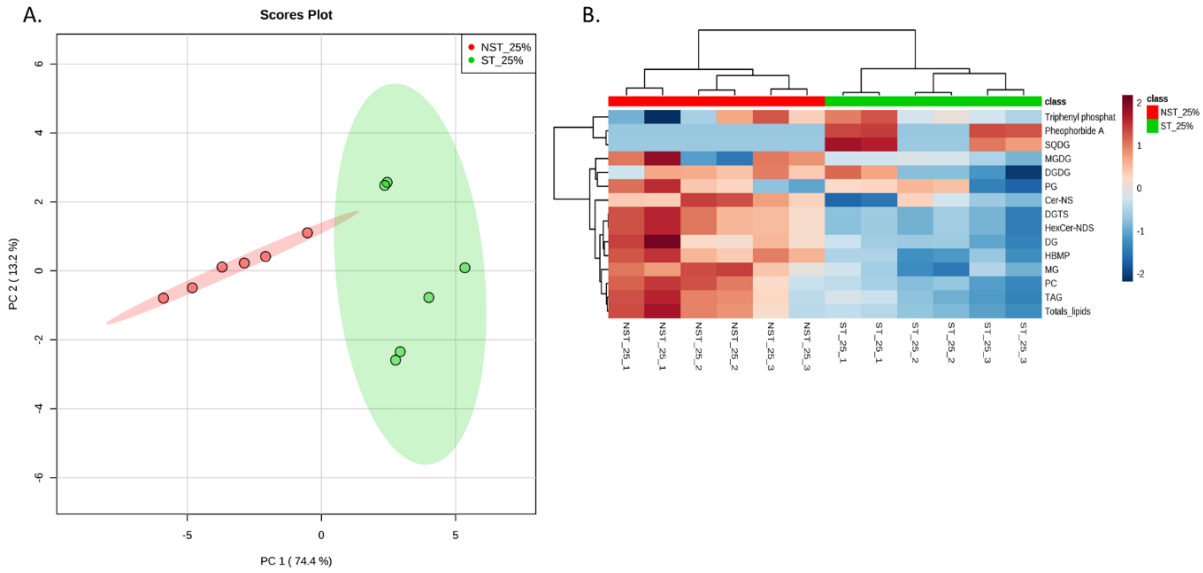

Figure 5.7.1: Differences in known (targeted) lipid classes in *Eragrostis nindensis* under dehydrated (25% relative water content (RWC)) conditions between non-senescent tissue (NST), in red, and senescent tissue (ST), in green, represented by a (A) PCA plot and (B) heatmap. Refer to Table 5.1 for abbreviations.

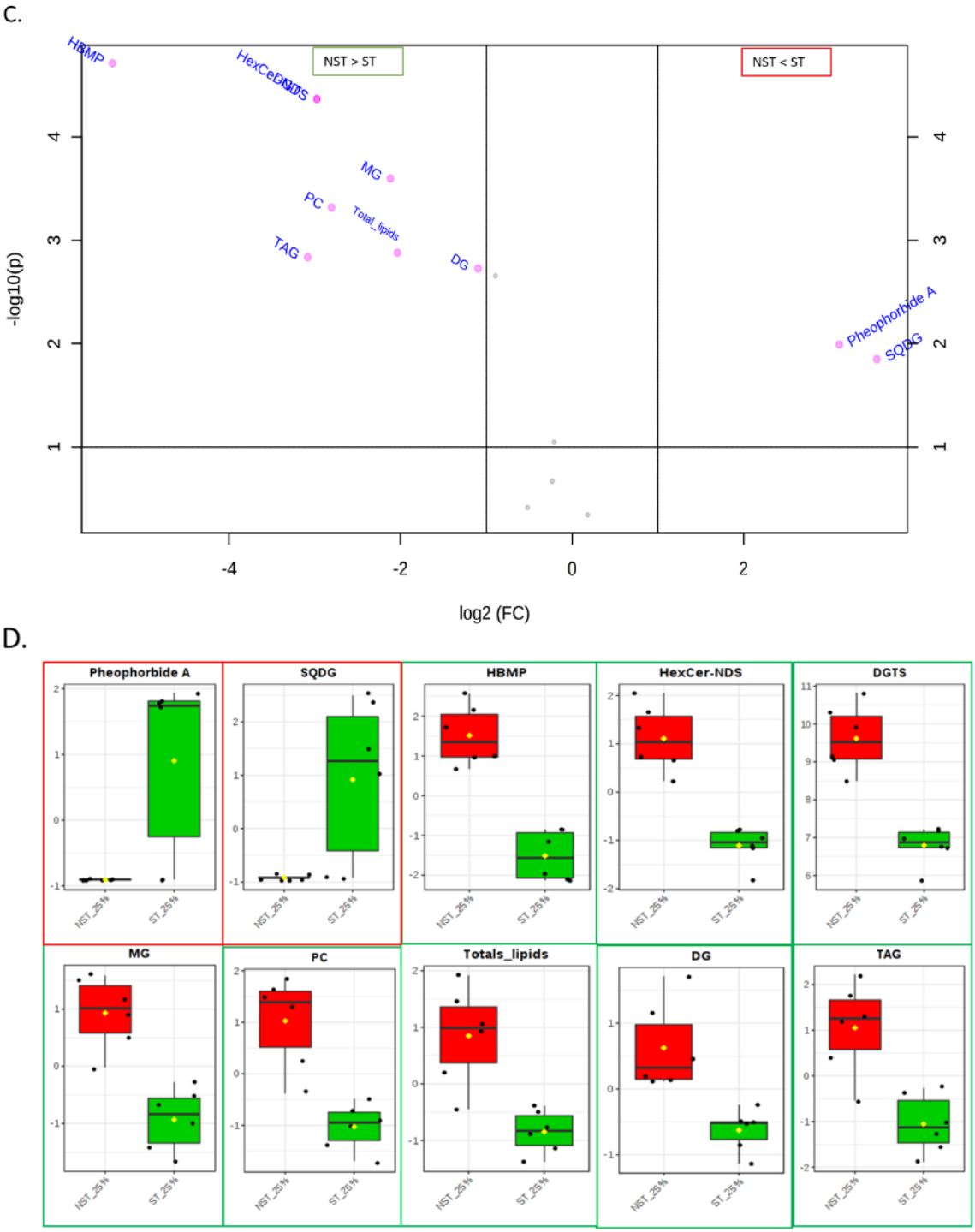

Figure 5.7.2: Differences in known (targeted) lipid classes in *Eragrostis nindensis* under dehydrated (25% relative water content (RWC)) conditions between non-senescent tissue (NST), in red, and senescent tissue (ST), in green, represented by (C) volcano plot and (D) corresponding box plots. Statistically significant changes in lipid class fold change are represented as box plots (D), where a log_2 fold change of <-1 represents lipid classes with higher abundances in the NST compared to ST at 100% RWC (indicated in green box). Similarly, a log_2 fold change of >1 represents significantly lower lipid class abundances in the NST compared to the ST at 100% RWC (indicated in red box). Refer to Table 5.1 for abbreviations.

5.3.2.3 Differences during drying in the NST

Changes in lipid classes from fully hydrated (100% RWC) to dehydrated (25% RWC) were assessed in the NST. There were differences in lipid class composition between the two water contents, as displayed by the clear sample separation in the PCA and heatmap (Figure 5.8.1). Three lipid classes (SQDG, pheophorbide A, and HBMP) diminished in abundance upon dehydration to 25% RWC and showed the strongest decrease in abundance during drying (Figure 5.8.2, C), with the former two being almost undetectable in the dehydrated state. Two glycerolipids (MG and TAG) and two glycerophospholipids (PC and PG) accumulated upon dehydration (Figure 5.8.2, D, represented as red box). There was an increase in total lipids during drying in the NST.

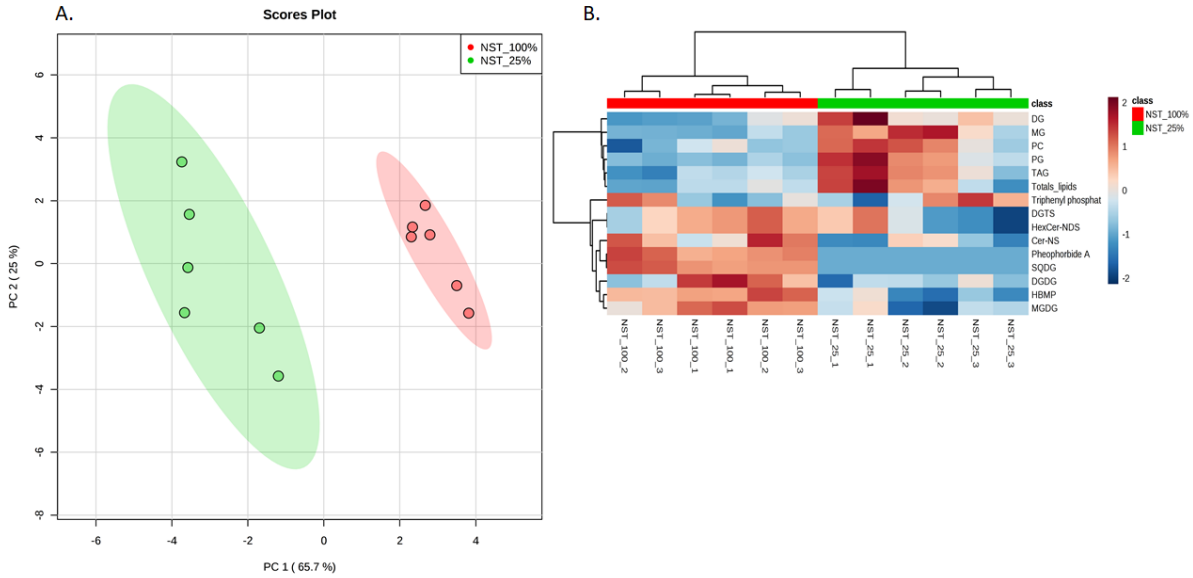

Figure 5.8.1: Differences in known (targeted) lipid classes in the non-senescent tissue (NST) of *Eragrostis nindensis* between hydrated (100% relative water content (RWC), in red) and dehydrated (25% RWC, in green) conditions represented by a (A) PCA plot and (B) heatmap.

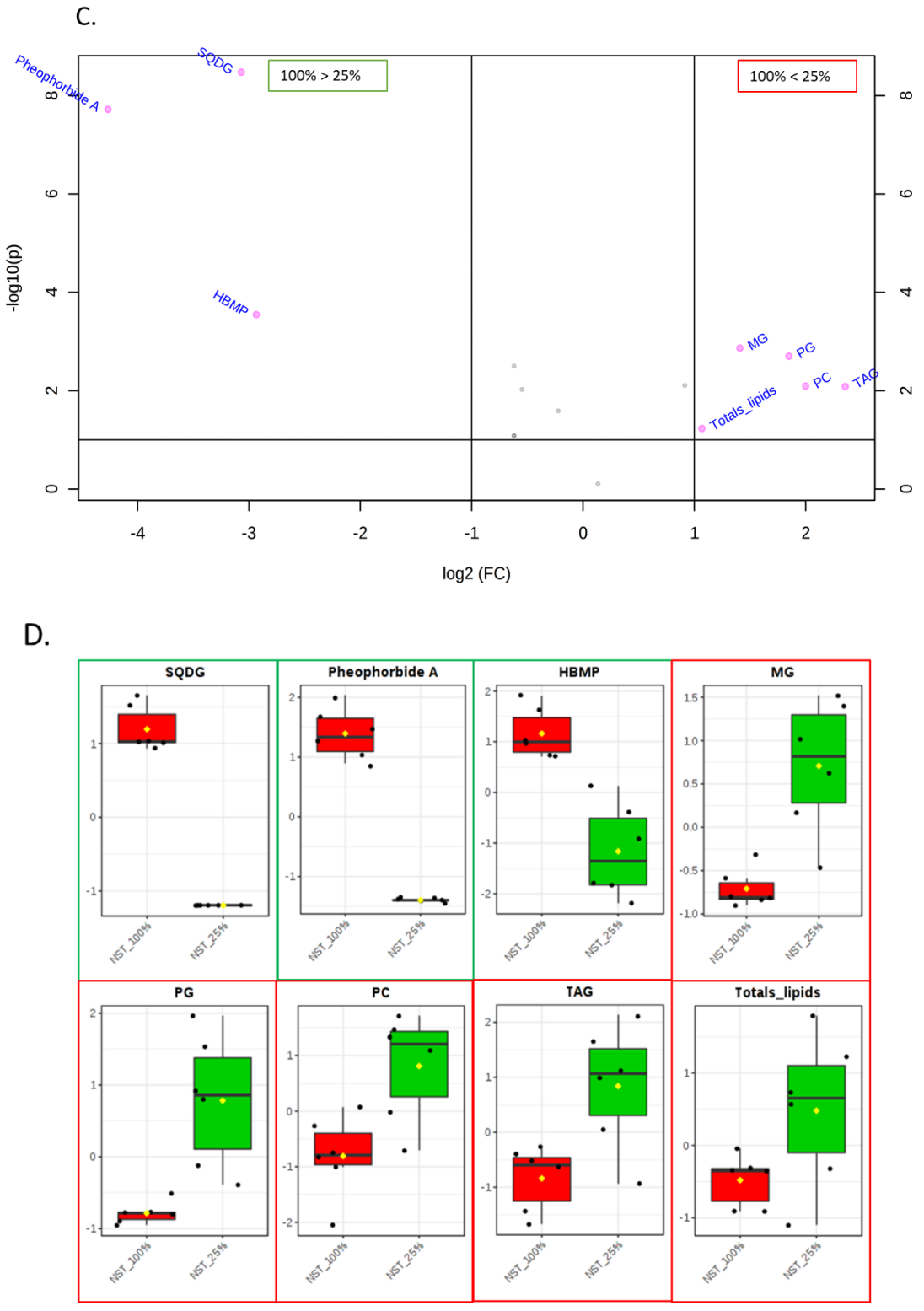

Figure 5.8.2: Differences in known (targeted) lipid classes in the non-senescent tissue (NST) of *Eragrostis nindensis* between hydrated (100% relative water content (RWC), in red) and dehydrated (25% RWC, in green) conditions represented by (C) volcano plot and (D) corresponding box plots. Statistically significant changes in lipid class fold change are represented as box plots (D), where a log_2 fold change of <-1 represents samples significantly lower in abundance in hydrated leaves (100% RWC) compared to dehydrated (25% RWC, indicated in green box) leaves in the NST, whereas a log_2 fold change of >1 represents significant higher lipid class abundances at 25% RWC, where MG, PG, PC, TAG and total lipids were significantly higher in abundance at 25% RWC, indicated in red box. Refer to Table 5.1 for abbreviations.

5.3.2.4 Differences during drying in the ST

According to the PCA and heatmap, there were differences in lipid class composition between the two water contents (Figure 5.9.1). The dehydrated ST showed six lipid classes diminishing in abundances, with only PG increasing in abundance (Figure 5.9.2) compared to the hydrated control.

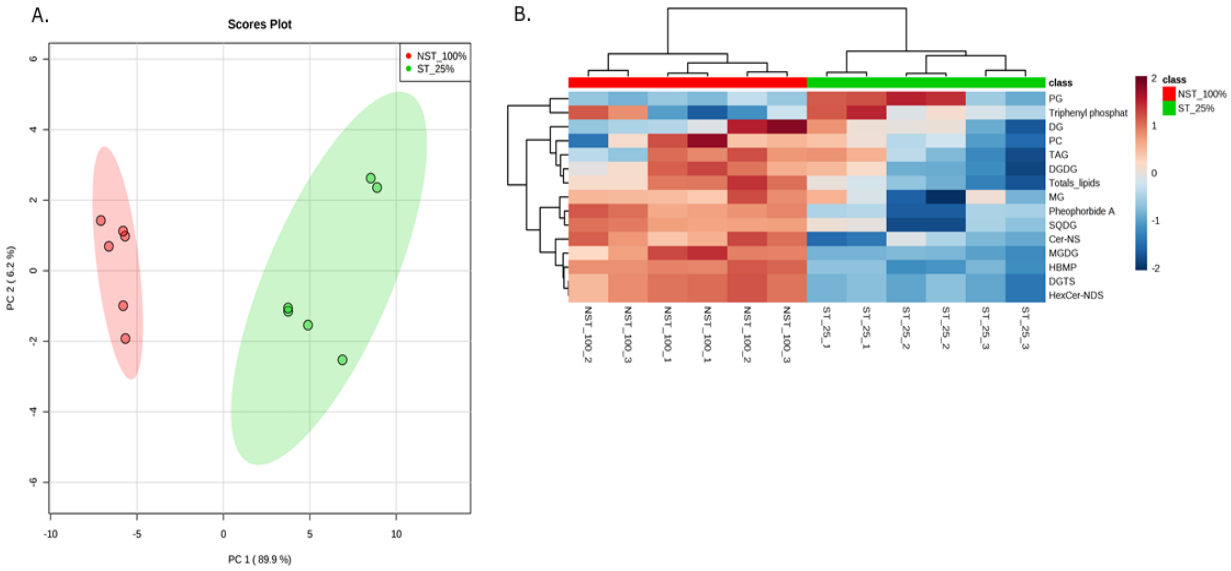

Figure 5.9.1: Differences in known (targeted) lipid classes in the hydrated (100% relative water content (RWC), in red) non-senescent tissue (NST) and the and dehydrated (25% RWC, in green) senescent tissue (ST) of *Eragrostis nindensis* represented by a (A) PCA plot and (B) heatmap. Refer to Table 1 for abbreviations.

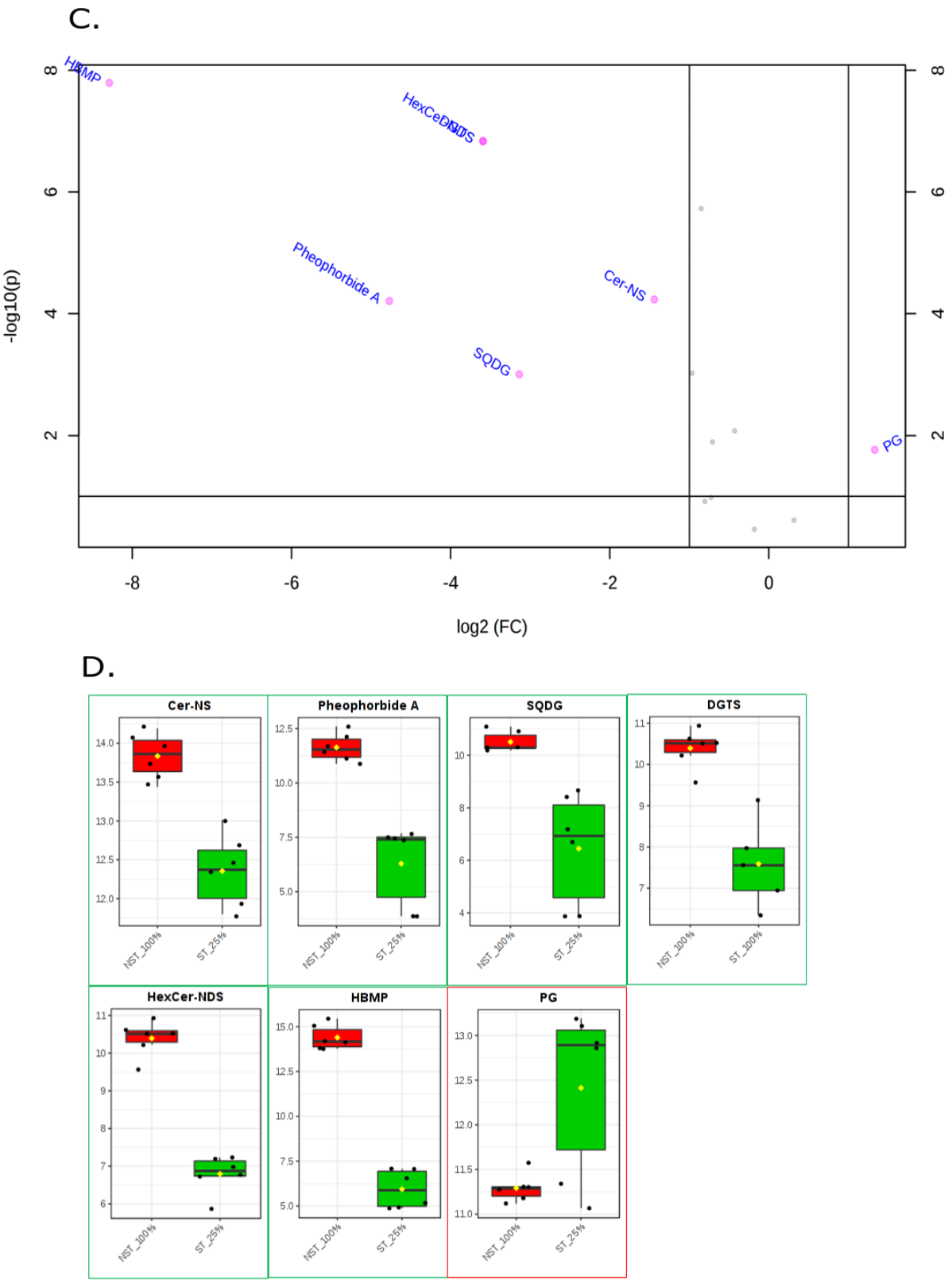

Figure 5.9.2: Differences in known (targeted) lipid classes in the senescent tissue (ST) of *Eragrostis nindensis* between hydrated (100% relative water content (RWC), in red) and dehydrated (25% RWC, in green) conditions represented by (C) volcano plot and (D) corresponding box plots. Statistically significant changes in lipid class fold change are represented as box plots (D), where a log_2 fold change <-1 represents samples significantly lower in abundance in the control (100% RWC NST) compared to dehydrated (25% RWC, green box) leaves in the ST, whereas a log_2 fold change of >1 represents significantly higher lipid class abundances at 25% RWC, red box. PG was significantly higher in abundance at 25% RWC, represented with a red box. Refer to Table 5.1 for abbreviations.

5.3.3. Changes in TAG composition upon dehydration

TAG consistently showed a strong accumulation in the NST upon dehydration, and this change was reflected in the relative amounts of TAG species (n = 30) during drying (Figure 5.10). The dominant trend occurred in TAG 54:8 (comprising of TAG 18:2/18:3/18:3) and TAG 54:9 (comprising of TAG 18:3/18:3/18:3), which increased upon dehydration, particularly in the NST (Figure 5.10). These TAGs are therefore proposed as markers for desiccation tolerance. The ST showed a more homogenous composition, whereas the dehydrated NST showed large preferences towards unsaturated TAGs (Figure 5.10). Of the 30 TAG species, 13 significantly accumulated upon dehydration in the NST, several of which showed major accumulation. Four TAG species increased in the ST during drying (TAG 18:0/18:1/18:2, TAG 18:3/18:3/20:0, TAG 18:3/18:3/183 and TAG 18:1/18:3/18:3), however, these TAGs accumulated significantly more in the NST (Figure 5.10, filled triangle in B), indicating that their increase can be used as a biomarker for desiccation tolerance.

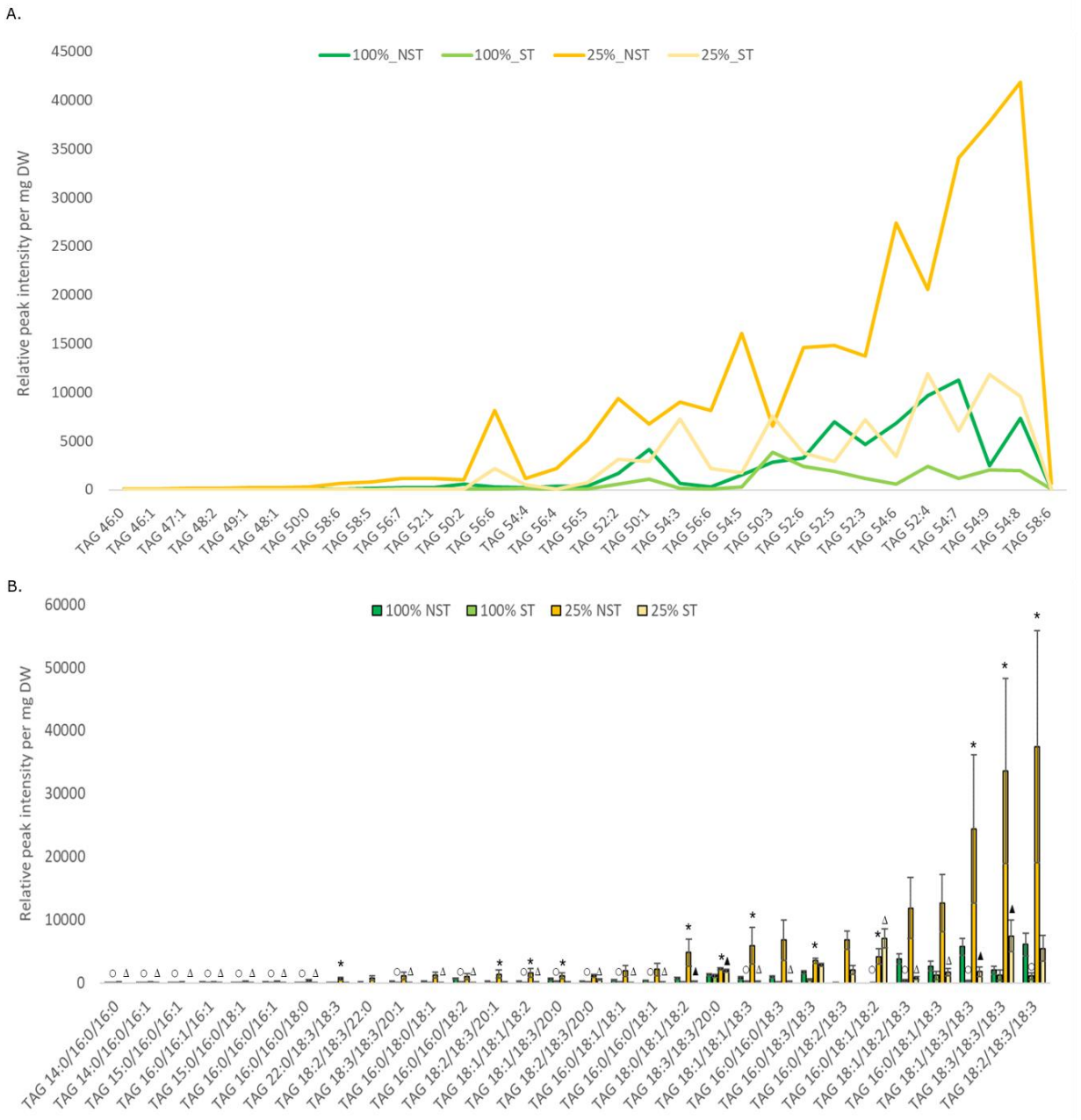

Figure 5.10: Changes in triacylglycerol (TAG) species composition in the non-senescent tissue (NST) and senescent tissue (ST) of the resurrection plant *Eragrostis nindensis* under hydrated (100% relative water content (RWC), in green) and dehydrated (25% RWC, in yellow) conditions. (A) Relative changes in peak intensities were derived from LC-HRMS analyses. TAG species composition (e.g. 54:9) are indicated by total carbon chain length (54) and number of double bonds (9). TAG 54:8 and TAG 54:9 accumulated strongly upon dehydration in the NST. (B) Bar graph representing the relative peak intensities (unnormalised) of TAG compositional changes and statistical significance (based on log transformation and pareto scaling). Significant differences derived from a Students t-test ($p<0.05$) using the hydrated control (100% RWC, NST) are indicated and are as follows: TAG consistently decreased (open circle) in ST at 100% RWC, consistently increased (asterisk) in the NST at 25% RWC, while both increased (filled triangle) and decreased (open triangle) in the ST at 25% RWC. Values are means with ± standard error bars (n= 3). TAG species in (A) correlate with the respective composition in (B).

5.3.4. Lipid-related transcript abundance

The transcriptome (**Chapter 3**) was used to investigate lipid-related expression trends to establish which key transcripts might function in lipid metabolism. Observations from the global lipid analysis showed an increase in total lipid and TAG at 25% RWC and therefore DGAT1, the final enzyme in TAG biosynthesis and oleosin biosynthesis (Chapman *et al.* 2012a), was investigated. DGAT1 significantly accumulated upon dehydration in both tissue types (Figure 5.11), however, the timing of expression differed, where the ST displayed earlier expression at 60% RWC only, whereas the NST showed delayed expression at 40% and 25% RWC. In general, transcript expression trends were similar in both tissue types, however, three DEGs, belonging to 3-KETOACYL-COA SYNTHASE 11 (AT2G26640), were exclusively expressed in the ST at 25% RWC (Figure 5.11). This enzyme is involved in the biosynthesis of very long chain fatty acids (VLCFA), which are carbon chains of 20 or longer, and tend to form waxes (Kim *et al.* 2019), which can enhance drought resistance through reduced water loss (Seo *et al.* 2011a). The transport of FAs from chloroplast to the ER is facilitated by, *inter alia*, LONG CHAIN FATTY ACID COA LIGASE (LACs) (Wang *et al.* 2012b; Aid 2019). These DEGs strongly accumulated in abundance during drying from 60% RWC throughout desiccation and rehydration in the NST, and during drying in the ST (Figure 5.11). TAG degradation and β-oxidation of FAs is a prerequisite for energy release (Wang *et al.* 2019) and an enzyme responsible for this degradation (ACYL COA REDUCTASE DEHYDROGENASE, AT3G51840) accumulated during drying, which correlated with the energy requirement upon rehydration. In general, ACYL COA REDUCTASE (AT5G22500) diminished in transcript abundance from 25% RWC in both tissue types. This enzyme promotes FA saturation by reducing double bonds and is required to make waxes (Kosma *et al.* 2012). Of the 13 DEGs annotated as CYCLOARTENOL SYNTHASE 1 (AT2G07050), which are involved in sterol biosynthesis and thylakoid organisation (Jin *et al.* 2017), 12 diminished during drying (predominantly in the NST), whereas one transcript (AT2G07050) only accumulated in the desiccated and rehydrated states (Figure 5.11). In general, there were few differences between the NST and ST, however, the ST accumulated β-oxidative transcripts at 18% RWC. The transcriptome supports the maintenance of active lipid metabolism, from TAG biosynthesis to FA transport and β-oxidation.

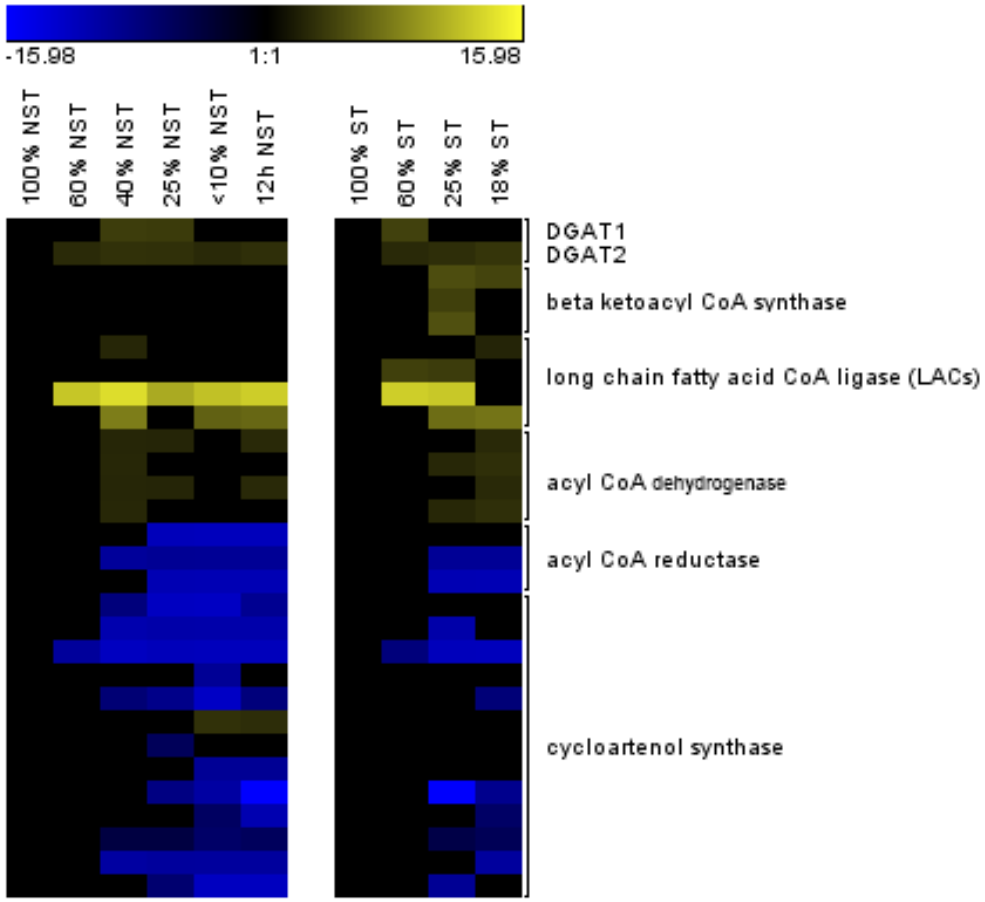

Figure 5.11: Heatmap showing transcript abundance trends of lipid-related transcripts depicting differential transcript abundance trends of desiccation tolerant, non-senescent tissue (NST) and desiccation sensitive, senescent tissue (ST) of the resurrection plant *Eragrostis nindensis* during drying (represented as relative water content, %) and rehydration (12h). Only differentially expressed genes (DEGs) are depicted, derived from the statistically significant change (>2 or <-2 log_2 fold change values, FDR <0.05) in transcript abundance compared to the control (NST, 100% RWC). The colour scale represents log_2 fold change values.

5.3.5. Oleosin transcript abundance

Of the 11 oleosin transcripts present in the transcriptome, eight were differentially expressed in the NST, and six in the ST, during drying and rehydration (Figure 5.12). Despite the OLE1 antibody being derived from Arabidopsis seed, the proline knot is highly conserved, which is a hallmark of oleosin (Fang *et al.* 2014). In addition, the OLE1 antibody had sequencing similarity to three of the DEGs, namely Eni_009916 (67%), Eni_003038 (67%) and Eni_007625 (57%) (Figure 5.12, red box).

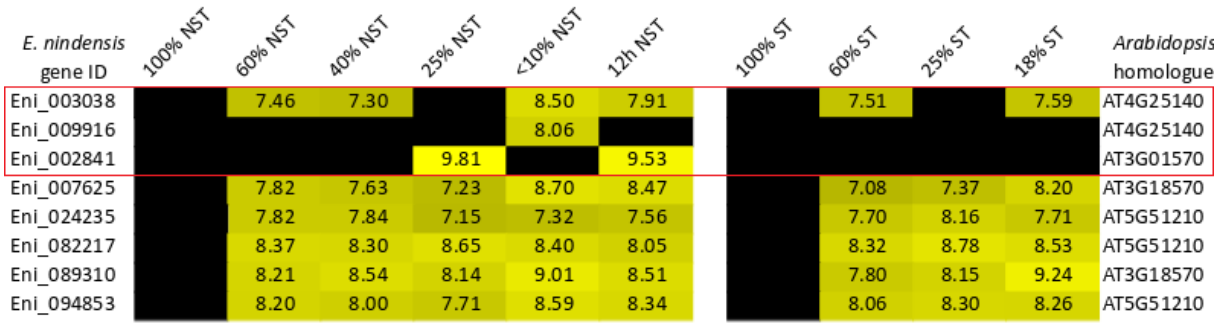

E. nindensis gene ID	100% NST	60% NST	40% NST	25% NST	<10% NST	12h NST	100% ST	60% ST	25% ST	18% ST	*Arabidopsis* homologue
Eni_003038		7.46	7.30		8.50	7.91		7.51		7.59	AT4G25140
Eni_009916					8.06						AT4G25140
Eni_002841				9.81		9.53					AT3G01570
Eni_007625		7.82	7.63	7.23	8.70	8.47		7.08	7.37	8.20	AT3G18570
Eni_024235		7.82	7.84	7.15	7.32	7.56		7.70	8.16	7.71	AT5G51210
Eni_082217		8.37	8.30	8.65	8.40	8.05		8.32	8.78	8.53	AT5G51210
Eni_089310		8.21	8.54	8.14	9.01	8.51		7.80	8.15	9.24	AT3G18570
Eni_094853		8.20	8.00	7.71	8.59	8.34		8.06	8.30	8.26	AT5G51210

Figure 5.12: Oleosin transcript abundance changes upon water-deficit stress (represented at relative water content, %), in the in the non-senescent tissue (NST) and senescent-tissue (ST) of the resurrection plant *Eragrostis nindensis*. Red box indicates sequence similarity to the anti-oleosin (OLE1) antibody used for the western blot. Yellow denotes accumulating transcripts, derived from the statistically significant change (>2 log_2 fold change values, FDR <0.05) in transcript abundance compared to the control (NST, 100% RWC). The colour scale represents log_2 fold change values.

5.3.6. Oleosin protein expression

There were distinct changes in the protein expression of oleosin across RWCs and between tissue types (Figure 5.13). In the NST, oleosin was barely detectable in the fully hydrated state but was consistently expressed at 40% RWC in all three biological replicates and positively correlated with decreases in RWC. In general, oleosin expression peaked at 25% RWC and remained stably expressed during desiccation (<10% RWC). Upon 12h of rehydration, the protein expression was variable, with two biological replicates showing a reduction, and one an increase, in oleosin expression (Figure 5.13). This reflected the variable nature of rehydration.

In the ST, the protein expression of oleosin during drying was observed, however, this was barely detectable (Figure 5.13, B). Despite the faint bands, the ST showed an increase in oleosin expression during drying, like the NST. Since the observed oleosin protein expression was detected from 40% RWC onwards (Figure 5.13), this implies that the antibody most likely bound to Eni_003038, as this was the only transcript with significant sequence similarity that had accumulating transcript abundance changes prior to the observed oleosin expression (Figure 5.12). The fold change of the comparative RWCs (e.g. 7.45 in the NST vs 7.51 in the ST at 60% RWC) of this transcript was similar between the tissue types (Figure 5.12), suggesting that the protein turnover should also be similar. However, the expression of oleosin differed between the two tissue types, where the NST exhibited higher oleosin expression during drying (Figure 5.13). This suggests that protein expression in the ST is retarded or inefficient.

The expected molecular weight of oleosin is 18.5 kDa (Shimada *et al.* 2008), however, the majority of OLE1 antibodies bound to proteins of ~33 kDa in both tissue types (Figure 5.13). It is therefore possible that the antibody bound to an oleosin or oleosin-like protein of a higher molecular weight, that there

was non-specific antibody binding, or that post-translational modification of the oleosin had occurred. Although the first two cannot be ruled out, the role of post-translational modification is suspected in *E. nindensis* and explained in the Discussion.

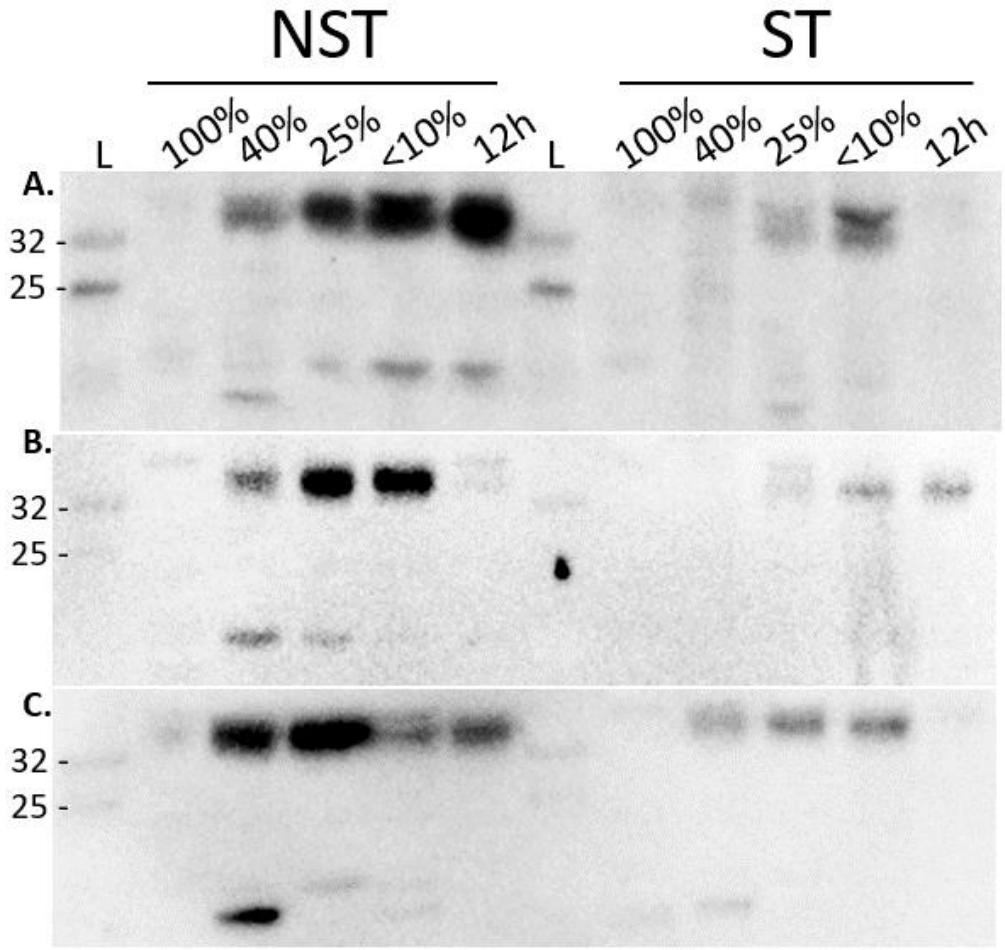

Figure 5.13: Protein expression of oleosin differed between the non-senescent tissue (NST) and senescent tissue (ST) of the resurrection plant *Eragrostis nindensis* during drying (represented as relative water content, %) and rehydration (12h). Three membranes (A-C), representing biological replicates, were probed with the anti-oleosin (OLE1) antibody (PhytoAB). Equal amounts of protein (40 µg/µl) was loaded, and Ponceau confirmed equal transfer to the membrane (Appendix, Figure A4). The Color Prestained Protein Standard, Broad Range (11–245 kDa) ladder (L) was used.

5.3.7. Ultrastructural changes

The ultrastructural changes are shown in Figure 5.14 to again highlight the lipid specific structural changes in the bundle sheath cells during drying. There was an accumulation of small, regularly shaped LDs that localised around the periphery of the cell, along the plasmalemma in the NST. In this tissue, LDs clearly increased during drying, particularly at 40% and 25% RWC, and were absent during rehydration (Figure 5.14, A). This reflected the trend observed in the oleosin expression in the NST

(Figure 5.14) and suggests that the small, regular lipids observed in the NST are a product of oleosins that regulate LD size, which act as storage organelles for TAG, along with functions associated with oleosin-coated LDs (discussed below). In contrast, the large, irregularly spaced LDs (osmophilic bodies) in the ST are typical of LDs devoid of oleosins (Figure 5.14, B, see Siloto *et al.* (2006)), which reflected insufficient oleosin protein expression observed (Figure 5.13). These TAG-filled LDs appear fused, resulting in enlarged structures, which showed less organisation around the plasmalemma, indicating a failure to both maintain a regular size and to translocate to the periphery as observed in the NST.

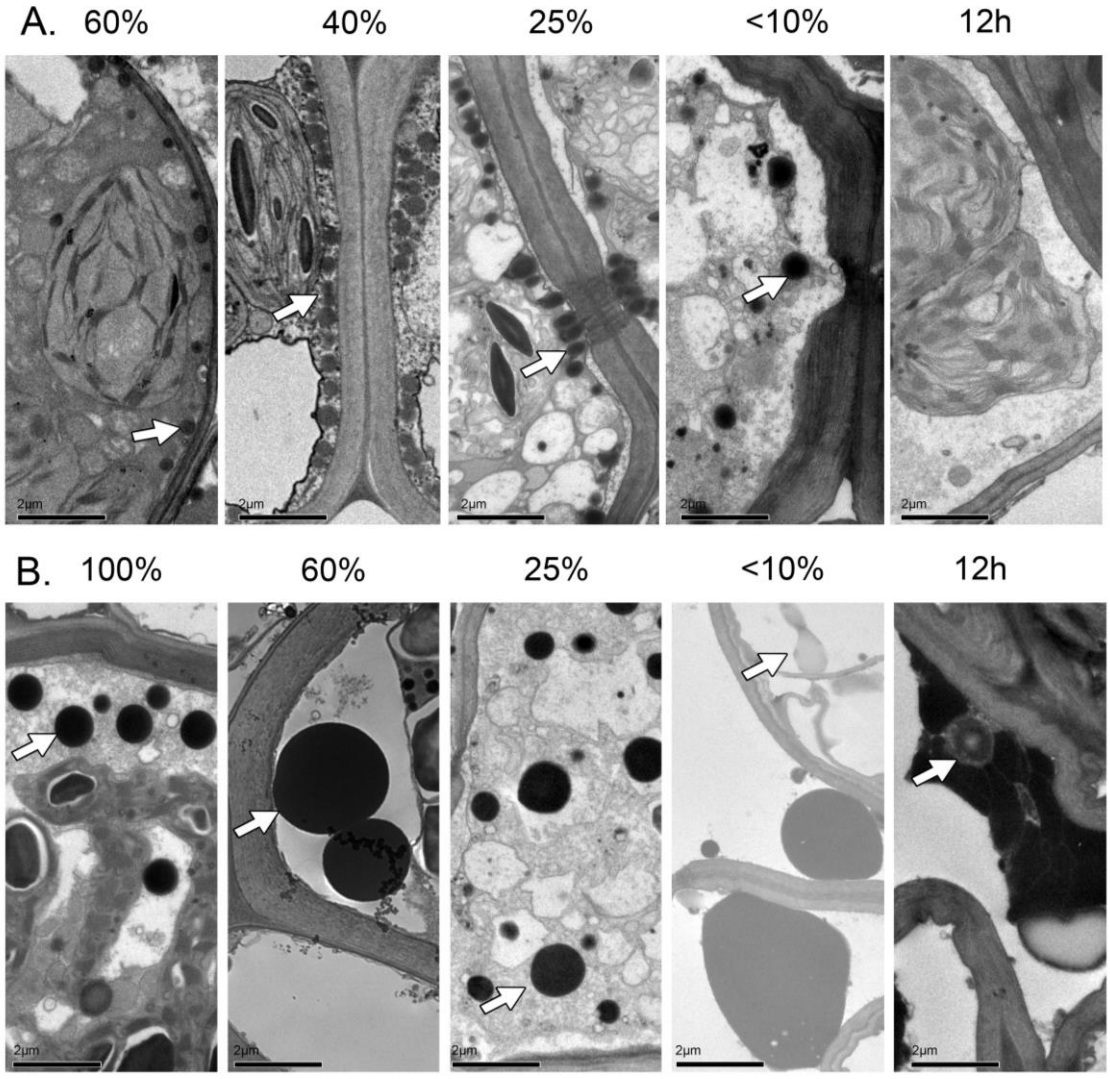

Figure 5.14: Accumulation of lipid droplets (LDs, white arrows) in the bundle sheath cells differ in size and distribution between the (A) desiccation tolerant leaves (non-senescent tissue (NST)) and (B) desiccation sensitive leaves (senescent tissue (ST)) of *Eragrostis nindensis* during drying (represented as relative water content, %) was identified through transmission electron microscopy. (A) LDs accumulating along the plasmalemma were small and regular. LDs accumulated from 60% RWC and increased in abundance at 40% RWC, peaked at 25% RWC, diminished in the desiccated state (<10% RWC), and were absent by 12h rehydration. (B) LDs (osmophilic bodies) occurred in the hydrated state (100% RWC), and accumulated strongly from 60% RWC, where their large and less ordered distribution differed starkly from the regulated LDs along the plasmalemma in the NST. Enlarged LDs remained abundant throughout desiccation and were not degraded during rehydration (12h). During rehydration, the cells had collapsed and cellular debris containing lipids remained, indicating cell death.

5.4. DISCUSSION

5.4.1. Global lipid changes

The dominance of TAG (and its precursors MG, DG) accumulation upon dehydration in the NST (Figure 5.4, Figure 5.8.2, Figure 5.10) confirms the hypothesis that the large darkly-stained droplets in the ultrastructural images are lipids (Figure 5.14). This also demonstrates that *E. nindensis* has a lipid-storage strategy and to a lesser extent other storage reserves, such as starch and sugars. Compared to sugars, lipids have received little attention in the resurrection plant field. Although in-depth studies exist (Navari-Izzo *et al.* 1995; Quartacci *et al.* 1997; Gasulla *et al.* 2013; Li *et al.* 2014; Tshabuse *et al.* 2018) these have not identified lipids as the major energy store in a resurrection plant, but rather reflect changes in thylakoid and membrane lipids. Total lipid content increased in dehydrated NST, suggesting some storage for potential energy release during rehydration. Furthermore, Figure 5.6 shows developmentally determined lipid compositional changes, as the NST and ST were both fully hydrated, yet the NST shows significantly higher accumulation of glycerolipids associated with the formation of chloroplasts. There was also major lipid reshuffling. The biosynthesis of acyls with more double bonds upon water-deficit stress in *E. nindensis* is clearly shown, especially for TAG 54:8 and TAG 54:9 (Figure 5.10). This TAG composition and peak intensity dominance is therefore a hallmark of desiccation tolerance in this species. TAGs also accumulate in senescing tissues (Kaup *et al.* 2002; Lin *et al.* 2008; Slocombe *et al.* 2009; Watanabe *et al.* 2013), and although some saturated TAGs in the ST of *E. nindensis* showed increases during drying, the overall TAG content showed no statistical difference from the hydrated state. This reiterates that unsaturated TAG accumulation is dominant in the NST and is thus could be a biomarker of desiccation tolerance in *E. nindensis*. This, however, must be assessed in other resurrection plants to see if this is a universal phenomenon.

TAG accumulation is supported by the transcriptome (DGAT, Figure 5.11), and although DGAT1 is the final step in TAG biosynthesis, it is not the cause of TAG accumulation alone. Lipid accumulation in the NST might be due to high lipid turn-over rates. The supply of FAs, rather than the demand for TAGs, controls TAG biosynthesis (Ohlrogge *et al.* 1997). Therefore, it seems that the excess of FAs is the main driver of TAG accumulation. In *E. nindensis*, drying induced major structural changes in the chloroplasts (thylakoid breakdown), altering the main site for FA biosynthesis and producing an excess of chloroplast constituents (Figure 2.10 and 2.12). This is likely due to its poikilochlorophyllous nature. These breakdown products could form plastoglobuli but could also be temporarily sequestered into LDs upon desiccation (see Figure 2.15, B). The ST accumulated lower TAG levels when compared to the NST and seemed to accumulate more plastoglobuli. This might be an indication that the process of exporting FAs from the chloroplast into the ER for the biosynthesis of TAGs is dysfunctional or

inefficient. Most DEGs involved in thylakoid organisation diminished during drying (predominantly in the NST) validating observed thylakoid disassembly, whereas one transcript (AT2G07050) accumulated during drying in the desiccated and rehydrated state (Figure 5.11), hinting at preparation for rehydration. Surprisingly, there was not a significant reduction in MGDG or an increase in DGDG, as reported in other resurrection plants (Li *et al.* 2016; Tshabuse *et al.* 2018; Chen *et al.* 2018) and increasing the biological replicate sample size might help to clarify differences. Nevertheless, the observed chlorophyll breakdown (Figure 2.10) and thylakoid disassembly with subsequent plastoglobuli and LD accumulation (Figure 2.12) during drying correlated with the increase in TAG upon dehydration in both tissue types. This suggests that excess lipids are removed and exported to the ER, where they can be packaged and stored as TAG-filled LDs. The stable transcript expression of FA transport transcripts (LACs, Figure 5.11) and the increase in TAG-containing cytosolic LDs (Figure 5.14) supports this.

In addition, SQDG, which is critical for photosynthesis (Wang *et al.* 2012b), is degraded upon dehydration (Figure 5.5). It is possible that SQDG, which is the smallest contributing lipid to photosynthetic membranes, is degraded first to ensure prompt photosynthetic shutdown. MGDG was expected to decrease upon dehydration due to trends in other resurrection plants, and although MGDG did diminish in abundance, the changes were not statistically significant. This indicates that whatever degradation has occurred has not been sufficient, that MGDG degrades later in drying (below 25% RWC), or that the biological replicate sample size needs to be increased. The presence of HBMP in high quantities in the hydrated NST is notable, as there is no known information regarding the function of this molecule. It is depleted during drying in both tissue types. It is also possible that this lipid is involved in lipid reshuffling and particular TAG formation, however, this is speculation and must be experimentally confirmed.

While enlarged LDs (osmophilic bodies) dominated the cell during drying in the ST, these are unlikely to be entirely TAG dominant, as TAG content did not increase significantly compared to the hydrated control (Figure 5.9). It is possible that FAs are transported from the ST to the NST upon mild water-deficit stress, as LDs were already observed in the hydrated ST (Figure 5.14, B) and LACs was expressed from 60% RWC. However, the lack of regulation in the ST of *E. nindensis* during drying (**Chapter 4**), coupled with the observed enlarged LDs that do not degrade upon desiccation or rehydration, suggests that cell biogenesis is dysfunctional in the ST, and is a consequence of the attrition of lipid metabolism.

The structural lipid, PG, accumulated at 25% RWC in both tissue types, but more so in the NST (Figure 5.5), whereas PC accumulated in the NST only (Figure 5.8.2), indicating that lipid remodelling occurs

during water-deficit stress. A decline in PC was also observed in senescent Arabidopsis leaves (Watanabe *et al.* 2013). PC is the substrate for galactolipid synthesis and 18:3 plants, such as *E. nindensis* (Figure 5.2), rely completely on the import of PC from the ER for the synthesis of MGDG (Andersson *et al.* 2004; Michaud *et al.* 2019). PC is also required for ER-chloroplast transport, representing contact-sites for lipid transfer (Wang *et al.* 2012b). The stronger increase in these structural lipids in the NST could suggest that PC is pooled for the imminent synthesis of MGDG on rehydration, should levels have been further compromised below 25% RWC, as suggested above. If so, this would suggest that only the NST is capable of this, since the ST is devoid of PC pools. This suggests a tighter regulation and control over lipid biogenesis and reinforces the controlled expression and regulation that characterises the NST, as seen in **Chapter 4**. This is important, as the transfer of lipids from the chloroplast to ER occurring via contact-sites is required to sustain cell growth and to coordinate changes in response to stress (Michaud *et al.* 2019; Lee *et al.* 2019). Contact sites were observed in the desiccated state in the NST (Figure 2.12, E).

5.4.2. Oleosin: a driver of desiccation tolerance

The accumulation of oleosin protein, coupled with the ordered plasmalemma LD accumulation in response to water-deficit stress, reiterates that *E. nindensis* has opted for a lipid-storage strategy during drying, particularly in the NST. Since LDs are coated with oleosins, and the presence of oleosin was confirmed with western blotting, the small peripheral LDs in the NST of *E. nindensis* are assumed to be coated with oleosin. It is important to highlight that oleosins are not known to occur in the absence of LDs, and the majority of studies have investigated oleosins in the context of seeds (Horn *et al.* 2013). Although the transcript abundance patterns of some lipid-specific proteins (such as oleosin) have been described (see VanBuren *et al.* 2017, 2018a), the role of LDs as an entity have not been earmarked as common traits of resurrection plants. This might be due to the less important role of storage lipids observed in other resurrection plants. Furthermore, where the presence of LDs have been confirmed, for example in *O. thomaeum* through nile red staining, their localisation or changes in abundances during drying were not identified and remain unknown (VanBuren *et al.* 2017).

The lipase-binding sites on LDs are unknown, and although oleosins have been suspected to play a role (Huang 1992), conclusive evidence has yet to be shown (Huang 2018). However, oleosins are unlikely to promote lipase binding as LD accumulation was observed throughout drying in the NST of *E. nindensis,* indicating that the LDs were not entirely degraded. Also, the enzymatic activity of lipases could only occur after oleosins were removed by trypsin, thus suggesting that oleosins actually prevent lipase access to TAG in LDs (Tzen *et al.* 1992; Pyc *et al.* 2017). Oleosins therefore have an additional

function to both physically and oxidatively stabilise LDs, functioning as an antioxidant by preventing access to excess acyl chains to uncontrolled degradation with harmful consequences (Wijesundera *et al.* 2013). Moreover, Deruyffelaere *et al.* (2015) showed that oleosins first needed to be degraded in order to release TAGs, providing evidence that oleosins protect the LDs from premature or unwanted lipase degradation. In support of this, oleosins and LDs disappear rapidly during seedling growth, showing their mobilisation during rehydration and growth in *Zea mays* seeds (Huang 1992). There is no *a priori* reason to believe that this is different in vegetative tissues, and this is supported by the lack of observed LDs (Figure 5.14), and the concurrent decline in relative oleosin protein expression (Figure 5.13) by 12h rehydration in *E. nindensis*. As in the study by Deruyffelaere *et al.* (2015) in Arabidopsis seeds, the role of oleosin in *E. nindensis* NST showed precise and ordered accumulation of oleosin during drying and subsequent degradation during rehydration (Figure 5.13). This demonstrates the specific role of oleosin in preventing lipid mobilisation until the TAG-rich energy supply of LDs is needed during rehydration. The energy benefit is particularly important for resurrection plants, where photosynthetic carbon gain is shut down during drying, and thus energy stores need to be sufficient to supply metabolic readjustment and resumption during drying and rehydration. Furthermore, the increase in oleosin expression has been linked with accumulating TAG and LDs (Sadeghipour *et al.* 2002; Froissard *et al.* 2009; Deruyffelaere *et al.* 2015), and this is concomitantly observed in *E. nindensis* during drying in the NST (Figure 5.5, Figure 5.10). The regulated control of oleosin synthesis and degradation is a key component of the timing of energy release, and this mechanism is thus a key component of desiccation tolerance in this species.

The molecular weight of the oleosin protein was higher than expected, at ~33 kDa (Figure 5.13), given the expected antibody weight and range of oleosin of 15 - 26 kDa (Huang *et al.* 2015). Several isoforms of oleosin exist, and larger oleosin molecules have been encountered, likely due to the hydrophilic domains having variable amino acid sizes (Kim *et al.* 2002; Hsieh *et al.* 2004; Huang *et al.* 2013). However, this is unlikely to explain the higher molecular weight observed. Alternatively, the observed molecular weight could indicate post-translational modification of oleosin, due to the following: In a novel study, Hsaio and Tzen (2011) showed conclusively that oleosin was mono-ubiquitinated in Arabidopsis seeds after germination, resulting in a 32 kDa band. This was the first study to show that oleosins are targeted for ubiquitination. Another study by Deruyffelaere *et al.* (2015) illustrated that oleosin was mono-ubiquitinated, showing a 32.5 kDa band, and concluded that oleosin needed to be degraded prior to germination. The dominant function of ubiquitin is to tag proteins for selective degradation by the 26S proteasome, removing damaged or misfolded proteins, and thus maintaining cellular homeostasis (Von Kampen *et al.* 1996; Hasselgren *et al.* 1997; Sharma *et al.* 2016a). Furthermore, ubiquitination has been used as an indicator of protein damage upon desiccation in two

resurrection plants (*S. stapfianus* and *Syntrichia ruralis*, O'Mahony *et al.* 1999). This post-translational modification of proteins by ubiquitination therefore plays a critical role in desiccation tolerance by controlling the timing and rate of degradation, and the molecular weight of oleosin observed might be due to post-translational modification.

Most oleosin protein expressed in *E. nindensis* was ~33 kDa implying potential mono-ubiquitination (as previously observed in Tzen *et al.* 1992; Deruyffelaere *et al.* 2015). The expected band of ~19 kDa was evident, predominantly at 40% RWC (Figure 5.13, particularly in C), however, the dominant signal showed that oleosin expression occurred at ~33 kDa. This might suggest that the oleosin are forming stable dimers (as shown in Pons *et al.* 1998, 2005; Li *et al.* 2002), or that LDs in *E. nindensis* are potentially being tagged by ubiquitin. However, LDs are not degraded during drying. On the contrary, they accumulated at 25% RWC, which does not indicate immediate degradation. This raises the question as to why the oleosin in *E. nindensis* would be ubiquitinated early (at 40% RWC) when LD degradation is destined for energy requirements during rehydration. However, mono-ubiquitination does not necessarily implicate the ubiquitinated molecule for immediate degradation, but rather acts as a "priming event" for future ubiquitination (Petroski *et al.* 2007; Komander 2009). Furthermore, the function of ubiquitination is context-specific, as mono-ubiquitination of molecules can act as signals for DNA repair or vesicle trafficking (Johnson 2002; Sharma *et al.* 2016a), and therefore not necessarily degradation. Since the addition of the first ubiquitin molecule is the rate-limiting step, and at least four ubiquitin molecules are required for degradation via the proteasome 26S pathway (Petroski *et al.* 2007), it is possible that the oleosin in *E. nindensis* is being tagged in preparation for future breakdown in response to energy and lipid requirements. This "primed" oleosin could therefore facilitate rapid degradation in response to rehydration. Such mono-ubiquitination in turn, could tag the oleosin for rapid degradation in preparation for rapid TAG mobilisation for energy release and membrane repair, or enable other functions, such as vesicle trafficking.

The NST of *E. nindensis* showed strong oleosin protein accumulation during drying, whereas this protein was barely detectable in the ST (Figure 5.13). Given the oleosin protein and transcript expression trends, coupled with the ultrastructural observations, it is therefore reasonable to conclude that the observed irregular and enlarged LDs in the ST are due to the deficiency of oleosin. The reduced surface to volume ratio can impede the efficient release of energy during dehydration when compared to the small, regular LDs in the NST (Figure 5.14) that also provide a mechanical stabilisation function. The contrast between the localisation of these LDs between the NST (periphery) and ST (various cytoplasmic regions) also suggests a strong role in desiccation tolerance, other than oleosin aiding in quick energy release. The differences in localisation is evident as the LDs of NSTs simultaneously accumulated along the plasmalemma, particularly around the plasmodesmata (Figure

5.14, A), which was not detected in the ST (Figure 5.14, B). The organisation of the NST LDs during drying reflected that of orthodox seeds (Shimada *et al.* 2008), where vacuoles and nuclei are located in the centre of the cell, with LDs surrounding them on the periphery (Shimada *et al.* 2018). Rinne *et al.* (2001) observed a similar displacement of LDs along the plasmalemma and noted the increased congregation of LDs around the plasmodesmata during chilling stress in birch (*Betula pubescens*), shoot apices. The distinct localisation of LDs in the NST of *E. nindensis* showed the same localisation trend in Arabidopsis seeds and birch, showing clear parallels between LD localisation along the plasmalemma and tolerance (to freezing or desiccation). In addition, all of these tissues enter dormancy and require mechanisms of LD-mediated protein targeting to ensure cell communication (Siloto *et al.* 2006; van der Schoot *et al.* 2011; Paul *et al.* 2014). The localisation of LDs at the cells' periphery in the NST therefore shows a structural change during drying, which suggests that this is a signature of desiccation tolerance in *E. nindensis* and implies a role of these LDs in water-deficit stress response.

Furthermore, the lipid-dominated energy strategy of *E. nindensis* is intriguing, because lipids (especially unsaturated lipids) are prone to peroxidation, are targets of ROS (Ruiz *et al.* 2018) and are expensive to make (Heldt 1997; Subramanian *et al.* 2013), thus being a potential liability to the cell (Ruiz *et al.* 2018). However, this species is capable of strong lipid accumulation. The mechanical stabilisation and protection of cells during drying and rehydration, is due in part, to oleosin that stabilises these vital energy stores, acts as signalling molecules and mechanically stabilises organelles.

In summary, the enlarged LDs in the ST of *E. nindensis* during drying is in stark contrast to the regular sized and ordered distribution of LDs in the NST and can be attributed to oleosin. The transcript abundance patterns of oleosin showed similarities in the NST and ST (Figure 5.12). Oleosins have been explored in resurrection plants, but these studies have been restricted to changes in transcript abundance, and have not confirmed the presence or relative changes of oleosin protein in vegetative tissues. VanBuren *et al.* (2018) showed that more oleosin transcripts were expressed in a desiccation tolerant species and at higher transcript abundances (500 TPM, *L. brevidens*) compared to a desiccation sensitive relative (30 TPM, *L. subracemosa*) during drying. Baseline transcript abundances cannot explain the differences in oleosin protein expression in *E. nindensis* as they are similar (Figure 5.12), reinforcing the hypothesis that senescence is regulated at the translational level (**Chapter 4**). The translational failure in the ST resulted in insufficient oleosin proteins required to maintain small LD sizes, which therefore fused, resulting in large, unstable LDs that are not carriers of proteins to sites of activity. The lack of oleosin protein expression (Figure 5.12) and irregular enlarged LDs (Figure 5.14, B) illustrates the failure of the ST to undergo basic cell maintenance, production and function upon

desiccation, and therefore senesce and die. The lack of oleosin can therefore be considered a marker of senescence in *E. nindensis* and demonstrates how translational failure can result in cell death.

5.5. CONCLUSION

This **Chapter** shows for the first time, that lipids accumulate in *E. nindensis* during drying, and that the changes in lipid composition and species and proposes that some, such as TAG 54:8, can be used as biomarkers for desiccation tolerance. By comparing desiccation tolerant and desiccation sensitive tissue of the same species, the roles of oleosin-coated LDs were evident. Although TAG accumulation has been documented in other resurrection plants and sensing tissues, this **Chapter** demonstrated that it is rather the composition of these TAGs (e.g. TAG 54:8) and how they are packaged (in oleosin-coated LDs) that is important. The stabilisation and potential lipid signalling role of oleosin-coated LDs only occurred only in the NST of *E. nindensis* due to the expression of oleosin protein through intact translational machinery, as found in **Chapter 4.** Conversely, stable LDs are distinctly absent in the ST. Oleosins can therefore be used as a marker for desiccation tolerance in *E. nindensis,* and could apply to other resurrection plants, especially the lipid-rich species. LDs are highly dynamic organelles with various biochemical and structural functions rather than inert storage organelles as previously thought.

Chapter 6

DESICCATION TOLERANCE AND SENESCENCE IN *E. NINDENSIS*: CONCLUSIONS AND A WAY FORWARD

6.1. DESICCATION INDUCED SENESCENCE DIFFERS BETWEEN TISSUES

To meet the increasing demand for agricultural output, resilience to climatic demands needs to be introduced, either into current cultivars or by alternative forms of productive agriculture. Orphan crops are a route that has had strong advocacy in recent years (Tadele 2018). Drought-induced crop failure necessitates the introduction of stress-adaptive traits, such as resistance to, or tolerance of, water loss under drought and the prevention of senescence. In order to prevent cell death, a deeper understanding of the regulation of senescence and desiccation tolerance is required. Research has focussed on factors that enable tolerance, rather than investigating those that make a resurrection plant lose tolerance, as is evidenced by loss of viability and death of some tissues within the plant. This thesis has approached the question of how and why older leaf tissues die under water-deficit stress in *E. nindensis* from a unique perspective, thus identifying the crux of how senescence is regulated in this, and possibly other, resurrection plant species. Although there is an age-associated component of senescence in the ST, **Chapter 4** demonstrated that senescence is actively regulated in response to stress. A summary of the findings of this thesis can be found in Figure 6.1. What is apparent is that the ST failed to produce sufficient protective molecules and did not mitigate mechanical or oxidative stress below 25% RWC. The early response to water-deficit stress can therefore be considered a drought response, whereas from 25% RWC only desiccation tolerant tissues survive. This study demonstrated that a desiccation-specific senescence programme exists in *E. nindensis*.

One of the hallmarks of senescence in resurrection plants is the general suppression of genes and transcripts associated with senescence to block senescence signals during drying, as observed in *Sporobolus stapfianus* by Griffiths *et al.* (2014). A similar trend was observed in *E. nindensis*, where the overall senescence regulatory pathway was, in general, suppressed, particularly in the NST. Furthermore, this thesis adds to the knowledge of the general phenomenon of senescence in resurrection plants (see **Chapter 3** and **4**) and is the first comprehensive analysis linking components of the physiological, ultrastructural, molecular, proteomic (albeit limited) and lipidomic aspects of two

phenotypically diverse tissues that occur within a single species. This study formed a critical baseline for future studies working on desiccation tolerance and senescence suppression in resurrection plants, which in turn could lead to transformation of crops, for example *E. tef*, with improved tolerance to extended drought.

A major objective of this thesis was to demonstrate transcriptional differences between surviving (non-senescent) and senescent leaf tissues in response to desiccation. The transcriptomes of both tissues contribute to the global molecular data on resurrection plants, and so adds knowledge to the field. The transcriptomes, together with phenotypic and biochemical observations made between the tissue types under water-deficit stress, adds insight into how senescence can be regulated and suppressed, and how this knowledge can be used to improve crops, animal feed or biofuels.

Senescence is complex. It involves molecular and physiological control of several biological processes and is not fully understood. Senescence has the same complexity as desiccation tolerance, and the two concepts are interlinked: Thus, to understand desiccation tolerance one needs to understand senescence, and vice versa. One reason for this complexity is because similar processes occur during both senescence and desiccation tolerance, such as photosynthetic shutdown, chlorophyll breakdown (**Chapter 2**), and TAG accumulation (**Chapter 5**). This also calls for a renewed definition of senescence that is specific to resurrection plants, to differentiate between processes that end in a metabolically quiescent state displaying tolerance from those that exhibit excess damage and die. What defines desiccation tolerance is whether these processes are reversible (e.g. photosynthetic resumption) or not, and this could not be determined from the transcriptional expression of known traits of desiccation tolerance alone. To add to this complexity, the transcriptomic signature of known desiccation tolerant traits was similar in both tissue types (**Chapter 4**), disproving the notion that senescence occurs due to the inability of the ST to transcribe transcripts required for desiccation tolerance (such as LEAs, HSPs, antioxidants or transcripts involved in sucrose pathways, **Chapter 4**). The expression of desiccation tolerance transcripts in the ST was an unexpected result and demonstrated that senescence is not regulated at the individual transcript level.

A crucial difference between tissue types was the exclusive over-enrichment of transcript abundance relating to protein and RNA maintenance and protection in the NST and the suppression of senescence (**Chapter 4)**. The tighter translational control in the NST, reflected in both the transcriptome and protein synthesis (**Chapter 4**), indicates greater activation, and hence control, of the translational machinery (Figure 6.1). *E. nindensis* therefore engages in a regulation of senescence at the translational level in the NST, rather than a fine-tuned transcriptional regulation in the ST. This might be an evolutionary conserved strategy to continue transcription upon abiotic stress, but not exhaust

resources on expensive translation in the ST. This is a possible "hedge-betting" strategy, in that having these transcripts available means that they can still be translated in the ST to enable recovery in the event of rainfall during early drying. However, following drying to 25% RWC, only desiccation tolerant tissue can survive, as the required protective mechanisms and metabolic reshuffling needs to be laid down to prevent the deleterious consequences of desiccation prior to entering the airdry state (Figure 6.1). Thus, the main finding of this study is that transcription is maintained during drying in *E. nindensis*, in both tissue types, but that only the NST is capable of regulating and stabilising RNA and maintaining control of translational machinery. The NST protected RNA and showed structured cellular organisation during drying, reflecting the switch towards the desiccation tolerance programme. In contrast, the ST failed to regulate RNA processing, was unable to suppress senescence, and had inadequate translation of the required proteins, resulting in cell death.

Chapter 3 demonstrated the distinct metabolic reshuffling at different stages of water-deficit stress in the NST; from photosynthetic and metabolic shutdown, accumulation of protective molecules, to regulation of transcription and translation. In addition, this thesis showed that *E. nindensis* favours a lipid-storage strategy during drying, favouring lipids as a complex reserve rather than solely starch or simple reserves, such as sucrose, which is typical of most resurrection plants (**Chapter 4**). This is an interesting trait as the accumulation of peripheral lipid droplets has not been identified in other resurrection plants. Lipids were a common thread and their significance was shown throughout: their accumulation was a striking feature in **Chapter 2**, and the transcriptomic signature of diminishing starch catabolism in favour of accumulating lipid storage in **Chapter 3** was echoed in **Chapter 4**, where '*lipid storage*' transcripts accumulated in abundance in both tissue types and this corresponded with diminishing '*lipid transport*' transcript abundances, and finally, was further validated in **Chapter 5**, where unsaturated TAG (TAG 54:9) accumulation and oleosin-coated lipid droplets were proposed to be considered as biomarkers for desiccation tolerance in this, and possibly other, resurrection plant species. The consequence of an inefficient translational machinery was illustrated by the expression of the protein oleosin (**Chapter 5**). Here, the insufficient expression of oleosin in the ST is proposed to have failed to prevent lipid droplets from coalescing, thus yielding enlarged lipid droplets that were not targeted to the periphery of the cell, thereby failing to invoke their membrane repair and stabilisation roles, which contributed to cell death (**Chapter 5**). This demonstrated the deleterious consequence of inadequate protein translation and showed that these proteins are markers of desiccation tolerance in *E. nindensis*. Furthermore, there was no difference in transcript abundance of the oleosin transcripts between tissue types, therefore reinforcing the hypothesis that the transcription of desiccation tolerance traits is maintained in the ST, which could be (*inter alia*) a resurrection plant specific response to senescence.

Given the overall trends of the two tissue types, the senescence programme in *E. nindensis* is novel and does not entirely reflect classical senescence, because there is some degree of order during dehydration at 60% RWC. However, at 25% RWC the tissue is clearly phenotypically different. Most importantly, the transcriptional programme is generally maintained (desiccation tolerance response), however, translation is prevented (non-resurrection plant response). It is therefore critical to have a systems biology approach to understanding molecular processes like desiccation tolerance or senescence, as a holistic understanding of the interplay between transcription, translation, and the functional role of translated proteins is required to contextualise plant stress responses. This thesis was explorative, with the aims of understanding how different tissues respond to water-deficit stress on a molecular level through bioinformatic techniques and how this relates to observed physiological traits. The characterisation of the transcriptome provides a resource to further investigate candidate genes that could guide crop engineering towards increased drought resilience.

This explorative PhD has, for the first time, tackled a systems biology approach to the unravelling of senescence in a resurrection plant and has highlighted the critical role of RNA processing and regulation, maintenance of translational machinery, and the benefits of a lipid-dominated strategy during drying in *E. nindensis*.

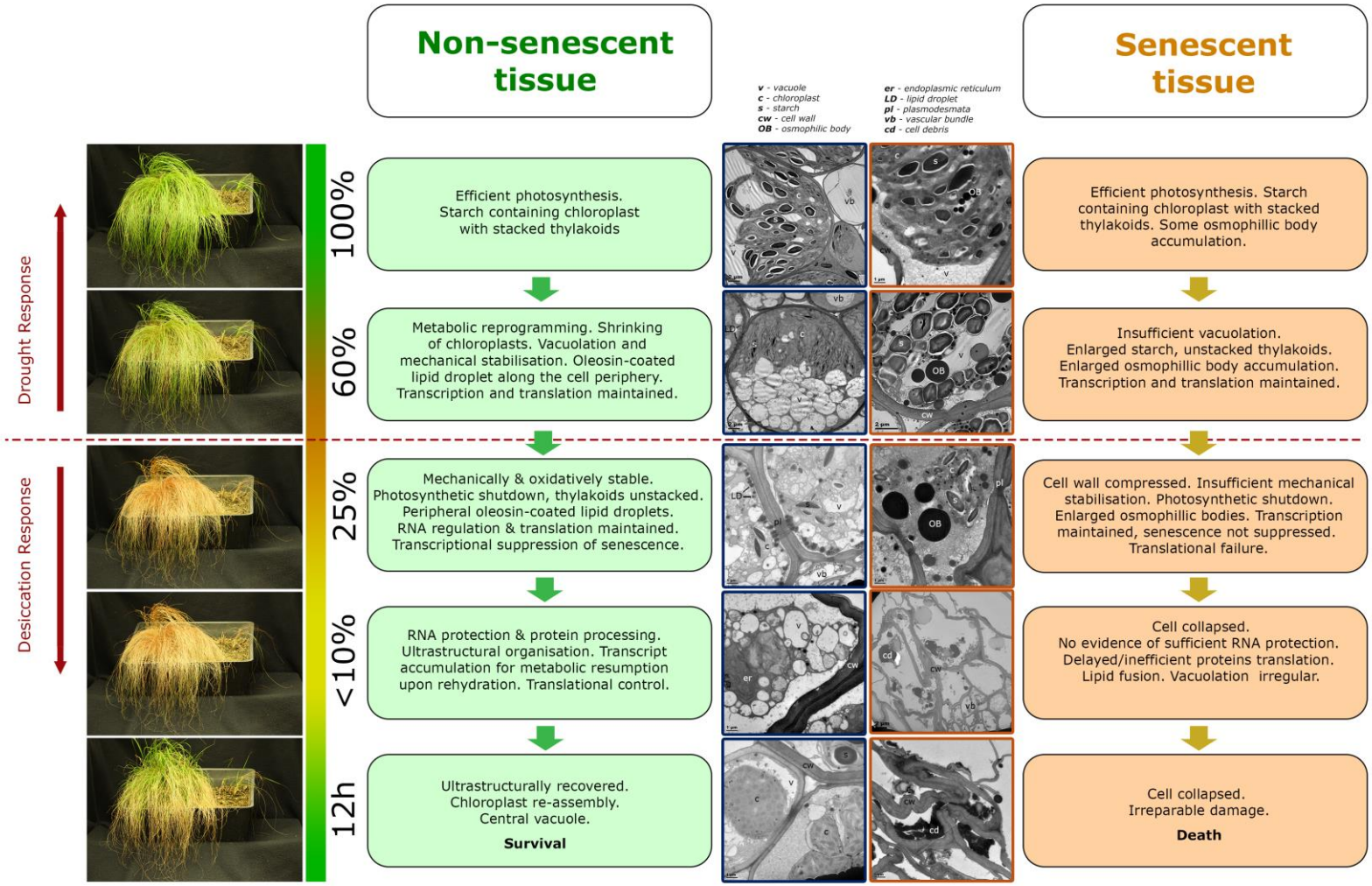

Figure 6.1: Summary flow diagram of key components of non-senescent and senescent tissue of the resurrection plant *Eragrostis nindensis* during water-deficit stress (%, relative water content (RWC)) and rehydration (12h). Boxes describe major physiological and molecular changes during drying and rehydration in both tissue types. These are correlated with whole-plant images (left) and transmission electron images (centre) to indicate physiological changes that occur at the described RWCs. Changes above 60% RWC represent a general response to drought (red arrow), whereas only desiccation tolerant tissue survives below 25% RWC, as indicated by the desiccation response (red arrow).

6.2. LIMITATIONS OF THE CURRENT STUDY

Sample variation was a limitation in that the seed samples were collected in the wild with natural genetic variation and were not genetically outbred, such as in Arabidopsis. The biological variation was sometimes large, as seen by gas exchange measurements and changes in global lipids, making it difficult to attain statistical significance. However, the goal of depicting broad trends was achieved, although larger biological replicate sample sizes and better quantitative techniques could be used to reduce sample variation.

Having better phenotyping tools for whole-plant, rather than individual leaves, would have been beneficial, due to leaf curling during drying in *E. nindensis* as it was difficult to measure gas exchange effectively below 40% RWC.

As the genome of *E. nindensis* had not been sequenced at the time that the *de novo* assembly was constructed, due to financial limitations, only one of the three biological replicates was paired-end sequenced. This introduced variation into the data, however, the PCA confirmed that RWC was the strongest determinant of sample variation and showed that the data was robust.

6.3. FUTURE WORK

The constructed transcriptome from this study is a valuable output and offers a platform for future work on senescence and desiccation tolerance in grasses (Poaceae). The research potential from the transcriptome is far-reaching, and DEGs identified here have to date provided a baseline for PhD research on the cross-talk of drought and salinity stress, and transcript data on the potential fungal endophytes in this species is being utilised in a PhD thesis aimed at identifying these fungi and their metabolites at the University of Cape Town. It has informed regulation of mitochondrial and chloroplast signalling during desiccation (in collaboration with Prof. Jürgen Soll at Ludwig Maximilian University of Munich) and informed the genome construction in Pardo *et al.* (2019). Furthermore, significant, but lowly expressed (i.e. <2 or >-2 $\log_2$ fold change) transcripts can be explored to gain insights into subtle signalling and regulation (e.g. apoptosis). An investigation into transcription factors that regulate stress response and their promotor regions would be worthwhile. It would also be worthwhile to get an energy cost estimate of making and storing transcripts and compare this to the cost of translation, to confirm the hypothesis that the opportunity cost of transcription is outweighed by fine-tuning transcription in the ST. A key follow-up research area is the translatome (see Bai *et al.* 2018), to investigate which RNA is being selected for storage and protection, how processing-bodies

form, and what transcripts are required for their synthesis, storage and degradation. Furthermore, an investigation into the cytoskeletal changes during drying between tissue types would be highly informative to disentangle whether the lipid droplets are unable to migrate to the periphery of the cell due to the failed roles of tubulin or actin, or whether oleosins are the signal for plasmalemma migration. No study has investigated changes in the cytoskeleton of a resurrection plant, and this would be of great import, especially in the context of senescence.

Given the importance of oleosin protein expression in *E. nindensis* upon water-deficit stress, a comprehensive proteomic analysis between the tissue types would discern the roles of proteins and thus divulge how they convey desiccation tolerance. This study explored the role of one protein (oleosin) and the associated consequences of failed expression in the ST. Extending this to a comprehensive proteome would significantly contribute to identifying which proteins are expressed and protected under stress and inform functional significance of said proteins in desiccation tolerance and senescence. In addition, fluxome studies using tracers could tag nitrogen and other molecules and identify whether nutrients are being reshuffled from the ST to the NST or stored in roots. Similarly, the origin of TAG species and whether they are derived from degraded chloroplast membranes can be determined through carbon-13 labelling and should be pursued. A comprehensive analysis on the full non-targeted and targeted lipidomic profile, including the degree of unsaturation and highly abundant lipids indicating biomarkers for desiccation tolerance, should be further investigated. *E. nindensis* is a good model plant for biofuel crop engineering, as it naturally increases large amounts of TAG during drying. This has application potential, as increasing vegetative TAG content is a desired agronomic trait for the biofuel industry or increasing nutrition in crops or fodder. The long-term goal is for this data to contribute to the development of increased drought resistance in crops, particularly the phylogenetically related orphan crop *E. tef*.

REFERENCES

Aid, F. (2019). Plant lipid metabolism. In Lipid metabolism (pp. 1–16). https://doi.org/DOI: http://dx.doi.org/10.5772/intechopen.81355

Alamillo, J. M., & Bartels, D. (2001). Effects of desiccation on photosynthesis pigments and the ELIP-like dsp 22 protein complexes in the resurrection plant *Craterostigma plantagineum*. Plant Science, 160(6), 1161–1170. https://doi.org/10.1016/S0168-9452(01)00356-9

Alexandratos, N., & Bruinsmam, J. (2012). World agriculture towards 2030/2050: the 2012 revision. ESA Workin(No. 12-03 Rome, FAO).

Allu, A. D., Soja, A. M., Wu, A. H., Szymanski, J., & Balazadeh, S. (2014). Salt stress and senescence: identification of cross-talk regulatory components. Journal of Experimental Botany, 65(14), 3993–4008. https://doi.org/10.1093/jxb/eru173

Alonso, A., Marsal, S., & Julià, A. (2015). Analytical methods in untargeted metabolomics: State of the art in 2015. Frontiers in Bioengineering and Biotechnology, 3(23), 1–20. https://doi.org/10.3389/fbioe.2015.00023

Andersson, M. X., Kjellberg, J. M., & Sandelius, A. S. (2004). The involvement of cytosolic lipases in converting phosphatidyl choline to substrate for galactolipid synthesis in the chloroplast envelope. Biochimica et Biophysica Acta - Molecular and Cell Biology of Lipids, 1684(1–3), 46–53. https://doi.org/10.1016/j.bbalip.2004.06.003

Anderson, P., & Kedersha, N. (2009). RNA granules: Post-transcriptional and epigenetic modulators of gene expression. Nature Reviews Molecular Cell Biology, 10(6), 430–436. https://doi.org/10.1038/nrm2694

Angeles-Núñez, J. G., & Tiessen, A. (2010). Arabidopsis sucrose synthase 2 and 3 modulate metabolic homeostasis and direct carbon towards starch synthesis in developing seeds. Planta, 232(3), 701–718. https://doi.org/10.1007/s00425-010-1207-9

Arce, D. P., Godoy, A. V., Tsuda, K., Yamazaki, K., Valle, E. M., Iglesias, M. J., … Casalongué, C. A. (2010). The analysis of an Arabidopsis triple knock-down mutant reveals functions for MBF1 genes under oxidative stress conditions. Journal of Plant Physiology, 167(3), 194–200. https://doi.org/10.1016/j.jplph.2009.09.003

Artur, M. A. S., Zhao, T., Ligterink, W., Schranz, M. E., & Hilhorst, H. W. M. (2018). Dissecting the genomic diversification of LATE EMBRYOGENESIS ABUNDANT (LEA) protein gene families in plants. Genome Biology and Evolution, 11(2), 459–471. https://doi.org/10.1093/gbe/evy248

Artur, M. A. S., Costa, M. C. D., Farrant, J. M., & Hilhorst, H. W. M. (2019). Genome-level responses to the environment: plant desiccation tolerance. Emerging Topics in Life Sciences, 3, 1–11. https://doi.org/10.1042/ETLS20180139

Asami, P., Mundree, S., & Williams, B. (2018). Saving for a rainy day: Control of energy needs in resurrection plants. Plant Science, 271(February), 62–66. https://doi.org/10.1016/j.plantsci.2018.03.009

Asami, P., Rupasinghe, T., Moghaddam, L., Njaci, I., Roessner, U., Mundree, S., & Williams, B. (2019). Roots of the resurrection plant *Tripogon loliiformis* survive desiccation without the activation of autophagy pathways by maintaining energy reserves. Frontiers in Plant Science, 10(April). https://doi.org/10.3389/fpls.2019.00459

Avila-Ospina, L., Moison, M., Yoshimoto, K., & Masclaux-Daubresse, C. (2014). Autophagy, plant senescence, and nutrient recycling. Journal of Experimental Botany, 65(14), 3799–3811. https://doi.org/10.1093/jxb/eru039

Bai, B., Peviani, A., van der Horst, S., Gamm, M., Snel, B., Bentsink, L., & Hanson, J. (2017). Extensive translational regulation during seed germination revealed by polysomal profiling. New Phytologist, 214(1), 233–244. https://doi.org/10.1111/nph.14355

Bai, B., Novák, O., Ljung, K., Hanson, J., & Bentsink, L. (2018). Combined transcriptome and translatome analyses reveal a role for tryptophan-dependent auxin biosynthesis in the control of DOG1-dependent seed dormancy. New Phytologist, 217(3), 1077–1085. https://doi.org/10.1111/nph.14885

Bajic, J. (2006). Exploring the longevity of dry *Craterostigma wilmsii* (homoiochlorophyllous) and *Xerophyta humilis* (poikilochlorophyllous) under simulated field conditions. https://doi.org/10.3390/su8020190

Balazadeh, S., Riaño-Pachón, D. M., & Mueller-Roeber, B. (2008). Transcription factors regulating leaf senescence in *Arabidopsis thaliana*. Plant Biology, 10(1), 63–75. https://doi.org/10.1111/j.1438-8677.2008.00088.x

Balazadeh, S. Siddiqui, H. Allu, A. Matallana-Ramirez, L. Caldana, C. Mehrnia, M. Zanor, M. Köhler, B. Mueller-Roeber, B. (2010). A gene regulatory network controlled by the NAC transcription

factor ANAC092/AtNAC2/ORE1 during salt-promoted senescence. Plant Journal, 62(2), 250–264. https://doi.org/10.1111/j.1365-313X.2010.04151.x

Baroja-Fernandez, E., Munoz, F. J., Li, J., Bahaji, A., Almagro, G., Montero, M., … Pozueta-Romero, J. (2012). Sucrose synthase activity in the sus1/sus2/sus3/sus4 Arabidopsis mutant is sufficient to support normal cellulose and starch production. Proceedings of the National Academy of Sciences, 109(1), 321–326. https://doi.org/10.1073/pnas.1117099109

Barratt, D. H. P., Derbyshire, P., Findlay, K., Pike, M., Wellner, N., Lunn, J., … Smith, A. M. (2009). Normal growth of Arabidopsis requires cytosolic invertase but not sucrose synthase. Proceedings of the National Academy of Sciences, 106(31), 13124–13129. https://doi.org/10.1073/pnas.0900689106

Barrs, H., & Weatherley, P. (1962). A re-examination of the relative turgidity technique for estimating water deficits in leaves. Australian Journal of BioLogical Sciences, 15, 413–428. https://doi.org/10.1071/bi9620413

Bartels, D., Schneider, K., Terstappen, G., Piatkowski, D., & Salamini, F. (1990). Molecular cloning of abscisic acid-modulated genes which are induced during desiccation of the resurrection plant *Craterostigma plantagineum*. Planta, 181(1), 27–34. https://doi.org/10.1007/bf00202321

Bartels, D., & Salamini, F. (2001). Desiccation tolerance in the resurrection plant *Craterostigma plantagineum*. A contribution to the study of drought tolerance at the molecular level. Scientific Correspondance, 127(December), 1346–1353. https://doi.org/10.1104/pp.010765.stress

Bartels, D., & Sunkar, R. (2005). Drought and salt tolerance in plants. Critical Reviews in Plant Sciences, 24(1), 23–58. https://doi.org/10.1080/07352680590910410

Barth, O., Vogt, S., Uhlemann, R., Zschiesche, W., & Humbeck, K. (2009). Stress induced and nuclear localized HIPP26 from *Arabidopsis thaliana* interacts via its heavy metal associated domain with the drought stress related zinc finger transcription factor ATHB29. Plant Molecular Biology, 69(1–2), 213–226. https://doi.org/10.1007/s11103-008-9419-0

Baskin, C., & Baskin, J. (2014). Seeds: ecology, biogeography, and evolution of dormancy and germination. San Diego: Academic Press.

Batailler, B., Lemaître, T., Vilaine, F., Sanchez, C., Renard, D., Cayla, T., … Dinant, S. (2012). Soluble and filamentous proteins in Arabidopsis sieve elements. Plant, Cell and Environment, 35(7), 1258–1273. https://doi.org/10.1111/j.1365-3040.2012.02487.x

Baud, S., Vaultier, M. N., & Rochat, C. (2004). Structure and expression profile of the sucrose synthase multigene family in Arabidopsis. Journal of Experimental Botany, 55(396), 397–409. https://doi.org/10.1093/jxb/erh047

Baud, S., & Lepiniec, L. (2010). Physiological and developmental regulation of seed oil production. Progress in Lipid Research, 49(3), 235–249. https://doi.org/10.1016/j.plipres.2010.01.001

Bechtold, U., & Field, B. (2018). Molecular mechanisms controlling plant growth during abiotic stress. Journal of Experimental Botany, 69(11), 2753–2758. https://doi.org/10.1093/jxb/ery157

Beck, E. H., Fettig, S. F., Knake, C. K., Hartig, K. H., & Bhattarai, T. (2007). Specific and unspecific responses of plants to cold and drought stress. Journal of Biosciences, 32(3), 501–510.

Beckett, M., Loreto, F., Velikova, V., Brunetti, C., Di Ferdinando, M., Tattini, M., … Farrant, J. M. (2012). Photosynthetic limitations and volatile and non-volatile isoprenoids in the poikilochlorophyllous resurrection plant *Xerophyta humilis* during dehydration and rehydration. Plant, Cell and Environment, 35(12), 2061–2074. https://doi.org/10.1111/j.1365-3040.2012.02536.x

Benjamini, Y., & Hochberg, Y. (1995). Controlling the False Discovery Rate: a practical and powerful approach to multiple testing. Journal of the Royal Statistical Society, 57(1), 289–300.

Benning, C. (2009). Mechanisms of lipid transport involved in organelle biogenesis in plant cells. Annual Review of Cell and Developmental Biology, 25(1), 71–91. https://doi.org/10.1146/annurev.cellbio.042308.113414

Berjak, P., & Pammenter, N. W. (2013). Implications of the lack of desiccation tolerance in recalcitrant seeds. Frontiers in Plant Science, 4(478), 1–9. https://doi.org/10.3389/fpls.2013.00478

Bianchi, G., Gamba, A., Murelli, C., Salamini, F., & Bartels, D. (1991). Novel carbohydrate metabolism in the resurrection plant *Craterostigma plantagineum*. The Plant Journal, 1(3), 355–359.

Bieniawska, Z., Paul Barratt, D. H., Garlick, A. P., Thole, V., Kruger, N. J., Martin, C., … Smith, A. M. (2007). Analysis of the sucrose synthase gene family in Arabidopsis. Plant Journal, 49(5), 810–828. https://doi.org/10.1111/j.1365-313X.2006.03011.x

Biju, S., Fuentes, S., & Gupta, D. (2017). Silicon improves seed germination and alleviates drought stress in lentil crops by regulating osmolytes, hydrolytic enzymes and antioxidant defense system. Plant Physiology and Biochemistry, 119, 250–264. https://doi.org/10.1016/j.plaphy.2017.09.001

Blomstedt, C. K., Griffiths, C. A., Fredericks, D. P., Hamill, J. D., Gaff, D. F., & Neale, A. D. (2010). The resurrection plant *Sporobolus stapfianus*: An unlikely model for engineering enhanced plant biomass? Plant Growth Regulation, 62(3), 217–232. https://doi.org/10.1007/s10725-010-9485-6

Blomstedt, C. K., Griffiths, C. A., Gaff, D. F., Hamill, J., & Neale, A. (2018). Plant desiccation tolerance and its regulation in the foliage of resurrection "flowering-plant" species. Agronomy, 8(8), 146. https://doi.org/10.3390/agronomy8080146

Blum, A., & Tuberosa, R. (2018). Dehydration survival of crop plants and its measurement. Journal of Experimental Botany, (January), 1–7. https://doi.org/10.1093/jxb/erx445

Bobik, K., & Burch-Smith, T. M. (2015). Chloroplast signaling within, between and beyond cells. Frontiers in Plant Science, 6(October), 1–26. https://doi.org/10.3389/fpls.2015.00781

Bohnert, H. J., Nelson, D. E., & Jensen, R. G. (1995). Adaptations to environmental stresses. The Plant Cell, 7(7), 1099–1111. https://doi.org/10.1105/tpc.7.7.1099

Bolger, A. M., Lohse, M., & Usadel, B. (2014). Trimmomatic: A flexible trimmer for Illumina sequence data. Bioinformatics, 30(15), 2114–2120. https://doi.org/10.1093/bioinformatics/btu170

Bondino, H. G., Valle, E. M., & ten Have, A. (2012). Evolution and functional diversification of the small heat shock protein/α-crystallin family in higher plants. Planta, 235(6), 1299–1313. https://doi.org/10.1007/s00425-011-1575-9

Botella, C., Jouhet, J., & Block, M. A. (2017). Importance of phosphatidylcholine on the chloroplast surface. Progress in Lipid Research, 65, 12–23. https://doi.org/10.1016/j.plipres.2016.11.001

Boyle, N. R., Page, M. D., Liu, B., Blaby, I. K., Casero, D., Kropat, J., … Merchant, S. S. (2012). Three acyltransferases and nitrogen-responsive regulator are implicated in nitrogen starvation-induced triacylglycerol accumulation in *Chlamydomonas*. Journal of Biological Chemistry, 287(19), 15811–15825. https://doi.org/10.1074/jbc.M111.334052

Breeze, E., Harrison, E., McHattie, S., Hughes, L., Hickman, R., Hill, C., … Buchanan-Wollaston, V. (2011). High-resolution temporal profiling of transcripts during Arabidopsis leaf senescence reveals a distinct chronology of processes and regulation. The Plant Cell, 23(3), 873–894. https://doi.org/10.1105/tpc.111.083345

Bremer, K., & Moyes, C. D. (2014). mRNA degradation: an underestimated factor in steady-state transcript levels of cytochrome c oxidase subunits? Journal of Experimental Biology, 217(12), 2212–2220. https://doi.org/10.1242/jeb.100214

Bresson, J., Bieker, S., Riester, L., Doll, J., & Zentgraf, U. (2018). A guideline for leaf senescence analyses: From quantification to physiological and molecular investigations. Journal of Experimental Botany, 69(4), 769–786. https://doi.org/10.1093/jxb/erx246

Brocard, L., Immel, F., Coulon, D., Esnay, N., Tuphile, K., Pascal, S., … Bréhélin, C. (2017). Proteomic analysis of lipid droplets from Arabidopsis aging leaves brings new insight into their biogenesis and functions. Frontiers in Plant Science, 8(May). https://doi.org/10.3389/fpls.2017.00894

Brown, T. B., Cheng, R., Sirault, X. R., Rungrat, T., Murray, K. D., Trtilek, M., … Borevitz, J. O. (2014). TraitCapture: genomic and environment modelling of plant phenomic data. Curr Opin Plant Biol, 18, 73–79. https://doi.org/10.1016/j.pbi.2014.02.002

Bryant, D. M., Johnson, K., DiTommaso, T., Tickle, T., Couger, M. B., Payzin-Dogru, D., … Whited, J. L. (2017). A tissue-mapped axolotl *De novo* transcriptome enables identification of limb regeneration factors. Cell Reports, 18(3), 762–776. https://doi.org/10.1016/j.celrep.2016.12.063

Buchanan-Wollaston, V., Page, T., Harrison, E., Breeze, E., Pyung, O. L., Hong, G. N., … Leaver, C. J. (2005). Comparative transcriptome analysis reveals significant differences in gene expression and signalling pathways between developmental and dark/starvation-induced senescence in Arabidopsis. Plant Journal, 42(4), 567–585. https://doi.org/10.1111/j.1365-313X.2005.02399.x

Buchanan, B. B., Gruissem, W., & Jones, R. L. (2015). Biochemistry and molecular biology of plants. British Journal of Psychiatry (second, Vol. 112). https://doi.org/10.1192/bjp.112.483.211-a

Buitink, J., & Leprince, O. (2004). Glass formation in plant anhydrobiotes: Survival in the dry state. Cryobiology, 48, 215–228. https://doi.org/10.1016/j.cryobiol.2018.07.002

Buitink, J., Leger, J. J., Guisle, I., Vu, B. L., Wuilleme, S., Lamirault, G., … Leprince, O. (2006). Transcriptome profiling uncovers metabolic and regulatory processes occurring during the transition from desiccation-sensitive to desiccation-tolerant stages in *Medicago truncatula* seeds. Plant Journal, 47(5), 735–750. https://doi.org/10.1111/j.1365-313X.2006.02822.x

Butow, R. A., & Avadhani, N. G. (2004). Review Mitochondrial Signaling: The Retrograde Response grade signaling pathways, focusing largely on yeast and animal cells. Molecular Cell, 14, 1–15.

Cannarozzi, G., Plaza-Wuthrich, S., Esfeld, K., Larti, S., Wilson, Y. S., Girma, D., … Tadele, Z. (2014). Genome and transcriptome sequencing identifies breeding targets in the orphan crop tef (Eragrostis tef). BMC Genomics, 15, 581. https://doi.org/10.1186/1471-2164-15-581

Capell, T., Campos, J. L., & Tiburcio, A. F. (1993). Antisenescence properties of guazatine in osmotically stressed oat leaves. Phytochemistry, 32(4), 785–788. https://doi.org/10.1016/0031-9422(93)85205-6

Challabathula, D., Puthur, J. T., & Bartels, D. (2016). Surviving metabolic arrest: Photosynthesis during desiccation and rehydration in resurrection plants. Annals of the New York Academy of Sciences, 1365(1), 89–99. https://doi.org/10.1111/nyas.12884

Chantarachot, T., & Bailey-Serres, J. (2018). Polysomes, Stress Granules, and Processing Bodies: A Dynamic Triumvirate Controlling Cytoplasmic mRNA Fate and Function. Plant Physiology, 176(1), 254–269. https://doi.org/10.1104/pp.17.01468

Chapman, K. D., & Ohlrogge, J. B. (2012a). Compartmentation of triacylglycerol accumulation in plants. Journal of Biological Chemistry, 287(4), 2288–2294. https://doi.org/10.1074/jbc.R111.290072

Chapman, K. D., Dyer, J. M., & Mullen, R. T. (2012b). Biogenesis and functions of lipid droplets in plants. Journal of Lipid Research, 53(2), 215–226. https://doi.org/10.1194/jlr.R021436

Chapman, K. D., Dyer, J. M., & Mullen, R. T. (2013). Commentary: Why don't plant leaves get fat? Plant Science, 207(June 2013), 128–134. https://doi.org/10.1016/j.plantsci.2013.03.003

Charuvi, D., Nevo, R., Shimoni, E., Naveh, L., Zia, A., Adam, Z., … Reich, Z. (2015). Photoprotection conferred by changes in photosynthetic protein levels and organization during dehydration of a homoiochlorophyllous resurrection plant. Plant Physiology, 167(4), 1554–1565. https://doi.org/10.1104/pp.114.255794

Charuvi, D., Nevo, R., Aviv-Sharon, E., Gal, A., Kiss, V., Shimoni, E., … Reich, Z. (2019). Chloroplast breakdown during dehydration of a homoiochlorophyllous resurrection plant proceeds via senescence-like processes. Environmental and Experimental Botany, 157, 100–111. https://doi.org/10.1016/j.envexpbot.2018.09.027

Chen, L.-Q., Hou, B. H., Lalonde, S., Takanaga, H., Hartung, M. L., Qu, X.-Q., … Frommer, W. B. (2010). Sugar transporters for intercellular exchange and nutrition of pathogens. Nature, 468(7323), 527–532. https://doi.org/10.1038/nature09606.Sugar

Chen, L. Q., Qu, X. Q., Hou, B. H., Sosso, D., Osorio, S., Fernie, A. R., & Frommer, W. B. (2012). Sucrose efflux mediated by SWEET proteins as a key step for phloem transport. Science, 335(6065), 207–211. https://doi.org/10.1126/science.1213351

Chen, L.-Q., Lin, I. W., Qu, X.-Q., Sosso, D., McFarlane, H. E., Londoño, A., … Frommer, W. B. (2015). A Cascade of Sequentially Expressed Sucrose Transporters in the Seed Coat and Endosperm

Provides Nutrition for the Arabidopsis Embryo. The Plant Cell, 27(3), 607–619. https://doi.org/10.1105/tpc.114.134585

Chen, Y., Lun, A. T. L., & Smyth, G. K. (2016). From reads to genes to pathways: differential expression analysis of RNA-Seq experiments using Rsubread and the edgeR quasi-likelihood pipeline. F1000Research, 5(May), 1438. https://doi.org/10.12688/f1000research.8987.2

Chen, D., Wang, S., Qi, L., Yin, L., & Deng, X. (2018). Galactolipid remodeling is involved in drought-induced leaf senescence in maize. Environmental and Experimental Botany, 150(November 2017), 57–68. https://doi.org/10.1016/j.envexpbot.2018.02.017

Christ, B., Egert, A., Süssenbacher, I., Kräutler, B., Bartels, D., Peters, S., & Hörtensteiner, S. (2014). Water deficit induces chlorophyll degradation via the "PAO/phyllobilin" pathway in leaves of homoio- (*Craterostigma pumilum*) and poikilochlorophyllous (*Xerophyta viscosa*) resurrection plants. Plant, Cell and Environment, 37(11), 2521–2531. https://doi.org/10.1111/pce.12308

Collett, H., Butowt, R., Smith, J., Farrant, J. M., & Illing, N. (2003). Photosynthetic genes are differentially transcribed during the dehydration-rehydration cycle in the resurrection plant, *Xerophyta humilis*. Journal of Experimental Botany, 54(392), 2593–2595. https://doi.org/10.1093/jxb/erg285

Collett, H., Shen, A., Gardner, M., Farrant, J. M., Denby, K. J., & Illing, N. (2004). Towards transcript profiling of desiccation tolerance in *Xerophyta humilis*: Construction of a normalized 11 k X. humilis cDNA set and microarray expression analysis of 424 cDNAs in response to dehydration. *Physiologia Plantarum*, *122*(1), 39–53. https://doi.org/10.1111/j.1399-3054.2004.00381.x

Cominelli, E., Conti, L., Tonelli, C., & Galbiati, M. (2013). Challenges and perspectives to improve crop drought and salinity tolerance. New Biotechnology, 30(4), 355–361. https://doi.org/https://doi.org/10.1016/j.nbt.2012.11.001

Conesa, A., & Götz, S. (2008). Blast2GO: A comprehensive suite for functional analysis in plant genomics. International Journal of Plant Genomics, 2008. https://doi.org/10.1155/2008/619832

Conesa, A., Madrigal, P., Tarazona, S., Gomez-Cabrero, D., Cervera, A., McPherson, A., … Mortazavi, A. (2016). A survey of best practices for RNA-seq data analysis. Genome Biology, 17(1), 1–19. https://doi.org/10.1186/s13059-016-0881-8

Consentino, L., Lambert, S., Martino, C., Jourdan, N., Bouchet, P. E., Witczak, J., … Ahmad, M. (2015). Blue-light dependent reactive oxygen species formation by Arabidopsis cryptochrome may

define a novel evolutionarily conserved signaling mechanism. New Phytologist, 206(4), 1450–1462. https://doi.org/10.1111/nph.13341

Cooper, K., & Farrant, J. M. (2002). Recovery of the resurrection plant *Craterostigma wilmsii* from desiccation: protection versus repair. Journal of Experimental Botany, 53(375), 1805–1813. https://doi.org/10.1093/jxb/erf028

Corvalan, C., Hales, S., & McMichael, A. (2005). Ecosystems and human well-being: health synthesis: a report of the Millennium Ecosystem Assessment. In World Health Organisation (Vol. 5). https://doi.org/10.1196/annals.1439.003

Costa, M. C. D., Artur, M. A. S., Maia, J., Jonkheer, E., Derks, M. F. L. L., Nijveen, H., … Hilhorst, H. W. (2017a). A footprint of desiccation tolerance in the genome of *Xerophyta viscosa*. Nature Plants, 3(4), 17038. https://doi.org/10.1038/nplants.2017.38

Costa, M. C. D., Cooper, K., Hilhorst, H. W. M., & Farrant, J. M. (2017b). Orthodox seeds and resurrection plants: two of a kind? Plant Physiology, (96033), pp.00760.2017. https://doi.org/10.1104/pp.17.00760

Costa, M. C. D., Farrant, J. M., Oliver, M. J., Ligterink, W., Buitink, J., & Hilhorst, H. M. W. (2016). Key genes involved in desiccation tolerance and dormancy across life forms. Plant Science, 251, 162–168. https://doi.org/10.1016/j.plantsci.2016.02.001

Covarrubias, A. A., Cuevas-Velazquez, C. L., Romero-Pérez, P. S., Rendón-Luna, D. F., & Chater, C. (2017). Structural disorder in plant proteins: where plasticity meets sessility. Cellular and Molecular Life Sciences, 74(17), 3119–3147. https://doi.org/10.1007/s00018-017-2557-2

Dace, H., Sherwin, H. W., Illing, N., & Farrant, J. M. (1998). Use of metabolic inhibitors to elucidate mechanisms of recovery from desiccation stress in the resurrection plant *Xerophyta humilis*. Plant Growth Regulation, 24(3), 171–177. https://doi.org/10.1023/A:1005883907800

Dace, H. (unpublished). Metabolic aspects of vegetative desiccation tolerance. Unpublished doctoral dissertation. University of Wageningen, Wageningen, Netherlands. Intended hand-in date: 2021.

Danielson, J. Å. H., & Johanson, U. (2008). Unexpected complexity of the Aquaporin gene family in the moss *Physcomitrella patens*. BMC Plant Biology, 8, 1–15. https://doi.org/10.1186/1471-2229-8-45

De Abreu-Neto, J. B., Turchetto-Zolet, A. C., De Oliveira, L. F. V., Bodanese Zanettini, M. H., & Margis-Pinheiro, M. (2013). Heavy metal-associated isoprenylated plant protein (HIPP):

Characterization of a family of proteins exclusive to plants. FEBS Journal, 280(7), 1604–1616. https://doi.org/10.1111/febs.12159

Delhomme, N., Mähler, N., Schiffthaler, B., & Sundell, D. (2014). Guidelines for RNA-Seq data analysis. Epigenesys Protocol, 1–24.

Dempewolf, H., Baute, G., Anderson, J., Kilian, B., Smith, C., & Guarino, L. (2017). Past and future use of wild relatives in crop breeding. Crop Science, 57(3), 1070–1082. https://doi.org/10.2135/cropsci2016.10.0885

Deruyffelaere, C., Bouchez, I., Morin, H., Guillot, A., Miquel, M., Froissard, M., … Andrea, S. D. (2015). Ubiquitin-mediated proteasomal degradation of oleosins is involved in oil body mobilization during post-germinative seedling growth in Arabidopsis. Plant and Cell Physiology, 56(April), 1374–1387. https://doi.org/10.1093/pcp/pcv056

Dessimoz, C., & Škunca, N. (2017). The Gene Ontology Handbook. Methods in Molecular Biology (1446th ed., Vol. 1446; D. C. & Š. N., Eds.). https://doi.org/10.1007/978-1-4939-3743-1

Dietz, K. J., Mittler, R., & Noctor, G. (2016). Recent progress in understanding the role of reactive oxygen species in plant cell signaling. Plant Physiology, 171(3), 1535–1539. https://doi.org/10.1104/pp.16.00938

Dinakar, C., Djilianov, D., & Bartels, D. (2012). Photosynthesis in desiccation tolerant plants: Energy metabolism and antioxidative stress defense. Plant Science, 182(1), 29–41. https://doi.org/10.1016/j.plantsci.2011.01.018

Dinakar, C., & Bartels, D. (2013). Desiccation tolerance in resurrection plants: new insights from transcriptome, proteome and metabolome analysis. Frontiers in Plant Science, 4(November), 482. https://doi.org/10.3389/fpls.2013.00482

Dinakar, C., Zhang, Q., Bartels, D., Challabathula, D., Zhang, Q., & Bartels, D. (2018). Protection of photosynthesis in desiccation-tolerant resurrection plants. Journal of Plant Physiology, 227(November 2017), 84–92. https://doi.org/10.1016/j.jplph.2018.05.002

Dłużewska, J., Szymańska, R., Gabruk, M., Kós, P. B., Nowicka, B., & Kruk, J. (2016). Tocopherol cyclases-substrate specificity and phylogenetic relations. PloS One, 11(7), e0159629. https://doi.org/10.1371/journal.pone.0159629

Dobrenel, T., Marchive, C., Azzopardi, M., Clément, G., Moreau, M., Sormani, R., … Meyer, C. (2013). Sugar metabolism and the plant target of rapamycin kinase: a sweet operaTOR? Frontiers in Plant Science, 4(April), 1–6. https://doi.org/10.3389/fpls.2013.00093

Durand, M., Porcheron, B., Hennion, N., Maurousset, L., Lemoine, R., & Pourtau, N. (2016). Water deficit enhances C export to the roots in *A. thaliana* plants with contribution of sucrose transporters in both shoot and roots. Plant Physiology, 170(March), pp.01926.2015. https://doi.org/10.1104/pp.15.01926

Durgud, M., Gupta, S., Ivanov, I., Omidbakhshfard, A., Benina, M., Alseekh, S., … Gechev, T. (2018). Molecular mechanisms preventing senescence in response to prolonged darkness in a desiccation-tolerant plant. Plant Physiology, 177(July), pp.00055.2018. https://doi.org/10.1104/pp.18.00055

Durrett, T. P., Benning, C., & Ohlrogge, J. (2008). Plant triacylglycerols as feedstocks for the production of biofuels. Plant Journal, 54(4), 593–607. https://doi.org/10.1111/j.1365-313X.2008.03442.x

Dussert, S., Serret, J., Bastos-Siqueira, A., Morcillo, F., Déchamp, E., Rofidal, V., … Joët, T. (2018). Integrative analysis of the late maturation programme and desiccation tolerance mechanisms in intermediate coffee seeds. Journal of Experimental Botany, 69(7), 1583–1597. https://doi.org/10.1093/jxb/erx492

Dutt, S., Parkash, J., Mehra, R., Sharma, N., Singh, B., Raigond, P., … Singh, B. P. (2015). Translation initiation in plants: roles and implications beyond protein synthesis. Biologia Plantarum, 59(3), 401–412. https://doi.org/10.1007/s10535-015-0517-y

Eichmann, R., & Schäfer, P. (2012). The endoplasmic reticulum in plant immunity and cell death. Frontiers in Plant Science, 3(August), 1–6. https://doi.org/10.3389/fpls.2012.00200

Elsayed, A. I., Rafudeen, M. S., & Golldack, D. (2014). Physiological aspects of raffinose family oligosaccharides in plants: Protection against abiotic stress. Plant Biology, 16(1), 1–8. https://doi.org/10.1111/plb.12053

Endo, S., Iwai, Y., & Fukuda, H. (2018). Cargo-dependent and cell wall-associated xylem transport in Arabidopsis. New Phytologist, 222(1), 159–170. https://doi.org/10.1111/nph.15540

Eom, J. S., Chen, L. Q., Sosso, D., Julius, B. T., Lin, I. W., Qu, X. Q., … Frommer, W. B. (2015). SWEETs, transporters for intracellular and intercellular sugar translocation. Current Opinion in Plant Biology, 25, 53–62. https://doi.org/10.1016/j.pbi.2015.04.005

Erb, T. J., & Zarzycki, J. (2018). A short history of RubisCO: the rise and fall (?) of Nature's predominant CO2fixing enzyme. Current Opinion in Biotechnology, 49, 100–107. https://doi.org/10.1016/j.copbio.2017.07.017

Esteves, A. R., Oliveira, C. R., & Cardoso, S. M. (2013). Autophagy, the “master” regulator of cellular quality control: What happens when autophagy fails? In Autophagy - A Double-Edged Sword - Cell Survival or Death? (pp. 81–120). https://doi.org/http://dx.doi.org/10.5772/55196

Fahy, E., Cotter, D., Sud, M., & Subramaniam, S. (2011). Lipid classification, structures and tools. Biochimica et Biophysica Acta, 1811(11), 637–647. https://doi.org/10.1016/j.bbalip.2011.06.009

Fallahi, H., Scofield, G. N., Badger, M. R., Chow, W. S., Furbank, R. T., & Ruan, Y. L. (2008). Localization of sucrose synthase in developing seed and siliques of *Arabidopsis thaliana* reveals diverse roles for SUS during development. Journal of Experimental Botany, 59(12), 3283–3295. https://doi.org/10.1093/jxb/ern180

Fan, J., Andre, C., & Xu, C. (2011). A chloroplast pathway for the *de novo* biosynthesis of triacylglycerol in *Chlamydomonas reinhardtii*. FEBS Letters, 585(12), 1985–1991. https://doi.org/10.1016/j.febslet.2011.05.018

Fan, J., Yan, C., Andre, C., Shanklin, J., Schwender, J., & Xu, C. (2012). Oil accumulation is controlled by carbon precursor supply for fatty acid synthesis in *Chlamydomonas reinhardtii*. Plant and Cell Physiology, 53(8), 1380–1390. https://doi.org/10.1093/pcp/pcs082

Fan, G., Zhang, K., Huang, H., Zhang, H., Zhao, A., Chen, L., … Lu, G. dong. (2017). Multiprotein-bridging factor 1 regulates vegetative growth, osmotic stress, and virulence in *Magnaporthe oryzae*. Current Genetics, 63(2), 293–309. https://doi.org/10.1007/s00294-016-0636-9

Fang, Y., Zhu, R. L., & Mishler, B. D. (2014). Evolution of oleosin in land plants. PLoS ONE, 9(8), 1–10. https://doi.org/10.1371/journal.pone.0103806

FAO. (2011). The State of the World’s land and water resources for Food and Agriculture (SOLAW) - Managing systems at risk. In Food and Agriculture Organization of the United Nations, Rome and Earthscan. https://doi.org/978-1-84971-326-9

FAO. (2017). The future of food and agriculture. Trends and Challenges. Rome.

FAO, IFAD, UNICEF, W. and W. (2018). The state of food security and nutrition in the world 2018. Building climate resilience for food security and nutrition. In Building climate resilience for food security and nutrition. https://doi.org/10.1093/cjres/rst006

Farrant, Jill M., Cooper, K., Kruger, L. A., & Sherwin, H. W. (1999). The effect of drying rate on the survival of three desiccation-tolerant angiosperm species. Annals of Botany, 84(3), 371–379. https://doi.org/10.1006/anbo.1999.0927

Farrant, Jill M. (2000). A comparison of mechanisms of desiccation tolerance among three angiosperm resurrection plant species. Plant Ecology, 151(1), 29–39. https://doi.org/10.1023/A:1026534305831

Farrant, Jill M., Brandt, W., & Lindsey, G. G. (2007). An overview of mechanisms of desiccation tolerance in selected angiosperm resurrection plants. Plant Stress, 1(1), 72–84. https://doi.org/10.1002/9780470376881.ch3

Farrant, J.M., Cooper, K. and Nell, J.S. (2012). Desiccation tolerance. In S. Shabala (Eds.), *Plant Stress Physiology* (pp 238-265). CAB International, Wallingford, UK. ISBN 1845939956

Farrant, Jill M., Cooper, K., Hilgart, A., Abdalla, K. O., Bentley, J., Thomson, J. A., … Rafudeen, M. S. (2015). A molecular physiological review of vegetative desiccation tolerance in the resurrection plant *Xerophyta viscosa* (Baker). Planta, 242(2), 407–426. https://doi.org/10.1007/s00425-015-2320-6

Farrant, Jill M., Cooper, K., Dace, H. J. W., Bentley, J., & Hilgart, A. (2017). Desiccation Tolerance. In Plant stress physiology (pp. 238–265). https://doi.org/10.1079/9781845939953.0000

Fernandes-Júnior, P. I., Aidar, S. de T., Morgante, C. V., Gava, C. A. T., Zilli, J. É., de Souza, L. S. B., … Martins, L. M. V. (2015). The resurrection plant Tripogon spicatus (Poaceae) harbors a diversity of plant growth promoting bacteria in northeastern Brazilian Caatinga. Revista Brasileira de Ciencia Do Solo, 39(4), 993–1002. https://doi.org/10.1590/01000683rbcs20140646

Folch, J., Lees, M., & Stanley, G. H. S. (1956). A simple method for the isolation and purification of total lipides from animal tissues. Journal of Biochemistry, 226(1), 497–509. https://doi.org/10.1016/j.athoracsur.2011.06.016

Forterre, Y. (2013). Slow, fast and furious: understanding the physics of plant movements. Journal of Experimental Botany, 64(15), 4745–4760. https://doi.org/10.1093/jxb/ert230

Foyer, C. H., & Shigeoka, S. (2011). Understanding oxidative stress and antioxidant functions to enhance photosynthesis. plant physiology, 155(1), 93–100. https://doi.org/10.1104/pp.110.166181

Frandsen, G. I., Mundy, J., & Tzen, J. T. C. (2001). Oil bodies and their associated proteins, oleosin and caleosin. Physiologia Plantarum, 112(3), 301–307. https://doi.org/10.1034/j.1399-3054.2001.1120301.x

Froissard, M., D'Andréa, S., Boulard, C., & Chardot, T. (2009). Heterologous expression of AtClo1, a plant oil body protein, induces lipid accumulation in yeast. FEMS Yeast Research, 9(3), 428–438. https://doi.org/10.1111/j.1567-1364.2009.00483.x

Fu, L., Niu, B., Zhu, Z., Wu, S., & Li, W. (2012). CD-HIT: Accelerated for clustering the next-generation sequencing data. Bioinformatics, 28(23), 3150–3152. https://doi.org/10.1093/bioinformatics/bts565

Gaff, D. F. (1971). Desiccation-Tolerant Flowering Plants in Southern Africa. Science, 174(4013), 1033–1034.

Gaff, D. F., & Ellis, R. P. (1974). Southern African grasses with foliage that revives after dehydration. Bothalia, 3(11), 305–308.

Gaff, D. F., & Churchill, D. M. (1976). *Borya nitida* Labill.-An Australian species in the liliaceae with desiccation-tolerant leaves. Australian Journal of Botany, 24(2), 209–224. https://doi.org/10.1071/BT9760209

Gaff, D. F., & Giess, W. (1986). Drought resistance in water plants in rock pools of Southern Africa. Dinteria, 18(18), 17–37.

Gaff, D. F. (1986). Desiccation tolerant "resurrection" grasses from Kenya and West Africa. Oecologia, 70, 118–120.

Gaff, D. F., Bartels, D., & Gaff, J. L. (1997). Changes in gene expression during drying in a desiccation-tolerant grass *Sporobolus stapfianus* and a desiccation-sensitive grass *Sporobolus pyramidalis*. Functional Plant Biology, 24, 617–622.

Gaff, D. F., Blomstedt, C. K., Neale, A. D., Le, T. N., Hamill, J. D., & Ghasempour, H. R. (2009). *Sporobolus stapfianus*, a model desiccation-tolerant grass. Functional Plant Biology, 36(7), 589. https://doi.org/10.1071/FP08166

Gaff, D. F., & Oliver, M. J. (2013). The evolution of desiccation tolerance in angiosperm plants: A rare yet common phenomenon. Functional Plant Biology, 40(4), 315–328. https://doi.org/10.1071/FP12321

Gao, B., Li, X., Zhang, D., Liang, Y., Yang, H., Chen, M., … Wood, A. J. (2017). Desiccation tolerance in bryophytes: The dehydration and rehydration transcriptomes in the desiccation-tolerant bryophyte *Bryum argenteum*. Scientific Reports, 7(1), 7571. https://doi.org/10.1038/s41598-017-07297-3

Gao, W., Xu, F.-C., Guo, D.-D., Zhao, J.-R., Liu, J., Guo, Y.-W., … Song, C.-P. (2018). Calcium-dependent protein kinases in cotton: insights into early plant responses to salt stress. BMC Plant Biology, 18(1), 15. https://doi.org/10.1186/s12870-018-1230-8

Garber, M., Grabherr, M. G., Guttman, M., & Trapnell, C. (2011). Computational methods for transcriptome annotation and quantification using RNA-seq. Nature Methods, 8(6), 469–477. https://doi.org/10.1038/nmeth.1613

Gasulla, F., Dorp, K., Dombrink, I., Za, U., Gisch, N., Do, P., & Bartels, D. (2013). The role of lipid metabolism in the acquisition of desiccation tolerance in *Craterostigma plantagineum*: a comparative approach. The Plant Journal, 75, 726–741. https://doi.org/10.1111/tpj.12241

Gechev, T. S., Dinakar, C., Benina, M., Toneva, V., & Bartels, D. (2012). Molecular mechanisms of desiccation tolerance in resurrection plants. Cellular and Molecular Life Sciences, 69(19), 3175–3186. https://doi.org/10.1007/s00018-012-1088-0

Geigenberger, P., & Stitt, M. (1993). Sucrose synthase catalyses a readily reversible reaction in vivo in developing potato tubers and other plant tissues. Planta, 189(3), 329–339. https://doi.org/10.1007/BF00194429

Georgieva, Katya, Dagnon, S., Gesheva, E., Bojilov, D., Mihailova, G., & Doncheva, S. (2017a). Antioxidant defense during desiccation of the resurrection plant *Haberlea rhodopensis*. Plant Physiology and Biochemistry, 114, 51–59. https://doi.org/10.1016/j.plaphy.2017.02.021

Georgieva, K., Rapparini, F., Bertazza, G., Mihailova, G., Sárvári, Solti, & Keresztes. (2017b). Alterations in the sugar metabolism and in the vacuolar system of mesophyll cells contribute to the desiccation tolerance of *Haberlea rhodopensis* ecotypes. Protoplasma, 254(1), 193–201. https://doi.org/10.1007/s00709-015-0932-0

Ghasempour, H. R., Gaff, D. F., Williams, R. P. W., & Gianello, R. D. (1998). Contents of sugars in leaves of drying desiccation tolerant flowering plants, particularly grasses. Plant Growth Regulation, 24(3), 185–191. https://doi.org/10.1023/A:1005927629018

Giarola, V., Challabathula, D., & Bartels, D. (2015). Quantification of expression of dehydrin isoforms in the desiccation tolerant plant *Craterostigma plantagineum* using specifically designed reference genes. Plant Science, 236, 103–115. https://doi.org/10.1016/j.plantsci.2015.03.014

Giarola, V., Hou, Q., & Bartels, D. (2017). Angiosperm plant desiccation tolerance: Hints from transcriptomics and genome sequencing. Trends in Plant Science, 22(8), 705–717. https://doi.org/10.1016/j.tplants.2017.05.007

Giauque, H., Connor, E. W., & Hawkes, C. V. (2019). Endophyte traits relevant to stress tolerance, resource use and habitat of origin predict effects on host plants. New Phytologist, 221(4), 2239–2249. https://doi.org/10.1111/nph.15504

Ginbot, Z. G., & Farrant, J. M. (2011). Physiological response of selected eragrostis species to water-deficit stress. African Journal of Biotechnology, 10(51), 10405–10417. https://doi.org/10.5897/AJB11.1124

Godfray, H. C., Beddington, J. R., Crute, I. R., Haddad, L., Lawrence, D., Muir, J. F., … Toulmin, C. (2010). Food security: the challenge of feeding 9 billion people. Science, 327(5967), 812–818. https://doi.org/10.1126/science.1185383

Goyal, K., Walton, L. J., & Tunnacliffe, A. (2005). LEA proteins prevent protein aggregation due to water stress. The Biochemical Journal, 388(Pt 1), 151–157. https://doi.org/10.1042/BJ20041931

Grabherr, M. G., Haas, B. J., Yassour, M., Levin, J. Z., Thompson, D. A., Amit, I., … Regev, A. (2011). Full-length transcriptome assembly from RNA-Seq data without a reference genome. Nature Biotechnology, 29(7), 644–652. https://doi.org/10.1038/nbt.1883

Graham, I. A. (2008). Seed Storage Oil Mobilization. Annual Review of Plant Biology, 59(1), 115–142. https://doi.org/10.1146/annurev.arplant.59.032607.092938

Green, M. M., Blankenhorn, G., & Hart, H. (1975). Which starch fraction is water soluble, amylose or amylopectin? Journal of Chemical Education, 52(11), 729–730. https://doi.org/10.1021/ed052p729

Grennan, A. K. (2007). The role of trehalose biosynthesis in plants. Plant Physiology, 144(1), 3–5. https://doi.org/10.1104/pp.104.900223

Griffiths, C. A. (2015). Functional analysis of dehydration responsive genes in the resurrection grass *Sporobolus stapfianus*. Unpublished doctoral dissertation. Monash University, Melbourne, Australia.

Griffiths, C. A., Gaff, D. F., & Neale, A. D. (2014). Drying without senescence in resurrection plants. Frontiers in Plant Science, 5(February), 36. https://doi.org/10.3389/fpls.2014.00036

Guiboileau, A., Sormani, R., Meyer, C., & Masclaux-Daubresse, C. (2010). Senescence and death of plant organs: Nutrient recycling and developmental regulation. Comptes Rendus - Biologies, 333(4), 382–391. https://doi.org/10.1016/j.crvi.2010.01.016

Guo-chao, Y., Nikolic, M., YE, M. jun, XIAO, Z. xi, & LIANG, Y. chao. (2018). Silicon acquisition and accumulation in plant and its significance for agriculture. Journal of Integrative Agriculture, 17(10), 2138–2150. https://doi.org/10.1016/S2095-3119(18)62037-4

Guo, Yi, Cai, Z., & Gan, S. (2004). Transcriptome of Arabidopsis leaf senescence. Plant, Cell and Environment, 27(5), 521–549. https://doi.org/10.1111/j.1365-3040.2003.01158.x

Guo, X., Fan, C., Chen, Y., Wang, J., Yin, W., Wang, R. R. C., & Hu, Z. (2017). Identification and characterization of an efficient acyl-CoA: Diacylglycerol acyltransferase 1 (DGAT1) gene from the microalga Chlorella ellipsoidea. BMC Plant Biology, 17(1), 1–16. https://doi.org/10.1186/s12870-017-0995-5

Guo, Yongfeng. (2018). Plant senescence: Methods and protocols (Yongfeng Guo, Ed.). Qingdao, Shandong, China: Springer Nature.

Haas, B. J., Papanicolaou, A., Yassour, M., Grabherr, M., Philip, D., Bowden, J., … Pochet, N. (2013). *De novo* transcript sequence reconstruction from RNA-Seq: reference generation and analysis with Trinity. In Nature Protocols (Vol. 8). https://doi.org/10.1038/nprot.2013.084.De

Hardoim, P. R., Overbeek, L. S. Van, Berg, G., Pirttilä, M., Compant, S., Campisano, A., & Döring, M. (2015). The hidden world within plants: ecological and evolutionary considerations for defining functioning of microbial endophytes. Microbiology and Molecular Biology Reviews, 79(3), 293–320. https://doi.org/10.1128/MMBR.00050-14

Hasselgren, P. O., & Fischer, J. E. (1997). The ubiquitin-proteasome pathway: Review of a novel intracellular mechanism of muscle protein breakdown during sepsis and other catabolic conditions. Annals of Surgery, 225(3), 307–316. https://doi.org/10.1097/00000658-199703000-00011

He, Y., & Gan, S. (2002). A gene encoding an acyl hydrolase is involved in leaf senescence in Arabidopsis. The Plant Cell, 14(4), 805–815. https://doi.org/10.1105/tpc.010422

Heffernan, O. (2013). The dry facts. Nature, 501(7468), S2-3. https://doi.org/10.1038/501S2a

Heldt, H.-W. (1997). Plant biochemistry and molecular biology (1st ed.; H.-W. Heldt, Ed.). Oxford: Oxford University Press.

Herrmann, K. M., & Weaver, L. M. (1999). The shikimate pathway. Annual Review of Plant Physiology and Plant Molecular Biology, 50(1), 473–503. https://doi.org/10.1146/annurev.arplant.50.1.473

Higashi, Y., Okazaki, Y., Myouga, F., Shinozaki, K., & Saito, K. (2015). Landscape of the lipidome and transcriptome under heat stress in *Arabidopsis thaliana*. Scientific Reports, 5, 1–7. https://doi.org/10.1038/srep10533

Higashi, Y., & Saito, K. (2019). Lipidomic studies of membrane glycerolipids in plant leaves under heat stress. Progress in Lipid Research, 100990. https://doi.org/10.1016/j.plipres.2019.100990

Hilhorst, H. W. M., Costa, M. C. D., & Farrant, J. M. (2018). A Footprint of Plant Desiccation Tolerance. Does It Exist? Molecular Plant. https://doi.org/10.1016/j.molp.2018.07.001

Hilhorst, H. W. M., & Farrant, J. M. (2018). Plant desiccation tolerance: A survival strategy with exceptional prospects for climate-smart agriculture. Annual Plant Reviews Online, 1, 1–27. https://doi.org/10.1002/9781119312994.apr0637

Hoekstra, F., Golovina, E., & Buitink, J. (2001). Mechanisms of plant desiccation tolerance. Trends in Plant Science, 6(9), 431–438. https://doi.org/10.1016/S1360-1385(01)02052-0

Hölzl, G., & Dörmann, P. (2019). Chloroplast lipids and their biosynthesis. Annual Review of Plant Biology, 70(1), 51–81. https://doi.org/10.1146/annurev-arplant-050718-100202

Hong-Bo, S., Zong-Suo, L., & Ming-An, S. (2005). LEA proteins in higher plants: Structure, function, gene expression and regulation. Colloids and Surfaces B: Biointerfaces, 45(3–4), 131–135. https://doi.org/10.1016/j.colsurfb.2005.07.017

Horn, P. J., James, C. N., Gidda, S. K., Kilaru, A., Dyer, J. M., Mullen, R. T., … Chapman, K. D. (2013). Identification of a new class of lipid droplet-associated proteins in plants. Plant Physiology, 162(4), 1926–1936. https://doi.org/10.1104/pp.113.222455

Horn, P. J., & Benning, C. (2016). The plant lipidome in human and environmental health. Science, 353(6305), 1228–1233. Retrieved from http://www.riss.kr/link?id=T11736684

Hossain, M. M., Khatun, M. A., Haque, M. N., Bari, M. A., Alam, M. F., Mandal, A., & Kabir, A. H. (2018). Silicon alleviates arsenic-induced toxicity in wheat through vacuolar sequestration and ROS scavenging. International Journal of Phytoremediation, 20(8), 796–804. https://doi.org/10.1080/15226514.2018.1425669

Hou, Q., & Bartels, D. (2015). Comparative study of the aldehyde dehydrogenase (ALDH) gene superfamily in the glycophyte *Arabidopsis thaliana* and *Eutrema* halophytes. Annals of Botany, 115(3), 465–479. https://doi.org/10.1093/aob/mcu152

Hou, Q., Ufer, G., & Bartels, D. (2016). Lipid signalling in plant responses to abiotic stress. Plant Cell and Environment, 39(5), 1029–1048. https://doi.org/10.1111/pce.12666

Hsiao, E. S. L., & Tzen, J. T. C. (2011). Ubiquitination of oleosin-H and caleosin in sesame oil bodies after seed germination. Plant Physiology and Biochemistry, 49(1), 77–81. https://doi.org/10.1016/j.plaphy.2010.10.001

Hsieh, K., & Huang, A. H. (2004). Endoplasmic reticulum, oleosins, and oils in seeds. Plant Physiology, 136(November), 3427–3434. https://doi.org/10.1104/pp.104.051060.1

Hsieh, K., & Huang, A. H. (2005). Lipid-rich tapetosomes in Brassica tapetum are composed of oleosin-coated oil droplets and vesicles, both assembled in and then detached from the endoplasmic reticulum. Plant Journal, 43(6), 889–899. https://doi.org/10.1111/j.1365-313X.2005.02502.x

Hu, Z., Ren, Z., & Lu, C. (2012). The phosphatidylcholine diacylglycerol cholinephosphotransferase is required for efficient hydroxy fatty acid accumulation in transgenic Arabidopsis. Plant Physiology, 158(4), 1944–1954. https://doi.org/10.1104/pp.111.192153

Huang, A. H. (1992). Oil bodies and oleosins in seeds. Annual Review of Plant Physiology and Plant Molecular Biology, 43(1), 177–200. https://doi.org/10.1146/annurev.pp.43.060192.001141

Huang, C. Y., Chen, P.-Y., Huang, M.-D., Tsou, C.-H., Jane, W.-N., & Huang, A. H. (2013). Tandem oleosin genes in a cluster acquired in Brassicaceae created tapetosomes and conferred additive benefit of pollen vigor. Proceedings of the National Academy of Sciences of the United States of America, 110(35), 14480–14485. https://doi.org/10.1073/pnas.1305299110

Huang, M.-D., & Huang, A. H. (2015). Bioinformatics reveal five lineages of oleosins and the mechanism of lineage evolution related to structure/function from green algae to seed plants. Plant Physiology, 169(1), 453–470. https://doi.org/10.1104/pp.15.00634

Huang, A. H. (2018). Plant lipid droplets and their associated oleosin and other proteins: potential for rapid advances. Plant Physiology, 176, 1894–1918. https://doi.org/10.1104/pp.17.01677

Illing, N., Denby, K. J., Collett, H., Shen, A., & Farrant, J. M. (2005). The signature of seeds in resurrection plants: A molecular and physiological comparison of desiccation tolerance in seeds and vegetative tissues. Integrative and Comparative Biology, 45(5), 771–787. https://doi.org/10.1093/icb/45.5.771

Ingle, R. A., Collett, H., Cooper, K., Takahashi, Y., Farrant, J. M., & Illing, N. (2008). Chloroplast biogenesis during rehydration of the resurrection plant *Xerophyta humilis*: Parallels to the

etioplast-chloroplast transition. Plant, Cell and Environment, 31(12), 1813–1824. https://doi.org/10.1111/j.1365-3040.2008.01887.x

Ismail, A. M., & Horie, T. (2017). Genomics, physiology, and molecular breeding approaches for improving salt tolerance. Annu Rev Plant Biol. https://doi.org/10.1146/annurev-arplant-042916-040936

Ivanov, P., Kedersha, N., & Anderson, P. (2018). Stress granules and processing bodies in translational control. Cold Spring Harbor Perspectives in Biology, a032813. https://doi.org/10.1101/cshperspect.a032813

Jacinto, E., Guo, B., Arndt, K. T., Schmelzle, T., & Hall, M. N. (2001). TIP41 interacts with TAP42 and negatively regulates the TOR signaling pathway. Molecular Cell, 8(5), 1017–1026. https://doi.org/10.1016/S1097-2765(01)00386-0

Jameson, P. E., Dhandapani, P., Novak, O., & Song, J. (2016). Cytokinins and expression of SWEET, SUT, CWINV and AAP genes increase as pea seeds germinate. International Journal of Molecular Sciences, 17(12), 1–13. https://doi.org/10.3390/ijms17122013

Jang, G.-J., Yang, J.-Y., Hsieh, H.-L., & Wu, S.-H. (2019). Processing bodies control the selective translation for optimal development of Arabidopsis young seedlings. Proceedings of the National Academy of Sciences, 116(13), 6451–6456. https://doi.org/10.1073/pnas.1900084116

Jeong, C. Y., Lee, W. J., Truong, H. A., Trinh, C. S. N., Jin, J. Y., Kim, S., … Lee, H. (2018). Dual role of SND1 facilitates efficient communication between abiotic stress signalling and normal growth in Arabidopsis. Scientific Reports, 8(1), 1–10. https://doi.org/10.1038/s41598-018-28413-x

Jin, Y., Fei, M., Rosenquist, S., Jin, L., Gohil, S., Sandström, C., … Sun, C. (2017). A dual-promoter gene orchestrates the sucrose-coordinated synthesis of starch and fructan in barley. Molecular Plant, 10(12), 1556–1570. https://doi.org/10.1016/j.molp.2017.10.013

Johnson, E. S. (2002). Ubiquitin branches out. Nature Cell Biology, 4(12). https://doi.org/10.1038/ncb1202-e295

Johnston-Monje, D., & Raizada, M. N. (2011). Plant and endophyte relationships. In Comprehensive Biotechnology (Second Edi, Vol. 1). https://doi.org/10.1016/b978-0-08-088504-9.00264-6

Jones, L., & McQueen-Mason, S. (2004a). A role for expansins in dehydration and rehydration of the resurrection plant *Craterostigma plantagineum*. FEBS Letters, 559(1–3), 61–65. https://doi.org/10.1016/S0014-5793(04)00023-7

Jones, P. M., & George, A. M. (2004b). The ABC transporter structure and mechanism: Perspectives on recent research. Cellular and Molecular Life Sciences, 61(6), 682–699. https://doi.org/10.1007/s00018-003-3336-9

Joshi, R., Wani, S. H., Singh, B., Bohra, A., Dar, Z. A., Lone, A. A., … Singla-Pareek, S. L. (2016). Transcription factors and plants response to drought stress: Current understanding and future directions. Frontiers in Plant Science, 7(July), 1029. https://doi.org/10.3389/fpls.2016.01029

Juergens, M. T., Disbrow, B., & Shachar-Hill, Y. (2016). The relationship of triacylglycerol and starch accumulation to carbon and energy flows during nutrient deprivation in *Chlamydomonas reinhardtii*. Plant Physiology, 171(4), 2445–2457. https://doi.org/10.1104/pp.16.00761

Juszczak, I., & Bartels, D. (2017). LEA gene expression, RNA stability and pigment accumulation in three closely related Linderniaceae species differing in desiccation tolerance. Plant Science, 255, 59–71. https://doi.org/10.1016/j.plantsci.2016.10.003

Kalamaki, M. S., Alexandrou, D., Lazari, D., Merkouropoulos, G., Fotopoulos, V., Pateraki, I., … Kanellis, A. K. (2009). Over-expression of a tomato N-acetyl-L-glutamate synthase gene (SlNAGS1) in *Arabidopsis thaliana* results in high ornithine levels and increased tolerance in salt and drought stresses. Journal of Experimental Botany, 60(6), 1859–1871. https://doi.org/10.1093/jxb/erp072

Kanehisa, M., Sato, Y., & Morishima, K. (2016). BlastKOALA and GhostKOALA: KEGG tools for functional characterization of genome and metagenome sequences. Journal of Molecular Biology, 428(4), 726–731. https://doi.org/10.1016/j.jmb.2015.11.006

Kang, J., Park, J., Choi, H., Burla, B., Kretzschmar, T., Lee, Y., & Martinoia, E. (2011). Plant ABC transporters. American Society of Plant Biologists, 1–25. https://doi.org/10.1016/S0005-2736(00)00132-2

Kannadan, S., & Rudgers, J. A. (2008). Endophyte symbiosis benefits a rare grass under low water availability. Functional Ecology, 22(4), 706–713. https://doi.org/10.1111/j.1365-2435.2008.01395.x

Karbaschi, M. R., Williams, B., Taji, A., & Mundree, S. G. (2016). *Tripogon loliiformis* elicits a rapid physiological and structural response to dehydration for desiccation tolerance. Functional Plant Biology, 43(February), 643–655. https://doi.org/10.1071/FP15213

Kaup, M. T., Froese, C. D., & Thompson, J. E. (2002). A role for diacylglycerol acyltransferase during leaf senescence. Plant Physiology, 129(4), 1616–1626. https://doi.org/10.1104/pp.003087

Kazan, K., & Lyons, R. (2016). The link between flowering time and stress tolerance. Journal of Experimental Botany, 67(1), 47–60. https://doi.org/10.1093/jxb/erv441

Kigel, J., & Galili, G. (1995). Seed development and germination. In Plant Hormones. DOI: https://doi.org/10.1017/S0960258500002907

Kim, H. U., Hsieh, K., Ratnayake, C., & Huang, A. H. C. (2002). A novel group of oleosins is present inside the pollen of Arabidopsis. Journal of Biological Chemistry, 277(25), 22677–22684. https://doi.org/10.1074/jbc.M109298200

Kim, R. J., Kim, H. U., & Suh, M. C. (2019). Development of camelina enhanced with drought stress resistance and seed oil production by co-overexpression of MYB96A and DGAT1C. Industrial Crops and Products, 138(June), 111475. https://doi.org/10.1016/j.indcrop.2019.111475

Kind, T., Okazaki, Y., Saito, K., & Fiehn, O. (2014). LipidBlast templates as flexible tools for creating new in-silico tandem mass spectral libraries. Analytical Chemistry, 86(22), 11024–11027. https://doi.org/10.1021/ac502511a

Kleines, M., Elster, R. C., Rodrigo, M. J., Blervacq, A. S., Salamini, F., & Bartels, D. (1999). Isolation and expression analysis of two stress-responsive sucrose-synthase genes from the resurrection plant *Craterostigma plantagineum* (Hochst.). Planta, 209(1), 13–24. https://doi.org/10.1007/s004250050602

Knorr, & WWF. (2019). 50 Foods for Healthier People and a Healthier Planet.

Koelmel, J. P., Kroeger, N. M., Ulmer, C. Z., Bowden, J. A., Patterson, R. E., Cochran, J. A., … Yost, R. A. (2017). LipidMatch: an automated workflow for rule-based lipid identification using untargeted high-resolution tandem mass spectrometry data. BMC Bioinformatics, 18(331), 1–11. https://doi.org/10.1186/s12859-017-1744-3

Komander, D. (2009). The emerging complexity of protein ubiquitination. Biochemical Society Transactions, 37(5), 937–953. https://doi.org/10.1042/bst0370937

Kosma, D. K., Molina, I., Ohlrogge, J. B., & Pollard, M. (2012). Identification of an Arabidopsis fatty alcohol: Caffeoyl-Coenzyme a acyltransferase required for the synthesis of alkyl hydroxycinnamates in root waxes. Plant Physiology, 160(1), 237–248. https://doi.org/10.1104/pp.112.201822

Kranner, I., Beckett, R. P., Wornik, S., Zorn, M., & Pfeifhofer, H. W. (2002). Revival of a resurrection plant correlates with its antioxidant status. Plant Journal, 31(1), 13–24. https://doi.org/10.1046/j.1365-313X.2002.01329.x

Kuang, J., Gaff, D. F., Gianello, R. D., Blomstedt, C. K., Neale, A. D., & Hamill, J. D. (1995). Changes in in vivo protein complements in drying leaves of the desiccation-tolerant grass *Sporobolus stapfianus* and the desiccation-sensitive grass Sporobolus pyramidalis. Australian Journal of Plant Physiology, 22(6), 1027–1034. https://doi.org/10.1071/PP9951027

Kushwah, S., & Laxmi, A. (2017). The interaction between glucose and cytokinin signaling in controlling *Arabidopsis thaliana* seedling root growth and development. Plant Signaling and Behavior, 12(5), 1–8. https://doi.org/10.1080/15592324.2017.1312241

Lämmli, U. K. (1970). Cleavage of Structural Proteins during the Assembly of the Head of Bacteriophage T4. Nature, 227(5259), 680–685. https://doi.org/10.1038/227680a0

Lata, R., Chowdhury, S., Gond, S. K., & White, J. F. (2018). Induction of abiotic stress tolerance in plants by endophytic microbes. Letters in Applied Microbiology, 66(4), 268–276. https://doi.org/10.1111/lam.12855

Law, S. R., Chrobok, D., Juvany, M., Delhomme, N., Lindén, P., Brouwer, B., … Keech, O. (2018). Darkened leaves use different metabolic strategies for senescence and survival. Plant Physiology, pp.00062.2018. https://doi.org/10.1104/pp.18.00062

Le, T. N., Blomstedt, C. K., Kuang, J., Tenlen, J., Gaff, D. F., Hamill, J. D., & Neale, A. D. (2007). Desiccation-tolerance specific gene expression in leaf tissue of the resurrection plant *Sporobolus stapfianus*. Functional Plant Biology, 34(7), 589–600. https://doi.org/10.1071/FP06231

Lee, E., Vanneste, S., Pérez-Sancho, J., Benitez-Fuente, F., Strelau, M., Macho, A. P., … Rosado, A. (2019). Ionic stress enhances ER–PM connectivity via phosphoinositide-associated SYT1 contact site expansion in Arabidopsis. Proceedings of the National Academy of Sciences of the United States of America, 116(4), 1420–1429. https://doi.org/10.1073/pnas.1818099116

Leprince, O., Van Aelst, A. C., Pritchard, H. W., & Murphy, D. J. (1998). Oleosins prevent oil-body coalescence during seed imbibition as suggested by a low-temperature scanning electron microscope study of desiccation-tolerant and -sensitive oilseeds. Planta, 204(1), 109–119. https://doi.org/10.1007/s004250050236

Leprince, Olivier, & Buitink, J. (2010). Desiccation tolerance: From genomics to the field. Plant Science, 179(6), 554–564. https://doi.org/10.1016/j.plantsci.2010.02.011

Leprince, Olivier, & Buitink, J. (2015). Introduction to desiccation biology: from old borders to new frontiers. Planta, 242(2), 369–378. https://doi.org/10.1007/s00425-015-2357-6

Li-Beisson, Y., Shorrosh, B., Beisson, F., Andersson, M. X., Arondel, V., Bates, P. D., … Ohlrogge, J. B. (2013). Acyl-lipid metabolism. In The Arabidopsis book (Vol. 8, p. e0133). https://doi.org/10.1199/tab.0133

LI-COR. (2012). Manual. In Using the LI-6400/Version 6. Retrieved from www.licor.com

Lin, L-J., Tai, S.S.K., Peng, C-C., Tzen, J.T.C. (2002). Steroleosin, a sterol-binding dehydrogenase in seed oil bodies. Plant Physiology, 128(4) 1200-1211. doi:10.1104/pp.010928

Li, W., & Godzik, A. (2006). Cd-hit: A fast program for clustering and comparing large sets of protein or nucleotide sequences. Bioinformatics, 22(13), 1658–1659. https://doi.org/10.1093/bioinformatics/btl158

Li, A., Wang, D., Yu, B., Yu, X., & Li, W. (2014). Maintenance or collapse: Responses of extraplastidic membrane lipid composition to desiccation in the resurrection plant *Paraisometrum mileense*. PLoS ONE, 9(7), 1–14. https://doi.org/10.1371/journal.pone.0103430

Li, Q., Zheng, Q., Shen, W., Cram, D., Brian Fowler, D., Wei, Y., & Zou, J. (2015). Understanding the biochemical basis of temperature-induced lipid pathway adjustments in plants. Plant Cell, 27(1), 8–103. https://doi.org/10.1105/tpc.114.134338

Li, N., Xu, C., Li-Beisson, Y., & Philippar, K. (2016). Fatty Acid and Lipid Transport in Plant Cells. Trends in Plant Science, 21(2), 145–158. https://doi.org/10.1016/j.tplants.2015.10.011

Lill, R., Dutkiewicz, R., Freibert, S. A., Heidenreich, T., Mascarenhas, J., Netz, D. J., … Mühlenhoff, U. (2015). The role of mitochondria and the CIA machinery in the maturation of cytosolic and nuclear iron-sulfur proteins. European Journal of Cell Biology, 94(7–9), 280–291. https://doi.org/10.1016/j.ejcb.2015.05.002

Lim, P. O., Woo, H. R., & Nam, H. G. (2003). Molecular genetics of leaf senescence in Arabidopsis. Trends in Plant Science, 8(6), 272–278. https://doi.org/10.1016/S1360-1385(03)00103-1

Lim, P. O., Kim, H. J., & Nam, H. G. (2007). Leaf Senescence. Annual Review of Plant Biology, 58(1), 115–136. https://doi.org/10.1146/annurev.arplant.57.032905.105316

Lin, W., & Oliver, D. J. (2008). Role of triacylglycerols in leaves. Plant Science, 175(3), 233–237. https://doi.org/10.1016/j.plantsci.2008.04.003

Liu, J.-X., & Howell, S. H. (2010). Endoplasmic reticulum protein quality control and its relationship to environmental stress responses in plants. The Plant Cell, 22(9), 2930–2942. https://doi.org/10.1105/tpc.110.078154

Liu, P., Yin, L., Deng, X., Wang, S., Tanaka, K., & Zhang, S. (2014). Aquaporin-mediated increase in root hydraulic conductance is involved in silicon-induced improved root water uptake under osmotic stress in *Sorghum bicolor* L. Journal of Experimental Botany, 65(17), 4747–4756. https://doi.org/10.1093/jxb/eru220

Liu, J., Rice, A., Mcglew, K., Shaw, V., Park, H., Clemente, T., … Durrett, T. P. (2015). Metabolic engineering of oilseed crops to produce high levels of novel acetyl glyceride oils with reduced viscosity, freezing point and calorific value. Plant Biotechnology Journal, 13(6), 858–865. https://doi.org/10.1111/pbi.12325

Liu, P. L., Du, L., Huang, Y., Gao, S. M., & Yu, M. (2017). Origin and diversification of leucine-rich repeat receptor-like protein kinase (LRR-RLK) genes in plants. BMC Evolutionary Biology, 17(1), 1–16. https://doi.org/10.1186/s12862-017-0891-5

Liu, Q., Luo, L., & Zheng, L. (2018). Lignins: Biosynthesis and biological functions in plants. International Journal of Molecular Sciences, 19(2). https://doi.org/10.3390/ijms19020335

Liu, Xiaoxiao, Ma, D., Zhang, Z., Wang, S., Du, S., Deng, X., & Yin, L. (2019a). Plant lipid remodeling in response to abiotic stresses. Environmental and Experimental Botany, 165(March), 174–184. https://doi.org/10.1016/j.envexpbot.2019.06.005

Liu, Xun, Challabathula, D., Quan, W., & Bartels, D. (2019b). Transcriptional and metabolic changes in the desiccation tolerant plant *Craterostigma plantagineum* during recurrent exposures to dehydration. Planta, 249(4), 1017–1035. https://doi.org/10.1007/s00425-018-3058-8

Lockshon, D., Surface, L. E., Kerr, E. O., Kaeberlein, M., & Kennedy, B. K. (2007). The sensitivity of yeast mutants to oleic acid implicates the peroxisome and other processes in membrane function. Genetics, 175(1), 77–91. https://doi.org/10.1534/genetics.106.064428

Lohse, M., Nagel, A., Herter, T., May, P., Schroda, M., Zrenner, R., … Usadel, B. (2014). Mercator: A fast and simple web server for genome scale functional annotation of plant sequence data. Plant, Cell and Environment, 37(5), 1250–1258. https://doi.org/10.1111/pce.12231

López-Pozo, M., Gasulla, F., García-Plazaola, J. I., & Fernández-Marín, B. (2019). Unraveling metabolic mechanisms behind chloroplast desiccation tolerance: Chlorophyllous fern spore as a new promising unicellular model. Plant Science, 281(July 2018), 251–260. https://doi.org/10.1016/j.plantsci.2018.11.012

Lough, T. J., & Lucas, W. J. (2006). Integrative plant biology: Role of phloem long-distance macromolecular trafficking. Annual Review of Plant Biology, 57(1), 203–232. https://doi.org/10.1146/annurev.arplant.56.032604.144145

Lundquist, P. K., Poliakov, A., Bhuiyan, N. H., Zybailov, B., Sun, Q., & van Wijk, K. J. (2012). The functional network of the Arabidopsis plastoglobule proteome based on quantitative proteomics and genome-wide coexpression analysis. Plant Physiology, 158(3), 1172–1192. https://doi.org/10.1104/pp.111.193144

Luo, Y., Na, Z., & Slavoff, S. A. (2018a). P-Bodies: Composition, properties, and functions. Biochemistry, 57(17), 2424–2431. https://doi.org/10.1021/acs.biochem.7b01162

Luo, K.-R., Huang, N.-C., & Yu, T.-S. (2018b). Selective targeting of mobile mRNAs to plasmodesmata for cell-to-cell movement. Plant Physiology, 177(2), 604–614. https://doi.org/10.1104/pp.18.00107

Lyska, D., Meierhoff, K., & Westhoff, P. (2013). How to build functional thylakoid membranes: From plastid transcription to protein complex assembly. Planta, 237(2), 413–428. https://doi.org/10.1007/s00425-012-1752-5

Ma, J. F., Tamai, K., Yamaji, N., Mitani, N., Konishi, S., Katsuhara, M., … Yano, M. (2006). A silicon transporter in rice. Nature, 440(7084), 688–691. https://doi.org/10.1038/nature04590

Ma, C., Wang, H., Macnish, A. J., Estrada-Melo, A. C., Lin, J., Chang, Y., … Jiang, C. Z. (2015). Transcriptomic analysis reveals numerous diverse protein kinases and transcription factors involved in desiccation tolerance in the resurrection plant Myrothamnus flabellifolia. Horticulture Research, 2(May). https://doi.org/10.1038/hortres.2015.34

Maere, S., Heymans, K., & Kuiper, M. (2005). BiNGO: A Cytoscape plugin to assess overrepresentation of gene ontology categories in biological networks. Bioinformatics, 21(16), 3448–3449. https://doi.org/10.1093/bioinformatics/bti551

Magwanga, R. O., Lu, P., Kirungu, J. N., Dong, Q., Hu, Y., Zhou, Z., … Liu, F. (2018). Cotton late embryogenesis abundant (LEA2) genes promote root growth and confer drought stress tolerance in transgenic *Arabidopsis thaliana*. Genes|Genomes|Genetics, 8(8), 2781–2803. https://doi.org/10.1534/g3.118.200423

Mao, Z., & Sun, W. (2015). Arabidopsis seed-specific vacuolar aquaporins are involved in maintaining seed longevity under the control of ABSCISIC ACID INSENSITIVE 3. Journal of Experimental Botany, 66(15), 4781–4794. https://doi.org/10.1093/jxb/erv244

Mariaux, J. B., Bockel, C., Salamini, F., & Bartels, D. 1998. Desiccation- and Abscisic Acid-responsive genes encoding major intrinsic proteins (MIPs) from the resurrection plant *Craterostigma plantagineum*. Plant Molecular Biology 38 (6): 1089–99. https://doi.org/10.1023/A:1006013130681.

Mariotti, M., De Benedictis, L., Avon, E., & Maier, J. A. M. (2000). Interaction between endothelial differentiation-related factor-1 and calmodulin in vitro and vivo. Journal of Biological Chemistry, 275(31), 24047–24051. https://doi.org/10.1074/jbc.M001928200

Martinelli, T., Whittaker, A., Masclaux-Daubresse, C., Farrant, J. M., Brilli, F., Loreto, F., & Vazzana, C. (2007). Evidence for the presence of photorespiration in desiccation-sensitive leaves of the C4 "resurrection" plant *Sporobolus stapfianus* during dehydration stress. Journal of Experimental Botany, 58(14), 3929–3939. https://doi.org/10.1093/jxb/erm247

Martinelli, T. (2008). In situ localization of glucose and sucrose in dehydrating leaves of *Sporobolus stapfianus*. Journal of Plant Physiology, 165(6), 580–587. https://doi.org/10.1016/j.jplph.2007.01.019

Martinoia, E., Klein, M., Geisler, M., Bovet, L., Forestier, C., Kolukisaoglu, Ü., … Schulz, B. (2002). Multifunctionality of plant ABC transporters - More than just detoxifiers. Planta, 214(3), 345–355. https://doi.org/10.1007/s004250100661

Massawe, F., Mayes, S., & Cheng, A. (2016). Crop diversity: An unexploited treasure trove for food security. Trends in Plant Science, 21(5), 365–368. https://doi.org/10.1016/j.tplants.2016.02.006

Maurel, C., Boursiac, Y., Luu, D.-T., Santoni, V., Shahzad, Z., & Verdoucq, L. (2015). Aquaporins in plants. Physiological Reviews, 95, 1321–1358. https://doi.org/10.1111/j.1748-1716.2006.01563.x

McCarthy, D. J., Chen, Y., & Smyth, G. K. (2012). Differential expression analysis of multifactor RNA-Seq experiments with respect to biological variation. Nucleic Acids Research, 40(10), 4288–4297. https://doi.org/10.1093/nar/gks042

Mekonnen, M. M., & Hoekstra, A. Y. (2016). Four billion people facing severe water scarcity. Science Advances, 2(2). https://doi.org/10.1126/sciadv.1500323

Meryman, H. T. (1974). Freezing injury and its prevention in living cells. Annual Review of Biophysics and Bioengineering, 3(1), 341–363. https://doi.org/10.1146/annurev.bb.03.060174.002013

Michaud, M., & Jouhet, J. (2019). Lipid trafficking at membrane contact sites during plant development and stress response. Frontiers in Plant Science, 10(January), 1–10. https://doi.org/10.3389/fpls.2019.00002

Millar, A. A., Wrischer, M., & Kunst, L. (1998). Accumulation of very-long-chain fatty acids in membrane glycerolipids is associated with dramatic alterations in plant morphology. The Plant Cell, 10(11), 1889–1902. https://doi.org/10.1105/tpc.10.11.1889

Miller, G., Suzuki, N., Ciftci-Yilmaz, S., & Mittler, R. (2010). Reactive oxygen species homeostasis and signalling during drought and salinity stresses. Plant Cell and Environment, 33(4), 453–467. https://doi.org/10.1111/j.1365-3040.2009.02041.x

Miquel, M., Trigui, G., Andréa, S., Kelemen, Z., Baud, S., Berger, A., … Dubreucq, B. (2014). Specialization of oleosins in oil body dynamics during seed development in Arabidopsis Seeds. Plant Physiology, 164(April), 1866–1878. https://doi.org/10.1104/pp.113.233262

Mittler, R, Vanderauwera, S., Suzuki, N., Miller, G., Tognetti, V. B., Vandepoele, K., … Van Breusegem, F. (2011). ROS signaling: the new wave? Trends in Plant Science, 16(6), 300–309. https://doi.org/Doi 10.1016/J.Tplants.2011.03.007

Mittler, Ron. (2017). ROS are good. Trends in Plant Science, 22(1), 11–19. https://doi.org/10.1016/j.tplants.2016.08.002

Mohanta, T. K., Bashir, T., Hashem, A., & Abd Allah, E. F. (2017). Systems biology approach in plant abiotic stresses. Plant Physiology and Biochemistry, 121(September), 58–73. https://doi.org/10.1016/j.plaphy.2017.10.019

Mongrand, S., Bessoule, J. J., Cabantous, F., & Cassagne, C. (1998). The C(16:3)/C(18:3) fatty acid balance in photosynthetic tissues from 468 plant species. Phytochemistry, 49(4), 1049–1064. https://doi.org/10.1016/S0031-9422(98)00243-X

Moore, J. P., Westall, K. L., Ravenscroft, N., Farrant, J. M., Lindsey, G. G., & Brandt, W. F. (2005). The predominant polyphenol in the leaves of the resurrection plant *Myrothamnus flabellifolius*, 3,4,5 tri-O-galloylquinic acid, protects membranes against desiccation and free radical-induced oxidation. The Biochemical Journal, 385(Pt 1), 301–308. https://doi.org/10.1042/BJ20040499

Moore, J. P., Lindsey, G. G., Farrant, J. M., & Brandt, W. F. (2007). An overview of the biology of the desiccation-tolerant resurrection plant Myrothamnus flabellifolia. Annals of Botany, 99, 211–217.

Moore, J. P., Nguema-Ona, E. E., Vicré-Gibouin, M., Sørensen, I., Willats, W. G. T., Driouich, A., & Farrant, J. M. (2013). Arabinose-rich polymers as an evolutionary strategy to plasticize resurrection plant cell walls against desiccation. Planta, 237(3), 739–754. https://doi.org/10.1007/s00425-012-1785-9

Moore, D. S., Hansen, R., & Hand, S. C. (2016). Liposomes with diverse compositions are protected during desiccation by LEA proteins from *Artemia franciscana* and trehalose. Biochimica et Biophysica Acta, 1858(1). https://doi.org/10.1016/j.bbamem.2015.10.019

Moriyasu, Y., Hattori, M., Jauh, G. Y., & Rogers, J. C. (2003). Alpha tonoplast intrinsic protein is specifically associated with vacuole membrane involved in an autophagic process. Plant and Cell Physiology, 44(8), 795–802. https://doi.org/10.1093/pcp/pcg100

Morse, M., Rafudeen, M. S., & Farrant, J. M. (2011). An overview of the current understanding of desiccation tolerance in the vegetative tissues of higher plants. In Advances in Botanical Research (1st ed., Vol. 57). https://doi.org/10.1016/B978-0-12-387692-8.00009-6

Mowla, S. B., Thomson, J. A., Farrant, J. M., & Mundree, S. G. (2002). A novel stress-inducible antioxidant enzyme identified from the resurrection plant *Xerophyta viscosa* baker. Planta, 215(5), 716–726. https://doi.org/10.1007/s00425-002-0819-0

Muller, B., Pantin, F., Génard, M., Turc, O., Freixes, S., Piques, M., & Gibon, Y. (2011). Water deficits uncouple growth from photosynthesis, increase C content, and modify the relationships between C and growth in sink organs. Journal of Experimental Botany, 62(6), 1715–1729. https://doi.org/10.1093/jxb/erq438

Mundree, S. G., Baker, B., Mowla, S., Peters, S., Marais, S., Willigen, C. Vander, … Thomson, J. A. (2002). Physiological and molecular insights into drought tolerance. Minireview African Journal of Biotechnology, 1(2), 28–38. Retrieved from http://www.academicjournals.org/AJB

Munné-Bosch, S., & Alegre, L. (2002). Plant aging increases oxidative stress in chloroplasts. Planta, 214(4), 608–615. https://doi.org/10.1007/s004250100646

Munné-Bosch, Sergi, & Alegre, L. (2004). Die and let live: Leaf senescence contributes to plant survival under drought stress. Functional Plant Biology, 31(3), 203–216. https://doi.org/10.1071/FP03236

Murphy, R. C., Fiedler, J., & Hevko, J. (2001). Analysis of nonvolatile lipids by mass spectrometry. Chemical Reviews, 101(2), 479–526. https://doi.org/10.1021/cr9900883

Murphy, D. J. (2012). The dynamic roles of intracellular lipid droplets: From archaea to mammals. Protoplasma, 249(3), 541–585. https://doi.org/10.1007/s00709-011-0329-7

Myers, M. Y., Farrant, J. M., & Roden, L. C. (2010). Preliminary characterization of floral response of *Xerophyta humilis* to desiccation, vernalisation, photoperiod and light intensity. Plant Growth Regulation, 62(3), 213–216. https://doi.org/10.1007/s10725-010-9460-2

Navari-Izzo, F., Ricci, F., Vazzana, C., & Quartacci, M. F. (1995). Unusual composition of thylakoid membranes of the resurrection plant *Boea hygroscopica*: Changes in lipids upon dehydration and rehydration. Physiologia Plantarum, 94(1), 135–142. https://doi.org/10.1111/j.1399-3054.1995.tb00794.x

Naveed, M., Mitter, B., Reichenauer, T. G., Wieczorek, K., & Sessitsch, A. (2014). Increased drought stress resilience of maize through endophytic colonization by *Burkholderia phytofirmans* PsJN and Enterobacter sp. FD17. Environmental and Experimental Botany, 97, 30–39. https://doi.org/10.1016/j.envexpbot.2013.09.014

Naylor, R. L., Falcon, W. P., Goodman, R. M., Jahn, M. M., Sengooba, T., Tefera, H., & Nelson, R. J. (2004). Biotechnology in the developing world: A case for increased investments in orphan crops. Food Policy, 29(1), 15–44. https://doi.org/10.1016/j.foodpol.2004.01.002

Neale, A. D., Blomstedt, C. K., Bronson, P., Le, T. N., Guthridge, K., Evans, J., … Hamill, J. D. (2000). The isolation of genes from the resurrection grass *Sporobolus stapfianus* which are induced during severe drought stress. Plant, Cell and Environment, 23(3), 265–277. https://doi.org/10.1046/j.1365-3040.2000.00548.x

Neff, M. M., & Chory, J. (1998). Genetic interactions between phytochrome A, phytochrome B, and cryptochrome 1 during Arabidopsis development. Plant Physiology, 118(1), 27–36.

Nguyen, T. P., Cueff, G., Hegedus, D. D., Rajjou, L., & Bentsink, L. (2015). A role for seed storage proteins in Arabidopsis seed longevity. Journal of Experimental Botany, 66(20), 6399–6413. https://doi.org/10.1093/jxb/erv348

Nilson, S. E., & Assmann, S. M. (2010). Heterotrimeric G proteins regulate reproductive trait plasticity in response to water availability. New Phytologist, 185(3), 734–746. https://doi.org/10.1111/j.1469-8137.2009.03120.x

Nishizawa, A., Yabuta, Y., & Shigeoka, S. (2008). Galactinol and Raffinose Constitute a Novel Function to Protect Plants from Oxidative Damage. Plant Physiology, 147(3), 1251–1263. https://doi.org/10.1104/pp.108.122465

O'Mahony, P. J., & Oliver, M. J. (1999). The involvement of ubiquitin in vegetative desiccation tolerance. Plant Molecular Biology, 41(5), 657–667. https://doi.org/10.1023/A:1006330623364

Ohlrogge, J., & Browse, J. (1995). Lipid Biosynthesis. The Plant Cell, 7, 957–970. https://doi.org/10.2307/3870050

Ohlrogge, J. B., & Jaworski, J. G. (1997). Regulation of fatty acid synthesis. Annual Review of Plant Physiology and Plant Molecular Biology, 48, 109–136.

Olex, A. L., & Fetrow, J. S. (2011). SC2ATmd: A tool for integration of the figure of merit with cluster analysis for gene expression data. Bioinformatics, 27(9), 1330–1331. https://doi.org/10.1093/bioinformatics/btr115

Oliver, M. J. (1991). Influence of protoplasmic water loss on the control of protein synthesis in the desiccation-tolerant moss *Tortula ruralis*: Ramifications for a repair-based mechanism of desiccation tolerance. Plant Physiology, 97, 1501–1511. https://doi.org/10.1104/pp.97.4.1501

Oliver, M. J., Wood, A. J., & Mahony, P. O. (1998). "To dryness and beyond" – preparation for the dried state and rehydration in vegetative desiccation-tolerant plants. Plant Growth Regulation, 24(1), 193–201.

Oliver, M. J., Tuba, Z., & Mishler, B. D. (2000). The evolution of vegetative desiccation tolerance in land plants. Plant Ecology, 151(1), 85–100.

Oliver, M. J., Dowd, S. E., Zaragoza, J., Mauget, S. A., & Payton, P. R. (2004). The rehydration transcriptome of the desiccation-tolerant bryophyte *Tortula ruralis*: transcript classification and analysis. BMC Genomics, 5, 89. https://doi.org/10.1186/1471-2164-5-89

Oliver, M. J., Hudgeons, J., Dowd, S. E., & Payton, P. R. (2009). A combined subtractive suppression hybridization and expression profiling strategy to identify novel desiccation response transcripts from *Tortula ruralis* gametophytes. Physiologia Plantarum, 136(4), 437–460. https://doi.org/10.1111/j.1399-3054.2009.01245.x

Oliver, M. J., Guo, L., Alexander, D. C., Ryals, J. A., Wone, B. W. M., & Cushman, J. C. (2011). A sister group contrast using untargeted global metabolomic analysis delineates the biochemical regulation underlying desiccation tolerance in *Sporobolus stapfianus*. American Society of Plant Biologists, 23(4), 1231–1248.

Ono, H., Ishii, K., Kozaki, T., Ogiwara, I., Kanekatsu, M., & Yamada, T. (2015). Removal of redundant contigs from *de novo* RNA-Seq assemblies via homology search improves accurate detection of differentially expressed genes. BMC Genomics, 1–13. https://doi.org/10.1186/s12864-015-2247-0

Orlando, D. A., Brady, S. M., Koch, J. D., Dinneny, J. R., & Philip, N. (2009). Plant Systems Biology. 553(2), 1–18. https://doi.org/10.1007/978-1-60327-563-7

Otegui, M. S. (2018). Vacuolar degradation of chloroplast components: Autophagy and beyond. Journal of Experimental Botany, 69(4), 741–750. https://doi.org/10.1093/jxb/erx234

Páli, T., Garab, G., Horváth, L. I., & Kóta, Z. (2003). Functional significance of the lipid-protein interface in photosynthetic membranes. Cellular and Molecular Life Sciences, 60(8), 1591–1606. https://doi.org/10.1007/s00018-003-3173-x

Paliyath, G., & Droillard, M. (1992). The mechanisms of membrane deterioration and disassembly during senescence. Plant Physiology and Biochemistry, 30, 789–812.

Pammenter, N. W., & Berjak, P. (1999). A review of recalcitrant seed physiology in relation to desiccation-tolerance mechanisms. Seed Science Research, 9(1), 13–37. https://doi.org/10.1017/S0960258599000033

Panunzi, E. (2008). Are grasslands under threat? Brief analysis of FAO statistical data on pasture and fodder crops. In FAO. Retrieved from www.fao.org/uploads/media/grass_stats_1.pdf

Pardo, J., Wai, C. M., Chay, H., Madden, C. F., Hilhorst, H. W. M., Farrant, J. M., & VanBuren, R. (2019). Intertwined signatures of desiccation and drought tolerance in grasses. BioRxiv, 662379. https://doi.org/10.1101/662379

Parkhey, S., Tandan, M., & Keshavkant, S. (2014). Salicylic acid and acquisition of desiccation tolerance in *Pisum stivum* seeds. Biotechnology, 5, 217–225.

Patro, R., Duggal, G., Love, M. I., Irizarry, R. A., & Kingsford, C. (2017). Salmon: fast and bias-aware quantification of transcript expression using dual-phase inference. Nature Methods, 14(4), 417. https://doi.org/10.1038/NMETH.4197

Paul, L. K., Rinne, P. L. H., & Schoot, C. Van Der. (2014). Refurbishing the plasmodesmal chamber: a role for lipid bodies? Frontiers in Plant Science, 5(February), 1–10. https://doi.org/10.3389/fpls.2014.00040

Paul, M. J., Gonzalez-Uriarte, A., Griffiths, C. A., & Hassani-Pak, K. (2018). The role of trehalose 6-phosphate in crop yield and resilience. Plant Physiology, pp.01634.2017. https://doi.org/10.1104/pp.17.01634

Pauling, J. K., Hermansson, M., Hartler, J., Christiansen, K., Gallego, S. F., Peng, B., … Ejsing, C. S. (2017). Proposal for a common nomenclature for fragment ions in mass spectra of lipids. PLoS ONE, 12(11), 1–21. https://doi.org/10.1371/journal.pone.0188394

Peng, Z., He, S., Gong, W., Xu, F., Pan, Z., Jia, Y., … Du, X. (2018). Integration of proteomic and transcriptomic profiles reveals multiple levels of genetic regulation of salt tolerance in cotton. BMC Plant Biology, 18(1), 128. https://doi.org/10.1186/s12870-018-1350-1

Perea-Resa, C., Carrasco-López, C., Catalá, R., Turečková, V., Novak, O., Zhang, W., … Salinas, J. (2016). The LSM1-7 complex differentially regulates Arabidopsis tolerance to abiotic stress conditions by promoting selective mRNA decapping. The Plant Cell, 28(2), 505–520. https://doi.org/10.1105/tpc.15.00867

Perlikowski, D., Kierszniowska, S., Sawikowska, A., & Krajewski, P. (2016). Remodeling of Leaf Cellular glycerolipid composition under drought and re-hydration conditions in grasses from the *lolium-festuca* complex. 7(July), 1–15. https://doi.org/10.3389/fpls.2016.01027

Pertea, M., Kim, D., Pertea, G. M., Leek, J. T., & Salzberg, S. L. (2016). Transcript-level expression analysis of RNA- seq experiments with HISAT, StringTie and Transcript-level expression analysis of RNA-seq experiments with HISAT, StringTie and Ballgown. Nature Protocols, 11(9), 1650–1667. https://doi.org/10.1038/nprot.2016-095

Peters, S., Mundree, S. G., Thomson, J. A., Farrant, J. M., & Keller, F. (2007). Protection mechanisms in the resurrection plant *Xerophyta viscosa* (Baker): Both sucrose and raffinose family oligosaccharides (RFOs) accumulate in leaves in response to water deficit. Journal of Experimental Botany, 58(8), 1947–1956. https://doi.org/10.1093/jxb/erm056

Petroski, M. D., Zhou, X., Dong, G. Q., Daniel-Issakani, S., Payan, D. G., & Huang, J. (2007). Substrate modification with lysine 63-linked ubiquitin chains through the UBC13-UEV1A ubiquitin-conjugating enzyme. Journal of Biological Chemistry, 282(41), 29936–29945. https://doi.org/10.1074/jbc.M703911200

Petschnigg, J., Wolinski, H., Kolb, D., Zelling, G., Kurat, C. F., Natter, K., & Kohlwein, S. D. (2009). Good fat, essential cellular requirements for triacylglycerol synthesis to maintain membrane

homeostasis in yeast. Journal of Biological Chemistry, 284(45), 30981–30993. https://doi.org/10.1074/jbc.M109.024752

Phillips, J. R., Oliver, M. J., & Bartels, D. (2002). Molecular genetics of desiccation and tolerant systems. In M. B. and H. Pritchard. (Ed.), CAB International Desiccation and Survival in Plants: Drying without dying (pp. 319–341).

Phillips, Jonathan R., Fischer, E., Baron, M., Van Den Dries, N., Facchinelli, F., Kutzer, M., … Bartels, D. (2008). Lindernia brevidens: A novel desiccation-tolerant vascular plant, endemic to ancient tropical rainforests. Plant Journal, 54(5), 938–948. https://doi.org/10.1111/j.1365-313X.2008.03478.x

Pintó-Marijuan, M., Munné-Bosch, S., Pinto-Marijuan, M., & Munne-Bosch, S. (2014). Photo-oxidative stress markers as a measure of abiotic stress-induced leaf senescence: advantages and limitations. Journal of Experimental Botany, 65(14), 3845–3857. https://doi.org/10.1093/jxb/eru086

Pons, L., Olszewski, A., Guéant, J.L. (1998). Characterization of the oligomeric behavior of a 16.5 kDa peanut oleosin by chromatography and electrophoresis of the iodinated form. Journal Chromatography B: Biomedical Applications, 706(1) 131-140. doi:10.1016/S0378-4347(97)00530-6

Pons, L., Chéry, C., Mrabet, N., Schohn, H., Lapicque, F., Guéant, J.L. (2005). Purification and cloning of two high molecular mass isoforms of peanut seed oleosin encoded by cDNAs of equal sizes. Plant Physiological Biochemistry, 43(7) 659-668. doi:10.1016/j.plaphy.2005.06.002

Porra, R. J., Thompson, W. A., & Kriedemann, P. E. (1989). Determination of accurate extinction coefficients and simultaneous equations for assaying chlorophylls a and b extracted with four different solvents: verification of the concentration of chlorophyll standards by atomic absorption spectroscopy. BBA - Bioenergetics, 975(3), 384–394. https://doi.org/10.1016/S0005-2728(89)80347-0

Pourtau, N., Jennings, R., Pelzer, E., Pallas, J., & Wingler, A. (2006). Effect of sugar-induced senescence on gene expression and implications for the regulation of senescence in Arabidopsis. Planta, 224(3), 556–568. https://doi.org/10.1007/s00425-006-0243-y

Prerostova, S., Dobrev, P. I., Gaudinova, A., Knirsch, V., Körber, N., Pieruschka, R., … Vankova, R. (2018). Cytokinins: Their impact on molecular and growth responses to drought stress and recovery

in Arabidopsis. Frontiers in Plant Science, 9(May), 1–14. https://doi.org/10.3389/fpls.2018.00655

Pressel, S., & Duckett, J. G. (2010). Cytological insights into the desiccation biology of a model system: Moss protonemata. New Phytologist, 185(4), 944–963. https://doi.org/10.1111/j.1469-8137.2009.03148.x

Pyc, M., Cai, Y., Greer, M. S., Yurchenko, O., Chapman, K. D., Dyer, J. M., & Mullen, R. T. (2017). Turning over a new leaf in lipid droplet biology. Trends in Plant Science, 22(7), 596–609. https://doi.org/10.1016/j.tplants.2017.03.012

Quartacci, M. F., Forli, M., Rascio, N., Vecchia, F. D., Bochicchio, A., & Navari-Izzo, F. (1997). Desiccation-tolerant *Sporobolus stapfianus*: lipid composition and cellular ultrastructure during dehydration and rehydration. Journal of Experimental Botany, 48(6), 1269–1279. https://doi.org/10.1093/jxb/48.6.1269

Quartacci, M. F. (2002). Plasma membrane lipids in the resurrection plant *Ramonda serbica* following dehydration and rehydration. Journal of Experimental Botany, 53(378), 2159–2166. https://doi.org/10.1093/jxb/erf076

Rabino, I., & Mancinelli, A. L. (1986). Light, Temperature, and Anthocyanin Production. Plant Physiology, 81, 922–924.

Rajjou, L., Gallardo, K., Debeaujon, I., Vandekerckhove, J., Job, C., & Job, D. (2004). The effect of a-amanitin on the Arabidopsis seed proteome highlights the distinct roles of stored and neosynthesized mRNAs during germination. Plant Physiology, 134(4), 1598–1613. https://doi.org/10.1104/pp.103.036293

Ramanjulu, S., & Bartels, D. (2002). Drought-and desiccation-induced modulation of gene expression in plants. Plant, Cell and Environment, 25(Bray 1997), 141–151. https://doi.org/10.1046/j.0016-8025.2001.00764.x

Rascio, N., & La Rocca, N. (2005). Resurrection plants: The puzzle of surviving extreme vegetative desiccation. Critical Reviews in Plant Sciences, 24(3), 209–225. https://doi.org/10.1080/07352680591008583

Reynolds, E. S. (1963). The use of lead citrate at high pH as an electron-opaque stain in electron microscopy. The Journal of Cell Biology, 17(1), 208–212. https://doi.org/10.1083/jcb.17.1.208

Righetti, K., Vu, L., Pelletier, S., Vu, L., Glaab, E., Lalanne, D., … Buitink, J. (2015). Inference of longevity-related genes from a robust coexpression network of seed maturation identifies regulators

linking seed storability to biotic defense-related pathways. The Plant Cell Preview. 1–18. https://doi.org/10.1105/tpc.15.00632

Rinne, P. L. H., Kaikuranta, P. M., & Van Schoot, C. Der. (2001). The shoot apical meristem restores its symplasmic organization during chilling-induced release from dormancy. Plant Journal, 26(3), 249–264. https://doi.org/10.1046/j.1365-313X.2001.01022.x

Rinne, P. L. H., Welling, A., Vahala, J., Ripel, L., Ruonala, R., Kangasjärvi, J., & van der Schoot, C. (2011). Chilling of dormant buds hyper induces FLOWERING LOCUS T and recruits GA-inducible 1,3-β-Glucanases to reopen signal conduits and release dormancy in *Populus*. The Plant Cell, 23(1), 130–146. https://doi.org/10.1105/tpc.110.081307

Rivero, R. M., Kojima, M., Gepstein, A., Sakakibara, H., Mittler, R., Gepstein, S., & Blumwald, E. (2007). Delayed leaf senescence induces extreme drought tolerance in a flowering plant. Proceedings of the National Academy of Sciences, 104(49), 19631–19636. https://doi.org/10.1073/pnas.0709453104

Robinson, M. D., & Oshlack, A. (2010). A scaling normalization method for differential expression analysis of RNA-seq data. Genome Biology, 11(3), R25. https://doi.org/10.1186/gb-2010-11-3-r25

Rodriguez, M. C. S., Edsgärd, D., Hussain, S. S., Alquezar, D., Rasmussen, M., Gilbert, T., … Mundy, J. (2010). Transcriptomes of the desiccation-tolerant resurrection plant *Craterostigma plantagineum*. Plant Journal, 63(2), 212–228. https://doi.org/10.1111/j.1365-313X.2010.04243.x

Rottet, S., Besagni, C., & Kessler, F. (2015). The role of plastoglobules in thylakoid lipid remodeling during plant development. Biochimica et Biophysica Acta, 1847(9), 889–899. https://doi.org/10.1016/j.bbabio.2015.02.002

Rottmann, T., Zierer, W., Subert, C., Sauer, N., & Stadler, R. (2016). STP10 encodes a high-affinity monosaccharide transporter and is induced under low-glucose conditions in pollen tubes of Arabidopsis. Journal of Experimental Botany, 67(8), 2387–2399. https://doi.org/10.1093/jxb/erw048

Ruan, Y. L., Jin, Y., Yang, Y. J., Li, G. J., & Boyer, J. S. (2010). Sugar input, metabolism, and signaling mediated by invertase: Roles in development, yield potential, and response to drought and heat. Molecular Plant, 3(6), 942–955. https://doi.org/10.1093/mp/ssq044

Ruan, Y.-L. (2014). Sucrose metabolism: Gateway to diverse carbon use and sugar signaling. Annual Review of Plant Biology, 65(1), 33–67. https://doi.org/10.1146/annurev-arplant-050213-040251

Ruiz, M., Bodhicharla, R., Svensk, E., Devkota, R., Boren, J., & Pilon, M. (2018). Membrane fluidity is regulated by the *C . elegans* transmembrane protein FLD-1 and its human homologs TLCD1/2. ELife, 1–25.

Sablok, G., Powell, J. J., & Kazan, K. (2017). Emerging roles and landscape of translating mRNAs in plants. Frontiers in Plant Science, 8(September), 1–9. https://doi.org/10.3389/fpls.2017.01443

Sadeghipour, H. R., & Bhatla, S. C. (2002). Differential sensitivity of oleosins to proteolysis during oil body mobilization in sunflower seedlings. Plant Cell Physiology, 43(10), 1117–1126.

Sajeev, N., Bai, B., & Bentsink, L. (2019). Seeds: A unique system to study translational regulation. Trends in Plant Science, 1–9. https://doi.org/10.1016/j.tplants.2019.03.011

Sakuma, Y., Maruyama, K., Qin, F., Osakabe, Y., & Shinozaki, K. (2006). Dual function of an Arabidopsis transcription factor DREB2A in water-stress-responsive and heat-stress-responsive gene expression. PNAS, 103(49), 18822–18827.

Sato, N., & Awai, K. (2017). “Prokaryotic pathway” is not prokaryotic: Noncyanobacterial origin of the chloroplast lipid biosynthetic pathway revealed by comprehensive phylogenomic analysis. Genome Biology and Evolution, 9(11), 3162–3178. https://doi.org/10.1093/gbe/evx238

Sattler, S. E., Gilliland, L. U., Magallanes-Lundback, M., Pollard, M., & DellaPenna, D. (2004). Vitamin E is essential for seed longevity and for preventing lipid peroxidation during germination. The Plant Cell, 16(6), 1419–1432. https://doi.org/10.1105/tpc.021360

Schaffer, J. E. (2003). Lipotoxicity: when tissues overeat. Current Opinion in Lipidology, 14, 281–287. https://doi.org/10.1097/01.mol.0000073508.41685.7f

Schepetilnikov, M., & Ryabova, L. A. (2017). Recent discoveries on the role of TOR (Target of Rapamycin) Signaling in Translation in Plants. Plant Physiology, 176(2), 1095–1105. https://doi.org/10.1104/pp.17.01243

Schwacke, R., Ponce-Soto, G. Y., Krause, K., Bolger, A. M., Arsova, B., Hallab, A., … Usadel, B. (2019). MapMan4: A refined protein classification and annotation framework applicable to multi-omics data analysis. Molecular Plant, 12(6), 879–892. https://doi.org/10.1016/j.molp.2019.01.003

Scott, P. (2000). Resurrection plants and the secrets of eternal leaf. Annals of Botany, 85(2), 159–166. https://doi.org/10.1006/anbo.1999.1006

Seiwert, D., Witt, H., Janshoff, A., & Paulsen, H. (2017). The non-bilayer lipid MGDG stabilizes the major light- harvesting complex (LHCII) against unfolding. Scientific Reports, 7(June), 1–10. https://doi.org/10.1038/s41598-017-05328-7

Seo, P. J., & Park, C. M. (2011a). Cuticular wax biosynthesis as a way of inducing drought resistance. Plant Signaling and Behavior, 6(7), 125–127. https://doi.org/10.4161/psb.6.7.15606

Seo, P. J., Park, J. M., Kang, S. K., Kim, S. G., & Park, C. M. (2011b). An Arabidopsis senescence-associated protein SAG29 regulates cell viability under high salinity. Planta, 233(1), 189–200. https://doi.org/10.1007/s00425-010-1293-8

Serin, E. A. R., Nijveen, H., Hilhorst, H. W. M., & Ligterink, W. (2016). Learning from co-expression networks: Possibilities and challenges. Frontiers in Plant Science, 7(April), 1–18. https://doi.org/10.3389/fpls.2016.00444

Sesma, A., Castresana, C., & Castellano, M. M. (2017). Regulation of translation by TOR, eIF4E and eIF2α in plants: Current knowledge, challenges and future perspectives. Frontiers in Plant Science, 8(April), 2–8. https://doi.org/10.3389/fpls.2017.00644

Sessitsch, A., Mitter, B., Compant, S., Trognitz, F., & Brader, G. (2018). The plant microbiome: ecology and functioning of bacterial endophytes and how plants can benefit. 20th EGU General Assembly, EGU2018, Proceedings from the Conference Held 4-13 April, 2018 in Vienna, Austria, p.2201, 20, 2201. Retrieved from http://adsabs.harvard.edu/abs/2018EGUGA..20.2201S

Sharma, B., Joshi, D., Yadav, P. K., Gupta, A. K., & Bhatt, T. K. (2016a). Role of ubiquitin-mediated degradation system in plant biology. Frontiers in Plant Science, 7(June), 1–8. https://doi.org/10.3389/fpls.2016.00806

Sharma, S. S., Dietz, K. J., & Mimura, T. (2016b). Vacuolar compartmentalization as indispensable component of heavy metal detoxification in plants. Plant Cell and Environment, 39(5), 1112–1126. https://doi.org/10.1111/pce.12706

Sherwin, H. W., & Farrant, J. M. (1998). Protection mechanisms against excess light in the resurrection plants *Craterostigma wilmsii* and *Xerophyta viscosa*. Plant Growth Regulation, 24(3), 203–210. https://doi.org/10.1023/A:1005801610891

Shih, M. Der, Lin, S. C., Hsieh, J. S., Tsou, C. H., Chow, T. Y., Lin, T. P., & Hsing, Y. I. C. (2004). Gene cloning and characterization of a soybean (Glycine max L.) LEA protein, GmPM16. Plant Molecular Biology, 56(5), 689–703. https://doi.org/10.1007/s11103-004-4680-3

Shimada, T. L., Shimada, T., Takahashi, H., Fukao, Y., & Hara-nishimura, I. (2008). A novel role for oleosins in freezing tolerance of oilseeds in *Arabidopsis thaliana*. The Plant Journal, 55, 798–809. https://doi.org/10.1111/j.1365-313X.2008.03553.x

Shimada, T. L., Takano, Y., & Hara-Nishimura, I. (2015). Oil body-mediated defense against fungi: From tissues to ecology. Plant Signaling and Behavior, 10(2), 3–5. https://doi.org/10.4161/15592324.2014.989036

Shimada, T. L., Hayashi, M., & Hara-Nishimura, I. (2018). Membrane dynamics and multiple functions of oil bodies in seeds and leaves. Plant Physiology, 176(1), 199–207. https://doi.org/10.1104/pp.17.01522

Shivaraj, Y. N., Barbara, P., Gugi, B., Driouich, A., Govind, S. R., Devaraja, A., & Kambalagere, Y. (2018). Perspectives on structural, physiological, cellular, and molecular responses to desiccation in resurrection plants. Scientifica. 1-18.

Si, Y., Liu, P., Li, P., & Brutnell, T. P. (2014). Model-based clustering for RNA-seq data. Bioinformatics, 30(2), 197–205. https://doi.org/10.1093/bioinformatics/btt632

Siloto, R. M. P., Findlay, K., Lopez-Villalobos, Yeung, E. C., Nykiforruk, C. L., & Moloney, M. M. (2006). The accumulation of oleosins determines the size of seed oilbodies in Arabidopsis. The Plant Cell Online, 18(8), 1961–1974. https://doi.org/10.1105/tpc.106.041269

Silva, A. T., Ribone, P. A., Chan, R. L., Ligterink, W., & Hilhorst, H. W. M. (2016). A predictive coexpression network identifies novel genes controlling the seed-to-seedling phase transition in *Arabidopsis thaliana*. Plant Physiology, 170(4), 2218–2231. https://doi.org/10.1104/pp.15.01704

Simão, F. A., Waterhouse, R. M., Ioannidis, P., Kriventseva, E. V., & Zdobnov, E. M. (2015). BUSCO: Assessing genome assembly and annotation completeness with single-copy orthologs. Bioinformatics, 31(19), 3210–3212. https://doi.org/10.1093/bioinformatics/btv351

Slocombe, S. P., Cornah, J., Pinfield-Wells, H., Soady, K., Zhang, Q., Gilday, A., … Graham, I. A. (2009). Oil accumulation in leaves directed by modification of fatty acid breakdown and lipid synthesis pathways. Plant Biotechnology Journal, 7(7), 694–703. https://doi.org/10.1111/j.1467-7652.2009.00435.x

Šmarda, P., Bureš, P., Horová, L., Leitch, I. J., Mucina, L., Pacini, E., … Rotreklová, O. (2014). Ecological and evolutionary significance of genomic GC content diversity in monocots. Proceedings of the National Academy of Sciences, 111(39), E4096–E4102. https://doi.org/10.1073/pnas.1321152111

Solomon, M., Belenghi, B., Delledonne, M., Menachem, E., & Levine, A. (1999). The involvement of cysteine proteases and protease inhibitor genes in the regulation of programmed cell death in plants. The Plant Cell Online, 11(3), 431–443. https://doi.org/10.1105/tpc.11.3.431

Springmann, M., Clark, M., Mason-D'Croz, D., Wiebe, K., Bodirsky, B. L., Lassaletta, L., … Willett, W. (2018). Options for keeping the food system within environmental limits. Nature, 562(7728), 519–525. https://doi.org/10.1038/s41586-018-0594-0

Srivastava, S., Brychkova, G., Yarmolinsky, D., Soltabayeva, A., Samani, T., & Sagi, M. (2017). Aldehyde oxidase 4 plays a critical role in delaying silique senescence by catalyzing aldehyde detoxification. Plant Physiology, 173(4), 1977–1997. https://doi.org/10.1104/pp.16.01939

Stevenson, S. R., Kamisugi, Y., Trinh, C. H., Schmutz, J., Jenkins, J. W., Grimwood, J., … Cuming, A. C. (2016). Genetic analysis of *Physcomitrella patens* identifies ABSCISIC ACID NON-RESPONSIVE (ANR), a regulator of ABA responses unique to basal land plants and required for desiccation tolerance. The Plant Cell, 28(June), tpc.00091.2016. https://doi.org/10.1105/tpc.16.00091

Subramanian, S., Barry, A. N., Pieris, S., & Sayre, R. T. (2013). Comparative energetics and kinetics of autotrophic lipid and starch metabolism in chlorophytic microalgae: Implications for biomass and biofuel production. Biotechnology for Biofuels, 6(1), 1. https://doi.org/10.1186/1754-6834-6-150

Sun, C., Johnson, J. M., Cai, D., Sherameti, I., Oelmüller, R., & Lou, B. (2010). Piriformospora indica confers drought tolerance in Chinese cabbage leaves by stimulating antioxidant enzymes, the expression of drought-related genes and the plastid-localized CAS protein. Journal of Plant Physiology, 167(12), 1009–1017. https://doi.org/10.1016/j.jplph.2010.02.013

Sun, L., Liu, Y., Kong, X., Zhang, D., Pan, J., Zhou, Y., … Yang, X. (2012). ZmHSP16.9, a cytosolic class I small heat shock protein in maize (*Zea mays*), confers heat tolerance in transgenic tobacco. Plant Cell Reports, 31(8), 1473–1484. https://doi.org/10.1007/s00299-012-1262-8

Sun, R. Z., Lin, C. T., Zhang, X. F., Duan, L. X., Qi, X. Q., Gong, Y. H., & Deng, X. (2018). Acclimation-induced metabolic reprogramming contributes to rapid desiccation tolerance acquisition in

Boea hygrometrica. Environmental and Experimental Botany, 148(October 2017), 70–84. https://doi.org/10.1016/j.envexpbot.2018.01.008

Supek, F., Bošnjak, M., Škunca, N., & Šmuc, T. (2011). Revigo summarizes and visualizes long lists of gene ontology terms. PLoS ONE, 6(7). https://doi.org/10.1371/journal.pone.0021800

Suzuki, M., Kato, A., Nagata, N., & Komeda, Y. (2002). A xylanase, AtXyn1, is predominantly expressed in vascular bundles, and four putative xylanase genes were identified in the *Arabidopsis thaliana* genome. Plant and Cell Physiology, 43(7), 759–767. https://doi.org/10.1093/pcp/pcf088

Swiercz, A., Frohmberg, W., Kierzynka, M., Wojciechowski, P., Zurkowski, P., Badura, J., … Blazewicz, J. (2018). GRASShopPER—An algorithm for de novo assembly based on GPU alignments. PLoS ONE, 13(8), 1–23. https://doi.org/10.1371/journal.pone.0202355

Tadele, Z. (2009). New approaches to plant breeding of orphan crops in Africa (Z. Tadele, Ed.). Bern, Switzerland.

Tadele, Zerihun. (2018). African orphan crops under abiotic stresses: Challenges and opportunities. Scientifica, 2018, 1–19.

Taguchi, R., & Ishikawa, M. (2010). Precise and global identification of phospholipid molecular species by an Orbitrap mass spectrometer and automated search engine Lipid Search. Journal of Chromatography A, 1217(25), 4229–4239. https://doi.org/10.1016/j.chroma.2010.04.034

Takeno, K. (2016). Stress-induced flowering: The third category of flowering response. Journal of Experimental Botany, 67(17), 4925–4934. https://doi.org/10.1093/jxb/erw272

Tang, S., Li, L., Wang, Y., Chen, Q., Zhang, W., Jia, G., … Diao, X. (2017). Genotype-specific physiological and transcriptomic responses to drought stress in *Setaria italica* (an emerging model for Panicoideae grasses). Scientific Reports, 7(1), 1–15. https://doi.org/10.1038/s41598-017-08854-6

Tapia, H., & Koshland, D. E. (2014). Trehalose is a versatile and long-lived chaperone for desiccation tolerance. Current Biology, 24(23), 2758–2766. https://doi.org/10.1016/j.cub.2014.10.005

Thieme, C. J., Rojas-Triana, M., Stecyk, E., Schudoma, C., Zhang, W., Yang, L., … Kragler, F. (2015). Endogenous Arabidopsis messenger RNAs transported to distant tissues. Nature Plants, 1(April), 15025. https://doi.org/10.1038/nplants.2015.25https://www.nature.com/articles/nplants201525#supplementary-information

Thimm, O., Bläsing, O., Gibon, Y., Nagel, A., Meyer, S., Krüger, P., … Stitt, M. (2004). MAPMAN: A user-driven tool to display genomics data sets onto diagrams of metabolic pathways and other biological processes. Plant Journal, 37(6), 914–939. https://doi.org/10.1111/j.1365-313X.2004.02016.x

Thomas, H. (2013). Senescence, ageing and death of the whole plant. New Phytologist, 197, 696–711. https://doi.org/10.1111/nph.12047

TAIR (The Arabidopsis Information Resource). (2019a). https://www.arabidopsis.org/servlets/TairObject?type=locus&name=At1g50310, on www.arabidopsis.org, 2019.

TAIR (The Arabidopsis Information Resource). (2019b). https://www.arabidopsis.org/servlets/TairObject?id=32036&type=locus, on www.arabidopsis.org, 2019.

TAIR (The Arabidopsis Information Resource). (2019c). https://www.arabidopsis.org/servlets/TairObject?id=29379&type=locus, on www.arabidopsis.org, 2019.

Tjellström, H., Strawsine, M., & Ohlrogge, J. B. (2015). Tracking synthesis and turnover of triacylglycerol in leaves. Journal of Experimental Botany, 66(5), 1453–1461. https://doi.org/10.1093/jxb/eru500

Towbin, H., Staehelint, T., & Gordon, J. (1979). Electrophoretic transfer of proteins from polyacrylamide gels to nitrocellulose sheets: Procedure and some applications. Proceedings of the National Academy of Sciences, 76(9), 4350–4354.

Trapnell, C., Roberts, A., Goff, L., Pertea, G., Kim, D., Kelley, D. R., … Pachter, L. (2012). Differential gene and transcript expression analysis of RNA-seq experiments with TopHat and Cufflinks. Nature Protocols, 7(3), 562–578. https://doi.org/10.1038/nprot.2012.016

Trapnell, C., Hendrickson, D. G., Sauvageau, M., Goff, L., Rinn, J. L., & Pachter, L. (2013). Differential analysis of gene regulation at transcript resolution with RNA-seq. Nature Biotechnology, 31(1), 46–53. https://doi.org/10.1038/nbt.2450

Tshabuse, F., Farrant, J. M., Humbert, L., Moura, D., Rainteau, D., Espinasse, C., … Ruelland, E. (2018). Glycerolipid analysis during desiccation and recovery of the resurrection plant *Xerophyta humilis* (Bak) Dur and Schinz. Plant Cell and Environment, 41(3), 533–547. https://doi.org/10.1111/pce.13063

Tuba, Z., Lichtenthaler, H. K., Csintalan, Z., & Pócs, T. (1993). Regreening of desiccated leaves of the poikilochlorophyllous *Xerophyta scabrida* upon rehydration. Journal of Plant Physiology, 142(1), 103–108. https://doi.org/10.1016/S0176-1617(11)80115-X

Tuba, Z., & Lichtenthaler, H. K. (2011). Plant Desiccation Tolerance. In Plant Desiccation Tolerance. https://doi.org/10.1002/9780470376881

Tunnacliffe, A., & Wise, M. J. (2007). The continuing conundrum of the LEA proteins. Naturwissenschaften, 94(10), 791–812. https://doi.org/10.1007/s00114-007-0254-y

Turnbull, T. L., Deheinzelin, A. I., Adams, M. A., & Grains, W. (2017). Does triacylglycerol (TAG) serve a photoprotective function in plant leaves? An examination of leaf lipids under shading and drought. Physiol Plant, 161(3), 400–413. https://doi.org/10.1111/ppl.12601.Does

Tymms, M. J., Gaff, D. F., & Hallam, N. D. (1982). Protein synthesis in the desiccation tolerant angiosperm *Xerophyta villosa* during dehydration. Journal of Experimental Biology, 33(133), 332–343.

Tzen, J. T. C., & Huang, A. H. C. (1992). Surface structure and properties of plant seed oil bodies. Journal of Cell Biology, 117(2), 327–335. https://doi.org/10.1083/jcb.117.2.327

Umezawa, T., Fujita, M., Fujita, Y., Yamaguchi-Shinozaki, K., & Shinozaki, K. (2006). Engineering drought tolerance in plants: discovering and tailoring genes to unlock the future. Current Opinion in Biotechnology, 17(2), 113–122. https://doi.org/10.1016/j.copbio.2006.02.002

van der Schoot, C., Paul, L. K., Paul, S. B., & Rinne, P. L. H. (2011). Plant lipid bodies and cell-cell signaling a new role for an old organelle? Plant Signaling and Behavior, 6(11), 1732–1738. https://doi.org/10.4161/psb.6.11.17639

Van Loon, A. F., Gleeson, T., Clark, J., Van Dijk, A. I. J. M., Stahl, K., Hannaford, J., … Van Lanen, H. A. J. (2016). Drought in the Anthropocene. Nature Geoscience, 9(2), 89–91. https://doi.org/10.1038/ngeo2646

van Outshoorn, F. (2012). Guide to grasses of southern Africa (3rd ed.). Pretoria, South Africa: Briza Publications.

VanBuren, R., Bryant, D., Edger, P. P., Tang, H., Burgess, D., Challabathula, D., … Mockler, T. C. (2015). Single-molecule sequencing of the desiccation-tolerant grass Oropetium thomaeum. Nature, 527(7579), 508–511. https://doi.org/10.1038/nature15714

VanBuren, R., Wai, J., Zhang, Q., Song, X., Edger, P. P., Bryant, D., … Bartels, D. (2017). Seed desiccation mechanisms co-opted for vegetative desiccation in the resurrection grass Oropetium thomeaum. Plant, Cell & Environment, 40, 2292–2306. https://doi.org/10.1111/pce.13027

VanBuren, R., Wai, C. M., Pardo, J., Giarola, V., Ambrosini, S., Song, X., & Bartels, D. (2018). Desiccation tolerance evolved through gene duplication and network rewiring in Lindernia. The Plant Cell, 30(12), 2943–2958. https://doi.org/10.1105/tpc.18.00517

VanBuren, R., Pardo, J., Man Wai, C., Evans, S., & Bartels, D. (2019a). Massive tandem proliferation of ELIPs supports convergent evolution of desiccation tolerance across land plants. Plant Physiology, 179(3), 1040–1049. https://doi.org/10.1104/pp.18.01420

VanBuren, R., Wai, C. M., Pardo, J., Yocca, A. E., Wang, X., Wang, H., … Michael, T. P. (2019b). Exceptional subgenome stability and functional divergence in allotetraploid teff, the primary cereal crop in Ethiopia. BioRxiv, 580720. https://doi.org/10.1101/580720

Vance, J. E., & Vance, D. E. (2004). Phospholipid biosynthesis in mammalian cells. Biochemistry and Cell Biology, 82(1), 113–128. https://doi.org/10.1139/o03-073

Vander Willigen, C., Farrant, J. M., & Pammenter, N. W. (2001a). Anomalous pressure volume curves of resurrection plants do not suggest negative turgor. Annals of Botany, 88(4), 537–543. https://doi.org/10.1006/anbo.2001.1499

Vander Willigen, C., Pammenter, N. W., Mundree, S., & Farrant, J. (2001b). Some physiological comparisons between the resurrection grass, *Eragrostis nindensis*, and the related desiccation-sensitive species, *E. curvula*. Plant Growth Regulation, 35(2), 121–129. https://doi.org/10.1023/A:1014425619913

Vander Willigen, C., Pammenter, N. W., Jaffer, M. A., Mundree, S. G., & Farrant, J. M. (2003). An ultrastructural study using anhydrous fixation of *Eragrostis nindensis*, a resurrection grass with both desiccation-tolerant and -sensitive tissues. Functional Plant Biology, 30(3), 281–290. https://doi.org/10.1071/FP02221

Vander Willigen, C., Pammenter, N. W., Mundree, S. G., & Farrant, J. M. (2004). Mechanical stabilization of desiccated vegetative tissues of the resurrection grass *Eragrostis nindensis*: Does a TIP 3;1 and/or compartmentalization of subcellular components and metabolites play a role? Journal of Experimental Botany, 55(397), 651–661. https://doi.org/10.1093/jxb/erh089

Vanderlinde, E. M., Harrison, J. J., Muszyński, A., Carlson, R. W., Turner, R. J., & Yost, C. K. (2010). Identification of a novel ABC transporter required for desiccation tolerance, and biofilm formation in *Rhizobium leguminosarum* bv. viciae 3841. FEMS Microbiology Ecology, 71(3), 327–340. https://doi.org/10.1111/j.1574-6941.2009.00824.x

Varshney, R. K., Tuberosa, R., & Tardieu, F. (2018). Progress in understanding drought tolerance: from alleles to cropping systems. Journal of Experimental Botany, 69(13), 3175–3179. https://doi.org/10.1093/jxb/ery187

Veljovic-Jovanovic, S., Kukavica, B., Stevanovic, B., & Navari-Izzo, F. (2006). Senescence- and drought-related changes in peroxidase and superoxide dismutase isoforms in leaves of Ramonda serbica. Journal of Experimental Botany, 57(8), 1759–1768. https://doi.org/10.1093/jxb/erl007

Verbančič, J., Lunn, J. E., Stitt, M., & Persson, S. (2018). Carbon Supply and the Regulation of Cell Wall Synthesis. Molecular Plant, 11(1), 75–94. https://doi.org/10.1016/j.molp.2017.10.004

Vertucci, C. W., & Farrant, J. M. (1995). Acquisition and loss of desiccation tolerance. In J. Kigel & G. Galili (Eds.), *In Seed Development and Germination* (pp. 237–271). New York: Marcel Dekker Press Inc.

Vicré, M., Farrant, J. M., & Driouich, A. (2004). Insights into the cellular mechanisms of desiccation tolerance among angiosperm resurrection plant species. Plant, Cell and Environment, 27(11), 1329–1340. https://doi.org/10.1111/j.1365-3040.2004.01212.x

Von Kampen, J., Wettern, M., & Schulz, M. (1996). The ubiquitin system in plants. Physiologia Plantarum, 97(3), 618–624. https://doi.org/10.1034/j.1399-3054.1996.970326.x

Wallace, J. G., & May, G. (2018). Endophytes: The Other Maize Genome. In J. Bennetzen, S. Flint-Garcia, C. Hirsch, & R. Tuberosa (Eds.), The Maize Genome. Compendium of Plant Genomes. (pp. 213–246). Springer, Cham.

Walmsley, A. R., Barrett, M. P., Bringaud, F., & Gould, G. W. (1998). Sugar transporters from bacteria, parasites and mammals: Structure-activity relationships. Trends in Biochemical Sciences, 23(12), 476–481. https://doi.org/10.1016/S0968-0004(98)01326-7

Walters, C., Farrant, J. M., Pammenter, N. W., & Berjak, P. (2002). Desiccation and damage. In P. H. Black M (Ed.), Desiccation and Survival in Plants – Drying without Drying. Wallingford, UK: CABI Publishing.

Walz, C., Juenger, M., Schad, M., & Kehr, J. (2002). Evidence for the presence and activity of a complete antioxidant defence system in mature sieve tubes. Plant Journal, 31(2), 189–197. https://doi.org/10.1046/j.1365-313X.2002.01348.x

Wang, W., Vinocur, B., Shoseyov, O., & Altman, A. (2004). Role of plant heat-shock proteins and molecular chaperones in the abiotic stress response. Trends in Plant Science, 9(5), 244–252. https://doi.org/10.1016/j.tplants.2004.03.006

Wang, X., Chen, S., Zhang, H., Shi, L., Cao, F., Guo, L., … Dai, S. (2010). Desiccation tolerance mechanism in resurrection fern-ally *Selaginella tamariscina* revealed by physiological and proteomic analysis. Journal of Proteome Research, 9(12), 6561–6577. https://doi.org/10.1021/pr100767k

Wang, Z., & Benning, C. (2012a). Chloroplast lipid synthesis and lipid trafficking through ER–plastid membrane contact sites. Biochemical Society Transactions, 40(2), 457–463. https://doi.org/10.1042/bst20110752

Wang, Liping, Shen, W., Kazachkov, M., Chen, G., Chen, Q., Carlsson, A. S., … Zou, J. (2012b). Metabolic interactions between the lands cycle and the kennedy pathway of glycerolipid synthesis in Arabidopsis developing seeds. Plant Cell, 24(11), 4652–4669. https://doi.org/10.1105/tpc.112.104604

Wang, H., Airola, M. V, Reue, K., Coleman, R., & Hesselink, M. (2017). How lipid droplets “TAG” along: Glycerolipid synthetic enzymes and lipid. BBA - Molecular and Cell Biology of Lipids, 1862(10), 1131–1145. https://doi.org/10.1016/j.bbalip.2017.06.010

Wang, C., Schmich, F., Srivatsa, S., Weidner, J., Beerenwinkel, N., & Spang, A. (2018a). Context-dependent deposition and regulation of mRNAs in P-bodies. ELife, 7, 1–25. https://doi.org/10.7554/elife.29815

Wang, K., Tang, S. F., & Hou, X. (2018b). Molecular mechanism investigation on the interactions of copper (II) ions with glutathione peroxidase 6 from *Arabidopsis thaliana*. Spectrochimica Acta - Part A: Molecular and Biomolecular Spectroscopy, 203, 428–433. https://doi.org/10.1016/j.saa.2018.05.085

Wang, W., Li, X., Zhu, M., Tang, X., Wang, Z., Guo, K., Zhou, Y., Sun, Y., Zhang, W. & Li, X. (2019a). Arabidopsis GAAP1 to GAAP3 Play redundant role in cell death inhibition by suppressing the upregulation of salicylic acid pathway under endoplasmic reticulum stress. Frontiers in Plant Science 10 (August): 1–13. https://doi.org/10.3389/fpls.2019.01032.

Wang, Lishuan, Wang, C., Liu, X., Cheng, J., Li, S., Zhu, J. K., & Gong, Z. (2019b). Peroxisomal β-oxidation regulates histone acetylation and DNA methylation in Arabidopsis. Proceedings of the National Academy of Sciences of the United States of America, 116(21), 10576–10585. https://doi.org/10.1073/pnas.1904143116

Watanabe, M., Balazadeh, S., Tohge, T., Erban, A., Giavalisco, P., Kopka, J., … Hoefgen, R. (2013). Comprehensive dissection of spatiotemporal metabolic shifts in primary, secondary, and lipid metabolism during developmental senescence in Arabidopsis. Plant Physiology, 162(3), 1290–1310. https://doi.org/10.1104/pp.113.217380

Waters, E. R. (2013). The evolution, function, structure, and expression of the plant sHSPs. Journal of Experimental Botany, 64(2), 391–403. https://doi.org/10.1093/jxb/ers355

Wawer, I., Golisz, A., Sulkowska, A., Kawa, D., Kulik, A., & Kufel, J. (2018). mRNA decapping and 5'-3' decay contribute to the regulation of ABA signaling in *Arabidopsis thaliana*. Frontiers in Plant Science, 9(March), 1–12. https://doi.org/10.3389/fpls.2018.00312

Weaver, L. M., Gan, S., Quirino, B., & Amasino, R. M. (1998). A comparison of the expression patterns of several senescence-associated genes in response to stress and hormone treatment. Plant Molecular Biology, 37(3), 455–469. https://doi.org/10.1023/A:1005934428906

Weber, C., Nover, L., & Fauth, M. (2008). Plant stress granules and mRNA processing bodies are distinct from heat stress granules. Plant Journal, 56(4), 517–530. https://doi.org/10.1111/j.1365-313X.2008.03623.x

Weber, H., Borisjuk, L., Heim, U., Buchner, P., & Wobus, U. (1995). Seed coat-associated invertases of fava bean control both unloading and storage functions: Cloning of cDNAs and cell type-specific expression. The Plant Cell, 7(November), 1835–1846.

Welte, M. A. (2009). Fat on the move: intracellular motion of lipid droplets. Biochemical Society Transactions, 37(5), 991–996. https://doi.org/10.1042/bst0370991

Wesley-Smith, J. (2001). Freeze-substitution of dehydrated plant tissues: Artefacts of aqueous fixation revisited. Protoplasma, 218(3–4), 154–167. https://doi.org/10.1007/BF01306605

Whittaker, A., Bochicchio, A., Vazzana, C., Lindsey, G., & Farrant, J. M. (2001). Changes in leaf hexokinase activity and metabolite levels in response to drying in the desiccation-tolerant species *Sporobolus stapfianus* and *Xerophyta viscosa*. Journal of Experimental Botany, 52(358), 961–969. https://doi.org/10.1093/jexbot/52.358.961

Whittaker, A., Martinelli, T., Bochicchio, A., Vazzana, C., & Farrant, J. M. (2004). Comparison of sucrose metabolism during the rehydration of desiccation-tolerant and desiccation-sensitive leaf material of *Sporobolus stapfianus*. Physiologia Plantarum, 122(1), 11–20. https://doi.org/10.1111/j.1399-3054.2004.00346.x

Whittaker, A., Martinelli, T., Farrant, J. M., Bochicchio, A., & Vazzana, C. (2007). Sucrose phosphate synthase activity and the co-ordination of carbon partitioning during sucrose and amino acid accumulation in desiccation-tolerant leaf material of the C4 resurrection plant *Sporobolus stapfianus* during dehydration. Journal of Experimental Botany, 58(13), 3775–3787. https://doi.org/10.1093/jxb/erm228

Wijesundera, C., Boiteau, T., Xu, X., Shen, Z., Watkins, P., & Logan, A. (2013). Stabilization of fish oil-in-water emulsions with oleosin extracted from canola meal. Journal of Food Science, 78(9), 1–8. https://doi.org/10.1111/1750-3841.12177

Williams, B., Verchot, J., & Dickman, M. B. (2014). When supply does not meet demand-ER stress and plant programmed cell death. Frontiers in Plant Science, 5(June), 1–9. https://doi.org/10.3389/fpls.2014.00211

Williams, B., Njaci, I., Moghaddam, L., Long, H., Dickman, M. B., Zhang, X., & Mundree, S. (2015). Trehalose accumulation triggers autophagy during plant desiccation. PLoS Genetics, 11(12), 1–17. https://doi.org/10.1371/journal.pgen.1005705

Willigen, C. Vander. (2001). Comparisons of the resurrection grass, *Eragrostis nindensis*, with the related desiccation-sensitive species, *E. curvula*. Unpublished doctoral dissertation. University of Cape Town, Cape Town South Africa.

Wingler, A., Masclaux-Daubresse, C., & Fischer, A. M. (2009). Sugars, senescence, and ageing in plants and heterotrophic organisms. Journal of Experimental Botany, 60(4), 1063–1066. https://doi.org/10.1093/jxb/erp067

Woo, H. R., Kim, H. J., Nam, H. G., & Lim, P. O. (2013). Plant leaf senescence and death - regulation by multiple layers of control and implications for aging in general. Journal of Cell Science, 126(21), 4823–4833. https://doi.org/10.1242/jcs.109116

Woo, Hye Ryun, Masclaux-Daubresse, C., & Lim, P. O. (2018). Plant senescence: How plants know when and how to die. Journal of Experimental Botany, 69(4), 715–718. https://doi.org/10.1093/jxb/ery011

Wood, A. J., & Oliver, M. J. (1999). Translational control in plant stress: The formation of messenger ribonucleoprotein particles (mRNPs) in response to desiccation of *Tortula ruralis* gametophytes. Plant Journal, 18(4), 359–370. https://doi.org/10.1046/j.1365-313X.1999.00458.x

Wright, K. M., & Oparka, K. J. (2006). The ER within plasmodesmata. Plant Cell Monographs, 4(February), 279–308. https://doi.org/10.1007/7089_060

Xiao, L., Yang, G., Zhang, L., Yang, X., Zhao, S., Ji, Z., … He, Y. (2015). The resurrection genome of *Boea hygrometrica*: A blueprint for survival of dehydration. Proceedings of the National Academy of Sciences, 112(18), 5833–5837. https://doi.org/10.1073/pnas.1505811112

Xu, S. M., Brill, E., Llewellyn, D. J., Furbank, R. T., & Ruan, Y. L. (2012). Overexpression of a potato sucrose Synthase gene in cotton accelerates leaf expansion, reduces seed abortion, and enhances fiber production. Molecular Plant, 5(2), 430–441. https://doi.org/10.1093/mp/ssr090

Xu, Q., Chen, S., Yunjuan, R., Chen, S., & Liesche, J. (2018a). Regulation of sucrose transporters and phloem loading in response to environmental cues. Plant Physiology, 176(1), 930–945. https://doi.org/10.1104/pp.17.01088

Xu, Z., Xin, T., Bartels, D., Li, Y., Gu, W., Yao, H., … Chen, S. (2018b). Supplementary Data: Genome analysis of the ancient tracheophyte *Selaginella tamariscina* reveals evolutionary features relevant to the acquisition of desiccation tolerance. Molecular Plant, 11(7), 983–994. https://doi.org/10.1016/j.molp.2018.05.003

Yabe, T. (2004). The Arabidopsis chloroplastic NifU-like protein CnfU, which can act as an iron-sulfur cluster scaffold protein, is required for biogenesis of ferredoxin and photosystem I. The Plant Cell Online, 16(4), 993–1007. https://doi.org/10.1105/tpc.020511

Yamaji, N., & Ma, J. F. (2009). A Transporter at the Node Responsible for Intervascular Transfer of Silicon in Rice. The Plant Cell Online, 21(9), 2878–2883. https://doi.org/10.1105/tpc.109.069831

Yang, Z., & Ohlrogge, J. B. (2009). Turnover of fatty acids during natural senescence of Arabidopsis, brachypodium, and switchgrass and in Arabidopsis β-oxidation mutants. Plant Physiology, 150(4), 1981–1989. https://doi.org/10.1104/pp.109.140491

Yang, S., Zeng, X., Li, T., Liu, M., Zhang, S., Gao, S., … Yang, C. (2012). AtACDO1, an ABC1-like kinase gene, is involved in chlorophyll degradation and the response to photooxidative stress in

Arabidopsis. Journal of Experimental Botany, 63(2), 695–709. https://doi.org/10.1093/jxb/err313

Yang, Y., & Benning, C. (2018). Functions of triacylglycerols during plant development and stress. Current Opinion in Biotechnology, 49, 191–198. https://doi.org/10.1016/j.copbio.2017.09.003

Yau, Y.-Y., & Simon, P. W. (2003). A 2.5-kb insert eliminates acid soluble invertase isozyme II transcript in carrot (Daucus carota L.) roots, causing high sucrose accumulation. Plant Molecular Biology, 53, 151–162. https://doi.org/10.1023/b

Yobi, A., Schlauch, K. A., Tillett, R. L., Yim, W. C., Espinoza, C., Wone, B. W. M., … Oliver, M. J. (2017). *Sporobolus stapfianus*: Insights into desiccation tolerance in the resurrection grasses from linking transcriptomics to metabolomics. BMC Plant Biology, 17(1), 67. https://doi.org/10.1186/s12870-017-1013-7

Yolcu, S., Li, X., Li, S., & Kim, Y. J. (2018). Beyond the genetic code in leaf senescence. Journal of Experimental Botany, 69(4), 801–810. https://doi.org/10.1093/jxb/erx401

Yoshida, S. (1965). Chemical aspects of the role of silicon in physiology of the rice plant. Bulletin of the National Institute of Agricultural Sciences, 15, 1–58.

Zhang, L., Ohta, A., Takagi, M., & Imai, R. (2000). Expression of plant group 2 and group 3 lea genes in Saccharomyces cerevisiae revealed functional divergence among LEA proteins. Journal of Biochemistry, 127(4), 611–616. https://doi.org/10.1093/oxfordjournals.jbchem.a022648

Zhang, Z., Wang, B., Sun, D., & Deng, X. (2013). Molecular cloning and differential expression of sHSP gene family members from the resurrection plant Boea hygrometrica in response to abiotic stresses. Biologia (Poland), 68(4), 651–661. https://doi.org/10.2478/s11756-013-0204-4

Zhang, Q., & Bartels, D. (2016). Physiological factors determine the accumulation of D-glycero-D-ido-octulose (D-g-D-i-oct) in the desiccation tolerant resurrection plant *Craterostigma plantagineum*. Functional Plant Biology, 43(7), 684–694. https://doi.org/10.1071/FP15278

Zhang, Y., Zhao, L., Zhao, J., Li, Y., Wang, J., Guo, R., … Zhang, K. (2017). S5H/DMR6 Encodes a Salicylic Acid 5-Hydroxylase That Fine-Tunes Salicylic Acid Homeostasis. Plant Physiology, 175(3), 1082–1093. https://doi.org/10.1104/pp.17.00695

Zhang, Q., Song, X., & Bartels, D. (2016). Enzymes and Metabolites in Carbohydrate Metabolism of Desiccation Tolerant Plants. Proteomes, 4(4), 40. https://doi.org/10.3390/proteomes4040040

Zhang, Z. S., Liu, M. J., Scheibe, R., Selinski, J., Zhang, L. T., Yang, C., … Gao, H. Y. (2017). Contribution of the Alternative Respiratory Pathway to PSII Photoprotection in C3 and C4 Plants. Molecular Plant, 10(1), 131–142. https://doi.org/10.1016/j.molp.2016.10.004

Zhang, Q., Song, X., & Bartels, D. (2018). Sugar metabolism in the desiccation tolerant grass *Oropetium thomaeum* in response to environmental stresses. Plant Science, 270(November 2017), 30–36. https://doi.org/10.1016/j.plantsci.2018.02.004

Zhao, Y. (2012). Auxin biosynthesis: A simple two-step pathway converts tryptophan to indole-3-Acetic acid in plants. Molecular Plant, 5(2), 334–338. https://doi.org/10.1093/mp/ssr104

Zhu, Y., Wang, B., Phillips, J. R., Zhang, Z. N., Du, H., Xu, T., … Deng, X. (2015). Global transcriptome analysis reveals acclimation-primed processes involved in the acquisition of desiccation tolerance in Boea hygrometrica. Plant and Cell Physiology, 56(7), 1429–1441. https://doi.org/10.1093/pcp/pcv059

Zia, A., Walker, B. J., Oung, H. M. O., Charuvi, D., Jahns, P., Cousins, A. B., … Kirchhoff, H. (2016). Protection of the photosynthetic apparatus against dehydration stress in the resurrection plant *Craterostigma pumilum*. Plant Journal, 87(6), 664–680. https://doi.org/10.1111/tpj.13227

Zwack, P. J., Compton, M. A., Adams, C. I., & Rashotte, A. M. (2016). Cytokinin response factor 4 (CRF4) is induced by cold and involved in freezing tolerance. Plant Cell Reports, 35(3), 573–584. https://doi.org/10.1007/s00299-015-1904-8

APPENDIX 1

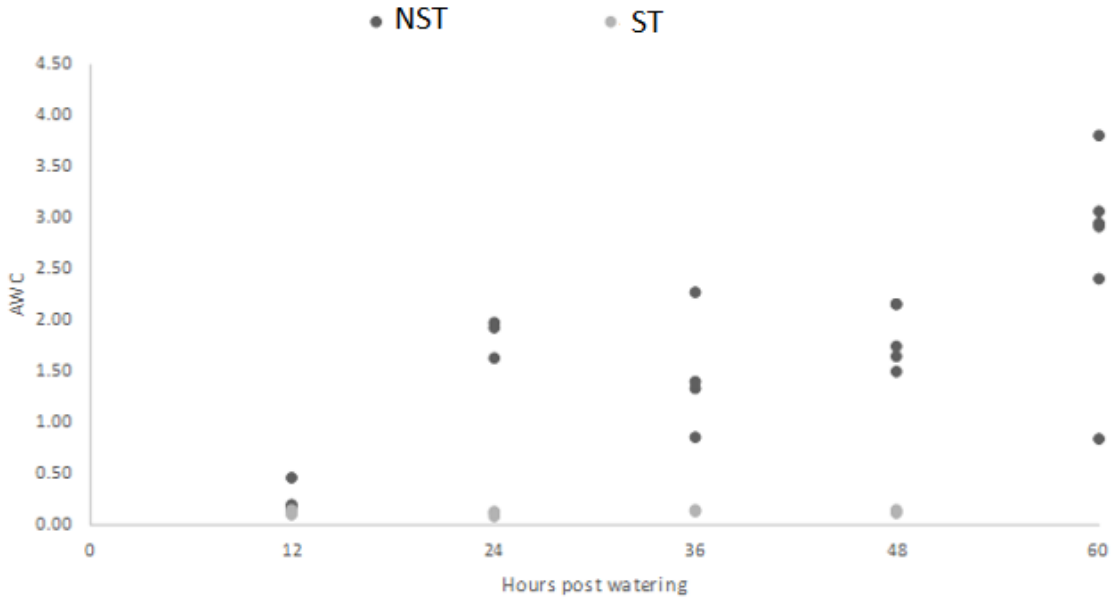

Figure A1: Changes in absolute water content (AWC) upon rehydration amongst individual plants of the resurrection plant *Eragrostis nindensis* in both desiccation tolerant (non-senescent tissue, NST) and desiccation sensitive (senescent tissue, ST) leaves.

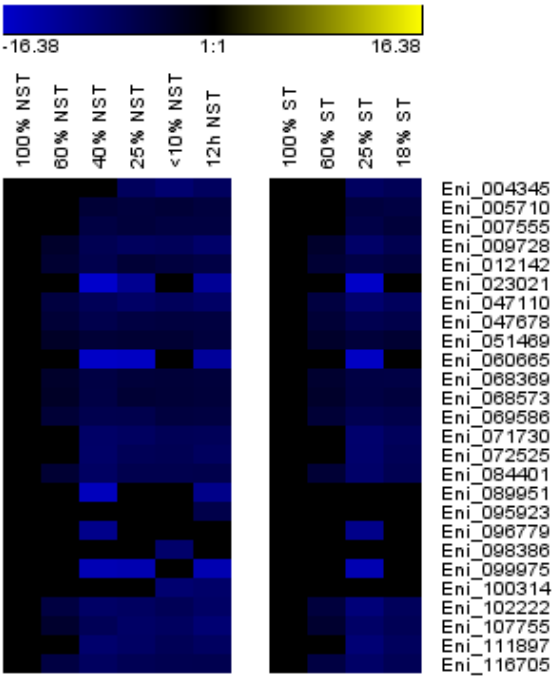

Figure A2: Heatmap showing transcript abundance trends of chlorophyll a/b binding transcripts diminishing in desiccation tolerant (non-senescent tissue, NST) and desiccation sensitive (senescent tissues, ST) leaves of the resurrection plant *Eragrostis nindensis* upon severe water-deficit stress (%) and rehydration (12h). Only differentially expressed genes (DEGs) are depicted, derived from the statistically significant change (>2 or <-2 log_2 fold change, FDR <0.05) in transcript abundance compared to the control (NST, 100% RWC). The colour scale represents log_2 fold change values.

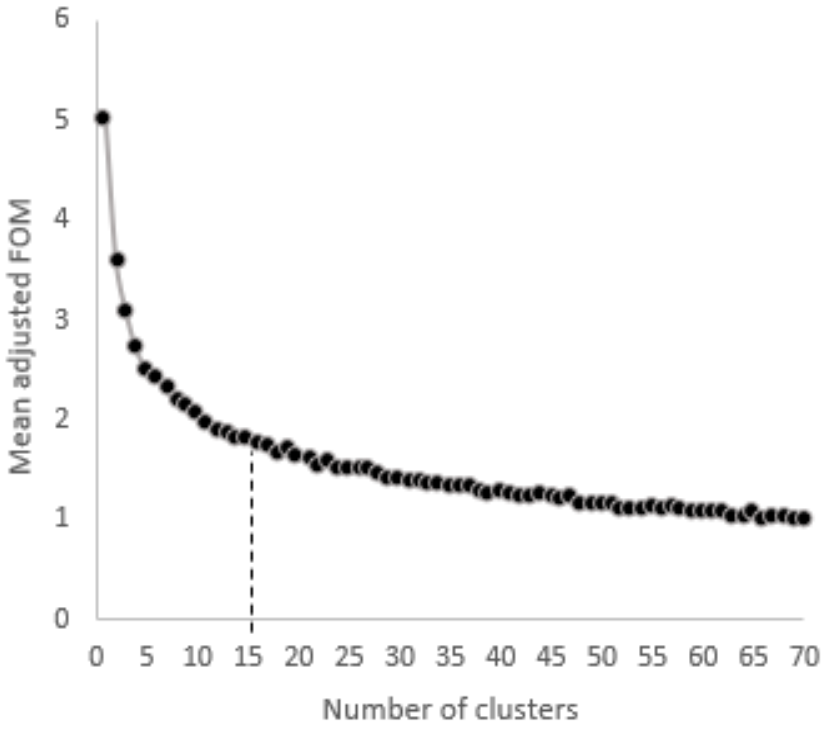

Figure A3: A FOM (Figures of Merit) was performed to find the number of clusters (15, dashed line) by generating reproducible clusters of co-expressed differentially expressed genes.

Gene ID	100% NST	60% NST	40% NST	25% NST	<10% NST	12 h NST	100% ST	60% ST	25% ST	18% ST	AT homologue	Mercator	Chapter
Eni_004103											AT1G58370	cell wall degradation	3
Eni_011626											AT5G50740	metal handling	3
Eni_064039											AT5G49940	protein assembly & cofactor ligation	3
Eni_066920											AT4G37670	NAGS2	4
Eni_109563											AT5G49690	UDP-glycosyltransferase	4
Eni_079766											AT3G22840	ELIP1	4
Eni_076914											AT3G22840	ELIP1	4
Eni_079064											AT3G22840	ELIP1	4
Eni_104042											AT3G22840	ELIP1	4
Eni_104044											AT4G14690	ELIP2	4
Eni_079763											AT4G14690	ELIP2	4
Eni_076909											AT4G14690	ELIP2	4
Eni_079767											AT4G14690	ELIP2	4
Eni_076917											AT4G14690	ELIP2	4
Eni_079059											AT3G22840	ELIP1	4
Eni_079771											AT4G14690	ELIP2	4
Eni_079773											AT4G14690	ELIP2	4
Eni_105818											AT3G14080	LSM domain	4

Figure A4: Heatmap showing DEGs mentioned in text of *Eragrostis nindensis* hat were differentially expressed during drying represented as relative water content (%) and rehydration (12h) in the non-senescent tissue (NST) and senescent tissue (ST). AT = *Arabidopsis thaliana.*

Table A1: Description of the number of plants used for each assay per dehydration curve experiment of *Eragrostis nindensis*.

Dehydration curve	No. plants	Age of plants	Assay
1	5	years	RWC determination
2	20	>8-months	gas exchange, microscopy
3	20	>8-months	gas exchange, chlorophyll
4	32	>8-months	RNAseq, protein, lipids
5	14	years	lipid, protein

Table A2: The transcriptome was constructed from high quality RNA (indicated by the RNA Integrity Number (RIN) and corresponding RNA concentration (ng/µl)) and had a high degree of mapping to the *E. nindensis* genome (90% average) using HISAT2. RNA extracted from three biological replicates from each relative water content (RWC) was assessed for quality before sequencing. RIN and RNA concentration (ng/µl) derived from bioanalysis and Q-bit analysis, respectively, were conducted at Queensland University of Technology (Australia) upon the arrival of the samples. Once sequenced, the samples were mapped to the *E. nindensis* genome using HISAT2 with the percentage (%) mapped shown.

RWC group	RWC (%)	Plant	Leaf type	RIN	RNA (ng/µl)	Mapped (%)
100%	98	3	NST	8.2	110	94%
100%	98	18	NST	8.3	109	87%
100%	94	23	NST	7.5	106	94%
100%	94	3	ST	7.3	132	95%
100%	97	18	ST	7.4	76.2	94%
100%	96	23	ST	7.5	110	88%
60%	59	7	NST	7.9	131	94%
60%	65	22	NST	8.1	151	95%
60%	64	26	NST	7.9	149	88%
60%	56	7	ST	7.7	121	95%
60%	62	22	ST	7.5	101	95%
60%	54	26	ST	8.1	131	87%
40%	42	10	NST	7.3	584	94%
40%	41	16	NST	8.3	97.8	87%
40%	40	32	NST	7.5	121	94%
25%	27	6	NST	7.9	120	92%
25%	25	8	NST	8.1	110	93%
25%	26	21	NST	8.3	116	78%
25%	23	9	ST	8.3	51.4	88%
25%	33	10	ST	8	130	92%
25%	28	21	ST	7.8	189	92%
18%	18	6	ST	7.4	69.2	91%
18%	17	8	ST	7.6	120	88%
18%	18	16	ST	7.8	98.6	85%
<10%	8	12	NST	7.6	150	90%
<10%	9	13	NST	7.8	278	81%
<10%	18	19	NST	7.1	270	93%
12 h	11	4	NST	7.5	132	90%
12 h	29	27	NST	6.5	188	91%
12 h	17	29	NST	7.7	450	82%

Table A3: Sequence quality of desiccation tolerant, non-senescent tissue (NST) and desiccation sensitive, senescent tissue (ST) of the resurrection plant *Eragrostis nindensis* was achieved by removing the adaptors from the reads with Trimmomatic v0.33 (Bolger *et al.* 2014). Representative paired-end reads are shown, with the corresponding GC-content and the number of sequences (seq) trimmed before and after quality control. Forward and reverse reads were properly aligned with the same number of reads (n = 559641524). The following parameters were used: HEADCROP – 12, CROP – 149, SLIDINGWINDOW 4, 24 and MINLEN 50. The minimum quality for all trimmed read nucleotide bases was a 24 PHRED score and the range of sequence length were 35-151 and 50-139 for the raw and trimmed reads respectively.

				raw reads		trimmed reads		
sample ID	**type**	**sample**	**RWC**	**#seq (raw)**	**GC%**	**#seq (trim)**	**GC%**	**% trimmed**
100%	NST	18i	98%	56111211	50	34598910	49	38
100%	ST	23o	96%	56949190	49	36240037	49	36
60%	NST	26i	64%	64323445	49	40856459	48	36
60%	ST	26o	54%	60582160	50	38068400	49	37
40%	NST	16i	41%	81909293	50	51872122	49	37
25%	NST	21i	26%	27012683	50	14361736	50	47
25%	ST	9o	23%	42201931	49	26764215	49	37
18%	ST	16o	18%	60142940	51	37224491	50	38
<10%	NST	13i	9%	49374085	53	29394062	52	40
12 h	NST	4i	11%	61034586	52	37081592	51	39
Total				559641524		346462024		39

Table A4: GO terms enriched in non-senescent tissue (NST) of *Eragrostis nindensis* exclusively accumulating in transcripts during 12h post rehydration. Categories highlighted in green are discussed in the thesis, Frequency (Freq.), uniqueness (Uniq.), dispensability (Disp.). Top 20 GO categories are shown.

Term ID	Description	Freq.	Uniq.	Disp.
GO:0046037	GMP metabolic process	0.12%	0.72	0
GO:0051329	mitotic interphase	0.00%	0.97	0
GO:0006807	nitrogen compound metabolic process	38.74%	0.96	0.02
GO:0071454	cellular response to anoxia	0.00%	0.77	0.02
GO:0061077	chaperone-mediated protein folding	0.04%	0.94	0.02
GO:0006457	protein folding	0.90%	0.93	0.03
GO:0017003	protein-heme linkage	0.02%	0.88	0.04
GO:0006606	protein import into nucleus	0.10%	0.8	0.06
GO:0080153	negative regulation of reductive pentose-phosphate cycle	0.00%	0.78	0.08
GO:0000082	G1/S transition of mitotic cell cycle	0.06%	0.88	0.13
GO:0006396	RNA processing	3.21%	0.81	0.19
GO:0018315	molybdenum incorporation into molybdenum-molybdopterin complex	0.00%	0.91	0.23
GO:0042040	metal incorporation into metallo-molybdopterin complex	0.00%	0.91	0.23
GO:0042221	response to chemical	3.07%	0.82	0.25
GO:0010288	response to lead ion	0.00%	0.85	0.3
GO:0015760	glucose-6-phosphate transport	0.00%	0.89	0.31
GO:0008652	cellular amino acid biosynthetic process	2.93%	0.6	0.31
GO:0046321	positive regulation of fatty acid oxidation	0.00%	0.73	0.31
GO:0009635	response to herbicide	0.00%	0.84	0.31
GO:0009308	amine metabolic process	0.52%	0.83	0.32

Table A5: GO terms enriched in non-senescent tissue (NST) of *Eragrostis nindensis* exclusively accumulating in transcripts upon drying. Frequency (freq.), uniqueness (uniq.), dispensability (disp.). Transcripts are the number of transcripts in the category. Ratio (expected to observed number of transcripts) represents the degree that each category is overrepresented, corrected p-value refers to significance * <0.05, ** <0.01, * <0.001. Categories highlighted in green indicate those represented in the exclusive analysis Figure 4.13.1. The top 20 GO categories are shown.**

Term ID	Description	Freq.	Uniq.	Disp.	Transcripts	Ratio	Corr p-val
GO:0009082	amino acid biosynthetic process	0.40%	0.66	0	7	0.02	***
GO:0009408	response to heat	0.17%	0.8	0	23	0.05	***
GO:0051131	chaperone-mediated protein complex assembly	0.02%	0.95	0.02	3	0.01	*
GO:0015760	glucose-6-phosphate transport	0.00%	0.83	0.05	3	0.01	**
GO:0010029	regulation of seed germination	0.01%	0.78	0.05	11	0.02	**
GO:0006396	RNA processing	3.21%	0.81	0.13	37	0.08	**
GO:0010467	gene expression	19.67%	0.91	0.22	92	0.21	*
GO:0032006	regulation of TOR signalling	0.04%	0.74	0.26	3	0.01	**
GO:0008380	RNA splicing	0.41%	0.81	0.35	19	0.04	**
GO:0016071	mRNA metabolic process	0.80%	0.83	0.37	25	0.06	**
GO:0006397	mRNA processing	0.56%	0.79	0.62	23	0.05	**
GO:0035303	regulation of dephosphorylation	0.05%	0.83	0.15	3	0.01	*
GO:0006808	regulation of nitrogen utilization	0.08%	0.86	0.18	3	0.01	*
GO:0080153	negative regulation of reductive pentose-phosphate cycle	0.00%	0.76	0.21	2	0.00	*
GO:0009749	response to glucose	0.03%	0.82	0.25	8	0.02	**
GO:0034641	cellular nitrogen compound metabolic process	34.14%	0.84	0.26	115	0.26	*
GO:0044106	cellular amine metabolic process	0.45%	0.82	0.26	23	0.05	*
GO:0046037	GMP metabolic process	0.12%	0.73	0.26	3	0.01	***
GO:0042991	transcription factor import into nucleus	0.02%	0.81	0.29	3	0.01	*
GO:0015990	electron transport coupled proton transport	0.01%	0.86	0.3	2	0.00	*

Table A6: GO terms enriched in senescent tissue (ST) of *Eragrostis nindensis* exclusively accumulating in transcripts upon drying. Frequency (freq.), uniqueness (uniq.), dispensability (disp.), transcripts = number of transcripts in the category. Ratio (expected to observed number of transcripts) represents the degree that each category is overrepresented, corrected p-value refers to significance * <0.05, ** <0.01, * <0.001. Categories highlighted in green indicate those represented in the exclusive analysis Figure 4.13.1. Only two categories were enriched.**

Term ID	Description	Freq.	Uniq.	Disp.	Transcripts	Ratio	Corr p-val
GO:0042776	mitochondrial ATP synthesis coupled proton transport	0.00%	0	0	3	0.02	*
GO:0031930	mitochondria-nucleus signaling pathway	0.00%	0	0.04	3	0.02	*

Table A7: GO terms enriched in non-senescent tissue (NST) of *Eragrostis nindensis* exclusively diminishing in transcripts upon drying. Frequency (freq.), uniqueness (uniq.), dispensability (disp.), transcripts = number of transcripts in the category. Ratio (expected to observed number of transcripts) represents the degree that each category is overrepresented, corrected p-value refers to significance * <0.05, ** <0.01, * <0.001. Categories highlighted in green indicate those represented in the exclusive analysis Figure 4.13.2. Top 20 GO categories are shown.**

Term ID	Description	Freq.	Uniq.	Disp.	Transcripts	Ratio	Corr p-val
GO:0010149	senescence	0.14%	0.98	0	25	0.02	***
GO:0006468	protein phosphorylation	4.14%	0.89	0	98	0.09	***
GO:0023052	signalling	6.77%	0.98	0	129	0.12	*
GO:0006865	amino acid transport	0.81%	0.8	0	22	0.02	***
GO:0008152	metabolic process	75.39%	0.99	0	654	0.63	*
GO:0009611	response to wounding	0.13%	0.82	0	47	0.05	***
GO:0050896	response to stimulus	12.21%	0.98	0	403	0.39	***
GO:0051703	intraspecies interaction between organisms	0.02%	0.97	0	4	0.00	*
GO:0051704	multi-organism process	0.75%	0.98	0	124	0.12	**
GO:0009812	flavonoid metabolic process	0.02%	0.96	0.04	17	0.02	*
GO:0010260	animal organ senescence	0.00%	0.87	0.04	25	0.02	***
GO:0006558	L-phenylalanine metabolic process	0.08%	0.76	0.07	11	0.01	***
GO:0051553	flavone biosynthetic process	0.00%	0.84	0.08	8	0.01	***
GO:0061014	positive regulation of mRNA catabolic process	0.01%	0.84	0.11	4	0.00	**
GO:0019748	secondary metabolic process	0.14%	0.89	0.11	58	0.06	*
GO:0009698	phenylpropanoid metabolic process	0.02%	0.86	0.12	36	0.03	**
GO:0006725	cellular aromatic compound metabolic process	29.63%	0.92	0.14	63	0.06	**
GO:0010586	miRNA metabolic process	0.00%	0.91	0.16	4	0.00	*
GO:0006793	phosphorus metabolic process	13.51%	0.92	0.18	127	0.12	**
GO:0055114	oxidation-reduction process	15.06%	0.84	0.19	115	0.11	**

Table A8: GO terms enriched in senescent tissue (ST) of *Eragrostis nindensis* exclusively diminishing in transcripts upon drying. Frequency (freq.), uniqueness (uniq.), dispensability (disp.), transcripts = number of transcripts in the category. Ratio (expected to observed number of transcripts) represents the degree that each category is overrepresented, corrected p-value refers to significance * <0.05, ** <0.01, * <0.001. Categories highlighted in green indicate those represented in the exclusive analysis Figure 4.13.2. Only nine categories were enriched.**

Term ID	Description	Freq.	Uniq.	Disp.	Transcripts	Ratio	Corr p-val
GO:0015979	photosynthesis	0.18%	0.82	0	15	0.04	**
GO:0010103	stomatal complex morphogenesis	0.00%	0.44	0	7	0.02	*
GO:0030155	regulation of cell adhesion	0.13%	0.8	0	2	0.01	*
GO:0019484	beta-alanine catabolic process	0.00%	0.78	0.03	2	0.01	*
GO:0006833	water transport	0.01%	0.68	0.04	5	0.01	*
GO:0015833	peptide transport	0.30%	0.63	0.19	9	0.03	*
GO:0042044	fluid transport	0.02%	0.68	0.31	5	0.01	*
GO:0048367	shoot system development	0.05%	0.53	0.47	20	0.06	*
GO:0048579	negative regulation of long-day photoperiodism, flowering	0.00%	0.47	0.57	3	0.01	*

Table A9: List of the 93 DEGs belonging to the *'RNA processing'* category exclusively enriched in the non-senescent tissue (NST) of the resurrection plant *Eragrostis nindensis* discussed in Chapter 4. The DEG with the highest fold change was an LSM (Like-Sm ribonucleoprotein) domain (highlighted), which is an LSM1B involved in the LSM1-7 decapping activator complex (see Wawer *et al.* 2018; Chantarachot *et al.* 2018). AT = *Arabidopsis thaliana*. Top 20 GO DEGs are shown.

Gene_ID	100%	60%	40%	25%	<10%	Swissprot	AT homologue
Eni_054248		8.7	8.1	9.0	7.1	AP2 domain	AT4G27950
Eni_016595		6.4	6.1	6.6	5.6	ethylene.signal transduction	AT4G27950
Eni_092268			7.2	6.9	8.2	Peptidase C13 family	AT1G62710
Eni_105818			11.2	10.7		LSM domain	AT3G14080
Eni_055506				7.8	8.3	unclassified	AT5G56120
Eni_029299				6.6	6.8	Survival motor neuron (SMN) interacting protein 1	AT1G54380
Eni_091124			3.9	3.7	4.1	DNA.synthesis/chromatin structure	AT5G04050
Eni_037167		2.7	2.6	2.5	3.0	Brix domain	AT3G15460
Eni_065587					9.9	unclassified	AT4G20330
Eni_034656			3.1	3.1	3.2	Domain of unknown function (DUF296)	AT4G12080
Eni_045468				9.3		mTERF	AT2G03050
Eni_033408				4.1	5.2	heat	AT2G25140
Eni_025385		3.3		2.9	2.8	bZIP transcription factor	AT1G45249
Eni_110050			2.6	3.2	3.1	RNA polymerase Rpb1; domain 1	AT4G35800
Eni_110630				4.3	4.4	initiation	AT5G38640
Eni_004184					8.3	HSF-type DNA-binding	AT2G26150
Eni_116442			8.0			Ribosomal protein S21e	AT5G27700
Eni_052264					7.9	RWP-RK domain	AT1G18790
Eni_099202				4.1	3.8	unclassified	AT2G29760
Eni_091960					7.8	No apical meristem (NAM) protein	AT1G61110

Table A10: Post-transcriptional related DEGs upon desiccation (denoted as relative water content, %) and rehydration (12h) in the non-senescent tissue (NST) and senescent tissue (ST) of the resurrection plant *Eragrostis nindensis*. The colour scale represents log_2 fold change values, FDR <0.05. AT = *Arabidopsis thaliana* homologues. Annotations were derived from Mercator v4.0 (Schwacke *et al.* 2019). Top 20 DEGs are shown.

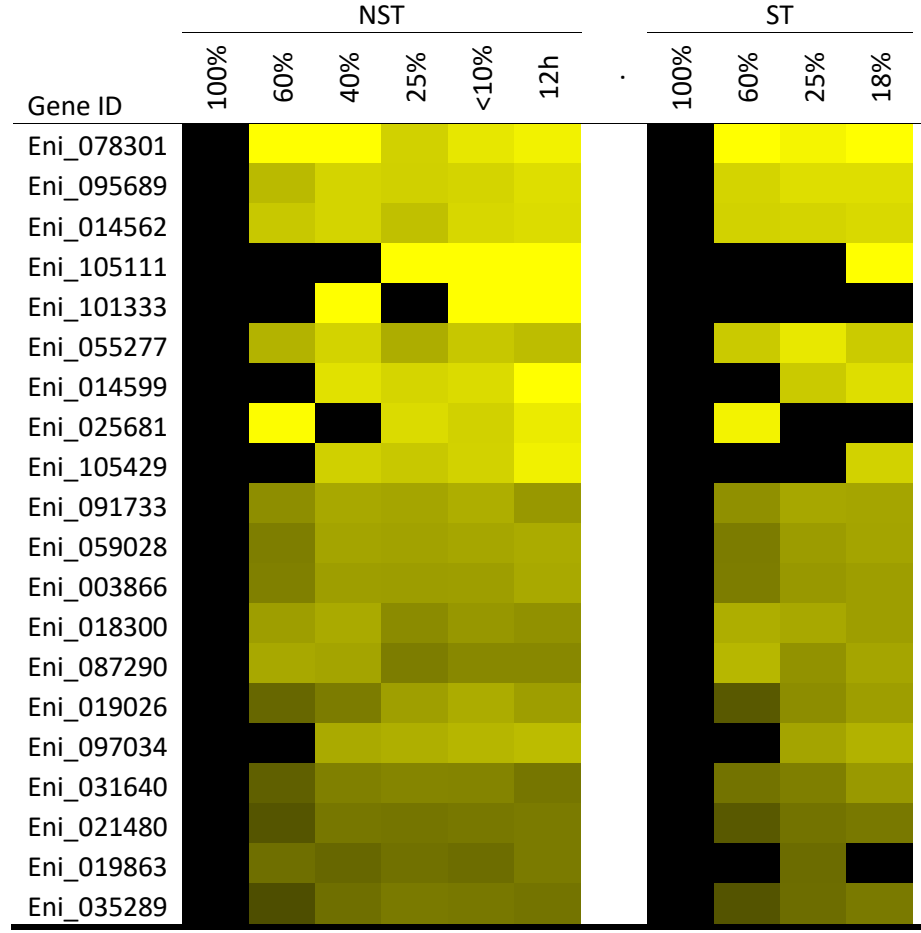

Gene ID	Mercator	AT homologue
Eni_078301	protein.postranslational modification	AT4G10010
Eni_095689	protein.postranslational modification	AT4G31750
Eni_014562	protein.postranslational modification	AT4G31750
Eni_105111	protein.postranslational modification	AT5G53140
Eni_101333	protein.postranslational modification.kinase.VII	AT5G02800
Eni_055277	protein.postranslational modification.kinase.VII	AT3G07070
Eni_014599	protein.postranslational modification.kinase	AT5G63370
Eni_025681	protein.postranslational modification.kinase.IV	AT4G00330
Eni_105429	protein.postranslational modification.kinase	AT5G63370
Eni_091733	protein.postranslational modification	AT4G33950
Eni_059028	protein.postranslational modification	AT4G33950
Eni_003866	protein.postranslational modification	AT4G33950
Eni_018300	protein.postranslational modification	AT4G10010
Eni_087290	protein.postranslational modification	AT1G71530
Eni_019026	protein.postranslational modification	AT4G33950
Eni_097034	protein.postranslational modification	AT4G33950
Eni_031640	protein.postranslational modification	AT3G25250
Eni_021480	protein.postranslational modification	AT5G58380
Eni_019863	protein.postranslational modification.kinase.IV	AT4G00330
Eni_035289	protein.postranslational modification	AT4G18700

Table A11: Protein synthesis related DEGs upon desiccation (denoted as relative water content, %) and rehydration (12h) in the non-senescent tissue (NST) and senescent tissue (ST) of the resurrection plant *Eragrostis nindensis*. The colour scale represents log_2 fold change values, FDR <0.05. AT = *Arabidopsis thaliana* homologues. Annotations were derived from Mercator v4.0 (Schwacke *et al.* 2019).

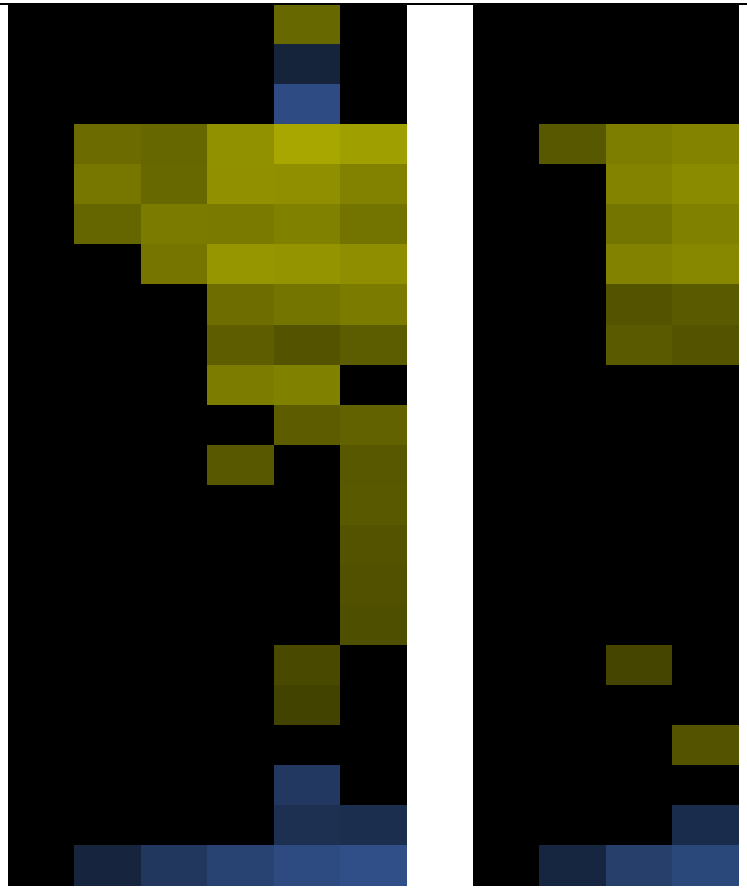

Gene ID	Mercator	AT homologue
Eni_062202	elongation	AT1G07910
Eni_081166	elongation	AT4G11120
Eni_078815	elongation	AT4G11120
Eni_055537	initiation	AT1G54290
Eni_073076	initiation	AT4G27130
Eni_003705	initiation	AT4G27130
Eni_064395	initiation	AT1G71350
Eni_034647	initiation	AT3G11400
Eni_095545	initiation	AT1G71350
Eni_110630	initiation	AT5G38640
Eni_090721	initiation	AT3G11400
Eni_116470	initiation	AT1G76820
Eni_069632	initiation	AT2G05830
Eni_051119	initiation	AT1G04170
Eni_029958	initiation	AT2G05830
Eni_086386	initiation	AT3G56150
Eni_041638	initiation	AT1G36730
Eni_107774	initiation	AT3G56150
Eni_072564	initiation	AT1G76720
Eni_013540	initiation	AT2G40780
Eni_073955	initiation	AT1G48410
Eni_063532	initiation	AT1G48410

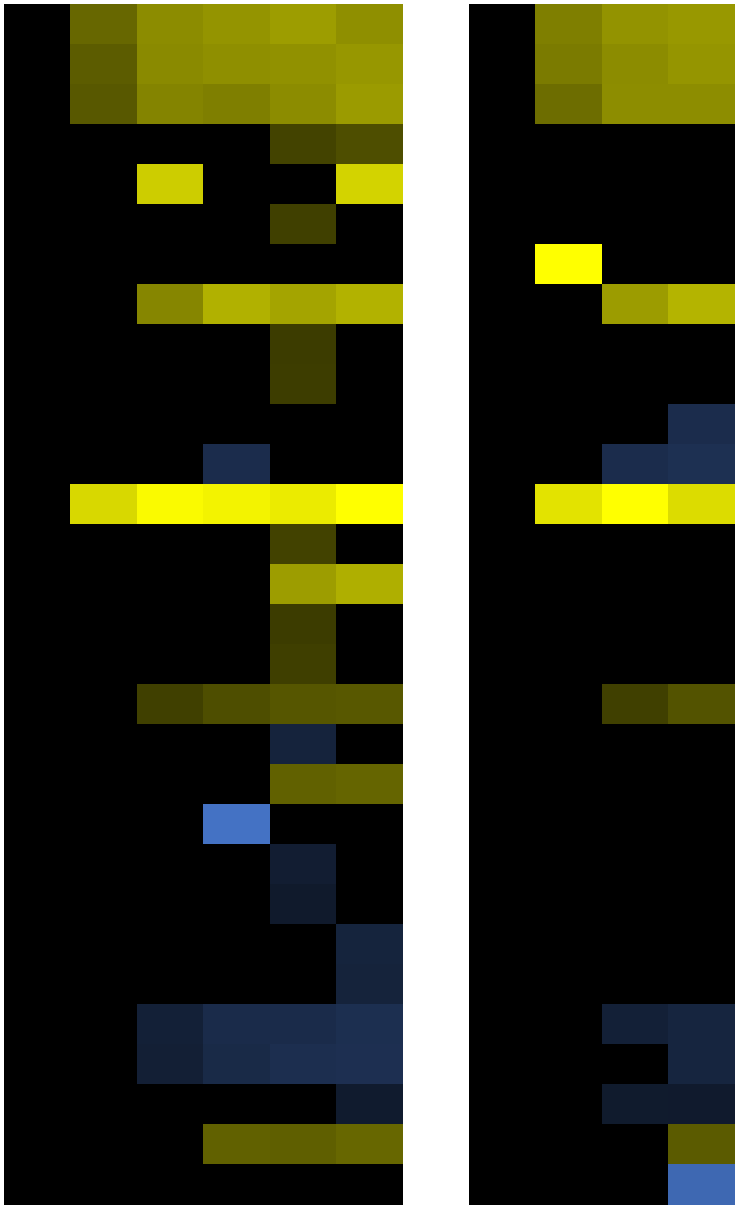

Eni_078417	release	AT3G26618
Eni_028587	release	AT3G26618
Eni_062974	release	AT3G26618
Eni_075348	40S subunit.S14	AT3G52580
Eni_116442	40S subunit.S21	AT5G27700
Eni_096330	40S subunit.S25	AT2G21580
Eni_005285	40S subunit.S27	AT1G23410
Eni_082639	40S subunit.S27	AT1G23410
Eni_052420	40S subunit.S3A	AT4G34670
Eni_008241	40S subunit.S7	AT3G02560
Eni_026487	40S subunit.S9	AT5G39850
Eni_034364	40S subunit.S9	AT5G39850
Eni_063765	60S subunit.L10	AT1G26910
Eni_078487	60S subunit.L12	AT2G37190
Eni_048460	60S subunit.L13	AT3G49010
Eni_021353	60S subunit.L13A	AT5G48760
Eni_089781	60S subunit.L18	AT5G27850
Eni_047742	60S subunit.L18A	AT2G34480
Eni_048113	60S subunit.L34	AT5G39785
Eni_099195	60S subunit.L34	AT3G01170
Eni_034485	60S subunit.L35A	AT1G74270
Eni_070430	chloroplast.30S subunit.S5	AT2G33800
Eni_068304	chloroplast.50S subunit.L15	AT3G25920
Eni_005352	chloroplast.50S subunit.L18	AT1G48350
Eni_022929	chloroplast.50S subunit.L21	AT1G35680
Eni_074969	chloroplast.50S subunit.L28	AT2G33450
Eni_096696	chloroplast.50S subunit.L28	AT2G33450
Eni_092023	chloroplast.50S subunit.L3	AT2G43030
Eni_060296	chloroplast.50S subunit.L34	AT3G06180
Eni_058077	chloroplast.50S subunit.L4	AT1G07320

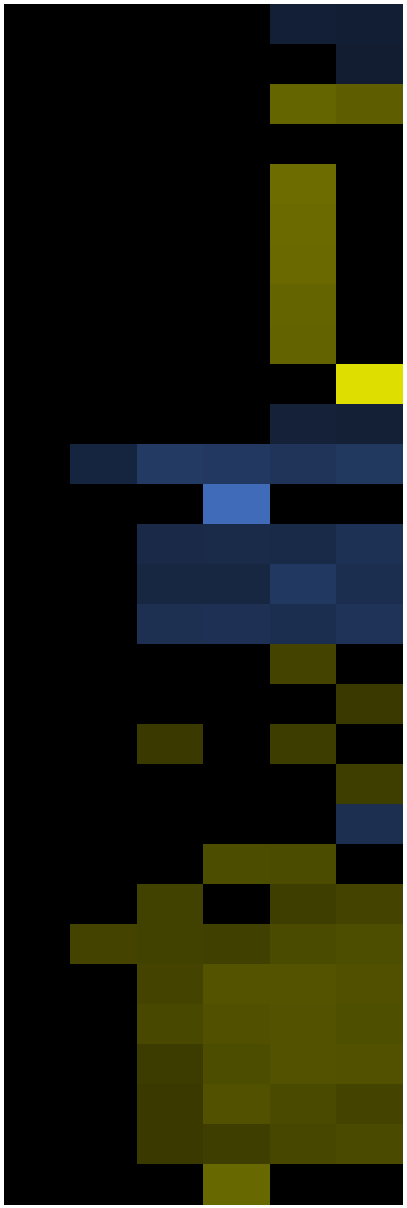

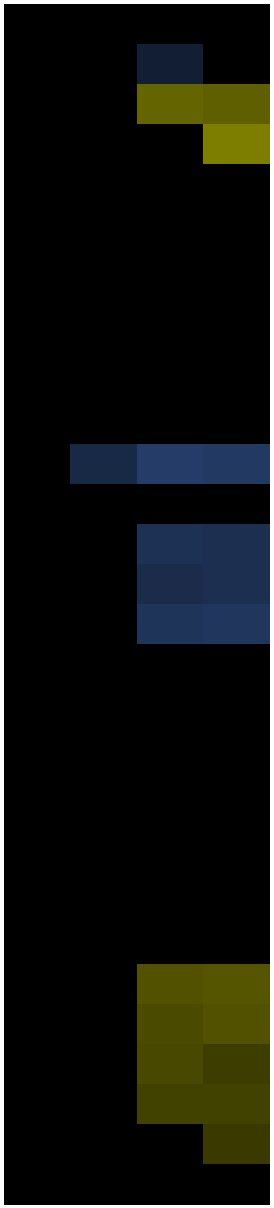

Eni_107911	chloroplast.50S subunit.L6	AT1G05190
Eni_040745	chloroplast.50S subunit.L9	AT3G44890
Eni_090880	mitochondrion.30S subunit.S2	AT3G03600
Eni_035976	mitochondrion.30S subunit.S2	AT3G03600
Eni_088712	mitochondrion.50S subunit.L2	ATMG00980
Eni_116575	mitochondrion.50S subunit.L2	ATMG00980
Eni_079977	mitochondrion.50S subunit.L2	ATMG00980
Eni_116058	mitochondrion.50S subunit.L2	ATMG00980
Eni_077820	mitochondrion.50S subunit.L2	ATMG00980
Eni_059035	unknown organellar.50S subunit.L10A	AT5G22440
Eni_066423	unknown organellar.50S subunit.L18	AT3G20230
Eni_004994	unknown organellar.50S subunit.L28	AT4G31460
Eni_109153	unknown organellar.50S subunit.L4	AT2G20060
Eni_107813	ribosomal protein.unknown.unknown	AT5G13720
Eni_001018	ribosomal protein.unknown.unknown	AT5G13720
Eni_065073	ribosomal protein.unknown.unknown	AT5G13720
Eni_061675	ribosomal RNA	AT2G37990
Eni_017332	ribosome biogenesis	AT3G22980
Eni_114114	ribosome biogenesis	AT1G52980
Eni_051642	ribosome biogenesis	AT1G42440
Eni_059837	ribosome biogenesis	AT5G38290
Eni_051146	ribosome biogenesis.Assembly factors.DExD-box helicases	AT5G05450
Eni_040198	ribosome biogenesis.Assembly factors.GTPases	AT1G06720
Eni_037167	ribosome biogenesis.BRIX	AT3G15460
Eni_005734	ribosome biogenesis.export from nucleus	AT5G60790
Eni_073820	ribosome biogenesis.export from nucleus	AT5G60790
Eni_062538	ribosome biogenesis.export from nucleus	AT1G43860
Eni_035881	ribosome biogenesis.export from nucleus	AT1G08410
Eni_107793	ribosome biogenesis.export from nucleus	AT1G08410
Eni_023161	ribosome biogenesis.export from nucleus	AT3G51270

Eni_041286	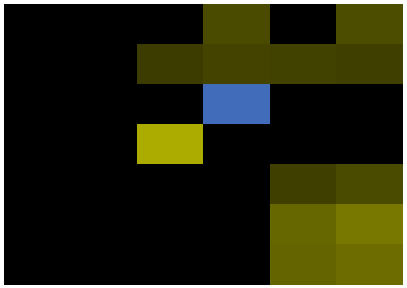	Pre-rRNA processing and modifications.DExD-box helicases	AT3G09720
Eni_020865		Pre-rRNA processing and modifications.methylotransferases	AT4G25730
Eni_051682		Pre-rRNA processing and modifications.methylotransferases	AT5G40530
Eni_030659		Pre-rRNA processing and modifications.misc	AT3G55620
Eni_109548		Pre-rRNA processing and modifications.misc	AT2G47420
Eni_072705		Pre-rRNA processing and modifications.WD-repeat proteins	AT5G14050
Eni_081488		Pre-rRNA processing and modifications.WD-repeat proteins	AT5G14050

Table A12: Protein degradation related DEGs upon drying (denoted as relative water content, %) and rehydration (12h) in the non-senescent tissue (NST) and senescent tissue (ST) of the resurrection plant *Eragrostis nindensis*. The colour scale represents log_2 fold change values, FDR <0.05. AT = *Arabidopsis thaliana* homologues. Annotations were derived from Mercator v4.0 (Schwacke *et al.* 2019). Top 20 accumulating DEGs are shown.

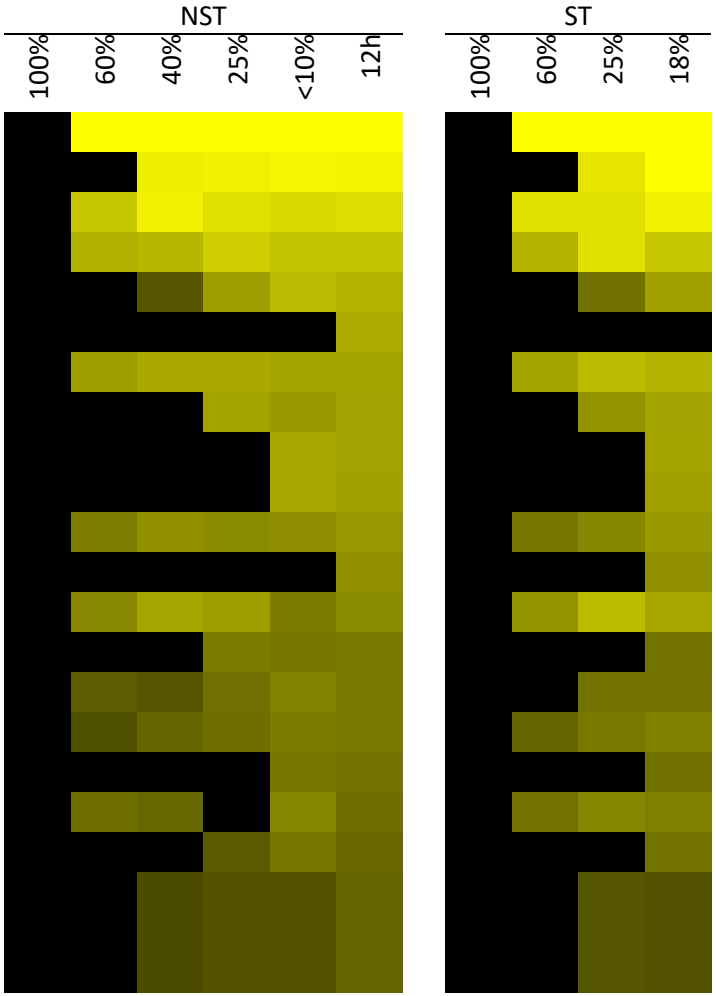

Gene ID	Mercator	AT homologue
Eni_084778	protein.degradation.ubiquitin.E3.RING	AT5G50170
Eni_068765	protein.degradation.ubiquitin.E3.RING	AT3G62690
Eni_037465	protein.degradation.ubiquitin.E3.RING	AT5G27420
Eni_107080	protein.degradation.ubiquitin.E3.RING	AT5G50170
Eni_034375	protein.degradation.ubiquitin.E3.RING	AT1G26800
Eni_023558	protein.degradation.ubiquitin	AT4G05230
Eni_054774	protein.degradation.ubiquitin.E3.RING	AT5G50170
Eni_084000	protein.degradation.ubiquitin.E3.RING	AT2G42360
Eni_053806	protein.degradation.ubiquitin	AT4G05230
Eni_018268	protein.degradation.ubiquitin	AT4G05230
Eni_075918	protein.degradation.ubiquitin.E3.RING	AT4G35840
Eni_112814	protein.degradation.ubiquitin.E3.RING	AT4G35840
Eni_107081	protein.degradation.ubiquitin.E3.RING	AT1G03370
Eni_013278	protein.degradation.ubiquitin.E3.RING	AT3G10910
Eni_040246	protein.degradation.ubiquitin.E3.SCF.FBOX	AT1G21410
Eni_109818	protein.degradation.ubiquitin.E3.RING	AT4G34370
Eni_053527	protein.degradation.ubiquitin.ubiquitin protease	AT5G10790
Eni_068319	protein.degradation.ubiquitin.E3.SCF.SKP	AT1G20140
Eni_077391	protein.degradation.ubiquitin.E3.RING	AT4G35840
Eni_032284	protein.degradation.ubiquitin.E3.RING	AT1G65430

Table A13: RT-qPCR correlation analyses comparing the genome and *de novo* based assembly to the quantitative real-time PCR (RT-qPCR) of selected genes of interest (GOI) during drying (represented as the relative water content, %) and rehydration (12h) in desiccation tolerant, non-senescent tissue (NST) and desiccation sensitive, senescent tissue (ST) of the resurrection plant *Eragrostis nindensis*. Transcript abundance profiles (normalised fold change ($2^{-\Delta\Delta Ct}$)) of GOI relating to desiccation tolerance (drought recovery, trehalose phosphatase, LEA3 (late embryogenesis abundant protein), RUBISCO (ribulose-1,5-bisphosphate carboxylase/oxygenase)) and senescence (senescence associate gene (SAG), WRKY, WRKY70) showed similar trends during drying and therefore validated the transcriptome. GOI expression patterns were normalised to the internal controls (GAPDH, F-Box and ubiquitin).

	Genome-based			*De novo* based		
Gene	r^2	p-value	Significance	r^2	p-value	Significance
Drought recovery	0.53	0.018	N/A	0.55	0.16	N/A
LEA	0.48	0.23	N/A	0.89	0.0034	***
RUBISCO	0.85	0.0078	**	0.74	0.035	*
SAG	0.67	0.099	N/A	-0.23	0.61	N/A
Trehalose	0.18	0.67	N/A	-0.11	0.79	N/A
WRKY	0.97	0.00037	***	0.98	0.000091	***
WRKY70	0.99	0.00000061	***	1	1e-8	***

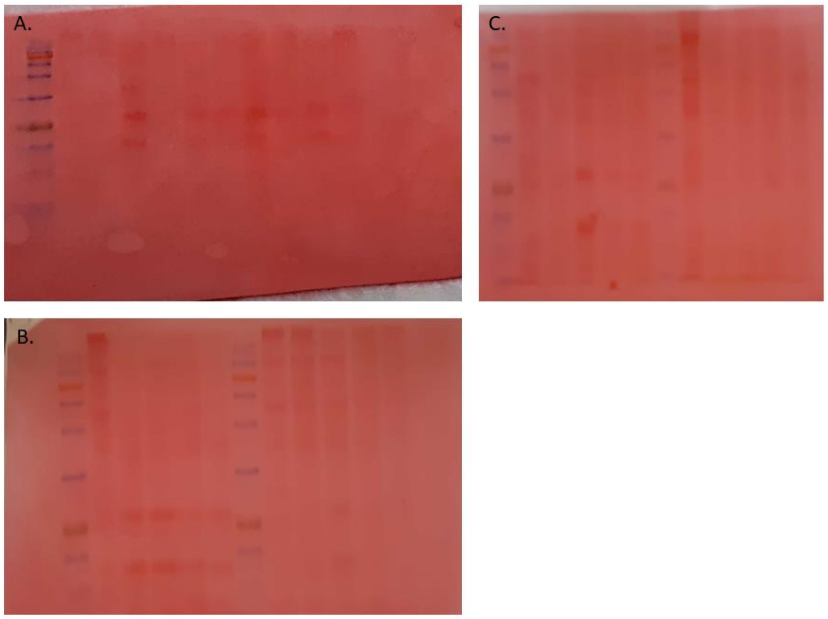

Figure A5: Ponceau staining of PVDF membrane post-transfer at 40V overnight of the three gels (A-C) used for the western blot analysis.

APPENDIX 2:

DE NOVO TRANSCRIPTOME ASSEMBLY OF *E. NINDENSIS*

Introduction

RNA-seq analyses generate very large, complex datasets that require fast and accurate software to transform contigs (fragmented DNA) into comprehensible and annotated genes (Pertea *et al.* 2016). New tools have been developed to robustly calculate transcript expression of non-model organisms of ecological and economic importance with or without the need of a previously constructed genome (Grabherr *et al.* 2011). Non-model organisms without genomes are challenging, especially with species that have complex genomes (e.g. polyploidy, such as *E. nindensis* (Pardo *et al.* 2019)). This **Chapter** briefly describes the bioinformatic pipeline used to construct the *de novo* assembly for *E. nindensis*. The *de novo* assembly was conducted prior to the sequencing of the genome and further analysis of the *de novo* assembly was discontinued when the genome was sequenced. The assembly approach constructs a single reference assembly by mapping all reads from the sequenced mRNA into long contiguous sequences (contigs) using de Bruijn's graphs complied in Trinity version 2.2.0 (Grabherr *et al.* 2011; Haas *et al.* 2013). Trinity uses these contigs and reports transcripts and isoforms, which are used as a reference assembly to which each individual cDNA library is mapped against, to generate a comprehensive transcript library with read counts. This protocol quantifies transcripts based on the assumption that the number of reads mapped to each transcript in each library is a function of transcript abundance, and therefore can be used to measure transcript abundance for downstream analyses (Haas *et al.* 2013).

Methods and results

De novo assembly construction

The trimmed FASTQ files containing RNA sequences described in **Chapter 3** were used to construct four *de novo* assemblies. Only paired-end reads were used for the *de novo* assembly to ensure the highest quality alignment. These reads encompass the range of transcripts expressed during water-deficit stress and recovery thereof in two tissue types (NST and ST), and the constructed reference assembly is therefore a good representative of which transcripts are expressed in *E. nindensis* in

response to water-deficit stress. The transcript assembler package Trinity version 2.2.0 (Garber *et al.* 2011) was used (see https://github.com/TheOfficialFloW/Trinity).

Three assemblies were initially constructed (prior to fungal discovery, discussed below) to assess which k-mer size yielded the highest quality assembly. Assembly #3 was chosen as the most appropriate assembly due to the lowest number of contigs in combination of the BUSCO (Benchmarking Universal Single-Copy Orthologs) score (Simão *et al.* 2015), and the high N50 value (Table B1). Fungal contamination of reads then became evident and following removal of the fungus (discussed below), a new assembly was created using the nine paired-end samples that passed the contamination threshold. After removing the contaminated samples, re-constructing the *de novo* assembly, and clustering homologous contigs, the assembly without fungal reads (#4) was chosen as the best overall assembly (Table B1). This assembly was used for downstream analysis of statistically significant changes in transcript abundances, referred to as differentially expressed genes (DEGs). Figure B1 describes the bioinformatic pipeline used to develop the four assemblies and indicates the tools used to, *inter alia,* generate the *de novo* assembly, quantify transcript abundances and perform enrichment analysis.

RT-qPCR was done using the same method as described in **Chapter 3**, where primers were designed based on the RNA sequences for housekeeping genes (F-Box, GAPDH, ubiquitin) and genes of interest to desiccation tolerance (DROUGHT RECOVERY, trehalose phosphatase, LEA3, RUBISCO) and senescence (SAG, WRKY, WRKY70, see Table 3.2). The housekeeping gene encoding transcripts were used as internal controls.

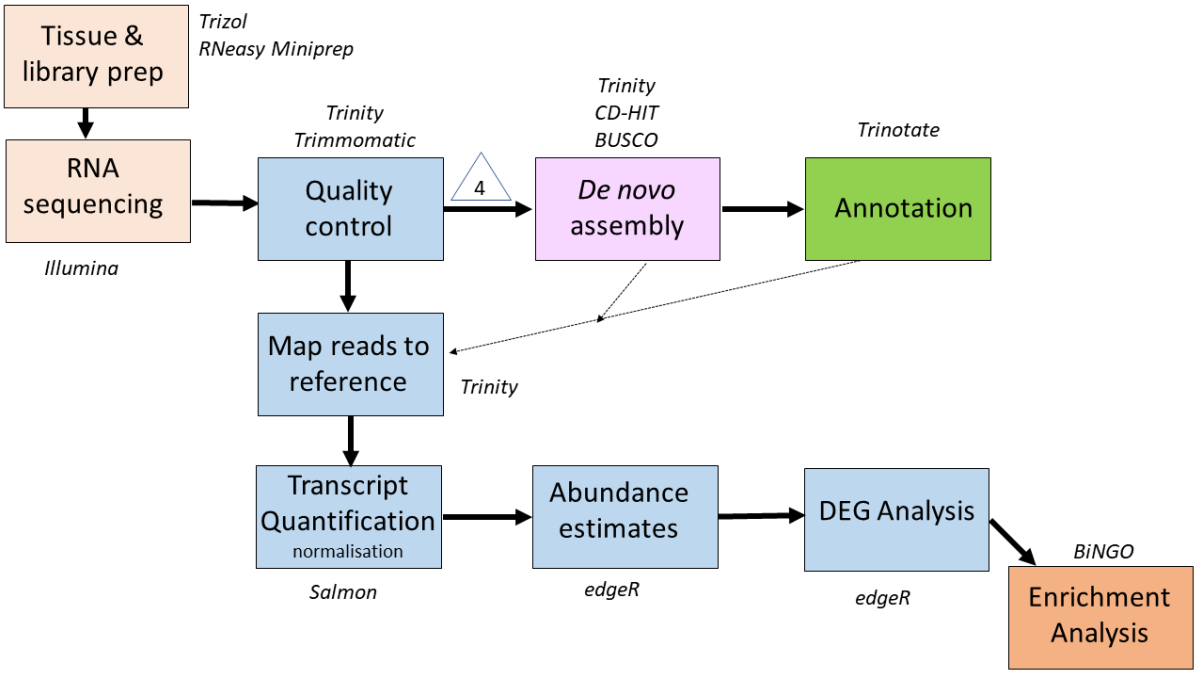

Figure B1: The bioinformatic pipeline used to derive differentially expressed transcript abundances, referred to as differentially expressed genes (DEGs), representing statistically significant changes in transcript abundances between the desiccation tolerant, non-senescent tissue (NST) and desiccation sensitive, senescent-tissue (ST) of the resurrection plant *Eragrostis nindensis* during water-deficit stress and rehydration. Triangle corresponds with *de novo* assembly constructed and indicates at which step in the pipeline fungus contaminants were removed. Assembly #4 removed five samples containing >2% fungal transcripts in the sample library and reconstructed the *de novo* assembly. Italicised words indicate the bioinformatic tools used to generate the outputs in the corresponding boxes.

Four *de novo* assemblies were constructed using different k-mer seed sizes (Table B1). The number of contigs generated *de novo* (208443 contigs) produced considerably more contigs compared to the transcriptome of a similar species, *Eragrostis tef*, which had 88078 contigs (Cannarozzi *et al.* 2014). This is because during the assembly of short reads, multiple contigs can be formed per gene due to incomplete reads being assembled (Ono *et al.* 2015). This results in redundant contigs, which must be removed to avoid falsely identifying contigs as differentially expressed, when they are in fact derived from the same gene (Ono *et al.* 2015). To remove redundant contigs from the *de novo* assembly, CD-HIT version 4.7 (Li *et al.* 2006; Fu *et al.* 2012) was used, which clustered homologues and duplicated reads with 90% identity coverage, retaining the representative sequence (longest contig). This reduced the assembly size to a more acceptable 137485 transcripts (assembly #4). Assembly completeness was assessed using BUSCO, as described in **Chapter 3.** The *de novo* assembly (#4) was constructed using a k-mer size of 30 and inchworm k-mer coverage parameter of 5.

Table B1: Comparisons of assembly completeness using BUSCO (Benchmarking Universal Single-Copy Orthologs, Simão *et al.* 2015) and assembly statistics using Trinity (Haas *et al.* 2013; Grabherr *et al.* 2011) across the four constructed *de novo* assemblies, and the genome (Pardo *et al.* 2019). *indicates normalisation. Bold indicates the *de novo* assembly with the highest quality.

		Raw de novo assembly			**No fungus**	Genome
	Assembly	#1	#2	#3	**#4**	-
BUSCO outputs	Complete	89.7% (1291)	86.2% (1241)	86.7% (1248)	**85.0% (1224)**	96% (1387)
	Single-copy	33.3% (479)	45.7% (658)	39.0% (561)	**69.2% (996)**	12% (176)
	Duplicated	56.4% (812)	40.5% (583)	47.7% (687)	**15.8% (228)**	84% (1211)
	Fragmented	6.4% (92)	7.6% (110)	7.2% (103)	**8.2% (118)**	3% (45)
	Missing	4.0% (57)	6.2% (89)	6.2% (89)	**6.8% (98)**	1% (8)
Assembly parameters	K-mer size*	25	27	30	**30**	-
	Max. coverage*	30	30	40	**30**	-
	Inchworm	1	5	5	**5**	-
	N50 (bp)	2057	1711	1862	**1434**	123358
	Contigs (total)	361753	213348	109611	**107486**	4368

Transcript quantification and read mapping

Raw sequencing reads (reads) were mapped against the reference assembly once it was constructed *de novo*. The alignment-free package Salmon v0.9.0 (Patro *et al.* 2017) was used to estimate and quantify transcript abundances for each sample library (Table B2). Salmon maps each sample back to the reference (*de novo*) assembly and estimates transcript abundance, fragment length and fragment number (count) for each transcript. Transcripts were normalised and corrected for biases in gene length and sequencing depth and expressed as transcripts per million (TPM). Lowly abundant transcripts, defined as a total TPM of less than five across all samples, were removed. A total of 121439 transcripts remained. The average mapping rate was 89% (Table B2), indicating that the reference assembly is a good representation of the sequenced reads. This is similar to the genome-based mapping rate in **Chapter 3** and thus validates the robustness of the constructed *de novo* assembly (Appendix, Table A).

Table B2: Mapping statistics for read alignment to the *de novo* assembly #4 (fungus removed) in Salmon v0.9.0 (Patro *et al.* 2017).

Sample	Mapped (%)	Reads mapped	Sample	Mapped (%)	Reads mapped
100% NST	88	79281444	40% NST	86	50236297
100% NST	95	32740146	40% NST	94	48850324
100% NST	88	41642167	40% NST	86	49135775
100% ST	87	36883193	25% NST	87	36468462
100% ST	87	63614409	25% NST	87	62260137
100% ST	94	34153433	25% NST	93	13358614
60% NST	86	43389807	25% ST	94	25124890
60% NST	86	51445960	25% ST	87	63614409
60% NST	94	38526645	<10% NST	87	63614409
60% ST	87	41102638	<10% NST	94	27633910
60% ST	87	51537774	<10% NST	86	38146982
60% ST	94	35973935	12 h NST	94	34894669
-	-	-	12 h NST	82	37347918

Functional annotation

Transcripts were annotated using the same tools as discussed in **Chapter 3**, with some modifications. Trinotate version 3.0, (http://trinotate.github.io, Bryant *et al.* 2017) was used to annotate the assembled genes (Figure B1). This comprehensive annotation tool incorporates several databases to functionally annotate transcripts, especially transcriptomes lacking an annotated genome (Haas *et al.* 2013). Annotations are based on similar sequence homology through BLAST+ and SwissProt, protein domain identification through HMMER and Pfam, protein signal peptide and transmembrane domain

prediction (through signalP and tmHMM) using the tool Transdecoder (version 2.1.0, https://github.com/TransDecoder), as well as Gene Ontology (GO, (Dessimoz *et al.* 2017)) and KEGG (Kyoto Encyclopedia of Genes and Genomes, (Kanehisa *et al.* 2016)) databases.

Various other methods were used to functionally annotate the transcriptome of *E. nindensis*. The transcriptome was BLASTed against the annotated transcriptome of *E. tef* (http://130.92.252.158/tef/version1/, Cannarozzi *et al.* 2014). Blast2GO, using the non-redundant protein dataset, provided some GO term annotation (Conesa *et al.* 2008). Trinotate provided the most comprehensive annotation and was used for the final *de novo* assembled transcriptome.

Differential transcript abundances

Differentially abundant transcripts (i.e. DEGs) were identified using the edgeR Bioconducter package (Robinson *et al.* 2010; McCarthy *et al.* 2012). Differential transcript abundance was calculated by pairwise comparisons of the treatments (drying plants) to the control (NST at 100% RWC). Every sample had three biological replicates, except 25% ST and 12h NST, which had two replicates, following the removal of contaminated samples (see below). The Trinity script "run_DE_analysis.pl" was used to generate transcript level expression. Transcripts were considered significantly differentially expressed when the fold change was > 2 (accumulating, $\log_2$ scale) or < 2 (diminishing, $\log_2$ scale), and the differences in expression between the control was $p \leq 0.05$ and a Benjamini & Hochberg (1995) minimum False Discovery Rate (FDR) correction of q-value ≤ 0.05.

PCA was performed to assess how well each biological replicate correlated within each treatment (Figure B2). The samples were observed to be grouped according to their RWC, demonstrating that water content is the main determinant of transcript variation. The hydrated samples (100% RWC) clearly separated from the drying samples, showing transcriptional differences during drying. Furthermore, the NST at 25% RWC are separated from the 25% in the ST, illustrating the transcriptional differences between these tissue types at lower water contents.

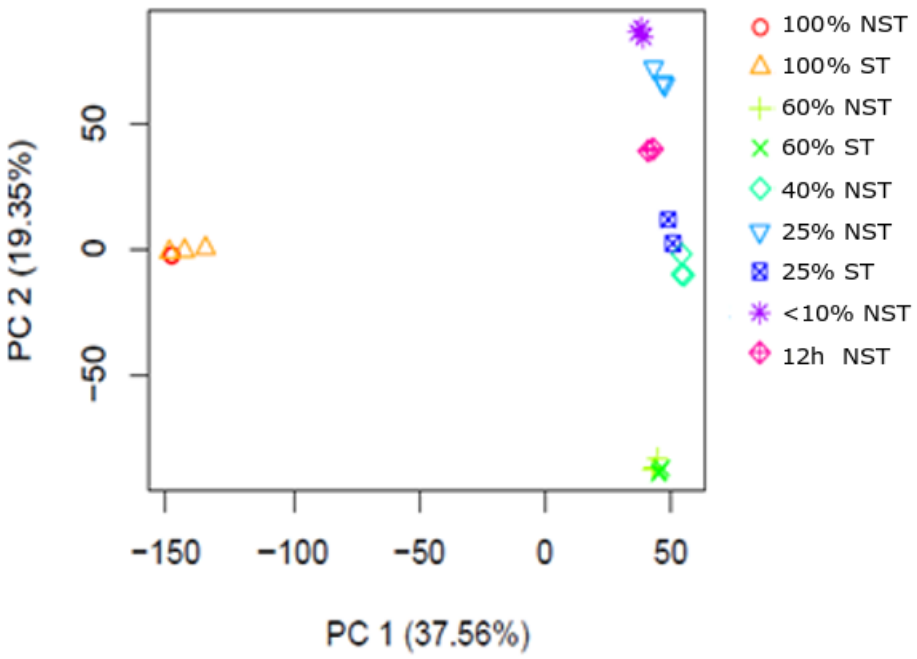

Figure B2: Principle component analysis (PCA) of transcriptomic sequencing data derived from fully hydrated (100% relative water content (RWC)) throughout drying in non-senescent tissue (NST) and senescent tissues (ST) of the resurrection plant *Eragrostis nindensis*.

Fungal discovery and removal

After identifying and annotating DEGs in each treatment an over-enrichment analysis was performed using BiNGO in Cytoscape as described in **Chapter 3.** This identified several enriched categories relating to fungus (‘*fungal-type cell wall biogenesis’*, ‘*hyphae growth’*, ‘*spore-bearing organ development’, ‘evasion or tolerance of host defences’,* amongst others) in the 18% ST sample (data not shown). A protocol detailing what an acceptable level of contamination is, and how these reads were removed, was not found in the literature. Contamination is not uncommon and reads of non-target taxa (i.e. fungus vs plant) are only identified after the construction and annotation of the transcriptome. Usually, high GC-content could indicate the presence of bacteria or fungi within plant samples (Delhomme *et al.* 2014), however, due to the naturally high GC-content of monocots, particularly grasses (Šmarda *et al.* 2014), this was not detected as contamination. Indeed, the genome confirmed the high GC-content (45.96%) in *E. nindensis* (Pardo *et al.* 2019).

A total of 4149 contigs (2.9% of the total assembly) were identified as fungal from the first constructed *de novo* assembly (142193 contigs remained). Although this seemed low, the enrichment of fungal-related categories in the 18% RWC ST sample was concerning. Fungal identification was re-confirmed by BLASTx-ing the *de novo* assembly against the non-redundant NCBI database (http://www.ncbi.nlm.nih.gov). Samples with high fungal contamination, defined as >2%, were

removed (Figure B3). This threshold was chosen to discard most of the fungus-related transcripts while keeping as many reads as possible. This removed all three biological replicates of 18% RWC ST as well as one 25% RWC ST and one 12h NST sample (black bars, Figure B3). All samples contained at least some degree of fungal reads, regardless of RWC.

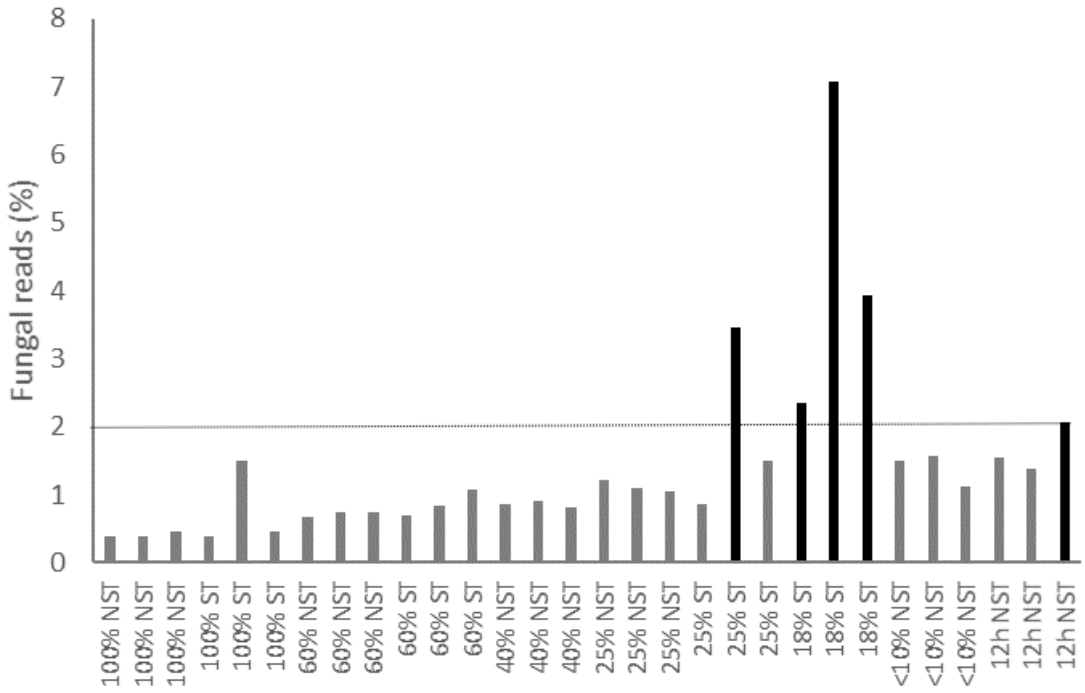

Figure B3: Identification of samples with fungal reads, defined as samples containing >2% reads annotated as fungal, were removed (black bars) in the desiccation tolerant, non-senescent tissue (NST) and desiccation sensitive, senescent-tissue (ST) of the resurrection plant *Eragrostis nindensis* during drying (represented as relative water content, %) and rehydration (12h).

Transcriptome validation

RT-qPCR was conducted to validate (Figure B4) whether transcript abundance trends reflected the mRNA abundances from the DEG analysis derived from the *de novo* assembly. Correlation analysis are depicted in Appendix, Table A13. In addition, the transcriptome was also validated against the genome once this had become available (Pardo *et al.* 2019) as shown in **Chapter 3** (Figure 3.17). Sequences from the constructed *de novo* assembly were aligned to the predicted transcripts from the genome using the genome-alignment tool LAST (http://last.cbrc.jp/). The *de novo* assembly transcripts mapped to 62171 unique genome-predicted transcripts with a sequence identity of >97%. These results are consistent with other projects (Swiercz *et al.* 2018) and validated the quality of the *de novo* assembly transcriptome construction.

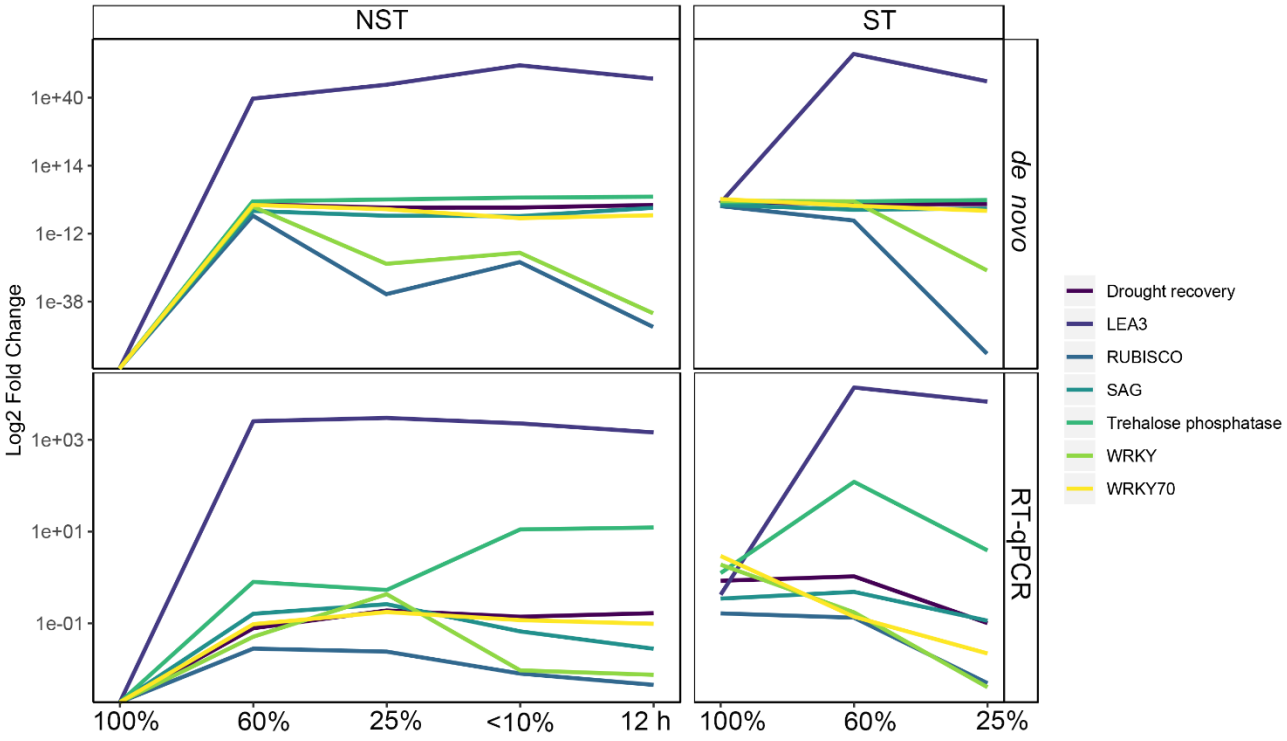

Figure B4: Transcript expression patterns of the various genes of interest during drying (relative water content, %) and rehydration (12h) in desiccation tolerant, non-senescent tissue (NST) and desiccation sensitive, senescent tissue (ST) of the resurrection plant *Eragrostis nindensis* in the *de novo* assembly constructed transcriptome. RT-qPCR (quantitative real-time polymerase chain reaction) analysis verified the transcript abundance trends derived from the RNA-seq analysis. GOI expression patterns are normalised to the internal controls (GAPDH, F-Box and ubiquitin).

Conclusion

A reference assembly for *E. nindensis* was successfully constructed. The assembly was of good quality, as shown by the high mapping rates (>80%) indicating strong read representation of the assembly, a good N50 value of 1434 bp, and high sequence similarity to the genome. Trends were also validated through RT-qPCR analysis, showing that the *in silico* differentially abundant transcripts (DEGs) were representative of mRNA abundances.

De novo assemblies, by their nature, lack a reference genome and are usually performed on non-model organisms. Novel transcripts are therefore present and non-target taxa genes cannot be eliminated based on the target genome. Quantifying the amount of “clean” reads and removing as many non-target taxa contigs while keeping as many samples is suggested. In this case, if > 2% of the library was identified from non-target taxa, the sample was removed, and a new assembly

constructed. The process of identifying and removing fungal contaminants was described to generate a reproducible method.

It is unsurprising that the tissues most afflicted with fungal infection were in the ST at lower water contents (25% and 18% RWC), as these tissues are sacrificed upon desiccation and experience general system failure (**Chapter 4**). Although transcripts enriched in *'defence response'* were diminishing during drying in both tissue types (Figure 4.1, B), the lack of discernible fungal infection in the NST suggests that there is a maintenance of a functional biotic defence in the NST at lower water contents, highlighting another difference between the NST and ST, and indicates a tighter regulation of the NST under water-deficit stress. All samples, regardless of RWC, contained some level of fungal reads (which is not uncommon). This might suggest the presence of fungal endophytes in *E. nindensis*. Endophytes can have a mutual or even beneficial effect on the plant (Naveed *et al.* 2014; Hardoim *et al.* 2015; Lata *et al.* 2018). For example, three fungal isolates from the class *Dothdemycetes* were associated with water-deficit stress in the C4 grass *Panicum virgatum* (Giauque *et al.* 2019). By screening for fungal traits of different endophytes in *P. virgatum*, Giauque *et al.* (2019) demonstrated that plant survival and stress tolerance effects can be predicted by fungal traits. It has been shown that the metabolites produced within the fungi benefit the host plant (e.g. production of antioxidants) (Sun *et al.* 2010; Sessitsch *et al.* 2018). Furthermore, the host plant's growth and water-use efficiency improved when it was inoculated with fungi that inhabit warmer drier regions (Giauque *et al.* 2019). Endophytic communities can thus be beneficial to plants and can play a role in drought resilience.

It would be useful to investigate the composition and potential function of endophytes within resurrection plants to see if plant-fungal relations help convey desiccation tolerance. To date this has not been reported, although endophytes isolated from a Brazilian resurrection plant, *Tripogon spicatus*, have been shown to promote the growth of rice via production of auxin (Fernandes Júnior *et al.*, 2015). Furthermore, relationships of grasses with endophytes are increasingly being explored due to their importance in crops with agronomic potential (Kannadan *et al.* 2008; Johnston-Monje *et al.* 2011; Wallace *et al.* 2018). Identifying endophytes with beneficial mechanisms to plants under stress could aid crop improvement (Naveed *et al.* 2014; Wallace *et al.* 2018) and offers an alternative (non-GM) approach to increasing drought resilience (Lata *et al.* 2018). Even maize, arguably one of the most well-studied plants, has no published data quantifying endophytes, except for an estimated range of 30-40 unique fungal species (Wallace *et al.* 2018). Because the endophytes in resurrection plants also undergo cycles of drying and rehydration, these taxa must induce within themselves mechanisms of desiccation tolerance to survive within the host plant. Therefore, these endophytes potentially harbour important abiotic-stress response mechanisms. *De novo* assemblies of non-model

organisms are thus potential resources for the discovery of fungal-plant relations that can improve water-use efficiency or stress tolerance in crops.